



NUREG/CR-7040
BNL-NUREG-94629-2011

Evaluation of JNES Equipment Fragility Tests for Use in Seismic Probabilistic Risk Assessments for U.S. Nuclear Power Plants

Evaluation of JNES Equipment Fragility Tests for Use in Seismic Probabilistic Risk Assessments for U.S. Nuclear Power Plants

Manuscript Completed: January 2011

Date Published: April 2011

Prepared by
R. Kennedy¹
J. Nie and C. Hofmayer²

¹RPK Structural Mechanics Consulting
28625 Mountain Meadow Road
Escondido, CA 92026

² Brookhaven National Laboratory
P.O. Box 5000
Upton, NY 11973-5000

S. Ali, NRC Project Manager

NRC Job Codes N6076 and N6998

ABSTRACT

The Japan Nuclear Energy Safety Organization (JNES) is conducting a multi-year equipment fragility test program to obtain realistic equipment fragility capacities for use in the seismic probabilistic risk assessments (SPRAs) of nuclear power plants (NPPs) in Japan. This test program started in 2002 and is planned to continue until 2012. The purpose of this test program is to improve the quality of the seismic fragility capacity database by determining realistic equipment fragility capacities from full-scale shaking table tests, and consequently to allow more accurate SPRAs to be performed to quantify the risk of NPPs during beyond-design-basis earthquakes. This test program reflects a philosophical shift from the design-proving test in the past that was intended to demonstrate the success of equipment under design basis or slightly larger earthquakes, to the current fragility test that determines the (ultimate) seismic capacity under beyond-design-basis earthquakes. This program consists of the test of a series of safety significant equipment, which are scheduled in two phases. Phase I includes large horizontal shaft pumps, large vertical shaft pumps, electrical panels, and control rod insertion capability and Phase II includes fans, valves, tanks, support structures, and overhead cranes.

As part of collaborative efforts between the United States and Japan on seismic issues, the U.S. Nuclear Regulatory Commission (NRC) and Brookhaven National Laboratory (BNL) participated in this program by evaluating the results of the JNES equipment fragility tests. The goal of this research effort was to compare the JNES fragility results with the fragility data typically used in current U.S. SPRAs and assess the impact that the new test results may have on current SPRAs and how this data can be utilized for future SPRAs. The JNES fragility results are also useful for seismic margin analyses (SMAs), which are important in design certification (DC) or combined license (COL) applications because of the lack of full SPRAs at the DC or COL stage. This report summarizes the BNL evaluation of the JNES equipment fragility test data and provides insights on the applicability and application of this data in U.S. SPRA practices.

TABLE OF CONTENTS

ABSTRACT	iii
LIST OF FIGURES	viii
LIST OF TABLES	xii
EXECUTIVE SUMMARY	xiii
ACKNOWLEDGEMENTS	xvii
1 INTRODUCTION	1
2 COMMON U.S. PRACTICE FOR ESTIMATING SEISMIC FRAGILITIES OF EQUIPMENT QUALIFIED BY TEST	3
2.1 Introduction	3
2.2 Equipment Fragilities Based on Generic Data	4
2.3 Equipment Fragilities Based on HCLPF Screening Levels.....	5
2.4 Advanced Light Water Reactor “Achievable” Fragilities	7
2.5 Comparison of Generic Fragility Estimates	7
3 JNES EQUIPMENT FRAGILITY TESTS.....	11
3.1 Overview of the JNES Equipment Fragility Test Program	11
3.2 Horizontal Shaft Pumps.....	13
3.2.1 Summary of Horizontal Shaft Pump Tests	13
3.2.1.1 Full Scale Test.....	13
3.2.1.2 Element Tests	14
3.2.2 Fragility Evaluation and Fragility Data	15
3.2.2.1 Fragility Evaluation for Active Function.....	15
3.2.2.2 Fragility Evaluation for Structural Strength	15
3.2.2.3 Summary of Fragility Data	16
3.3 Electrical Panels	16
3.3.1 Summary of Electrical Panel Tests.....	16
3.3.1.1 Full Scale Tests.....	16
3.3.1.2 Element (Device) Tests	18
3.3.2 Fragility Evaluation and Fragility Data	18
3.4 Control Rod Insertion Capability	20
3.4.1 PWR Control Rod Insertion Capability	20
3.4.1.1 Full Scale Test	20
3.4.1.2 Fragility Evaluation and Fragility data.....	21
3.4.2 BWR Control Rod Insertion Capability.....	21
3.4.2.1 Full Scale Test	21
3.4.2.2 Fragility Evaluation and Fragility Data	22
3.5 Large Size Vertical Shaft Pumps.....	23
3.5.1 Summary of Large Size Vertical Shaft Pump Test.....	23
3.5.1.1 Full Scale Test	23
3.5.1.2 Element Tests	24
3.5.2 Fragility Evaluation and Fragility Data	25
3.5.2.1 Fragility Evaluation for Structural Strength	26

3.5.2.2	Fragility Evaluation for Rotation Function	27
3.5.2.3	Summary of Fragility Data	27
4	EVALUATION OF JNES EQUIPMENT FRAGILITY TEST DATA.....	75
4.1	Introduction	75
4.2	Electrical Component Fragilities.....	77
4.3	Large Horizontal Shaft Pumps	79
4.4	Large Vertical Shaft Pump	81
4.5	Control Rod Insertion Capability	83
4.5.1	PWR Plants.....	83
4.5.2	BWR Plants	84
4.5.3	Applicability of Results for U.S. Fragility Assessments	84
5	CONCLUSIONS	87
5.1	Horizontal Shaft Pumps.....	87
5.2	Electrical Panels	88
5.3	Control Rod Insertion Capability	89
5.4	Large Size Vertical Shaft Pumps.....	90
5.5	Summary	90
6	REFERENCES	93
Appendix A	JNES FRAGILITY DATA OF EQUIPMENT FOR NUCLEAR FACILITIES BY SHAKING TESTS	A-I
Part-I	Introduction.....	A-1
1.	Background of Study	A-3
1.1	Necessity of Fragility Data of Equipment.....	A-3
1.2	Fragility Capacity Evaluation Test of Equipment and Its Progress, and Positioning of the Report.....	A-3
2.	Evaluation Process for Fragility Capacity of Equipment.....	A-5
Part-II	Development of Fragility Data.....	A-7
1.	Outline	A-9
1.1	Outcome of Fragility Capacity Tests for Equipment	A-10
1.1.1	Horizontal Shaft Pump	A-10
1.1.2	Electrical Equipment	A-11
1.1.3	Control Rod Inserting Capability	A-12
1.1.4	Large Size Vertical Shaft Pump	A-14
2.	Evaluation Method of Fragility Capacity	A-17
2.1	Horizontal Shaft Pump	A-17
2.2	Electrical Equipment	A-25
2.3	Control Rod Inserting Capability	A-28
2.4	Large Size Vertical Shaft Pump	A-33
3.	Fragility Data	A-47
3.1	Horizontal Shaft Pump	A-48
3.2	Electrical Equipment	A-55
3.3	Control Rod Inserting Capability	A-79
3.4	Large Size Vertical Shaft Pump	A-83

4. Summary	A-93
References	A-95
Appendix B ELECTRICAL PANEL TEST RESPONSE SPECTRA	B-1
B.1 Response Spectra Reported in September 2003	B-2
B.1.1 Reactor Control Center	B-3
B.1.2 Power Center	B-6
B.1.3 Device Tests	B-9
B.2 Response Spectra Reported in July 2004	B-21
B.2.1 Main Control Board	B-22
B.2.2 Logic Control Panel	B-26
B.2.3 Protection Instrument Rack	B-28
B.2.4 Instrument Rack	B-31
B.2.5 Reactor Control Center	B-32
B.2.6 Power Center	B-34
B.2.7 Metalclad Switchgear	B-37
B.2.8 Device Tests	B-39

LIST OF FIGURES

Figure 3-1 JNES Equipment Fragility Test Schedule	41
Figure 3-2 TADOTSU Shaking Table and the Amplification Device Table	41
Figure 3-3 RCW Pump Test Layout.....	42
Figure 3-4 Development of Envelop Floor Response Spectrum	43
Figure 3-5 Basis Input Acceleration Time History Generated From Envelop FRS for Horizontal Shaft Pump Test	43
Figure 3-6 Response Spectra at the Top of the Amplification Table for Excitation Levels of 2 g, 4g, and 6g in the Full Scale Horizontal Shaft Pump Test.....	44
Figure 3-7 Change of Acceleration at Bearing Case With Respect to Input Acceleration.....	45
Figure 3-8 Test Setup for Radial Ball Bearings	45
Figure 3-9 Test Setup for Thrust Ball Bearings	46
Figure 3-10 Surface Degradation of Bearings During Element Tests.....	46
Figure 3-11 Analytical Models for Single Stage Horizontal Shaft Pump	47
Figure 3-12 Analytical Models for Multi-stage Horizontal Shaft Pump.....	48
Figure 3-13 Basis Input Acceleration Time History for Electrical Panel Tests	49
Figure 3-14 Illustration of Electrical Panels.....	50
Figure 3-15 Test Setting for Electrical Panels.....	51
Figure 3-16 Comparison of Front-Back 6 g Level Response Spectra for Reactor Control Center Test	52
Figure 3-17 Gas Circuit Breaker Installed on a Support Frame in Element Test.....	52
Figure 3-18 JNES Target Range of the Fragility Tests	53
Figure 3-19 Test Setup for PWR Control Rod Insertion System	53
Figure 3-20 Mockup of A PWR Fuel Assembly	54
Figure 3-21 Section View of the Test Setup for PWR Control Rod Insertion System.....	55
Figure 3-22 Layout of 3 PWR Fuel Assemblies.....	55
Figure 3-23 Synthesized Wave for Full-Scale Test of PWR CRDM	56
Figure 3-24 Filtered Wave for Fuel Excitation	56
Figure 3-25 Comparison of PWR CRDM Target Input and Shaking Table Response (Still Water).....	57
Figure 3-26 Comparison of PWR CRDM Target Input and Shaking Table Response (With Core Flow).....	57
Figure 3-27 Comparison of PWR CRDM Target Input and Upper Core Plate Response (Still Water).....	58
Figure 3-28 Comparison of PWR CRDM Target Input and Lower Core Plate Response (Still Water).....	58
Figure 3-29 Comparison of PWR CRDM Target Input and CRDM Base Response (Still Water).....	59
Figure 3-30 Comparison of PWR CRDM Target Input and Upper Core Support Plate Response (Still Water).....	59
Figure 3-31 Delay Ratio of PWR Control Rod Insertion	60
Figure 3-32 Test Setup for BWR Control Rod Insertion System.....	60

Figure 3-33 Mockup of A BWR Fuel Assembly.....	61
Figure 3-34 Section View of the Test Setup for BWR Control Rod Insertion System	62
Figure 3-35 Layout of a BWR Fuel Assembly.....	62
Figure 3-36 BWR CRDM Basis Input Wave C with Center Frequency 4.8 Hz	63
Figure 3-37 BWR CRDM Basis Input Wave C with Center Frequency 5.8 Hz and 10% broadening.....	63
Figure 3-38 Comparison of BWR Target Input and Shaking Table Response	64
Figure 3-39 Delay Ratio of BWR Control Rod Insertion.....	64
Figure 3-40 Test Setup for Vertical Shaft Pump	65
Figure 3-41 Section View of the Test Setup for Vertical Shaft Pump	66
Figure 3-42 Response Spectrum for A-Wave.....	67
Figure 3-43 Response Spectra for D-Wave (Horizontal)	67
Figure 3-44 Response Spectra for D'-Wave (Horizontal).....	68
Figure 3-45 Comparison of A, D, and D' Waves.....	68
Figure 3-46 Response Spectra for Vertical Wave	69
Figure 3-47 Liner Ring and Shaft Bearing	69
Figure 3-48 Illustration of Shaft Bearing and the Nonlinear Load-Displacement Behavior.....	70
Figure 3-49 Structural Types of Large Size Vertical Shaft Pumps	70
Figure 3-50 Similar Structural Features of Vertical Mixed Flow Pump and Pit Barrel Type Pump.....	71
Figure 3-51 Equivalent Linear Stiffness of Barrel Support.....	71
Figure 3-52 Calculation of Impulsive Force.....	72
Figure 3-53 Stick Model for the Pit Barrel Type Pump	73
Figure 3-54 Two Mass Model for the Vertical Response Analysis for the Vertical Shaft Pumps	74
Figure B-1 Reactor Control Center Test – Child Table RS – 5 g (Side to Side).....	B-3
Figure B-2 Reactor Control Center Test – Base Plate RS – 5 g (Side to Side).....	B-3
Figure B-3 Reactor Control Center Test – Panel RS at the Installation Point of Magnetic Contactor – 5 g (Side to Side)	B-4
Figure B-4 Reactor Control Center Test – Child Table RS – 5 g (Back to Forth)	B-4
Figure B-5 Reactor Control Center Test – Base Plate RS – 5 g (Back to Forth)	B-5
Figure B-6 Reactor Control Center Test – Panel RS at the Installation Point of Magnetic Contactor – 5 g (Back and Forth).....	B-5
Figure B-7 Power Center Test – Child Table RS – 4 g (Side to Side)	B-6
Figure B-8 Power Center Test – Base Plate RS – 4 g (Side to Side)	B-6
Figure B-9 Power Center Test – Panel RS at the Installation Point of the Ratio Differential Relay – 4 g (Side to Side).....	B-7
Figure B-10 Power Center Test – Child Table RS – 3 g (Back and Forth).....	B-7
Figure B-11 Power Center Test – Base Plate RS – 3 g (Back and Forth)	B-8
Figure B-12 Power Center Test – Panel RS at the Installation Point of the Ratio Differential Relay – 3 g (Back and Forth)	B-8
Figure B-13 Ratio Differential Relay (MELCO TUB-2-D).....	B-9

Figure B-14 Over Current Relay (MELCO CO-18-D)	B-9
Figure B-15 Auxiliary Relay (MELCO NRD-81).....	B-10
Figure B-16 Comparator Card (MELCO HALN)	B-10
Figure B-17 AC Controller Card (MELCO HASN)	B-11
Figure B-18 Power Supply Equipment (MELCO -).....	B-11
Figure B-19 Magnetic Contactor (MELCO MSO-A80)	B-12
Figure B-20 Breaker for Wiring (MELCO NF-100-SH).....	B-12
Figure B-21 Module Switch (MELCO SSA-SD3-53)	B-13
Figure B-22 Over Current Relay (Toshiba VCR520) and Auxiliary Relay (Toshiba UP3A)....	B-13
Figure B-23 Controller (Toshiba TOSMAP)	B-14
Figure B-24 I/O Unit (Toshiba TOSMAP).....	B-14
Figure B-25 Power Supply Equipment (Toshiba TFV).....	B-15
Figure B-26 Differential Pressure Transmitter (Toshiba AP3107)	B-15
Figure B-27 Magnetic Contactor (Toshiba C-20J, T-20J) and Breaker for Wiring (Toshiba SH100)	B-16
Figure B-28 Auxiliary Relay (HITACHI MY4Z), Timer (HITACHI H3M), and Breaker for Wiring (HITACHI F type)	B-16
Figure B-29 Flat Display (HITACHI 18" type)	B-17
Figure B-30 Controller Display (HITACHI 18" type)	B-17
Figure B-31 Differential Pressure Transmitter (HITACHI EDR-N6).....	B-18
Figure B-32 Pressure Transmitter (HITACHI EPR-N6).....	B-18
Figure B-33 Cam Type Switch (HITACHI MS type) and Key Switch (HITACHI ACSNK type).....	B-19
Figure B-34 Test Module (S9186AW), Power Supply Module (S9016AW), and Monitor Module (S9146AW), All Produced by Yokogawa Electric Co.....	B-19
Figure B-35 Power Supply Module (S9980UD), Produced by Yokogawa Electric Co.....	B-20
Figure B-36 Differential Pressure Transmitter (UNE13), Produced by Yokogawa Electric Co.	B-20
Figure B-37 Main Control Board Test – Base Plate RS – 6 g.....	B-22
Figure B-38 Reactor Auxiliary Panel – Base Plate RS – 6g	B-23
Figure B-39 Reactor Auxiliary Panel Sensor Location	B-24
Figure B-40 Reactor Auxiliary Panel – Panel RS – 6 g (Side to Side)	B-24
Figure B-41 Reactor Auxiliary Panel – Panel RS – 6 g (Back and Forth)	B-25
Figure B-42 Logic Control Panel – Base Plate RS – 6 g.....	B-26
Figure B-43 Logic Control Panel – Panel RS – 6 g (Side to Side).....	B-27
Figure B-44 Logic Control Panel – Panel RS – 6 g (Back and Forth)	B-27
Figure B-45 Protection Instrument Rack – Base Plate RS – 6 g	B-28
Figure B-46 Protection Instrument Rack – Rack RS – 4 g (Side to Side).....	B-29
Figure B-47 Protection Instrument Rack – Rack RS – 4 g (Back and Forth)	B-29
Figure B-48 AC Controller Card – 7 g Excitation (Non-malfunction)	B-30
Figure B-49 AC Controller Card – 7.1 g Excitation (Malfunction)	B-30
Figure B-50 Instrument Rack – Base Plate RS – 6 g.....	B-31

Figure B-51 Reactor Control Center – Base Plate RS – 6 g.....	B-32
Figure B-52 Reactor Control Center – Panel RS – 6 g (Side to Side).....	B-33
Figure B-53 Reactor Control Center – Panel RS – 6 g (Back and Forth)	B-33
Figure B-54 Power Center – Base Plate RS – 6 g	B-34
Figure B-55 Power Center – Panel RS – 6 g (Side to Side)	B-35
Figure B-56 Power Center – Panel RS – 6 g (Back and Forth).....	B-35
Figure B-57 RS of Ratio Differential Relay (TUB-2-D), Malfunctioned in 6 g Full Scale Power Center Test (Back and Forth, 10.9 g)	B-36
Figure B-58 Metalclad Switchgear – Base Plate RS – 6 g	B-37
Figure B-59 Metalclad Switchgear – Panel RS – 3 g (Side to Side).....	B-38
Figure B-60 Metalclad Switchgear – Panel RS – 3 g (Back and Forth).....	B-38
Figure B-61 RS at Installation Points for Test Module (MHI S9166AW), Power Supply Module (MHI S9016AW), and Monitor Module (MHI S9146AW).....	B-39
Figure B-62 RS at Installation Points for Power Supply Equipment (MHI S9980UD) and Diode Unit (S9154UT).....	B-40
Figure B-63 RS for Differential Pressure Transmitter (MHI UNE13).....	B-41
Figure B-64 RS of Recorded Time History for Feed Breaker (DS-416) in Power Center – 5 g	B-42
Figure B-65 RS of Recorded Time History for Feed Breaker (DS-416) in Power Center – 6 g.....	B-42
Figure B-66 RS for Feed Breaker (DS-416) in Power Center – Malfunction	B-43
Figure B-67 RS for Feed Breaker (DS-416) in Power Center – Normal Function	B-43
Figure B-68 RS for Feed Breaker (DS-416) in Power Center.....	B-44
Figure B-69 RS for Feed Breaker (DS-416) in Power Center.....	B-44
Figure B-70 Test Module (MHI S9166AW), Power Supply Module (MHI S9016AW), and Monitor Module (MHI S9146AW) – Recorded Wave 10 g (Side to Side).....	B-45
Figure B-71 Test Module (MHI S9166AW), Power Supply Module (MHI S9016AW), and Monitor Module (MHI S9146AW) – Recorded Wave 10 g (Back and Forth)	B-45
Figure B-72 Test Module (MHI S9166AW), Power Supply Module (MHI S9016AW), and Monitor Module (MHI S9146AW) – Predicted Wave 10 g (Side to Side).....	B-46
Figure B-73 Power Supply Equipment (MHI S9980UD) and Diode Unit (MHI S9154UT) – Recorded Wave 10 g (Side to Side)	B-46
Figure B-74 Power Supply Equipment (MHI S9980UD) and Diode Unit (MHI S9154UT) – Recorded Wave 10 g (Back and Forth).....	B-47
Figure B-75 Power Supply Equipment (MHI S9980UD) and Diode Unit (MHI S9154UT) – Predicted Wave 10 g (Side to Side).....	B-47
Figure B-76 Power Supply Equipment (MHI S9980UD) and Diode Unit (MHI S9154UT) – Predicted Wave 10 g (Back and Forth)	B-48
Figure B-77 Differential Pressure Transmitter (MHI UNE13) – Recorded Wave 10 g (Side to Side)	B-48
Figure B-78 Differential Pressure Transmitter (MHI UNE13) – Recorded Wave 10 g (Back and Forth)	B-49

LIST OF TABLES

Table 2-1 Device Capacity Factors	8
Table 2-2 Estimated Generic Fragilities for Electrical Equipment	8
Table 2-3 Cabinet Amplification Factors	9
Table 2-4 “Function During” Spectral Acceleration SA Fragility for Pneumatic Timing Type Auxiliary Relay Panel Mounted in 15 Hz Control Cabinet.....	9
Table 2-5 Generic “Function After” Spectral Acceleration SA Fragility Levels in Terms of Component Input Motion Based on Screening Levels.....	9
Table 2-6 “Function During Achievable” Spectral Acceleration.....	10
Table 2-7 Comparison of Generic Fragilities for Typical Electrical Cabinets.....	10
Table 3-1 Types of Horizontal Shaft Pumps in Japan NPPs	29
Table 3-2 Element Types for Horizontal Shaft Pumps.....	29
Table 3-3 Summary of Selected Critical Values for the Fragility Evaluation.....	30
Table 3-4 Summary of Fragility Data for Horizontal Shaft Pumps.....	31
Table 3-5 Summary of Fragility Data for Ball Bearings used in Horizontal Shaft Pumps	31
Table 3-6 Summary of Fragility Data for Slide Bearings used in Horizontal Shaft Pumps.....	32
Table 3-7 Summary of Fragility Data for Liner Rings used in Horizontal Shaft Pumps	32
Table 3-8 Properties of the Tested Electrical Panels.....	33
Table 3-9 Electrical Parts in JNES Element Tests and Fragility Data	34
Table 3-10 Summary of Fragility Data for Electrical Panels	36
Table 3-11 Selected Results for the Full-scale Vertical Shaft Pump Test.....	37
Table 3-12 Element Types for Large Size Vertical Shaft Pumps.....	38
Table 3-13 Summary of Fragility Data for Large Size Vertical Shaft Pumps (Horizontal Vibration)	39
Table 3-14 Summary of Fragility Data for Large Size Vertical Shaft Pumps (Vertical Vibration)	39
Table 3-15 Summary of Fragility Data for Bearings and Liner Rings used in Large Size Vertical Shaft Pumps.....	40
Table 4-1 JNES Fragilities for Electrical Components	86

EXECUTIVE SUMMARY

This report presents an assessment of the equipment fragility test program performed by the Japan Nuclear Energy Safety Organization (JNES). JNES is carrying out a multi-year equipment fragility test program to obtain realistic equipment fragility capacities for use in the seismic probabilistic risk assessments (SPRAs) of nuclear power plants (NPPs) in Japan. The JNES equipment fragility test program started in 2002 and is planned to continue until 2012. The purpose of the JNES equipment fragility test program is to improve the quality of the seismic fragility capacity database by determining realistic equipment fragility capacities from full-scale shaking table tests, and consequently to allow more accurate SPRAs to be performed to quantify the risk of NPPs during beyond-design-basis earthquakes.

As part of collaborative efforts between the United States and Japan on seismic issues, the U.S. Nuclear Regulatory Commission (NRC) and Brookhaven National Laboratory (BNL) participated in the JNES program by evaluating the results of the JNES equipment fragility tests. The goal of this research effort was to compare the JNES fragility results with the fragility data typically used in current U.S. SPRAs and to assess the impact that the new test results may have on current SPRAs and how this data can be utilized for future SPRAs. The JNES fragility results are also useful for seismic margin analyses (SMAs), which are important in design certification (DC) or combined license (COL) applications because of the lack of full SPRAs at the DC or COL stage. All of the test results and information about the test equipment included in this report were provided by JNES to NRC/BNL. The unique advantage of this particular collaborative effort is obvious because of the rareness of full-scale high-level seismic equipment fragility data.

Seismic equipment fragilities, representing the seismic capacities of the equipment and the associated uncertainties, are the fundamental ingredient in SPRAs. The quality of seismic fragility capacity directly affects the quality of SPRAs in quantifying the risk of NPPs during beyond-design-basis earthquakes. The need for high quality seismic equipment fragility data led to many industry and U.S. NRC sponsored research programs, the results of which are still being applied in current SPRAs. Fragility capacities and the associated uncertainties of the most critical equipment items have historically been derived from qualification test data from equipment vendors. However, in situations when specific qualification data may not be readily available, generic component capacity data are commonly used. For various electrical components and relays, the Generic-Equipment-Ruggedness-Spectra (GERS) and the high confidence low probability of failure (HCLPF) capacities can be found in various industry and NRC publications. For many Central and Eastern U.S. (CEUS) SPRAs, the seismic fragilities of less critical components have been based on the HCLPF screening levels. These U.S. fragility data are all based on pre-1990 vintage components. The applicability of this data for modern components will depend upon the amount of changes that have occurred for any particular component class since 1990. More recently, EPRI TR-016780 [1999] presents “achievable” fragilities proposed to be used for preliminary analyses for modern advanced light water reactor (ALWR) seismic evaluations. However, they need to be verified by qualification tests before being used for any SPRA preceding fuel load.

Albeit the amount of the generic fragility data is large, it has been extremely rare, except perhaps in the case of relays, that fragility data is directly obtained from full-scale tests of equipment under seismic excitations that greatly exceed the design basis earthquake. In the equipment qualification tests, from which some high quality equipment fragilities have been derived, the input seismic waves are only at or slightly higher than the design basis earthquake. The prohibitive cost associated with full-scale seismic fragility tests is the major reason for the

unavailability of high excitation level test-based fragility data. The JNES equipment fragility test program is a very comprehensive and conscientious effort to determine realistic seismic equipment fragility capacities based on full-scale high-level shaking table tests.

The JNES equipment fragility test program consists of tests of a series of important equipment that were determined in an SPRA to be safety significant according to their effect on core damage frequency. The selected test equipment were typical for boiling water reactor (BWR) and pressurized water reactor (PWR) plants in Japan. The test program for the selected equipment was scheduled in two phases. The phase I test program includes large horizontal shaft pumps, large size vertical shaft pumps, electrical panels, and control rod insertion capability. The phase II test program includes fans, valves, tanks, support structures, and overhead cranes. This report documents the evaluation of the fragility data for the JNES phase I equipment. As additional information is made available by JNES for the phase II equipment, a supplement to this report will be prepared to document the corresponding evaluation results.

The fragility capacities of the tested equipment were developed based on the full-scale test results, element tests, and analyses. The JNES fragility evaluation considered both structural and functional limit states. In the full-scale tests, actual equipment as used in typical BWR and PWR nuclear power plants in Japan were shaken under excitations much larger than the design basis earthquakes which have been used in previous equipment qualification tests and design proving tests. The purpose of the full-scale tests was to identify critical acceleration levels and failure modes of the equipment. The element tests were conducted with multiple samples for each element type, and therefore their median capacity and the associated variation were able to be determined statistically. The purpose of the element tests was to evaluate threshold acceleration levels of parts and to assess median capacities and the associated uncertainties. The purpose of the various analyses was to estimate the seismic fragility capacities of the equipment based on the element fragility data and numerical models representing the appropriate failure modes as determined from the full-scale tests.

The horizontal shaft pump in the full-scale test was a reactor building closed cooling water (RCW) pump used in Japan BWR plants, which appears to be very similar to RCW pumps in U.S. nuclear plants. Therefore, it is judged that this test result could be used to estimate the median fragility of RCW pumps in U.S. plants. The function of the RCW pump was confirmed at a zero period acceleration (*ZPA*) of 6.0 g in the full-scale test. The median functional fragilities of the tested RCW pump, a larger RCW pump, and a charging injection pump were estimated to be 8.4 g, 8.6 g, and 17.3 g, respectively. The potentially controlling fragility appears to be slip of the motor on the pump frame. As large uncertainties exist for the slip phenomenon, calculated fragilities were designated as *reference* fragilities. The reference fragilities for the tested RCW pump, the larger RCW pump, and the charging injection pump were reported to be 6.1 g, 5.3 g, and 2.6 g.

For large and critical horizontal pumps such as RCW pumps and Charging High Pressure Injection pumps, it has been common U.S. fragility practice to base their fragility estimate on a review and scaling of the qualification stress report for the specific pump involved. For lower Central and Eastern U.S. (CEUS) seismic regions, and for less critical horizontal pumps, based on a screening level spectral acceleration of 1.2 g, the median *ZPA* capacity of horizontal pumps can be estimated to be about 2.0 g, which is much less than the function confirmed $ZPA = 6.0$ g obtained in the JNES RCW pump full-scale test. The JNES tests demonstrate that these screening level based fragility estimates are exceedingly conservative for horizontal pumps, and thus confirm the judgment that the screening level approach should not be used for risk important horizontal pumps.

Eight electrical panels were selected for the JNES full-scale tests, including a main control board, a reactor auxiliary control board, a logic circuit control panel, an instrumentation rack, a reactor protection rack, a reactor control center, a power center, and a 6.9 kV metal-clad switchgear. The median spectral fragilities for these panels, converted from the JNES test data, range between 5.5 g and 14.2 g; while the generic median fragilities in the U.S. SPRA practice range between 2.2 g and 5.1 g. This comparison indicates that generic fragilities commonly used in U.S. SPRAs for existing CEUS plants might be conservatively biased by more than a factor of two. The JNES test data median fragility levels for electrical components are comparable to the ALWR “achievable” fragilities, which are in the range of 8.3 g to 9.8 g.

However, the natural frequencies for all eight tested electrical components ranged between 21 Hz and 44 Hz. It is not clear whether these reported frequencies include local panel modes of vibration. Most of these electrical components in U.S. plants exhibit local panel mode frequencies in the 4 Hz to 15 Hz range when tested at higher shaking levels. Cabinet response amplification factors AF_C were reported for representative device mounting locations in the JNES tested components to be 1.0 to 2.5; while the recommended median AF_C values at the worst location for the existing U.S. cabinets range between 2.8 to 4.4. Based both on the natural frequency comparisons and the response amplification comparisons, it appears that the JNES tested electrical components are much stiffer than most electrical components in existing U.S. plants. The JNES reported median fragilities should not be used for U.S. electrical components unless it can be shown that the component has stiffnesses similar to those tested by JNES. However, they might be representative of electrical components to be used in new U.S. standard plants not yet built.

Electrical element tests included 37 types of devices. Seismic time history tests were conducted up to a $ZPA=10g$ level or slightly higher. All but eight of these 37 types of devices had function confirmed at ZPA levels of about 10g or slightly higher. The smallest ZPA at which loss of function occurred for eight types of devices was 2.5 g. Additional seismic reinforcement to some of the devices increased the fragility level. With the exception of the air and gas circuit breakers, and the grounded potential transformer, all of these device fragilities exceed the median fragility level used for similar devices in existing U.S. SPRAs. The circuit breaker and transformer capacities are consistent with those used in existing U.S. SPRAs. Because the tested devices are identified by manufacturer and model number, the JNES electrical equipment device fragility data is a highly valuable resource for future SPRAs.

JNES performed a full-scale test on a control rod drive mechanism, control rod, and fuel bundle assembly representative of 3 and 4 loop PWR plants. The fuel assembly was the 17x17 type. The input motion and resulting maximum fuel assembly displacement were 3.2 g (ZPA) and 48 mm, respectively. The reported computed median fragility for fuel assembly displacement is 77 mm. The median ZPA fragility for 3 and 4 loop PWR plants is estimated as 3.9 g in this report. For 2 loop PWR plants with 14x14 type fuel assembly, a median functional limit displacement of 66 mm and the median ZPA and displacement fragilities are estimated in this report as 3.7 g and 69 mm, respectively.

JNES also conducted a full-scale test on a control rod drive mechanism, control rod, and fuel bundle assembly representative of a BWR5 plant with a high speed scram type control rod drive mechanism. JNES estimated that the same fragility estimates were applicable for 80 mil and 120 mil channel boxes. The input motion and resulting maximum fuel bundle assembly displacement were 3.0 g (ZPA) and 83 mm, respectively. JNES estimated the median fragility for the fuel

bundle displacement was 91 mm. The corresponding median ZPA fragility is estimated as 3.1 g to 3.3 g.

The JNES fragility results are applicable for failure modes associated with fuel assembly displacements. Within the U.S., control rod insertion fragilities are generally derived based on a detailed review and scaling of NSSS vendor submitted qualification reported results. For PWR plants, the derived fragilities are generally controlled by the supports of the control rod drive mechanism. The failure modes that have typically been considered to be controlling in U.S. fragility assessments for control rod insertion could not have occurred during these tests because the entire fuel assembly was supported by very stiff frames in the JNES tests.

The large size vertical shaft pump in the full-scale test was a pit barrel type pump in the reactor residual heat removal system (RHR). Function was confirmed at an input ZPA of 1.6 g and a corresponding response ZPA of 14.0 g at the top of motor, and separately at an input ZPA of 2.8 g and a corresponding response ZPA of 31 g at the bottom of barrel. Based on the test results of the submerged bearings, the functional fragilities in terms of the bottom of barrel were estimated to be 37.1 g for the tested RHR pump. This computed submerged bearing functional limit was 20% higher than the highest test level. The functional failure of submerged bearings has not been considered in U.S. fragility analyses of vertical pumps. The JNES data on bearings should be considered in future U.S. practice; however, the submerged bearing functional limit data did not seem to control the pump fragilities.

Similarly as for the large horizontal pumps, the lowest reported fragility is a motor slip reference fragility reported in terms of the top of the motor ZPA response. The slip reference fragility for the tested RHR pump, a high pressure core injection system pump, a component cooling seawater pump (PWR), and a component cooling seawater pump (BWR) was 3.6 g, 3.5 g, 6.2 g, and 2.8 g, respectively. However, a fragility capacity of 14 g at the top of motor was achieved in the full-scale test after tightening the anchor bolts, confirming that large uncertainties exist for the slip reference fragility.

In summary, the JNES tests make a valuable contribution to the overall state of knowledge of equipment fragility levels for use in SPRAs. The JNES fragility capacities were determined based on full-scale component tests and element tests under simulated seismic excitations that were much larger than the design basis earthquakes commonly used in previous qualification tests or design proving tests. The fragility levels found in the JNES tests are in general much higher than those used in current U.S. SPRAs. Additional failure modes, such as relative motor slip on pump frame and functional failure of submerged bearings, have been identified for consideration by fragility analysts. These test results should be considered by fragility analysts in performing future SPRAs. However, caution must be applied to assess the applicability of the results to the specific equipment being considered. In particular, an analysis of the component anchorage and support fragility needs to be performed as a necessary supplement to the equipment fragility data for a proper application.

ACKNOWLEDGEMENTS

The research program described in this report was sponsored by the Office of Nuclear Regulatory Research of the U.S. Nuclear Regulatory Commission. The authors would like to express their gratitude to Dr. Syed Ali, NRC Project Manager, for the technical and administrative support he provided in performing this study.

This research program was performed as part of the Implementing Agreement between the U.S. Nuclear Regulatory Commission and the Japan Nuclear Energy Safety Organization (JNES) in the area of seismic engineering research. This agreement is an item of the Implementing Arrangement between the United States Nuclear Regulatory Commission and the Nuclear and Industrial Safety Agency (NISA) of Japan for Cooperation in the Field of Nuclear Regulatory Matters and Nuclear Safety Research and Development.

All of the test results and information about the test equipment included in this report were provided by JNES and are greatly appreciated. The authors especially thank Dr. Katsumi Ebisawa, Mr. Yuichi Uchiyama, Mr. Hiroshi Abe, and Dr. Kenichi Suzuki of JNES for their support and technical guidance throughout this collaborative study.

The authors also wish to express special thanks to Mrs. Lynda Fitz for her administrative support in the preparation of this report and throughout the duration of this project.

1 INTRODUCTION

Seismic equipment fragilities, representing the seismic capacities of the equipment and the associated uncertainties, are the fundamental ingredient in seismic probabilistic risk assessments (SPRAs) of nuclear power plants (NPPs). The quality of seismic fragility capacity directly affects the quality of SPRAs in quantifying the risk of NPPs during beyond-design-basis earthquakes. The need for high quality seismic equipment fragility data led to many industry and U.S. Nuclear Regulatory Commission (NRC) sponsored research programs, the results of which are still being applied in current SPRAs. Fragility capacities and the associated uncertainties of the most critical equipment items have historically been derived from qualification test data from equipment vendors. However, in situations when specific qualification data may not be readily available, generic component capacity data are commonly used. Generic-Equipment-Ruggedness-Spectra (GERS) are available for various electrical components and relays in EPRI NP-5223 and EPRI NP-7147 [Merz, 1991a, b]. In addition, HCLPF capacity data for various electrical components and relays is presented in NUREG/CR-4659 Vols. 1-4 [Bandyopadhyay and Hofmayer, 1986, Bandyopadhyay, et. al. 1987, 1990, 1991], NUREG/CR-4900 [Holman, et. al. 1987], and NUREG/CR-5470 [Tsai, et. al. [1989]. For many Central and Eastern U.S. (CEUS) SPRAs, the seismic fragilities of less critical components have been based on the HCLPF screening levels described in EPRI NP-6041-SL [1991].

The GERS, HCLPF, and HCLPF screening level data presented in the above references is all based on pre-1990 vintage components. The applicability of this data for modern components will depend upon the amount of changes that have occurred for any particular component class since 1990. More recently, EPRI TR-016780 [1999] presents “achievable” fragilities proposed to be used for preliminary analyses for modern advanced light water reactor (ALWR) seismic evaluations. However, they need to be verified by qualification tests before being used for any SPRA preceding fuel load.

Albeit the amount of the generic fragility data is large, it has been extremely rare, except perhaps in the case of relays, that fragility data is directly obtained from full-scale tests of equipment under seismic excitations that greatly exceed the design basis earthquake. In the equipment qualification tests, from which some high quality equipment fragilities have been derived, the input seismic waves are only at or slightly higher than the design basis earthquake. The prohibitive cost associated with full-scale seismic fragility tests is the major reason for the unavailability of high excitation level test-based fragility data. Nevertheless, the need to obtain the realistic (true) seismic equipment fragility capacities remains obvious so as to achieve higher quality SPRAs and consequently better risk management in NPPs in the U.S. and other countries.

As a very comprehensive and conscientious effort to fulfill such a need, a multi-year seismic equipment fragility test program is currently being carried out by the Japan Nuclear Energy Safety Organization (JNES) to obtain realistic equipment fragility capacities for use in SPRAs of nuclear power plants (NPPs) in Japan. The JNES equipment fragility test program started in 2002 and is planned to continue until 2012. The purpose of this test program is to improve the quality of the seismic fragility capacity database by determining realistic equipment fragility capacities from full-scale shaking table tests, and consequently to allow more accurate SPRAs to be performed to quantify the risk of NPPs during beyond-design-basis earthquakes. In contrast to the equipment qualification tests by vendors and some earlier design-proving tests performed by the Nuclear Power Engineering Corporation (NUPEC, Japan), in which the intent was to demonstrate the success of equipment under design basis or slightly larger earthquakes, the equipment fragility tests performed by JNES are aimed at determining the (ultimate) seismic capacity under beyond-design-basis earthquakes.

The JNES equipment fragility test program consists of tests of a series of important equipment that were determined in an SPRA to be safety significant according to their effect on core damage frequency. The selected test equipment were typical for boiling water reactor (BWR) and pressurized water reactor (PWR) plants in Japan. The test program for the selected equipment was scheduled in two phases. The phase I test program includes large horizontal shaft pumps, large size vertical shaft pumps, electrical panels, and control rod insertion capability. The phase II test program includes fans, valves, tanks, support structures, and overhead cranes. The fragility capacities of the tested equipment were developed based on the full-scale test results, element tests, and analyses. The JNES fragility evaluation considered both structural and functional limit states.

As part of collaborative efforts between the United States and Japan on seismic issues, the U.S. Nuclear Regulatory Commission (NRC) and Brookhaven National Laboratory (BNL) participated in this program by evaluating the results of the JNES equipment fragility test. The goal of this research effort was to compare the JNES fragility results with the fragility data typically used in current U.S. SPRAs and to assess the impact that the new test results may have on current SPRAs and how this data can be utilized for future SPRAs. The JNES fragility results are also useful for seismic margin analyses (SMAs), which are important in design certification (DC) or combined license (COL) applications because of the lack of full SPRAs at the DC or COL stage. All of the test results and information about the test equipment included in this report were provided by JNES to NRC/BNL. The unique advantage of this particular collaborative effort is obvious because of the rareness of full-scale, high-level seismic equipment fragility data.

This report summarizes the BNL evaluation of the JNES Phase I equipment fragility test data and provides the insights on the applicability and application of this data in the U.S. SPRA practices. Following this introduction, Section 2 presents a brief discussion of the current U.S. SPRA practices and in particular, the generic fragility data and screening levels as described in the references introduced in this section. Section 3 summarizes the JNES equipment fragility test program, fragility evaluation procedures, full-scale and element tests, and equipment fragility data, based on the JNES equipment fragility report 08TAIHATV-0027 [JNES, 2009] and other references provided by JNES. The JNES equipment fragility report 08TAIHATV-0027 is reproduced as Appendix A to this report for completeness of the fragility data presentation in this report. Appendix B describes the test response spectra for the electrical panel fragility tests. Section 4 describes a detailed evaluation of the JNES equipment fragility data and whether and how this data can be applied to the U.S. SPRA practices. The major insights obtained from this evaluation are summarized in Section 5.

It should be emphasized that the fragility data from the JNES equipment fragility tests, as well as from the equipment qualification tests, generic data, or screening levels, must be supplemented with an analysis of the component anchorage and support fragility. About half the time the overall component fragility is governed by anchorage or support capacity.

The details of the results of the JNES phase II tests are still being provided to NRC/BNL. When this transfer of information is complete, a supplement to this report will be prepared to address additional classes of equipment.

2 COMMON U.S. PRACTICE FOR ESTIMATING SEISMIC FRAGILITIES OF EQUIPMENT QUALIFIED BY TEST

2.1 Introduction

Within the U.S. practice for components qualified by test, component seismic fragilities are generally defined in terms of a 5% damped spectral acceleration SA for a broad frequency Test Response Spectrum (TRS). In a fragility analysis, this component fragility is defined in terms of a median $SA_{50\%}$ and randomness β_r and uncertainty β_u natural logarithm standard deviations (approximate coefficient of variations). In a seismic margin analysis, the component fragility is defined in terms of a conservatively biased High-Confidence-Low-Probability-of-Failure Capacity (HCLPF) SA_{HCLPF} equivalent to about a 1% non-exceedance probability capacity $SA_{1\%}$.

Guidance on estimating $SA_{50\%}$, β_r , and β_u are given on Pages 3-57 through 3-70 of EPRI TR-103959 [Reed and Kennedy 1994], whereas guidance on estimating SA_{HCLPF} are given in Appendix Q of EPRI NP-6041-SL [1991] for various types of available test data. This guidance will be briefly summarized in Section 2.2.

To define the fragility of the most critical equipment items qualified by test, it is preferable to start from the highest component specific qualification test data available for the specific equipment item. However, this information may not be readily available. In that situation, generic component capacity data is commonly used. Generic-Equipment-Ruggedness-Spectra (GERS) are available for various electrical components and relays in EPRI NP-5223 and EPRI NP-7147 [Merz, 1991a, b]. In addition, HCLPF capacity data for various electrical components and relays is presented in NUREG/CR-4659 Vols. 1-4 by Bandyopadhyay and Hofmayer [1986] and Bandyopadhyay, et. al. [1987, 1990, 1991], NUREG/CR-4900 by Holman, et. al. [1987], and NUREG/CR-5470 by Tsai, et. al. [1989]. These EPRI reports and NUREG/CR reports represent the generally available U.S. data base for generic fragilities.

For many Central and Eastern U.S. (CEUS) seismic probabilistic risk assessments (SPRAs), the seismic fragilities of less critical components have been based on the HCLPF screening levels SA_{SL} presented in Table 2-4 of EPRI NP-6041-SL [1991]. The use of these screening levels will be discussed in Section 2.3.

The GERS, HCLPF, and screening level data presented in the above references is all based on pre-1990 vintage components. The applicability of this data for modern components will depend upon the amount of changes that have occurred for any particular component class since 1990. Electrical component fragilities based on these references will be presented in the next two sections.

EPRI TR-016780 [1999] presents “achievable” fragilities proposed to be used for preliminary analyses for modern advanced light water reactor (ALWR) seismic evaluations. The basis for these fragility values could not be located during the course of this study. In any regard, they need to be verified by qualification tests before being used for any SPRA preceding fuel load. Electrical component fragilities based on EPRI TR-016780 will be presented in Section 2.4, and will be compared with fragilities based on GERS, HCLPF, and screening levels data as previously described.

Lastly, for equipment qualified by test, the fragility obtained from qualification test, generic data, or screening levels must be supplemented with an analysis of the component anchorage and

support fragility. About half the time the overall component fragility is governed by anchorage or support capacity.

2.2 Equipment Fragilities Based on Generic Data

EPRI TR-103959 [1994] recommends median factor $F_{D,50\%}$ and variabilities β_r and β_u to be used to convert qualification test, GERS, and HCLPF capacities into fragility estimates for a component, as shown in Table 2-1. The factors given in Table 2-1 depend on the operational requirements (i.e., “function during” or “function after”) and the physical results of the test (i.e., anomalies or no anomalies). If structural anomalies such as weld cracking, sheet metal tearing, screw pull out, local cabinet distortion, etc. are found, then the fragility analyst will have to use judgment to estimate how much higher the motion could be raised above the test level before damage is severe enough to cause the cabinet function to fail.

“Function during” fragilities are fragilities associated with a device within the equipment being able to appropriately change state during seismic shaking and are commonly associated with relay chatter or breaker trip during seismic shaking. “Function after” fragilities are fragilities associated with devices being capable of functioning properly after the strong shaking has ended. These “function after” fragilities are based on an unacceptable level of structural damage occurring to the device or cabinet. Their usage in an SPRA is conditioned on assuming that an operator can recover from an inappropriate change of state during seismic shaking.

Example electrical equipment fragilities based on GERS capacities [Merz, 1991a] are shown in Table 2-2 based on the $F_{D,50\%}$, β_r , and β_u values shown in Table 2-1. Specific caveats and checklist issues are listed in EPRI NP-5223 [Merz, 1991a] for use of these GERS capacities. Confirmation of compliance with these caveats and checklist issues need to be confirmed before using the generic fragilities. Two GERS capacities are reported for both low voltage and metal clad switchgear depending upon the degree of restraint provided for the breakers within the switchgear. The GERS based fragilities in Table 2-2 are shown for the purpose of comparison against fragilities reported by JNES for electrical equipment based on high amplitude shake table testing of Japanese equipment. This comparison will be made in Section 4.2 of this report.

Except as specifically noted in EPRI NP-5223 caveats, the GERS based fragilities are “function during” fragilities that include consideration of functionality of typical components within the relevant equipment classifications. However, to use these GERS based fragilities as “function during” fragilities, the analyst must confirm the lack of weak elements with the component.

The GERS based fragilities tend to be applicable only for the weakest tested equipment in the generic equipment class. Therefore, they are likely to be very conservatively biased for the majority of equipment in the generic equipment class. Typically, higher fragility estimates can be obtained using component specific test data.

“Function during” fragilities of electrical components are generally confirmed based upon element testing of the individual devices such as relays mounted within the electrical component. Relay specific test data can be obtained from testing conducted in accordance with IEEE C37.98 [1984]. For many relays, data is available in EPRI NP-7147 and NUREG/CR-4659. Table 2-1 provides recommended $F_{D,50\%}$, β_r , and β_u values to be applied to capacity data from these sources. The resulting device median fragility $SA_{D,50\%}$ is applicable for broad frequency input motion at the device. To obtain $SA_{50\%}$ at the base of cabinet, the device fragility must be divided by an appropriate cabinet amplification factor AF_C , i.e.:

$$SA_{50\%} = \frac{SA_{D,50\%}}{AF_{C,50\%}} \quad (2-1)$$

where $AF_{C,50\%}$ is the median value of AF_C .

The overall random variability β_r and β_u for this device fragility at the base of the cabinet are given by:

$$\beta_r = \sqrt{\beta_{r,D}^2 + \beta_{r,AF}^2} \quad (2-2)$$

$$\beta_u = \sqrt{\beta_{u,D}^2 + \beta_{u,AF}^2} \quad (2-3)$$

where $\beta_{r,D}$ and $\beta_{u,D}$ are device capacity variabilities from Table 2-1, and $\beta_{r,AF}$ and $\beta_{u,AF}$ are cabinet amplification factor variabilities. The resulting composite variability β_c is given by:

$$\beta_c = \sqrt{\beta_r^2 + \beta_u^2} \quad (2-4)$$

Cabinet amplification factor median, variability, and uncertainty values are recommended in EPRI TR-103959 [1994], as shown in Table 2-3. These recommended amplification factors were determined at the worst location using 5%-damped response spectra. As an example, Table 2-4 reports the estimated “function during” fragility for a pneumatic timing type auxiliary relay mounted on a panel in a 15 Hz control cabinet based on the relay GERS value from Page B-9 of EPRI NP-7147 [Merz, 1991b] and Table 2-1 and Table 2-3.

2.3 Equipment Fragilities Based on HCLPF Screening Levels

As previously noted, many CEUS SPRAs have used generic fragilities for less critical components based on HCLPF screening levels from EPRI NP-6041-SL [1991] in lieu of obtaining the highest available component specific qualification test data. This approach should not be used for higher seismic sites, or for components whose fragility significantly influences the reported seismic risk. However, currently, this seems to be a common practice. It should be noted that these HCLPF screening level based fragilities are only appropriate for “function after” fragilities since they don’t consider the ability of elements to properly function during strong shaking. Lastly, separate fragilities must also be computed for anchorage and component supports. Often these anchorage and support fragilities govern.

The screening level HCLPF capacities shown in Table 2-4 of EPRI NP-6041-SL [1991] are defined in terms of a broad frequency 5% damped spectral acceleration SA , and the following two screening levels are defined in that table:

$$SA_{SL} = 0.8g$$

$$SA_{SL} = 1.2g$$

Most components satisfy the conditions for the use of the $SA_{SL}=1.2g$ screening level.

Practice has varied concerning the development of fragility median values and composite β_c estimates based on these SA_{SL} screening levels. The following approach is recommended by the authors.

The component screening levels presented in Table 2-4 of EPRI NP-6041-SL were primarily developed by Campbell, Reed, and Kennedy based on the consideration of a diverse body of information summarized in Appendix A of EPRI NP-6041-SL. These component screening levels were defined in terms of the peak 5% damped spectral acceleration at the ground (SAG) instead of the peak 5% damped spectral acceleration (SA) at the base of the component. Most of the data base summarized in Appendix A of EPRI NP-6041-SL was reported in terms of ground motion instead of in-structure response spectra (ISRS). Furthermore, it was judged that realistic median ISRS might not exist in many cases where these component screening levels might be used. However, footnote (y) in Table 2-4 of EPRI NP-6041-SL cautions against the use of the SAG screening level for situations where the SA level from realistic ISRS exceeds $1.67 \cdot SAG$ (i.e. SA exceeds $2.0g$ for SAG of $1.2g$)

Furthermore, each component category in Table 2-4 of EPRI NP-6041-SL represents a broad diverse group of components from multiple manufacturers. For each diverse group, no “function after” failures have been observed below the screening level SA_{SL} and numerous successes have been observed for ground motions significantly exceeding SA_{SL} . Thus, for individual components within these broad diverse component class, it is recommended to use a composite variability β_c in the range of 0.4 to 0.5. Using a generic estimate for β_c of 0.45 for individual components:

$$\text{Median/HCLPF} = \exp[2.326(0.45)] = 2.85$$

Thus, for individual components:

$$\begin{aligned} SAG_{50\%} &= 2.85 SA_{SL} \\ \beta_c &= \beta_{SAG} = 0.45 \\ SAG_{HCLPF} &= SA_{SL} \end{aligned} \quad (2-5)$$

is appropriate.

The screening tables are in terms of ground motion SAG . Both the earthquake experience data and the past SPRA fragility data used to develop these screening tables are in terms of ground motion. The amplification factor AF and its variability β_{AF} are automatically embedded in these HCLPF screening levels and the overall β_{SAG} estimate. It is necessary to remove these amplification factor effects from the screening table data so as to have generic fragilities defined at the base of the component instead of at the ground. EPRI 1019200 [2009] Appendix B recommends an approach for estimating HCLPF and generic fragility levels for individual components in terms of SA at the base of the component from the screening level SA_{SL} given in Table 2-4 of EPRI NP-6041-SL. This approach is based on the following estimates of the median amplification factor $AF_{50\%}$ and its logarithmic standard deviation β_{AF} for the experience data:

$$AF_{50\%} = 1.4 \quad (2-6)$$

$$\beta_{AF} = 0.17 \quad (2-7)$$

The median $SA_{50\%}$, variability β_{SA} , and SA_{HCLPF} in terms of the ISRS SA for an individual component can then be estimated by:

$$SA_{50\%} = AF_{50\%} \cdot SAG_{50\%} = 4.0 SA_{SL} \quad (2-8)$$

$$\beta_{SA} = \sqrt{\beta_{SAG}^2 - \beta_{AF}^2} = 0.42 \quad (2-9)$$

$$SA_{HCLPF} = SA_{50\%} \cdot \exp(-2.326\beta_{SA}) = 1.5 SA_{SL} \quad (2-10)$$

since β_{AF} is included as part of the β_{SAG} estimate. Thus, for $SA_{SL}=1.2g$, the corresponding SA_{HCLPF} is reasonably estimated to be 1.8g. Table 2-5 shows the resulting recommended “function after” spectral acceleration SA fragilities in terms of motion at the component base. These screening level based generic fragilities shown in Table 2-5 will be compared with the JNES results in Section 4 of this report.

2.4 Advanced Light Water Reactor “Achievable” Fragilities

EPRI TR-016780 [1999] provides median “achievable” fragilities in terms of a broad frequency 5% damped spectral acceleration at the ground, $SAG_{50\%}$ and a corresponding composite β_{SAG} . In order to estimate fragility levels for individual components in terms of SA at the base of the component, the $AF_{50\%}$ and β_{AF} corrections shown in Equations 2-6 through 2-10 need to be applied. Table 2-6 shows representative natural frequencies and “achievable” fragilities for electrical components based on EPRI TR-016780.

2.5 Comparison of Generic Fragility Estimates

Table 2-7 compares generic fragilities for electrical components based on several data sources. Electrical component fragilities based on GERS [Merz, 1991a] and on screening levels [EPRI NP-6041-SL, 1991] are reasonably consistent with each other. However, these fragilities are based on data for pre-1990 vintage components. The ALWR “achievable” fragilities from EPRI TR-016780 are intended for preliminary evaluations for modern components. These fragility levels are about twice the GERS and screening level based fragilities. The basis for this increase could not be located during this study. As shown in Section 4, the JNES test data median fragility levels for electrical components are comparable to the ALWR “achievable” fragilities. However, all of the electrical components tested by JNES were very stiff and not representative of most similar existing electrical components in U.S. plants. Therefore, the use of the ALWR “achievable” fragilities requires verification by means of qualification tests.

Table 2-1 Device Capacity Factors

Data Source	$F_{D,50\%}$	β_r	β_u	$F_{D,HCLPF}$
HCLPF Capacities (NUREG/CR-4659 and NUREG/CR-4900)	1.75	0.11	0.23	1.0
GERS – Non relay (EPRI NP-5223)	1.45	0.11	0.23	0.83
GERS – Relay (EPRI NP-7147)	1.07	0.09	0.18	0.69
IEEE C37.98 – Relay Fragility	1.5	0.09	0.18	0.96
Qualification Test Function During	1.4	0.09	0.22	0.84
Function After (no anomalies)	1.95	0.09	0.28	1.06
Function After (anomalies)	1.1 – 1.65	0.09	0.28	0.6 – 0.9

Table 2-2 Estimated Generic Fragilities for Electrical Equipment

Component	5% Damped Spectral Acceleration Capacity SA (g)					
	GERS	$SA_{50\%}$	β_r	β_u	β_c	SA_{HCLPF}
Distribution Panels						
Floor Mounted	3.5	5.1	0.11	0.23	0.25	2.9
Wall Mounted	2.5	3.6	0.11	0.23	0.25	2.1
Motor Control Centers						
“Function After”	2.5	3.6	0.11	0.23	0.25	2.1
“Function During”	1.5	2.2	0.11	0.23	0.25	1.25
Switchgear						
Low Voltage	1.8 – 2.5	2.6 – 3.6	0.11	0.23	0.25	1.5 – 2.1
Metal Clad	1.8 – 2.5	2.6 – 3.6	0.11	0.23	0.25	1.5 – 2.1

Table 2-3 Cabinet Amplification Factors

Cabinet Types	AF_C		
	Median	β_r	β_u
Motor Control Center	2.8	0.10	0.23
Switchgear (flexible panels)	4.4	0.13	0.37
Control Room Electrical Benchboards and Panels (with frequency ≥ 13 Hz)	3.3	0.11	0.27

Table 2-4 “Function During” Spectral Acceleration SA Fragility for Pneumatic Timing Type Auxiliary Relay Panel Mounted in 15 Hz Control Cabinet

(Median $AF_C = 3.3$, $\beta_{r,AF} = 0.11$, $\beta_{u,AF} = 0.27$)

GERS SA_{GERS} (g)	Device Location			Cabinet Base				
	$SA_{D,50\%}$ (g)	$\beta_{r,D}$	$\beta_{u,D}$	$SA_{50\%}$ (g)	β_r	β_u	β_c	SA_{HCLPF} (g)
10.0	10.7	0.09	0.18	3.2	0.14	0.32	0.35	1.5

Table 2-5 Generic “Function After” Spectral Acceleration SA Fragility Levels in Terms of Component Input Motion Based on Screening Levels

Screening Level SA_{SL} (g)	Component Fragility Cabinet Base		
	Median $SA_{50\%}$ (g)	Composite Variability β_c	SA_{HCLPF} (g)
0.8	3.2	0.42	1.2
1.2	4.8	0.42	1.8

Table 2-6 “Function During Achievable” Spectral Acceleration

Component	Natural Frequency (Hz)	Ground Motion		Cabinet Base		
		$SAG_{50\%}$ (g)	β_{SAG}	$SA_{50\%}$ (g)	β_{SA}	SA_{HCLPF} (g)
Panel boards and Instrumentation Panels	5-10	7.0	0.46	9.8	0.43	3.6
Switchgear and Motor Control Centers	4-12	5.9	0.46	8.3	0.43	3.1

Table 2-7 Comparison of Generic Fragilities for Typical Electrical Cabinets

	GERS (Function During)	Screening Levels (Function After)	ALWR Achievable (Function During)
$SA_{50\%}$ (g)	2.2-5.1	3.2-4.8	8.3-9.8
β_{SA}	0.25	0.42	0.43
SA_{HCLPF} (g)	1.25-2.9	1.2-1.8	3.1-3.6

3 JNES EQUIPMENT FRAGILITY TESTS

3.1 Overview of the JNES Equipment Fragility Test Program

Japan Nuclear Energy Safety Organization (JNES) is carrying out a multi-year equipment fragility test program to obtain realistic equipment fragility capacities for use in the seismic probabilistic risk assessments (SPRAs) of nuclear power plants (NPPs) in Japan. As shown in Figure 3-1, the JNES equipment fragility test program started in 2002 and continued through 2009. Additional tests are planned during the period of 2009 to 2012. The purpose of this test program is to improve the quality of seismic fragility capacity database by determining realistic equipment fragility capacities from full-scale shaking table tests, and consequently to allow more accurate SPRAs to be performed to quantify the risk of NPPs during beyond-design-basis earthquakes.

This test program reflects a philosophical shift from the design-proving test in the past that was intended to demonstrate the success of equipment under design basis or slightly larger earthquakes, to the current fragility test that determines the (ultimate) seismic capacity under beyond-design-basis earthquakes. In the past, equipment fragility data were mostly not obtained from full-scale high level shaking tests, but, for example, by scaling equipment qualification test data or by converting from screening levels as described in Section 2. The true (realistic) equipment seismic fragility capacities have not been widely available because it is prohibitively costly to determine such capacities using high level shaking tests of full-scale equipment. Prior to the establishment of JNES, Nuclear Power Engineering Corporation (NUPEC, Japan) conducted multi-phase/multi-year proving tests of large structures, systems, and components (SSCs), but the shaking levels were not as great as the current JNES fragility tests (see Figure 3-1). The current fragility data used in the Japan SPRAs are either from Japanese lower level tests such as NUPEC tests or from the U.S. fragility databases. These fragility capacities are believed to be smaller than the actual values and accordingly the core damage frequency (CDF) may have been overestimated. The JNES equipment fragility tests were planned to identify the realistic seismic fragilities of important NPP equipment using high level shaking tests.

As stated above, a direct determination of median fragility capacity and the associated variation from full-scale tests is prohibitive. Therefore, in order for JNES to make the equipment fragility tests more achievable, element (device) tests, analyses, and use of some existing data are required along with the full-scale tests to establish the final fragility values. For each selected equipment category, only one or two representative full-scale equipment specimens were tested. The main purpose of the full-scale tests was to identify critical accelerations and failure modes of the equipment. The purpose of the element tests was to evaluate threshold acceleration of parts and median and deviation. The element tests were conducted with many samples, and therefore their median capacity and the associated variation were able to be determined statistically. For some cases, the variability was specified as those reported in the industry codes and standards. Based on the full-scale test results, analyses combined with element tests were performed to calculate the fragility capacities.

Some of the JNES equipment fragility tests were conducted at the TADOTSU shaking table of NUPEC. The TADOTSU shaking table has a plan dimension of 15 m × 15 m. Some of the test results were limited to the table capacity and therefore only function confirmed (FC) capacities were achieved. For some of the full-scale equipment tests and the element tests, higher acceleration input was required to identify their seismic fragility capacity. To this end, a vibration amplifying system was installed on top of the TADOTSU shaking table. Figure 3-2 illustrates how the amplification table was installed on top of the TADOTSU shaking table, also

showing an electrical panel sitting on top of the amplification table. The amplification table has a plan of 5 m × 5 m. The combined input acceleration capacity of the TADOTSU shaking table and the amplification table can reach about 6g around 10 Hz [Iijima, et al, 2004].

The input acceleration level was determined from JNES's sensitivity analysis of CDF. For example, it was shown in a preliminary SPRA that if the critical acceleration of a large horizontal shaft pump is higher than 4g or 5g, CDF was decreased by half. This finding was used to determine how much the capacity of the TADOTSU shaking table should be increased by an amplification table [Iijima, et al, 2004].

The JNES equipment fragility test program consists of a series of important equipment that were determined in a seismic probabilistic safety analysis (PSA) to be safety significant according to their effect on core damage frequency. More specifically, the F-V (Fussell-Vesely) importance measure was obtained in a preliminary seismic PSA performed by JNES and was used to select the safety significant equipment. The FV importance of a component is defined as the fraction that the baseline CDF would be reduced if the subject component was always available (with infinite high seismic fragility). Another criterion used for the equipment selection is that the equipment must be an active component, because the fragility of such active equipment is difficult to be estimated by analysis [Iijima, et al, 2004]. The test program for the selected equipment was scheduled in two phases, as shown in Figure 3-1. The phase I test program includes large horizontal shaft pumps, large vertical shaft pumps, electrical panels, and control rod insertion capability. The fragility data of the JNES phase I tests are documented in the JNES report 08TAIHATV-0027 [JNES, 2009], which is reproduced as Appendix A to this report for reference.

The JNES phase II test program includes fans, valves, tanks, support structures, and overhead cranes. The results of the JNES phase II tests were not yet available and will be evaluated and documented in the future once available.

The Phase I program was conducted from FY 2002 to 2005 (Japan). The fragility test equipment were typical for boiling water reactor (BWR) and pressure water reactor (PWR) plants in Japan. The phase I fragility test was conducted in three parts: Part 1 included the horizontal shaft pumps and electrical components, Part 2 included BWR and PWR equipment related to control rod inserting capacity, and Part 3 included large size vertical shaft pumps. Following these tests, a comprehensive evaluation was performed to produce the fragility data. During this comprehensive evaluation process, for electrical devices (elements) where an abnormality occurred at relatively low acceleration, some additional tests were performed after improvement was implemented to the devices. Fragility data were also developed using the test results of the improved devices. It should be pointed out that Appendix A of this report was prepared by JNES and is an English translation of the Chapter IV, "Development of Fragility Data," of the JNES comprehensive evaluation report.

Two limit states were considered for the fragility analysis for the Phase I equipment: (1) structural damage should not occur; (2) loss of active function should not occur during earthquake. Examples of active function include rotation for horizontal and vertical pumps, electrical state change for electrical components, and control rod insertion.

The JNES fragility report 08TAIHATV-0027 [JNES, 2009] presents the fragility capacities in terms of the maximum input acceleration (zero period acceleration, or ZPA), response accelerations or displacements, or a set of response multiplying factors with respect to input motion. As noted in the same report, response of equipment depends on the dynamic

characteristics of the equipment and the supporting structure as well as the earthquake condition at any particular site. More rigorous fragility capacity can be determined by using site-specific earthquake conditions.

The JNES fragility report 08TAIHATV-0027 [JNES, 2009] does not include test response spectra (TRS) associated with the ZPA fragilities. TRS for some tests were later provided by JNES separately using several JNES fragility reports in Japanese with English annotations. In general, these TRS are fairly narrow banded spectra developed for 1%, 4%, or 5% damping ratios, in contrast to the broad-frequency 5% damping response spectra typically used in U.S. qualification tests. The JNES TRS are representative of in-structure response spectra in Japanese NPPs, with many of the input spectra peaking in a frequency range of 7-10 Hz and containing little frequency content above about 12 Hz.

The 1% or 4% damping TRS may be converted to 5% damping TRS using appropriate methods, e.g., the random vibration methods or the empirical methods provided in NUREG/CR-6728 [McGuire, et al, 2001], if a direct assessment is needed for the applicability of these TRS in U.S. SPRAs. However, the accuracy of these methods must be evaluated and any potential bias induced by using these methods must be considered in the TRS-based fragility comparison.

The response spectra shown later in this section and in Appendix B were extracted from the annotated JNES fragility reports. The relevant legend and labels are created based on the annotations. The unit for the spectral acceleration may be in g, gal (cm/s^2), or m/s^2 , following the same convention as in the JNES fragility reports. Similarly, the horizontal axis can be in period (s) or in frequency (Hz).

This section provides a summary of the JNES phase I test program, based on various JNES presentations [e.g., Uchiyama, 2008a, b], the JNES equipment fragility report 08TAIHATV-0027 [JNES, 2009], and the annotated JNES fragility reports in Japanese. The fragility capacities are mostly described in this section in terms of input ZPA and peak response acceleration and/or displacement at critical locations, following the convention in the JNES report 08TAIHATV-0027. Whenever available and appropriate, the TRS associated with these fragility capacities are also documented in this section. Some more detailed TRS are documented in Appendix B particularly for electrical panels and devices, as more TRS data are available for these tests.

An evaluation of the JNES equipment fragility data and assessment of the impact of these data on the U.S. SPRA practices is provided in Section 4.

3.2 Horizontal Shaft Pumps

3.2.1 Summary of Horizontal Shaft Pump Tests

3.2.1.1 Full Scale Test

Table 3-1 shows a list of common horizontal shaft pumps in Japan BWR and PWR NPPs. JNES preliminary PSA analysis showed that single stage pumps have high F-V importance values. A reactor building closed cooling water (RCW) pump used in Japan BWR plants was selected as a representative single stage horizontal shaft pump for full-scale test. This pump has a flow rate of $1250 \text{ m}^3/\text{h}$, a length of 2.8 m, and a height of 1.5 m; and weighs $5.7 \times 10^3 \text{ kg}$. Figure 3-3 shows the layout of the full-scale RCW pump test system, which included the RCW pump, an electric motor, piping, valves, a tank, and power cabinets. It should be noted that the RCW pump and the motor were installed on top of the amplification table while other test elements were sitting on top of the main shaking table.

A basis input acceleration time history was generated from an envelope floor response spectrum (FRS) that covers FRSs at floors where major horizontal shaft pumps were located in Japan BWR and PWR plants, as shown in Figure 3-4 and Figure 3-5. The duration of the input waves were about 36 seconds. The basis input motion was scaled to a peak acceleration of 1g. The damping ratio was chosen as 1% for FRS. This basis input acceleration time history was gradually scaled from 2g to 6g in the test. The pump was tested in axial and transverse directions for both operating and standby conditions.

No damage was found up to the maximum input acceleration level of 6g, and no obvious decrease of performance was observed as well in terms of flow rate and head [Iijima, et al, 2005]. The TRS at the top of the amplification table for the 2 g, 4 g, and 6 g excitation levels are shown in Figure 3-6. These TRS are for the axial direction; however, they are reported to be fundamentally the same in the radial direction. The damping ratio for these spectra is 1%. As shown in Figure 3-7, acceleration measured at the bearing case showed only a slight increase as the input acceleration increased, from a base-line rattling acceleration about 10 m/s² to 18 m/s² before application of the simulated seismic motion. Significant damage to surface roughness of the bearing was not found during the post-test check.

3.2.1.2 Element Tests

Bearings and liner rings from both single stage and multi-stage horizontal shaft pumps were selected for the element tests. Liner rings were reported to have lower seismic margin than other parts and can be damaged due to impact between liner rings and the impeller during transverse vibration. Although bearings generally have high seismic margin, they are selected because they are the very fundamental parts for the pump's rotational function. Tested bearings included radial and thrust bearings of ball and slide types. Figure 3-8 and Figure 3-9 show the test setups for radial ball bearings and thrust ball bearings, respectively. Table 3-2 shows the types of element in the tests and their size and the number of specimens. As indicated in the note to Table 3-2, a ball bearing type 6316 and 270 mm liner ring were used for the RCW pump.

Two types excitations were used in the test: sinusoidal excitation and simulated seismic wave excitation. The sinusoidal excitation test was for investigation of the dynamic properties of the parts under large input excitation, which were then used in dynamic analysis. The seismic wave excitation test was for determination of fragility capacity and failure mode. For the seismic motion test, the basis input acceleration time history for the element tests was the same as the one for the full-scale test. For the type 6310 thrust ball bearing, the maximum input load for the sinusoidal test was about 10 kN, which in the test was equivalent to an acceleration of 12g; and the maximum input load for the seismic wave excitation test was about 33 kN, which in the test was equivalent to an acceleration of 39g. Input loads for other types of pump parts can be found in Appendix A.

Rattling acceleration at the bearing significantly increased after a threshold input load, which was about 20 kN (equivalent to 20g) for bearing 6310. The surface roughness of balls and the internal surface ball/slide bearing were degraded after the test, as shown Figure 3-10. However, this damage was found not to be significant enough to present an immediate stop of the pump, but the damage could cause a reduction of pump life. No significant damage was found for the tested liner rings. It is important to note that the input loads were very large (exceeding 10g equivalent force) when the minor damage occurred.

3.2.2 Fragility Evaluation and Fragility Data

3.2.2.1 Fragility Evaluation for Active Function

Safety related pumps in NPPs are required to operate continuously for a certain period of time after an earthquake. Although the full-scale test of the RCW pump showed no abnormality of the pump function up to an input acceleration of 6g, the element tests did show that at very large input load some degradation of the parts could lead to reduction of pump bearing life. Therefore, the load that could cause the bearing life reduction was conservatively specified as the critical load of the bearing. For cases where no abnormality occurred in the element tests, the maximum input load in the element test was specified as the critical load. The critical loads of the bearing were used in nonlinear time history analysis of pump models to determine the fragility capacities. Figure 3-11 and Figure 3-12 show the axial and lateral analytical models for a single stage horizontal shaft pump and for a multi-stage horizontal shaft pump, respectively. The axial models were single mass models, with the nonlinear spring constant and the damping factor obtained from the element sinusoidal tests. The lateral models were multi-mass systems, with the nonlinear spring constants for the bearings and liner rings determined from the element tests. The pump casing was assumed rigid in the analysis. For the parts other than the bearings and liner rings, the damping ratio was specified as 1% in the seismic response analyses, in line with the damping factor recommendation by JEAG 4601, "Technical Guidelines for Seismic Design of Nuclear Power Plants."

Table 3-3 summarizes selected critical values of the JNES fragility evaluation of the horizontal shaft pumps. It should be noted that for slide bearing, the surface pressure-velocity (PV) critical values were used as indicators of the contact pressure limit of the slide bearing in the fragility evaluation.

The median fragility value for active function was specified as the critical acceleration calculated based on the above procedure. Based on the element tests, maximum logarithmic standard deviations of 0.21 for the deep groove ball bearing and 0.12 for the slide (radial) bearing were used to represent the uncertainties in the fragility values.

3.2.2.2 Fragility Evaluation for Structural Strength

A simple static analysis method was used for the limit state of structural strength. The seismic acceleration used in the static analysis was specified as 1.2 times the floor response acceleration. Foundation bolts and mounting bolts between the pump/motor and pump frame were reported to have the lowest seismic margins among structural members, and therefore were evaluated for fragility capacity based on the static analysis procedure in JEAG 4601-1991.

Pump/motor relative slip motion on the pump frame can cause abnormality in the pump rotational function. As it was difficult to perform a detailed analysis of this slip phenomenon, a simplified static analysis using frictional force was used to estimate the acceleration that caused the relative slip. As noted in Appendix A, because many uncertainties exist for the slip phenomenon, the acceleration so determined by JNES was termed "reference fragility." Slip was not reported in the full-scale test of the RCW pump, which was tested to accelerations slightly less than the "reference fragility."

In the fragility evaluation, as shown in Table 3-3, the critical tensile stress was set to $0.75S_u/\eta$, where S_u is the design tensile stress as specified in the Japan Society of Mechanical Engineers (JSME), "Standards for Nuclear Power Generation Equipment: Design and Construction Standards." The median capacity was obtained by considering a 0.75 factor for thread portion

and a confidence coefficient η . The critical shear stress was specified as $S_u/\sqrt{3}$. For evaluation of relative slip of motor and pump on the pump frame, tightening force and pump/motor weight were considered for the frictional capacity. The fragility was calculated by comparing the seismic load in the horizontal direction to the frictional capacity.

The calculated bolt strength and critical slip acceleration were specified as median fragility capacities. The logarithmic standard deviation β in bolt strength was calculated to be 0.07 by assuming $0.75S_u$ as 1% and $0.75S_u/0.856$ as the median ($\eta = 0.856$ for general steel materials).

3.2.2.3 Summary of Fragility Data

Before the JNES horizontal shaft pump test, the seismic fragility capacity of horizontal shaft pumps in previous SPRAs was 1.6g, which was developed from previous vibration tests [Iijima, et al, 2005]. The function confirmed capacity of the RCW pump is 6g, about 4 times of the previously determined value.

Table 3-4 shows a summary of fragility data for three horizontal shaft pumps. Besides the RCW pump in the full-scale test, a larger RCW pump and a charging/HP injection pump were studied. The larger RCW pump is about 3.72 m long and 1.59 m tall, and has a flow rate of 2050 m³/h. Its mass is about 8.2×10^3 kg. The charging/HP injection pump was of a multi-stage centrifugal type, with a length of 2.6 m, a height of 1.5 m, a flow rate of 34.1 m³/h or 147 m³/h depending on pump head, and a mass of 6.05×10^3 kg.

The minimum median fragility for the functional limit state is 8.4g, about more than 5 times of the previously used fragility value. The reference fragility for the motor slip is 2.6 g for the charging/HP injection pump, about half of the other two horizontal pumps. This reference fragility capacity appears to be controlling; however, as the level of uncertainty in this estimate is unknown, further investigation is required to justify its proper use.

Table 3-5 through Table 3-7 summarizes the fragility data for tested ball bearings, slide bearings, and liner rings. For some, only function confirmed values are available. The tabulated values are indexed by their part id or diameters.

3.3 Electrical Panels

3.3.1 Summary of Electrical Panel Tests

JNES performed tests on full-scale electrical panels that were of the same types as in Japan NPPs to investigate their critical acceleration and failure modes due to seismic accelerations. It also conducted tests on elements (devices) with multiple specimens to obtain the dispersion in addition to the threshold acceleration. The fragility data were developed using results of the full-scale tests, element tests, and analyses.

3.3.1.1 Full Scale Tests

Eight electrical panels were selected for the JNES full-scale tests:

- Main control board (BWR)
- Reactor auxiliary control board (PWR)
- Logic circuit control panel (BWR)
- Instrumentation rack (BWR)
- Reactor protection rack (PWR)

- Reactor control center (PWR)
- Power center (PWR)
- 6.9 kV Metal-clad switchgear (BWR)

Table 3-8 shows the properties of these eight electrical panels, including their dimensions, weight, and fundamental frequency. The frequency of these electrical panels was in a range of 21 Hz to 44 Hz. The fundamental frequency of each panel was identified on a resonance curve that was generated in the low-level random wave excitation test before the fragility test. Figure 3-14 shows the major features and dimensions of these electrical panels [Iijima, et al, 2007]. Figure 3-15 shows the electrical panels sitting on the amplification table.

Similar to the full-scale horizontal shaft pump test, a basis seismic input wave was generated for the full-scale electrical panel tests using an FRS that enveloped the design FRS of the main electrical panels. The duration of the input seismic waves were about 36 seconds, as shown in Figure 3-13. The JNES preliminary SPRA showed that a fragility capacity of 5g to 6g would decrease the CDF by half; therefore, the amplified TADOTSU shaking table with a total capacity of 6g was judged to be satisfactory. The electrical panels were shaken in both front-to-back and side-to-side directions. Each panel was tested in the simulated operating condition, with some being tested with smaller current for safety reasons.

The main control board, the instrumentation rack, the reactor auxiliary control board, and the logic circuit control panel maintained their function up to a maximum input acceleration of 6g. The other four panels lost their functions during the test; the failure mode and the critical acceleration are summarized in the following:

Reactor control center: at an input acceleration of 6.1g in the front-back direction, chatter of auxiliary relays caused an error in the magnetic contactor. Figure 3-16 shows a comparison of the target response spectra and the response at the base plate for a 6 g level front back excitation in the reactor control center test. A 4% damping ratio was used for these spectra and all other response spectra for the electrical panel and device tests. The various levels of excitations were achieved in the JNES equipment fragility tests by scaling basis input motions. Therefore, a particular response spectrum at the base plate shows the characteristics of the frequency contents of the input motion but may not directly relate to the critical failure acceleration. Appendix B provides all available response spectra for the electrical panel and device tests.

Reactor protection rack: at an input acceleration of 4.3g in the side-side direction, chatter of miniature relays on the AC controller caused the malfunction of the panel.

Power center: at an input acceleration of 3.7g in the front-back direction, unexpected vibration of a manual close button caused an air circuit breaker to abnormally close. At a higher acceleration of 5g in the front-back direction, structural damage of the air circuit breaker occurred.

6.9 kV Metal-Clad Switchgear: at an input acceleration of 2.5g in the front-back direction, malfunction of a grounded potential transformer (GPT) occurred when the fuses fell out. At a higher acceleration of 4.1g in the side-side direction, structural damage of a vacuum breaker occurred.

For these loss-of-function cases, error or damage of electrical parts that caused the malfunction of the panels occurred before any damage to the panel structures.

3.3.1.2 Element (Device) Tests

For element tests, JNES selected more than 30 different types of electrical parts (devices) from an initial list of about 300 devices, considering their potential weakness under seismic motion. Table 3-9 lists the different types of devices in the element test, including the number of specimens. This table also includes four types of additional element tests of grounded potential transformer and breakers, as they failed in the full-scale panel tests at relatively low level excitation. In the additional test, the fuse that fell out from the grounded potential transformer in the full-scale test was improved by installing a fuse slide stopper. As shown in Figure 3-17, the parts were installed on a support frame that was attached to the shaking table. The support frame was intended to simulate the electrical panels. The installation of the parts in the element test was the same as in the panels, for example, using the same number and size of bolts.

Seismic waves for the element tests were generated from response analyses of the panels, in order to reflect the dynamic characteristics of the panels and the position of the devices in the panels. Therefore, the input waves for the element tests were different from each other. The devices were tested in both front-to-back and side-to-side directions, with the input maximum acceleration increased gradually from design level to about 10g. The TRS for the devices listed in Table 3-9 are shown in Appendix B.

Failure of a device during the shaking test occurred when the device could not maintain its normal function. For relays, their failure was defined as a chattering time longer than 2 ms according to the IEEE standard.

The input acceleration to the parts was measured at the mounting position. Most of the tested devices performed normally up to the maximum input accelerations, which were mostly about 10g, as shown in Table 3-9. Malfunction occurred for eight types of devices during the test, which include:

- 1 protection relay
- 1 auxiliary relay
- 1 AC controller card
- 2 air circuit breakers
- 1 vacuum circuit breaker
- 1 gas circuit breaker
- 1 grounded potential transformer

The critical acceleration for the devices that malfunctioned was as low as 2.5g. Some simple reinforcement to the devices that malfunctioned can greatly increase the seismic capacity as shown in Table 3-9. For example, the original GPT failed at an acceleration of 2.5g in the front-back direction, while the improved GPT reached an acceleration of 9.4g without evidence of malfunction.

3.3.2 Fragility Evaluation and Fragility Data

The fragility data of the 8 tested panels can be directly applied to those installed in current NPPs. However, as there are many more panels in NPPs that may not have similar configurations to those of the tested panels, JNES suggested an analytical method to compute the fragility of a panel based on the fragility data from the element tests. The full-scale panel tests showed that the malfunction of electrical parts, not the damage of the panel structure, caused the malfunction of the panels. The method includes four steps: (1) determine through analysis (e.g. finite element analysis) the amplification factor (AF_i) of the panel at the location of a device i ; (2) determine the

fragility capacity of the device f_{Di} , from the JNES device fragility database or from test if not available in the database; (3) the corresponding panel fragility f_{Pi} for the subject device i can be determined as $f_{Pi} = f_{Di}/AF_i$; and (4) find the minimum of f_{Pi} among all major devices in the panel.

Although structural strength is not controlling, the fragility capacity associated with the limit state of structural strength was also calculated using response spectrum analysis. The panel anchor bolts and housing structure were considered in the stress evaluation to determine the structural fragility capacity. The median tensile stress is defined as S_u/η , where $\eta = 0.856$ for general steel and S_u is the design tensile stress as specified in JSME “Standards for Nuclear Power Generation Equipment: Design and Construction Standards.”

The dispersion of an electrical component was assumed to take the dispersion of either the critical acceleration of electrical parts or critical stress of structural members, depending on which dominates the fragility capacity of the panel.

Table 3-9 also shows fragility data for those devices where malfunction occurred during the test, along with maximum input accelerations in the test for devices that did not lose their function. Appendix A provides fragility data for all devices. For cases where loss of function occurred, the fragility level was the average of the input acceleration at which loss-of-function occurred and the highest input acceleration when the function was maintained. For cases where no loss of function occurred, the fragility level was the average of the maximum input acceleration in the test and the assumed next step input acceleration at which loss-of-function was assumed.

Table 3-10 shows the seismic capacity determined from the full scale test for the electrical panels, as either function confirmed if no abnormality occurred or the critical acceleration at which abnormality occurred. Table 3-10 also presents the fragility data from analysis for functional and structural limit states. It can be seen that structural fragility capacities are generally much greater than the functional fragility capacities. For panels that did not fail in the full-scale test, the tabulated fragility from analysis is conservative, because the fragilities of the electrical parts were assumed to be the maximum input acceleration in the element test. For the power center and the 6.9 kV metal-clad switchgear, the fragilities (4.4g and 4.2 g, respectively) were estimated using the improved air circuit breaker and the improved GPT, respectively; therefore, the fragility capacities are higher than the loss of function accelerations (3.72 g and 2.52 g) in the full-scale test. For the reactor protection rack, the estimated fragility capacity (4.4 g) is very close to the loss of function acceleration (4.3 g) determined in the full-scale test. For the reactor control center, the fragility capacity was calculated to be 4.5 g based on the function critical acceleration of an auxiliary relay and the actual amplification factor at the mounting position of this auxiliary relay. It should be noted that the full-scale fragility test of this reactor control center reached an input acceleration of 6.12 g to generate abnormality. The reported smaller fragility capacity of this reactor control center was conservative. This difference may also be used to assess the level of uncertainty associated with the reported fragility capacity and in general with the hybrid experimental/analytical approach to derive the fragility capacities, although the reported uncertainties are generally very small in the JNES fragility report.

From earlier NUPEC vibration tests, JNES estimated the previous seismic fragility to be 3.6g, which had been applied uniformly to all electrical panels in Japan NPPs [Iijima, et al, 2007, Fujita, et al, 1997]. All estimated fragility capacities, using improved parts in two cases, are greater than 3.6 g. However, it should be noted that without improvement to the GPT, the 6.9 kV metal-clad switchgear had a loss of function acceleration of 2.52 g in the full-scale test, which is smaller than the estimated fragility (3.6g) based on the earlier NUPEC tests.

3.4 Control Rod Insertion Capability

The JNES control rod insertion capability tests included full size mockup specimens for PWR and BWR systems. The purpose of the tests was to examine the functional fragility of PWR and BWR control rod insertion systems during strong seismic motions that exceed the design level, to develop fragility evaluation methodology, and to establish a fragility database for PWR and BWR control rod insertion systems [Inagki, et al, 2006]. Figure 3-18 shows the target range of the fragility tests in terms of the insertion period versus the displacement response of the fuel assembly, showing a significant increase of displacement response compared to previous NUPEC tests.

A summary of the JNES tests will be presented separately for the PWR and BWR control rod insertion systems in the following subsections.

3.4.1 PWR Control Rod Insertion Capability

3.4.1.1 Full Scale Test

Figure 3-19 through Figure 3-22 show the test setup for the PWR control rod insertion capacity test, the mockup of a PWR fuel assembly, a section view of the test setup, and a plan view of the three fuel assemblies including the control rod, respectively. The main test components such as the fuel assemblies, control rod, and control rod drive mechanism (CRDM) were all manufactured with the same specification as in representative 3/4 loop PWR plants except for the material of the fuel pellets. The fuel assembly is 17×17 type. As shown in Figure 3-21, the test specimen stands above the top of the shaking table for 10 m (mainly the CRDM) and below the table for 6.3 m (mainly the fuel assemblies and control rod). The fuel assemblies and the control rod were enclosed in a cylindrical vessel, which was supported by tie rods connecting to a very sturdy frame above the shaking table and to the shaking table under the table. A pump flow loop was installed for the investigation of the effect of core flow on the control rod insertion.

Seismic input motion was generated based on a survey of Japanese PWR plant design conditions and a preliminary seismic analysis of the main test components. Input motion was controlled at the top of the shaking table. The magnitude of the input seismic motion was up to $3.3 \times S_2$, which is the extreme design earthquake ground motion in Japan. The maximum input acceleration in the JNES test was about 3.2 g, while it was 1.1 g in a similar earlier NUPEC test.

Figure 3-23 shows the response spectrum of the synthesized S_2 level input motion for the PWR CDRM tests, featuring two peaks of about the same magnitude. These two peaks correspond to the fundamental modes of the control rod cluster and the fuel bundle, respectively. Figure 3-24 shows a filtered version of the same spectrum that contains only the peak corresponding to the fuel bundles. The filtered input motion was used in the tests in order to achieve larger fuel response than using the unfiltered motion. These input motions were scaled to various levels to determine the fragility capacities. The scale factor for the unfiltered input motion was in the range of 0.25 to 3.3. Figure 3-25 through Figure 3-30 show comparison of the target input motion at $3.3 \times S_2$ level to responses at various locations (the top of the shaking table, upper core plate, lower core plate, CRDM base, and upper core support plate). Still water and core flow conditions were considered in the tests. The filtered input motion was scaled up to $3.6 \times S_2$ level. The damping ratio for these spectra is 5%.

Unlike the fragility tests for horizontal shaft pumps and electrical panels, element tests for the PWR control rod insertion capability was not intended to develop element fragility data but to identify the dynamic characteristic of the fuel assembly in water under large vibration. The maximum fuel response in water reached about 80 mm in the test. The results of this element test

were used to develop a stick model for the fuel assembly, which can reproduce the natural frequency and the response dependent damping.

Under an input seismic motion up to $3.3 \times S_2$, the maximum displacement of the fuel assemblies was about 48 mm (corresponding to a fuel response displacement of 45 mm), and no abnormality was found in the test. The maximum fuel displacement was more than twice the past test data (about 22 mm). The maximum displacement of the CRDM was about 17.2 mm, compared to 3.3 mm in the earlier NUPEC test. Figure 3-31 shows the test data for delay ratio of the PWR control rod insertion. The test results of PWR control rod insertion capability were in excellent agreement with the existing NUPEC test results for low range displacement response of the fuel assembly (proving test range). It should be emphasized that the JNES fragility test and the NUPEC proving test were performed using different test facilities and different input motions. The JNES fragility test also showed that the functional capacity of the control rod insertion system was at least twice of that proved in the previous NUPEC test [Inagaki, et al, 2006].

3.4.1.2 Fragility Evaluation and Fragility data

Based on results of the NUPEC seismic verification test of PWR core internals, displacement response of the fuel assembly was used by JNES as the control variable (performance indicator) in the fragility analysis. Excessive displacement of the fuel assemblies can cause damage to the guide thimble, which was considered as the critical event for the PWR control rod insertion system. Fragility data was developed based on an analytical method which was validated against the test results for the PWR control rod insertion capability.

Based on analysis considering the actual plant situation, such as operating temperature and flow rate, the median displacement of a fuel assembly was specified as 77 mm for 3/4 loop representative PWR plants, which corresponds to a seismic load of $4 \times S_2$. The logarithmic standard deviation was specified as 0.19, considering the dispersions of tensile strength and the dimensional tolerance of guide thimbles. This response dispersion was confirmed in the full-scale test.

For a 2 loop PWR plant with fuel assemblies of a 14×14 type, the median displacement of a fuel assembly was specified as 69 mm. The logarithmic standard deviation was specified as 0.19, the same as for 3/4 loop PWR plant.

In the past Japanese fragility evaluation, a scram time of 2.2 seconds was prescribed as the target of the control rod insertion time. However, an insertion time exceeding this scram time limit does not directly result in a problem. In NUPEC report INS/M03-05, "FY 2003, Report on Development of Probabilistic Safety Evaluation Method for Earthquake, Part III, Sophistication of Evaluation Method (In-core Thermal Hydraulic Analysis for Time Delay of Control Rod Insertion in PWR)," it was determined that core damage would not occur if the control rod can be inserted by the time when the pressurizer safety valve is initially actuated (about 8 seconds). This time limit was specified as the new target of the control rod insertion time used in the fragility capacity evaluation.

3.4.2 BWR Control Road Insertion Capability

3.4.2.1 Full Scale Test

Figure 3-32 through Figure 3-35 show the test setup for the BWR control rod insertion capacity test, the mockup of a BWR fuel assembly, a section view of the test setup, and a plan view of the fuel assemblies and the control rod, respectively. The main test components, such as the fuel assemblies, control rod, and CRDM, were manufactured with the same specification as in

representative BWR plants (BWR5) with 100 mil channel boxes, except for the material of the fuel pellets. The BWR5 plant features a high speed scram type CRDM. As shown in Figure 3-34, the test specimen stands above the top of the shaking table for 9.3 m (mainly the fuel assemblies and control rod) and below the table for 3.8 m (mainly the CRDM). The four fuel assemblies and the control rod were enclosed in a cylindrical vessel, which was supported by tie rods connecting to a very sturdy frame above the shaking table and to the shaking table under the table.

Seismic input motion was generated based on a survey of Japanese BWR plant design conditions and a preliminary seismic analysis of the main test components. Input motion was controlled at the top of the shaking table. The magnitude of the input seismic motion was up to $4 \times S_2$. The maximum input acceleration was about 3g, while it was 1.5g in the past NUPEC test.

Synthesized input motion (designated as Input Wave A) developed based on the envelop of the design spectra of Japanese BWR plants was found in the test not to be able to achieve adequate excitation, neither did a filtered version (designated as Input Wave B) that contains mainly the frequency contents for the fuel assembly. Therefore, the Input Wave C was developed by superposing sinusoidal wave components with dominant frequency range around 4.8 Hz, which is the fundamental frequency of the fuel assembly. The Input Wave C at S2 level is shown in Figure 3-36. The Input Wave C was further adjusted for use in the full scale test by shifting the center frequency to 5.8 Hz (measured frequency) and broadening the target spectrum by 10%, to consider the plastic behavior of the fuel assembly under large excitation. Figure 3-37 shows the adjusted Input Wave C. These motions were used in the test with various scale factors. Figure 3-38 shows a comparison of the target spectrum and the response at the top of the shaking table for a scale factor of 4.4. The damping ratio for these spectra is 5%.

The element test for BWR control rod insertion capability included a material test, buckling test, load-displacement history test, and repeated loading test of a channel box, which is the main structural member of a fuel assembly. The test confirmed that the plastic deformation at operating temperature was larger than at room temperature. The maximum fuel displacement was about 100 mm in the element test. The test results were also used to develop an analytical model.

Under an input seismic motion up to $4 \times S_2$, the maximum displacement of the fuel assemblies was about 83 mm and no abnormality was found in the test. The maximum fuel displacement was significantly larger than in the past test (about 34 mm). Figure 3-39 shows the test data for delay ratio of the BWR control rod insertion. The test results of BWR control rod insertion capability showed excellent agreement with the existing NUPEC test results for low range displacement response of the fuel assembly (proving test range). It should be emphasized that the JNES fragility test and the NUPEC proving test were performed using different test facilities and different input motions. The JNES fragility test also showed that the functional capacity of the control rod insertion system was at least twice of that proved in the previous NUPEC test [Inagaki, et al, 2006].

3.4.2.2 Fragility Evaluation and Fragility Data

Based on results of the NUPEC seismic verification test of a BWR in-core structure, displacement response of the fuel assembly was used by JNES as the control variable (performance indicator) in the fragility analysis. Excessive displacement of the fuel assemblies can cause collision of the fuel bundle and shroud, which was considered as the critical event for the BWR control rod insertion system and was defined as the fragility capacity limit. Fragility data was developed based on an analytical method which was validated against the test results for the PWR control rod insertion capability.

Based on analysis considering the actual plant situation such as temperature, the median displacement of a fuel assembly was calculated as 91mm for BWR plants with 100 mil channel boxes. This calculation assumed that the fuel displacement had a log-normal distribution, with 83 mm as the 5% percentile and 100 mm as the 95% percentile. The logarithmic standard deviation was specified as 0.10 (it appears that the calculated value should be 0.06 based on the above assumption).

For representative BWR plants with 80 mil or 120 mil channel boxes, the median fragility was specified as 91 mm, the same as for BWR plants with 100 mil channel boxes, while the logarithmic standard deviation was 0.1 for BWR plants with 80 mil channel boxes and 0.09 for BWR plants with 120 mil channel boxes.

In the past Japanese fragility evaluation, a scram time of 1.62 seconds was prescribed as the target of the control rod insertion time. However, an insertion time exceeding this scram time limit does not directly result in a problem. This prescribed scram time was also used in the fragility evaluation, because it was confirmed by analysis that the delay of the control rod insertion was still below the prescribed scram time even when the fuel assembly response reaches 100 mm, at which fuel-shroud collision would initiate (see Figure 3-39).

3.5 Large Size Vertical Shaft Pumps

3.5.1 Summary of Large Size Vertical Shaft Pump Test

The JNES test program for large size vertical shaft pumps included a full-scale equipment test for a pit barrel type pump of the reactor residual heat removal system (RHR) and element tests of submerged bearings, liner rings, and thrust bearings.

3.5.1.1 Full Scale Test

Figure 3-40 and Figure 3-41 show the test setup for the RHR pit barrel pump and a section view of the RHR pump installed on the TADOTSU shaking table. As shown in Figure 3-41, the RHR pump stands above the top of the shaking table for 7 m (mainly motor and motor stand) and below the table for 8 m (mainly the pump and pump barrel). The RHR pump has a flow rate of 1691 m³/h, a head of 92 m, and a mass of 61×10³ kg (about 49×10³ kg for pump and 13×10³ kg for motor). The test specimen also included piping and other components in order to simulate the operating condition. The diameter of the barrel support, as indicated in Figure 3-41, varied in the test such that the diametric clearance had a value of 1 mm, 2 mm, or 4 mm, depending on the test purposes.

Both horizontal and vertical excitations, while applied separately, were considered for normal operating conditions and shutdown conditions. The input seismic waves were generated using a response spectrum that envelops the design floor response spectra for large size vertical shaft pumps in Japanese BWR and PWR NPPs. Multiple simulated seismic waves utilized in the test had different frequency characteristics to investigate different parts of the pump system, e.g., the horizontal A wave for barrel without gap (16.1 Hz) and the horizontal D wave for barrel body (6.4 Hz).

Figure 3-42 through Figure 3-44 shows the response spectra for the A wave, D wave, and D' wave, respectively. Figure 3-45 shows a comparison of these three waves. The maximum acceleration is 1.24 g and the damping ratio for these horizontal spectra is 1%. Figure 3-46 shows a comparison of the response spectra for the target and the vertical wave. Quite differently

from the horizontal direction, the damping ratio for the vertical wave was 5%. The maximum acceleration for the vertical wave is 0.22 g. As indicated by Figure 3-45, the A wave was developed by filtering the D wave with a high pass filter with a corner frequency of 11.1 Hz, and the D' wave was developed by reducing by half the D wave response spectrum in the frequency vicinity around fundamental modes of the motor portion and the barrel portion with no gap. Both the A wave and the D wave are adequate if the gap at the barrel support is negligible, although the D wave produces smaller shaking table acceleration. For cases where the gap at the barrel support is not negligible, regardless of whether barrel collision would occur, the D wave is adequate but not the A wave. The test was performed in the following steps:

Step 1: Using A wave with 4 mm gap (design gap) for function limit test assuming gap effect at barrel support is negligible.

Step 2a: Using D (or D') wave with 4 mm gap to investigate the gap effect.

Step 2b: Using D (or D') wave with narrower gap (2 mm) to investigate the effect of gap width.

Step 2c: Using D (or D') wave with no gap (0 mm) to investigate the effect of gap width.

Step 3: Using vertical wave with 0 mm gap for function limit test.

Step 4: D (or D') wave (horizontal) and the vertical wave with 0 mm gap to compare responses obtained from one directional loading.

The horizontal test showed that although the motor mounting bolt yielded at a response acceleration of 12 g at the top of the motor (12 g-TOM, for short), motor function was maintained even at 14 g-TOM. The barrel yielded at a response acceleration of 31 g at the bottom of the barrel (31 g-BOB, for short). Nonlinear response behavior as a function of the diameter clearance at the barrel support was identified in the horizontal test. These horizontal confirmed response capacities greatly exceeded the existing function-confirmed response accelerations 10 g-BOB and 2.5 g-TOM as reported in JEAG4601. The vertical test showed that the function of the pump was maintained at 31 g-BOB and 12 g-TOM. No abnormality was found during the test and in the after-test disassembling inspection. Table 3-11 shows selected test results for the large size vertical shaft pump test.

3.5.1.2 Element Tests

Table 3-12 lists 9 parts that were included in JNES element tests for the large size vertical shaft pumps, including large and small size carbon bearings, solid lubricant distributed oilless bearings, resin bearings, rubber bearings, Kingsbury type thrust bearings, parallel plane type thrust bearings, and liner rings of two sizes. Three or four specimens were tested for each of the 9 parts. This table also presents the typical dimensions and materials of these parts. These parts were used in the selected large size vertical shaft pumps in the JNES equipment fragility evaluation. Figure 3-47 shows a liner ring sample and a bearing sample.

The selected elements (parts) were tested under simulated seismic excitations that were much larger than the excitations used for the full-scale test. The purpose of the element tests for the large size vertical shaft pumps was to confirm whether lose of function occurred for the parts subjected to very large seismic load and to obtain their dynamic characteristics (such as spring

constant, damping, and PV value (pressure-slide velocity)). Figure 3-48 shows the nonlinear load-displacement behavior of a shaft bearing under large excitation, in which the impulse shaped response was due to the diametric clearance.

The element tests showed that the rotation function of submerged bearings was maintained up to a surface pressure that was 5 times the design allowable surface pressure. Excessive deformation occurred for rubber and resin bearings although their rotation function was maintained. The rotation function of the liner rings was maintained under the maximum vibrating load of about 17.0 kN, which was equivalent to $3 \times S_2$ (S_2 was the enveloping design floor response of BWR/PWR plants, with a ZPA of 1.24 g). Using the spring constant that was determined from the tests, an uplift analysis showed that under a vertical acceleration of 1.3 to 1.5 g, the bearing load of the slide type thrust bearings reached the maximum load (determined in the element test) or collision occurred between the liner ring and the pump impeller. The acceleration that caused liner ring-impeller collision was conservatively defined as the uplift limit of the vertical shaft pumps. This level of acceleration corresponds to $6 \times S_2$ (S_2 was vertical ground motion with a ZPA of 0.22 g).

3.5.2 Fragility Evaluation and Fragility Data

According to their structural characteristics, large size vertical shaft pumps can be classified into three categories (as shown Figure 3-49): pit barrel type, vertical mixed flow type, and vertical single-stage floor type. Vertical single-stage floor type pumps are structurally very similar to the motor portion (above installation floor) of the other two types of vertical shaft pumps. It was further confirmed in the full-scale test that the response of the motor portion and that of the pump portion could be evaluated separately. Therefore, the vertical single-stage floor type pumps were not considered in the fragility analysis.

The pit barrel type pumps and the vertical shaft mixed flow pumps share many structural features, as shown Figure 3-50. The barrel support in the pit barrel type pumps is similar to the intermediate support in vertical mixed flow pumps. Therefore, the same analytical procedure was used for both types of pumps to calculate the seismic capacity for fragility analysis.

The full-scale test of the RHR pump showed that the response of the pump portion included both fundamental frequency response and high frequency response, the latter of which was due to the collision at the clearance of the barrel support. It was also confirmed that the response of the motor portion consisted of only fundamental frequency response.

For cases where the diametric clearance existed at the barrel support of pit barrel type pumps or the intermediate support of mixed flow pumps, an equivalent linear analysis and an impulse response analysis were performed for the pump portion to calculate the fundamental frequency response and the high frequency response, respectively. The overall response was the algebraic summation of the fundamental frequency response and the impulsive response. Seismic load at the motor portion was calculated by linear analysis using a model identical to the equivalent linear analysis for the pump portion. Figure 3-51 illustrates how the equivalent linear stiffness of the barrel support was obtained from the nonlinear stiffness (similar to the nonlinear load displacement relationship obtained in the element test, see Figure 3-48) at the maximum displacement y . The mode shape vector was used to determine the maximum displacement at the bottom of the pump.

In the impulsive analysis, the momentum change of the pump system in the collision of the barrel and barrel support was calculated, using equivalent lumped masses at the fundamental mode and

velocities at these masses, as shown in Figure 3-52. The impulsive force was then calculated assuming an impulsive duration $\Delta t = 1/600$ seconds, which was judged sufficiently small compared to the high frequency response below 100 Hz.

Figure 3-53 shows the one dimensional multi-mass model that JNES developed for the horizontal response analysis of the vertical shaft pumps. Both shear and flexible deformations were included in the beam model. Figure 3-54 shows the JNES two mass model for the vertical response analysis of the vertical shaft pumps. In the vertical response analysis, the uplift at the thrust bearing and the design clearance between the liner ring and impeller were considered as the criteria.

The damping ratios for various parts were chosen to be in the range of 1% to 3%.

Both rotating function and structural strength were considered in the fragility evaluation. For the rotating function limit state, the evaluation focused on the motor body, submerged bearing, and liner ring. For the structural strength limit state, the evaluation focused on the pump foundation bolt, mounting bolts (pump, motor, and motor stand), barrel, and column.

3.5.2.1 Fragility Evaluation for Structural Strength

Both earthquake load and the initial tightening force were considered in the evaluation of the tensile stress of bolts. The tensile stress was calculated using the overturning moment. The load factor for the bolts, which is the ratio of the portion of earthquake load taken by a bolt over the total earthquake load on the bolt connection, were conservatively assumed to be 0.5. The load factor for a bolt connection reflects the relative stiffness of the bolt versus the flange. The median value of the tensile stress of the bolt was specified S_u/η , where $\eta = 0.856$ for general steel or 0.885 for stainless steel (confidence coefficient) and S_u is the design tensile strength described in JSME “Standards for Nuclear Power Generation Equipment: Design and Construction Standards.” A critical stress of $0.75S_u/\eta$ was used in cases where nominal diameter of the bolt was used in the calculation.

Slip at the mounting surfaces was not identified in the full-scale test; however, as the relative slip between the motor and the pump may critically affect the rotation function of the pump, potential slip was evaluated at the motor mounting surface and at the motor stand mounting surface. The shear force during earthquake was assumed to be shared by all bolts in the same shear plane. The uncertainty in the torque was specified as $\beta = 0.25$ according to Japanese Industrial Standard “Points of Screw Tightening Mechanism Design.” A friction coefficient of 0.3 was used in the evaluation, with a logarithmic standard deviation $\beta = 0.123$, based on “Guide for Design and Construction of Lightweight Steel Structure, and its Interpretation” (a Japan standard). JNES recognized that many uncertain factors existed for the slip phenomena, and the resultant fragility capacity was reported as reference values. $S_u/(\sqrt{3}\eta)$ was specified as the critical shear stress based on shear stress strain theory.

For bolts that do not affect the rotation function of pumps, the dispersion of critical stresses was 0.07 for general steel and 0.05 for stainless steel. For bolts that may affect the rotation function of pumps, the dispersion of critical stresses was 0.09 for general steel and 0.07 for stainless steel.

For barrel and column, S_u/η was specified as the median tensile strength. The corresponding dispersion was specified as 0.07 for general steel and 0.05 for stainless steel. The strength of barrel and column was evaluated using the greater of the axial stress and the hoop stress. The

axial stress was the sum of the stresses due to bending moment, internal pressure, self-weight, and water weight in the barrel. The hoop stress was due to internal pressure.

3.5.2.2 Fragility Evaluation for Rotation Function

Up to the maximum vibration capacity of the shaking table, loss of function did not occur in the element tests for the submerged bearings and liner rings. Therefore, the minimum function confirmed PV values were conservatively specified as the rotation function limit. The median capacity and the corresponding logarithmic standard deviation were not calculated for the carbon bearing, solid lubricant distributed non-lubricated bearing, and liner ring. However, for rubber bearing and resin bearing, even though no loss of function had occurred, since the end surface of the bearings were found to be deformed at the maximum vibration load, the PV values were considered as indicators of the limit of rotation function. Accordingly, the median capacity and the logarithmic standard deviation were calculated as reference values. In the calculation of PV values, the velocity during the rated operation state of the pumps was used.

For the liner ring made of martensitic stainless steel, the PV values were specified based on the element test results in the horizontal shaft pump fragility test.

The maximum response acceleration 14 g-TOM (at the top of the motor) obtained in the full-scale test was considered to be a function confirmed response acceleration. The maximum response acceleration at the top of the motor was treated as the index variable for the rotating function limit of the pump system.

3.5.2.3 Summary of Fragility Data

In addition to the pit barrel type RHR pump which was tested in full scale, the JNES fragility evaluation for large size vertical shaft pumps also included a high pressure core injection system pump, a component cooling seawater pump (PWR), and a component cooling seawater pump (BWR).

The high pressure core injection system pump is a pit barrel type, with a flow rate of 727 m³/h, a total pump head of 190 m, and a mass of 62×10³ kg (about 52.5×10³ kg for pump portion and 8.5×10³ kg for motor portion).

The component cooling seawater pump (PWR) is a vertical mixed flow pump, with a flow rate of 5300 m³/h, a total pump head of 48 m, and a mass of 31×10³ kg (about 17.8×10³ kg for pump portion and 13×10³ kg for motor portion).

The component cooling seawater pump (BWR) is a vertical mixed flow pump, with a flow rate of 1080 m³/h, a total pump head of 40 m, and a mass of 15×10³ kg (about 10×10³ kg for pump portion and 5×10³ kg for motor portion).

Table 3-13 and Table 3-14 summarize some selected fragility data for the large size vertical shaft pumps under horizontal and vertical excitations, respectively. It should be emphasized that all reported fragility data related to loss of function of bearings or liner rings should be interpreted as function confirmed capacities, because the element tests and full-scale test of the RHR pump did not show any damage that would hinder the rotation functions of the parts. For horizontal excitations, the fragility data were reported as response acceleration at the top of the motor or at the bottom of the barrel; the corresponding input acceleration at the top of the shaking table was not reported. Most of the fragility data were estimated by analysis using element test data as shown in Table 3-15. The relative slip at the motor mounting surface was controlling, with

fragility capacities between 2.8 to 6.2 g-TOM. Since the slip phenomena involves a large amount of uncertainty and the corresponding capacity could be increased simply by tightening the anchor bolts, the fragility data were designated as reference values. In fact, a horizontal fragility capacity of 14 g-TOM was achieved in the full-scale test of the pit barrel type RHR pump after tightening the anchor bolts, compared to 3.6 g-TOM as estimated in the analysis.

Either no or a very small logarithmic standard deviation was reported for the large size vertical shaft pumps. A slightly larger logarithmic standard deviation β of 0.12 was calculated based on the distributions of friction factor of slip surface, torque constant of bolt, and tensile strength of material; while a smaller β of 0.09 was calculated based on distribution of tensile strength of material.

Table 3-15 shows the median capacities for the resin bearings and rubber bearings, and the minimum confirmed capacities for other submerged bearings, liner rings, and thrust bearings, which were determined in the element tests for the large size vertical shaft pumps. It should be pointed out that the fragility data was reported in terms of PV value ($\text{MPa} \times \text{m/s}$) and/or load (kN) in the JNES equipment fragility report, while only load capacities are summaries in Table 3-15. Most of the fragility capacities were function confirmed except for resin bearings and rubber bearings. In these cases excessive deformation occurred but rotational function was maintained in the test. The logarithmic standard deviation for the resin bearings and rubber bearings, 0.06 and 0.03, respectively, were derived using three samples (the 4th sample had different test conditions and was not counted in the statistics); these values were reported as reference values.

Table 3-1 Types of Horizontal Shaft Pumps in Japan NPPs
[from Iijima, et al, 2004]

Pumps	Reactor	Single Stage	Multi-stage
Reactor Building Closed Cooling Water Pump	BWR	×	
Residual Heat Removal Cooling Water Pump		×	
Emergency Equipment Cooling Water Pump		×	
High Pressure Core Spray Cooling Water Pump		×	
Reactor Core Isolation Cooling Pump			×
High Pressure Core Injection Pump			×
Component Cooling Water Pump	PWR	×	
Residual Heat Removal Pump		×	
C/V Spray Pump		×	
Charging Pump			×
Safety Injection Pump			×

Table 3-2 Element Types for Horizontal Shaft Pumps
[from Iijima, et al, 2005]

Element (Device)		Size (Type)	Number of Specimens
Radial Bearing	Ball	110 mm O.D. (6310)	3
		170 mm O.D. (6316)	3
	Slide	60 mm I.D. 80 mm I.D.	3 3
Thrust Bearing	Ball	110 mm O.D. (6310)	3
		170 mm O.D. (6316)	3
		170 mm O.D. (7316B)	3
	Slide	127 mm I.D.	3
Liner Ring	Flat	270 mm I.D.	3
		267 mm I.D.	3
		195 mm I.D.	3
		175 mm I.D.	3
		88 mm I.D.	3
	Groove	95.5 mm I.D.	3

★ Ball bearing type 6316 and 270 mm liner ring were used in the RCW pump.

Table 3-3 Summary of Selected Critical Values for the Fragility Evaluation

[from Appendix A, JNES, 2009]

Function	Direction	Critical portion	Fragility evaluation item		Description
			Item	Set value*	
Active function	Axial	Deep groove ball bearing	Bearing load	$Coa \times 1/3$	<ul style="list-style-type: none"> • Coa: Run-onto static rated load of bearing • To be set based on friction generation load which could cause decrease of operating life of bearing, using the element test results
		Angular ball bearing		Coa	<ul style="list-style-type: none"> • To be more conservatively set than function- confirmed load in the element test
		Slide bearing	PV value	$129MPa \cdot m/s$	<ul style="list-style-type: none"> • Minimum value of function-confirmed load in the element test
	Lateral	Deep groove ball bearing	Bearing load	$Cor \times 1/1.5$	<ul style="list-style-type: none"> • Cor: Basic static rated load of bearing • To be more conservatively set than function- confirmed load in the element test
		Angular ball bearing			
		Slide bearing	PV value	$121MPa \cdot m/s$	<ul style="list-style-type: none"> • To be set based on the minimum value of load due to shaft torque change, considering generation of plastic flow which could cause decrease of operating life of bearing
Structural strength	Axial/ Lateral	Foundation bolt Mounting bolt	Tensile stress Shear stress	$0.75Su/\eta$ $(Su/\sqrt{3})/\eta$	<ul style="list-style-type: none"> • Su: Design tensile stress • η: Confidence coefficient (general steel product: 0.856, stainless steel: 0.885) • Simplified evaluation for bolt strength
	Axial/ Lateral	Mounting bolt	Horizontal load	$\mu \cdot (F+W)$ (As reference value)	<ul style="list-style-type: none"> • μ: Friction coefficient (0.3) • F: Sum of bolt tightening forces • W: Dead load of pump or motor • Simplified evaluation for slip of mounting portion

* Set value: Reference value used for fragility evaluation in this report

Table 3-4 Summary of Fragility Data for Horizontal Shaft Pumps

Component	Limit State	Shaking Direction	Median Fragility (g)	Logarithmic Std (β)	Failure Mode
RCW Pump (full-scale test)	Functional	Axial	8.4	0.21	Wearing of ball bearing
	Structural	Lateral	28.5	0.07	Damage of foundation bolt
		Axial/ Lateral	6.1*	-	Slip of motor
RCW Pump 2	Functional	Axial	8.6	-	
	Structural	Lateral	23.5	0.07	Damage of foundation bolt
		Axial/ Lateral	5.3*	-	Slip of motor
Charging/HP Injection Pump	Functional	Axial	17.3	-	
	Structural	Lateral	11.0	0.07	Damage of foundation bolt
		Axial/ Lateral	2.6*	-	Slip of motor

* Reference fragility

Table 3-5 Summary of Fragility Data for Ball Bearings used in Horizontal Shaft Pumps

Model Number /Load Case	Median Fragility (kN)	Logarithmic Std (β)
6310 / Thrust	24.0	0.21
6316 / Thrust	25.3	0.01
7316B / Thrust	> 59	FC
6310 / Radial	26	FC
6316 / Radial	>31	FC

FC: function confirmed, no fragility value was specified.

Table 3-6 Summary of Fragility Data for Slide Bearings used in Horizontal Shaft Pumps

Diameter (mm) /Load Case	Median Fragility			Logarithmic Std (β)
	Function Critical Load (kN)	Maximum Surface Pressure (MPa)	Function Critical PV Value (MPa*m/s)	
80 I.D. / Radial	42.9	8.9	134	0.03
60 I.D. / Radial	21.2	8.0	121	0.12
127 O.D. / Thrust	45 (FC)	5.24	129	FC

FC: function confirmed, no fragility value was specified.

Table 3-7 Summary of Fragility Data for Liner Rings used in Horizontal Shaft Pumps

Inner Diameter (mm)	Function Confirmed Load (kN)	Maximum Surface Pressure (MPa)	Function Confirmed PV Value (MPa×m/s)
270	20.9	1.9	47.9
175	6.0	1.2	20.1
267	20.9	2.0	49.0
88	11.0	1.28	28.0
195	7	1.89	58
95.5	5	0.58	10

Note: all values are the smallest function confirmed values among the specimens.

Table 3-8 Properties of the Tested Electrical Panels

Panel	Dimension (m) W × H × D	Weight (kg)	Frequency (Hz)
Main Control Board	2.65 × 1.01 × 1.35	1010	44
Reactor Auxiliary Control Board	2.1 × 2.3 × 2.6	2580	31
Logic Circuit Control Panel	1.0 2.3 × 1.0	750	22
Reactor Protection Rack	1.8 × 2.3 × 0.9	2160	29
Instrumentation Rack	2.3 × 1.9 × 0.6	670	33
Reactor Control Center	0.8 × 2.3 × 0.8	640	36*
Power Center	1.8 × 2.3 × 2.0	4050	24
6.9 kV Metal-Clad Switchgear	2.0 × 2.3 × 2.5	5600	21

* Front-back direction, all other frequencies are for side-side direction.

Table 3-9 Electrical Parts in JNES Element Tests and Fragility Data

Part Category	Part Type	Number of Specimens	Front-Back		Side-Side		Failure Mode
			Median (g)	β	Median (g)	β	
Protection relay	TUB-2-D	3	9.5	0.13	10.0		chatter
	CO-18-D	9	10.6		10.0		
	VCR62D	3	12.0		12.7		
Auxiliary relay	NRD-81	9	5.9	0.0	10.6		Chatter
	UP3A	9	11.0		11.5		
	MY4Z	9	10.1		10.0		
Timer	H3M	9	10.1		10.0		
Comparator card	HALN	3	9.9		9.5		
AC controller card	HASN	3	9.9		8.3	0.17	Chatter of miniature relay
Flat display	18 inch	3	10.2		9.5		
Controller	18 inch	3	10.4		10.4		
Controller (CPU)	TOSMAP	3	10.8		10.9		
I/O Unit	TOSMAP	3	10.6		10.6		
Test module	S9166AW	3	10.5		10.1		
Power module	S9016AW	3	10.5		10.1		
Monitor module	S9146AW	3	10.5		10.1		
Power unit	TFV	3	11.0		10.2		
	S9980UD	1	10.5		10.1		
Differential pressure transmitter	EDR-N6L	4	10.0		10.1		
	AP3107	3	10.5		10.5		
	UNE13	3	10.0		10.0		

Part Category	Part Type	Number of Specimens	Front-Back		Side-Side		Failure Mode
			Median (g)	β	Median (g)	β	
Pressure transmitter	EPR-N6L	1	10.4		10.1		
Magnetic Contactor	MSO-A80	9	9.7		10.1		
	C-20J, T-20J	9	10.3		10.0		
Molded case circuit breaker	NF100-SH	9	9.8		9.6		
	SH100	9	10.4		10.1		
	F type	9	10.1		10.0		
Module Switch	SSA-SD3-53	9	10.3		9.9		
Cam-operated switch	MS	9	10.1		10.0		
Key switch	ACSNK	9	10.1		10.0		
GPT	VTZ-E6EP	1*	2.5	---	8.8	---	Fuses fell out
	VTZ-E6EP (improved)	1*	9.4		10.3		
Air circuit breaker	B10-1	1*	9.1		10.1		
	DS-416	1*	3.8	---	NA	NA	Error of closing
	DS-416 (improved)	1*	7.9		NA	NA	
	DS-840 (from panel test)	1	3.3	---	NA	NA	Error of closing
Gas circuit breaker	6-SFG-40S	1*	3.5	---	6.7		Structural damage
Vacuum circuit breaker	VF-6M63 (from panel test)	1	4.4	---	8.4	---	Structural damage

Notes: (1) * Additional test of GPT and breakers,

(2) A blank β means maximum tested acceleration at which no malfunction occurred for all specimens,

(3) A $\beta = ---$ means only one specimen tested, and β could not be evaluated,

(4) NA means not tested for the subject case or data was not available.

Table 3-10 Summary of Fragility Data for Electrical Panels

Panel	Test (g)	Abnormality	Analytical Fragility Evaluation			
			Limit State	Median (g)	β	Failure Mode
Main control board	5.69 (SS)	No	Functional	5.6 (SS)	-	Flat display
			Structural	42.2 (SS)	0.07	Foundation Bolt
Reactor auxiliary panel	5.90 (BF)	No	Functional	9.8 (BF)	0.02	Module switch
			Structural	82.4 (SS)	0.07	Cabinet
Logic circuit control panel	5.88 (BF)	No (but door hinge was broken)	Functional	6.7 (SS)	0.027	Power supply unit
			Structural	15.3 (SS)	0.07	Anchor bolt
Reactor protection rack	4.3 (SS)	Malfunction of Miniature relay	Functional	4.4 (SS)	0.166	AC controller card
			Structural	15.8 (SS)	0.07	Anchor bolt
Instrumentation Rack	5.69 (SS)	No	Functional	4.2 (SS)	-	Differential pressure transmitter
			Structural	18.2 (BF)	0.07	Anchor bolt
Reactor control center	6.12 (BF)	Malfunction of auxiliary relay	Functional	4.5 (BF)	-	Auxiliary relay
			Structural	22.6 (SS)	0.07	Foundation bolt
Power center	3.72 (BF)	Air circuit breaker closed	Functional	4.4 (BF)	-	Receiving circuit breaker
			Structural	8.1 (SS)	0.07	Housing
6.9 kV Metal-clad switchgear	2.52 (BF)	Fuse drop out	Functional	4.2 (SS)	-	Circuit breaker
			Structural	8.6 (SS)	0.07	Foundation bolt

Note: SS stands for the side to side direction;
 BF stands for back to forth direction

Table 3-11 Selected Results for the Full-scale Vertical Shaft Pump Test

Test Condition		Test Results			
Input Wave	Diametric Clearance (mm)	BOB Acceleration (g)	TOM Acceleration (g)	Input Acceleration (g)	Loss of Function
Horizontal D' (1)	1.0	31	-	2.8	No, but yield of barrel at barrel support
Horizontal D' (2)	1.0	35	-	2.8	No
Vertical	1.0	2.2	-	1.9	No
Horizontal A	4.0	-	14	1.6	No
Vertical	1.0	-	2.3	1.9	No
Horizontal D	1.0	-	12	1.5	No, but yield of motor mounting bolts

Notes:

BOB: bottom of barrel

TOM: top of motor

A wave: input wave including frequency content at 16.1 Hz for barrel (assuming no diametric clearance at barrel support)

D wave: input wave including frequency content at 6.4 Hz for barrel body (assuming diametric clearance is large enough to avoid collision)

D' wave: a modified D wave with the motor frequency content (at about 20 Hz) reduced by half, in order to suppress motor response but produce large barrel response

Table 3-12 Element Types for Large Size Vertical Shaft Pumps

Element Type	Inner Diameter (mm)	Length / Height (mm)	Diametric Clearance (mm)	Number of Specimens	Remarks
Carbon bearing (large)	100	115	0.41~0.48	3	Graphite
Carbon bearing (small)	55	50	0.41~0.48	3	Graphite
Solid lubricant distributed oilless bearing	100	80	0.39~0.58	4	Sintered metal of lead bronze alloy and graphite
Resin bearing	120	120	0.14~0.34	4	High polymer of fluorine and carbon
Rubber bearing	100	120	0.14~0.34	4	Copolymer of butadiene and acrylonitrile
Flat type liner ring	355	50	0.53	3	Austenitic stainless steel
Flat type liner ring	550	45	1.17	3	Austenitic stainless steel
Kingsbury type thrust bearing	270 (540 O.D.)	270	-	3	Slide bearing
Parallel plane type thrust bearing	250 (470 O.D.)	184	-	3	Slide bearing

Table 3-13 Summary of Fragility Data for Large Size Vertical Shaft Pumps (Horizontal Vibration)

Pump	Median Value (g)	β	Damage Mode
Pit barrel type RHR pump	37.1 (BOB)	-	Loss of function of submerged bearing
	3.6 (TOM)	0.12 (Reference)	Slip at motor mounting surface
	14.0 (TOM)	-	Achieved in the full-scale test after reinforcing mounting bolts
High pressure core injection system pump	17.7 (BOB)	-	Loss of function of submerged bearing
	3.5 (TOM)	0.12 (Reference)	Slip at motor mounting surface
	14.0 (TOM)	-	
Component cooling seawater pump (PWR)	96.9 (BOB)	-	Loss of function of submerged bearing
	6.2 (TOM)	0.12 (Reference)	Slip at motor mounting surface
	6.3 (TOM)	0.09	Yielding of motor stand mounting bolt
Component cooling seawater pump (BWR)	14.6 (BOB)	-	Loss of function of submerged bearing
	2.8 (TOM)	0.12 (Reference)	Slip at motor mounting surface
	4.3	0.09	Yielding of motor stand mounting bolt

Notes:

BOB: bottom of barrel

TOM: top of motor

Table 3-14 Summary of Fragility Data for Large Size Vertical Shaft Pumps (Vertical Vibration)

Pump	Maximum Input Acceleration (g)	Thrust Bearing Type
Pit barrel type RHR pump	1.9	Ball bearing
Component cooling seawater system pump (PWR)	1.5 (6.7S ₂)	Kingsbury bearing
High pressure core injection system pump	1.3 (5.7S ₂)	Parallel plane bearing

Table 3-15 Summary of Fragility Data for Bearings and Liner Rings used in Large Size Vertical Shaft Pumps

Element Type	Median / Minimum FC Loads (kN)	β
Carbon bearing (large)	95.9	FC
Carbon bearing (small)	51.9	FC
Solid lubricant distributed oilless bearing	98.8	FC
Resin bearing	61.1	0.06 (Reference)
Rubber bearing	69.8	0.03 (Reference)
Flat type liner ring (355 I.D.)	20.0	FC
Flat type liner ring (550 I.D.)	17.5	FC
Kingsbury type thrust bearing	1,500	FC
Parallel plane type thrust bearing	1,500	FC

Notes:

FC: function confirmed.

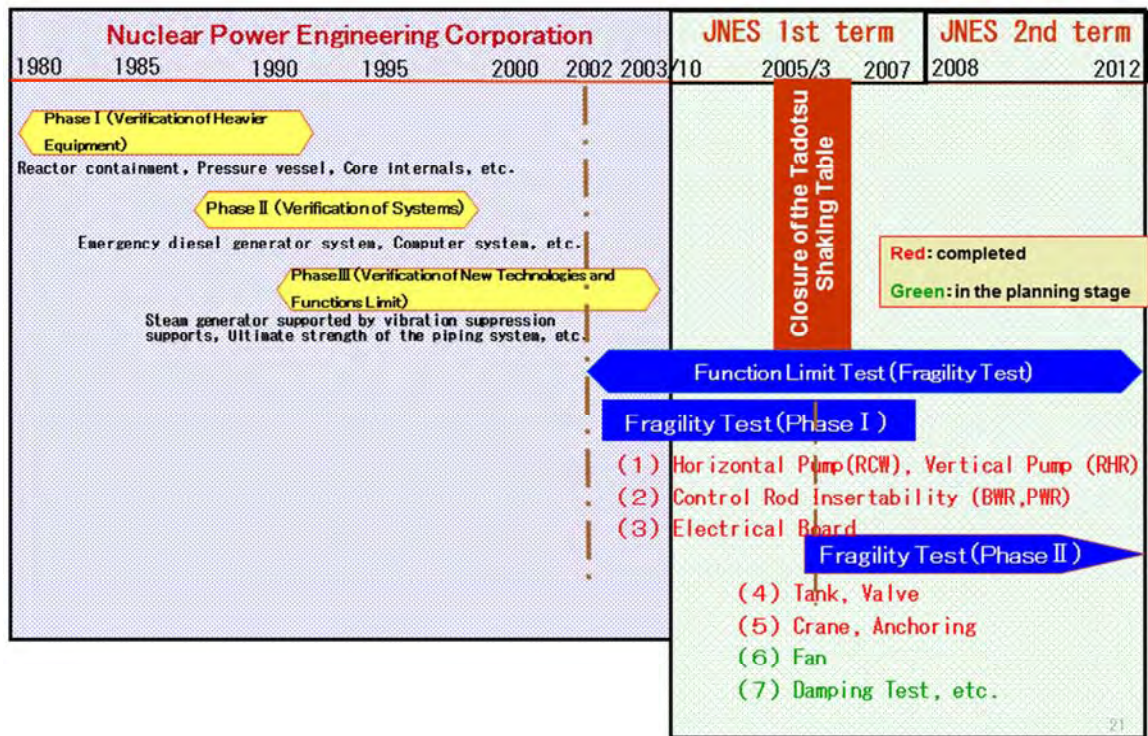


Figure 3-1 JNES Equipment Fragility Test Schedule

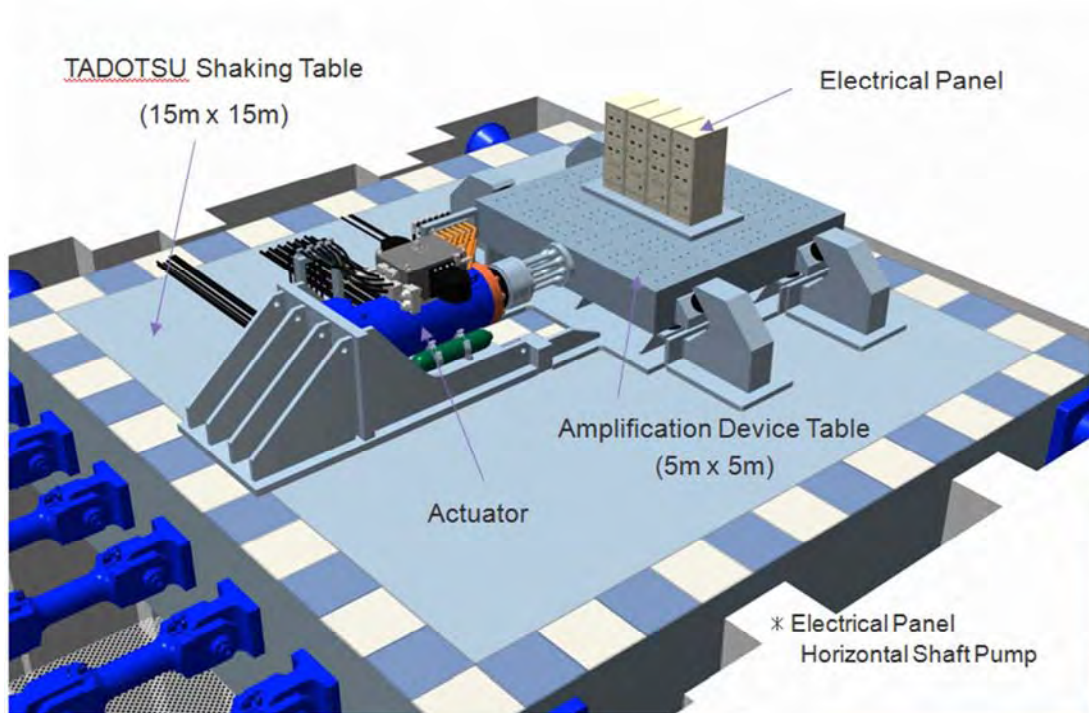


Figure 3-2 TADOTSU Shaking Table and the Amplification Device Table

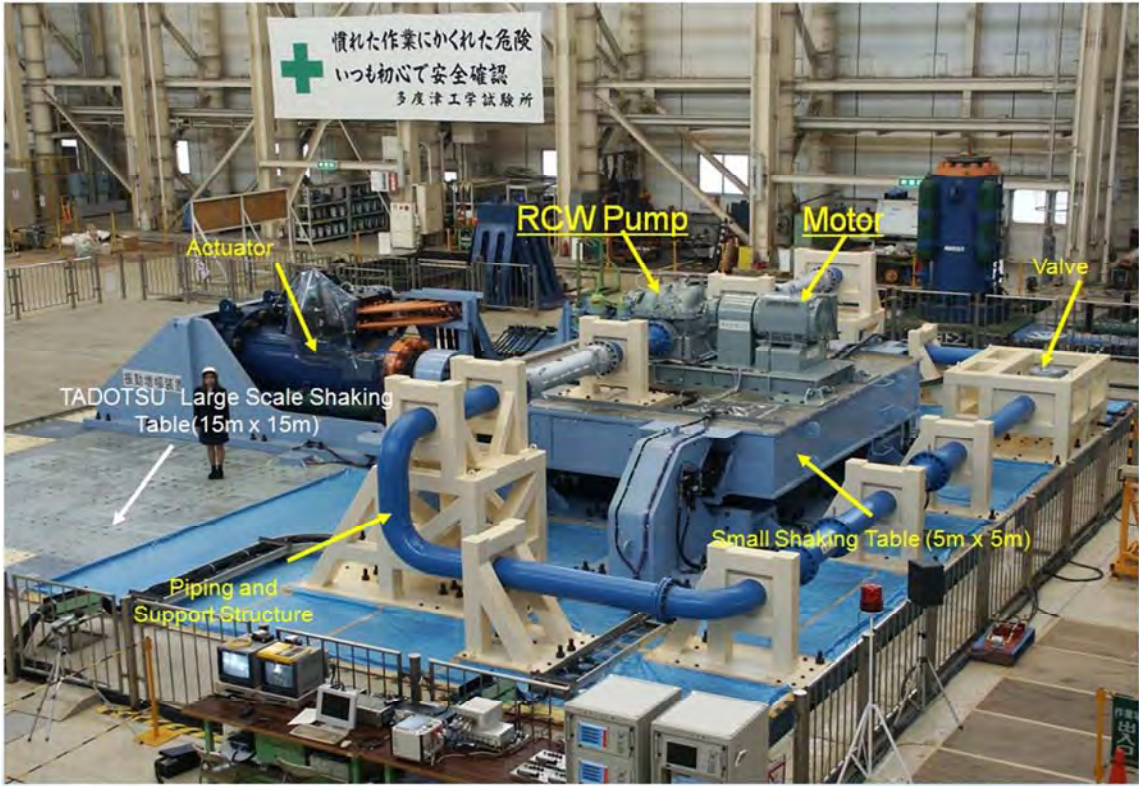


Figure 3-3 RCW Pump Test Layout

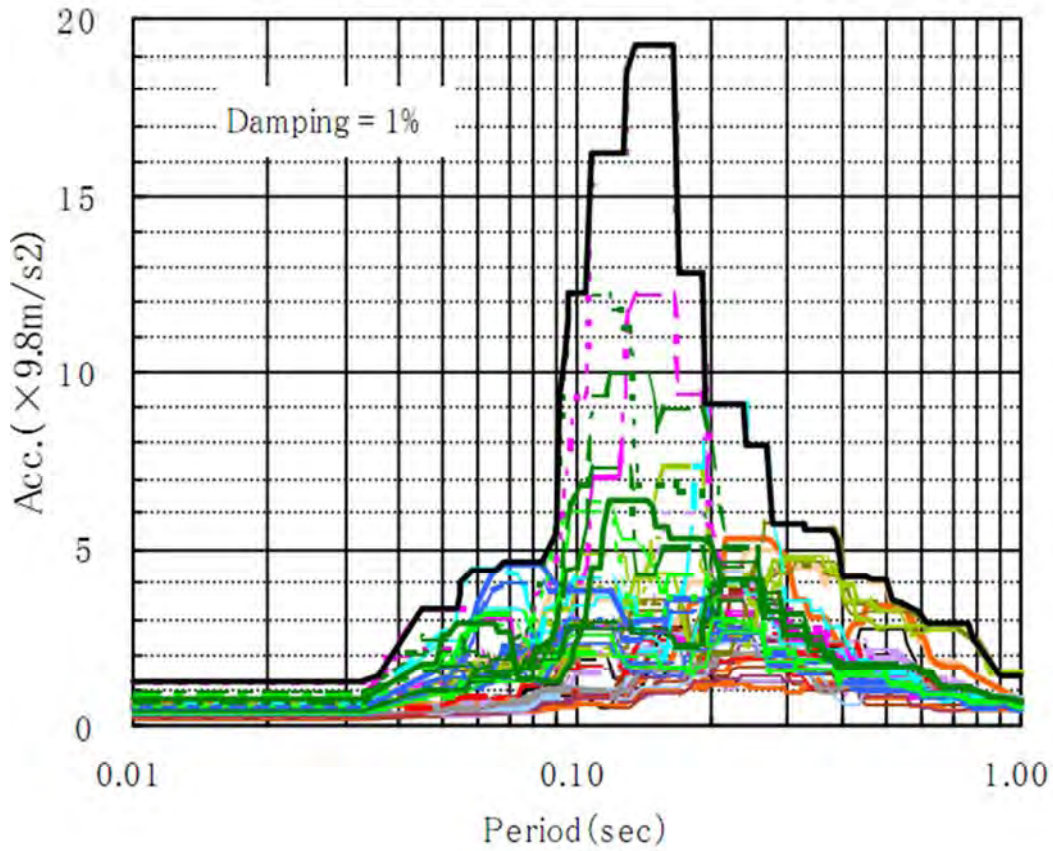


Figure 3-4 Development of Envelop Floor Response Spectrum

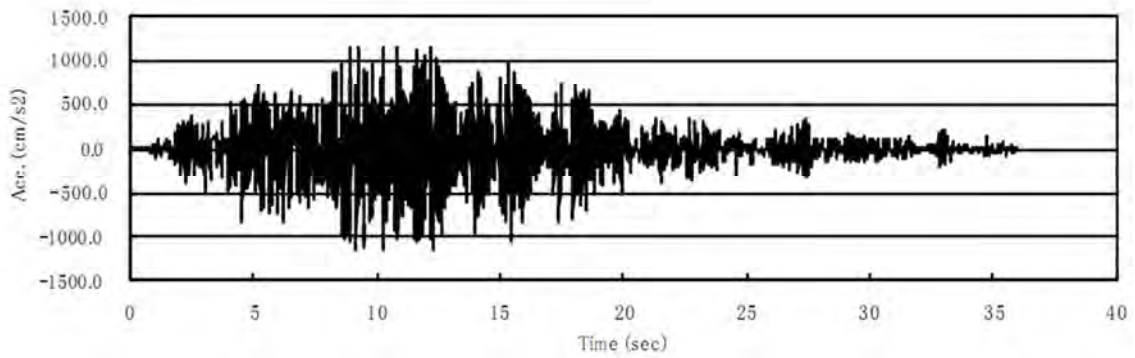


Figure 3-5 Basis Input Acceleration Time History Generated From Envelop FRS for Horizontal Shaft Pump Test

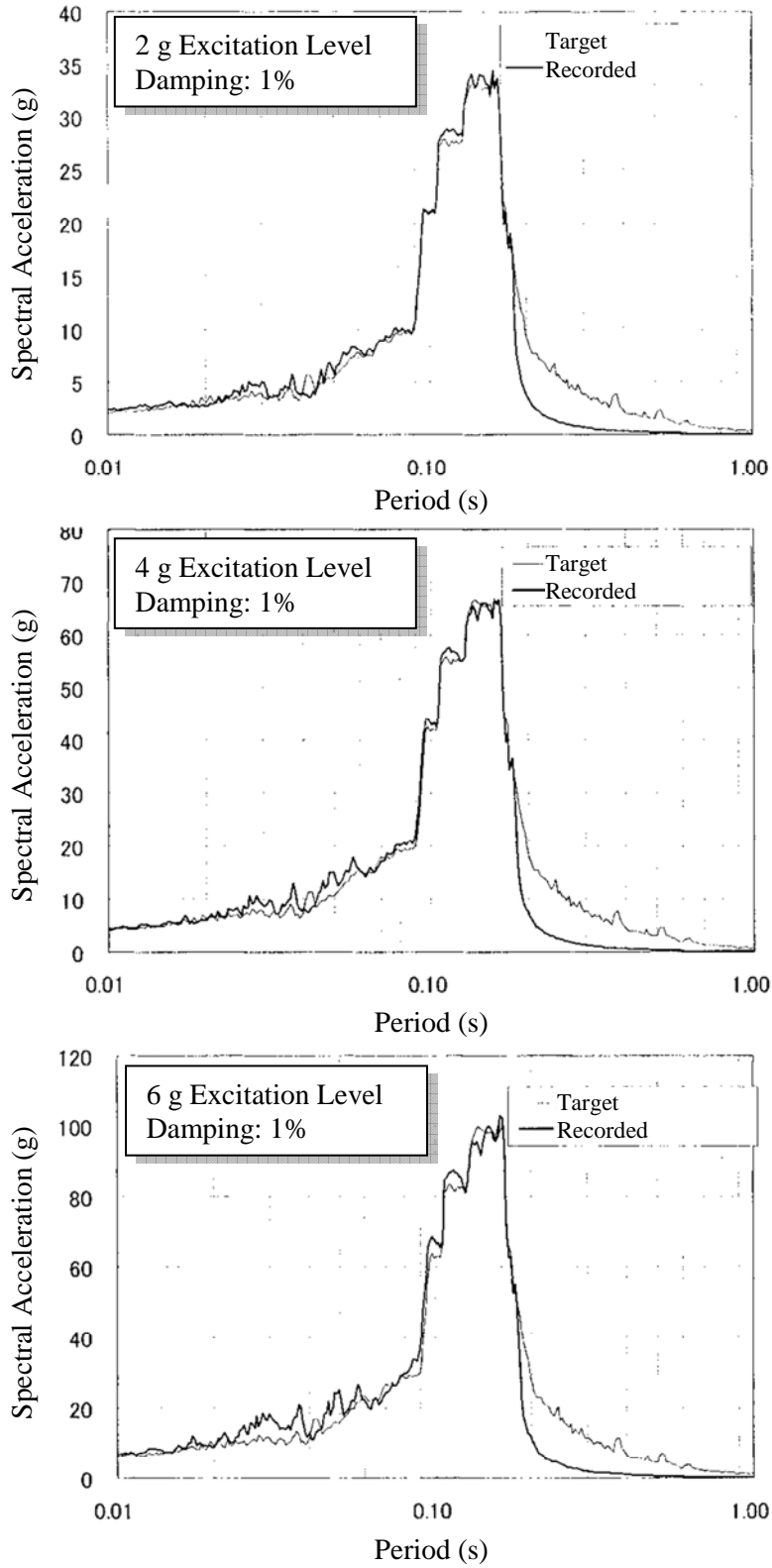


Figure 3-6 Response Spectra at the Top of the Amplification Table for Excitation Levels of 2 g, 4g, and 6g in the Full Scale Horizontal Shaft Pump Test

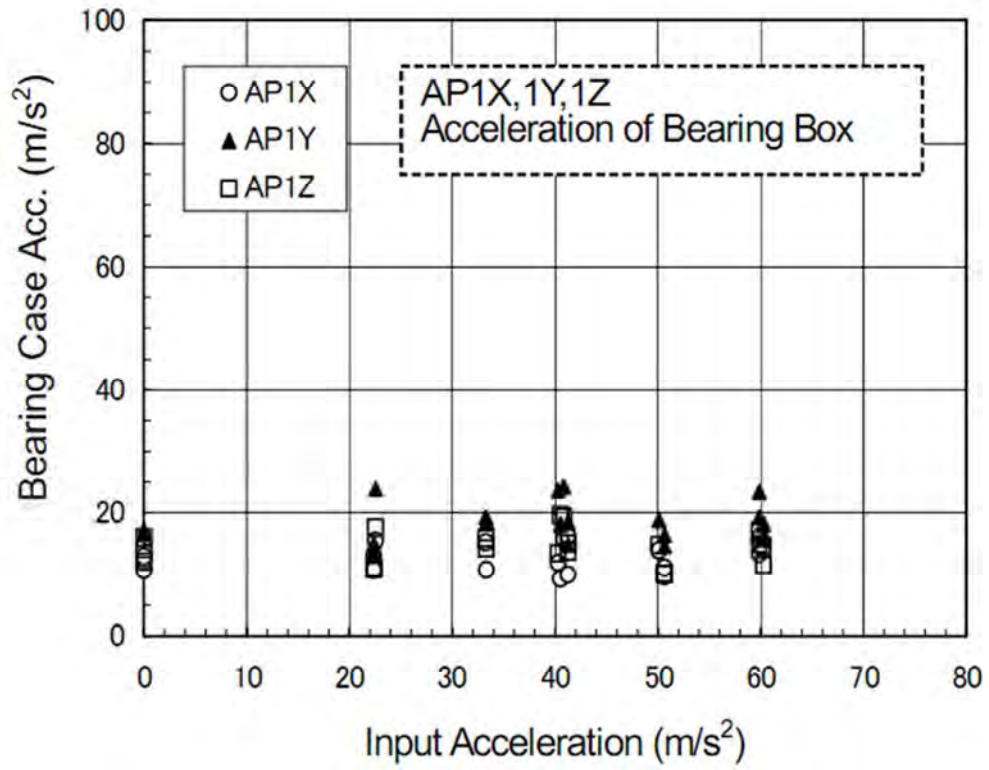


Figure 3-7 Change of Acceleration at Bearing Case With Respect to Input Acceleration

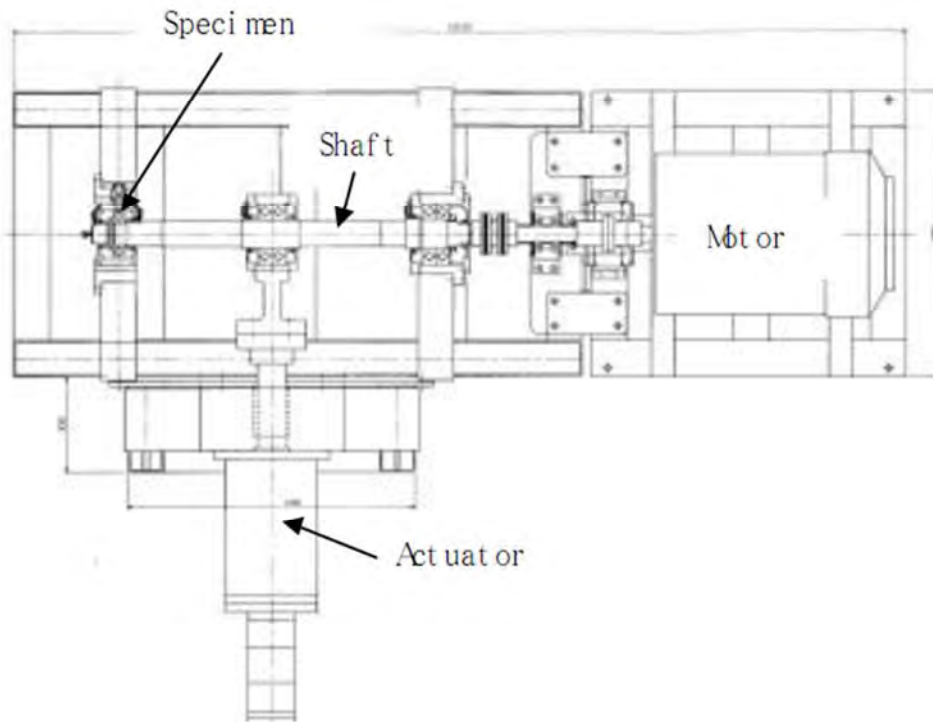


Figure 3-8 Test Setup for Radial Ball Bearings

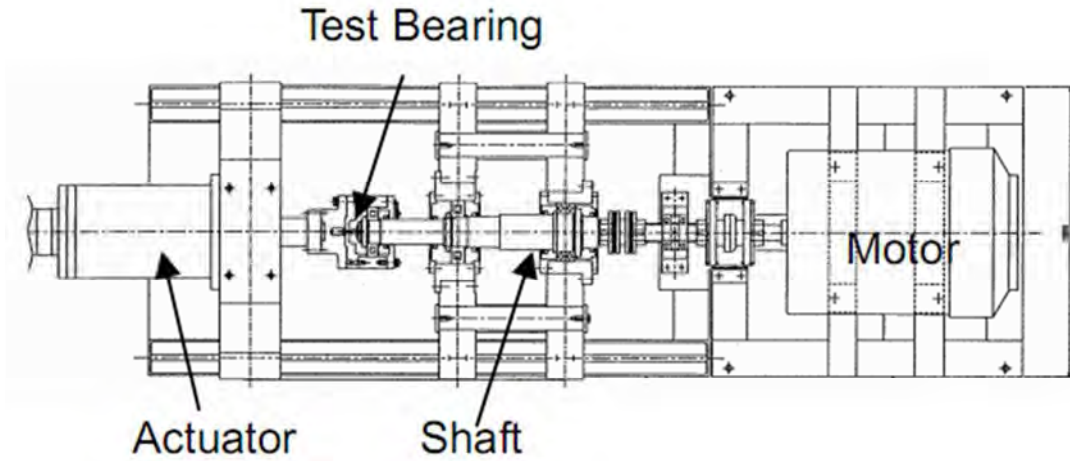
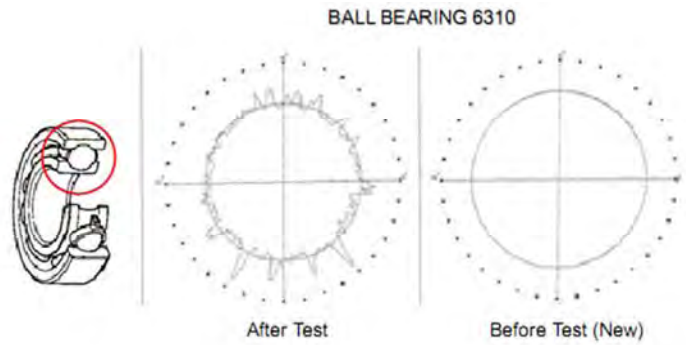
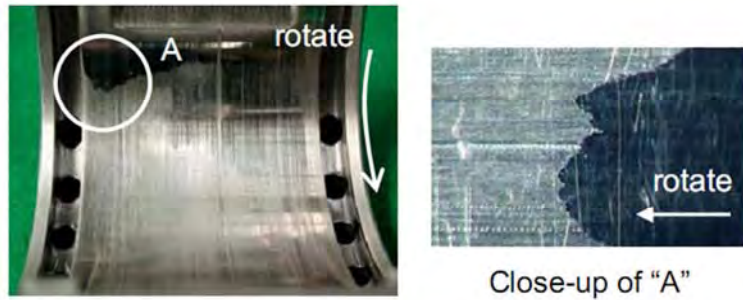


Figure 3-9 Test Setup for Thrust Ball Bearings

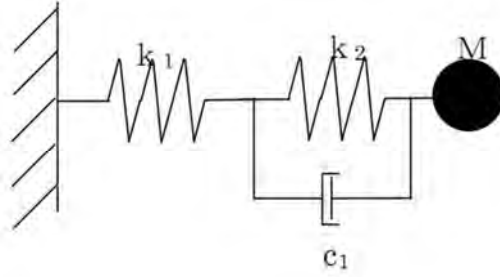


(A) Ball Surface Roughness of Bearing 6310



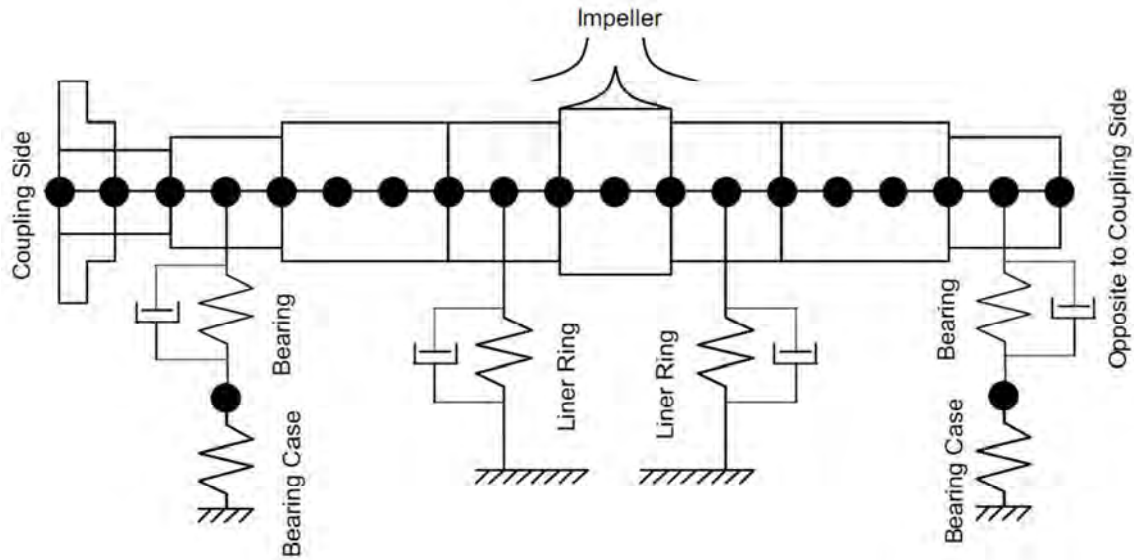
(B) Inner Surface Degradation of Slide Bearing (60 mm I.D.)

Figure 3-10 Surface Degradation of Bearings During Element Tests



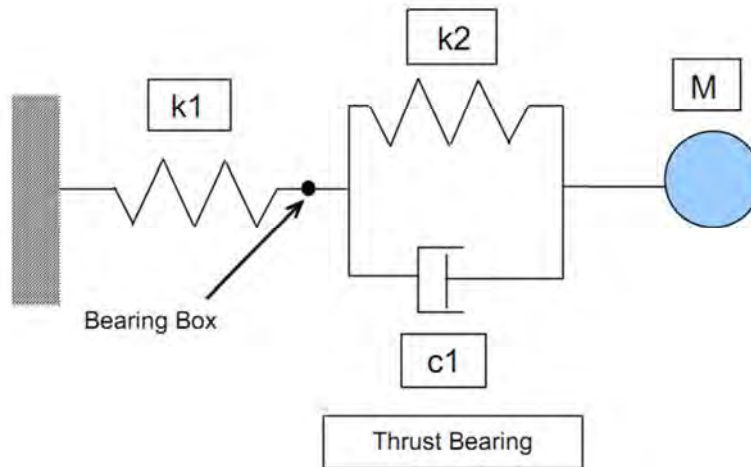
M: Mass of rotor system (including additional mass of water)
 k1: Spring constant of bearing box (linear)
 k2: Spring constant of bearing (non-linear)
 c1: Damping of bearing

(A) Model for Axial Direction



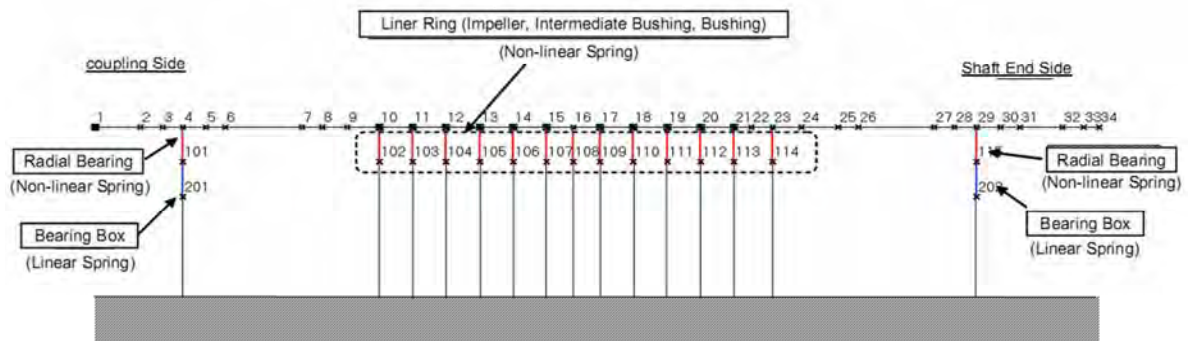
(B) Model for Lateral Direction

Figure 3-11 Analytical Models for Single Stage Horizontal Shaft Pump



M: Mass of rotating shaft system (including additional mass of water)
 K1: Spring constant of bearing bracket (linear)
 K2: Spring constant of thrust bearing (non-linear)
 c1: Damping factor of thrust bearing

(A) Model for Axial Direction



(B) Model for Lateral Direction

Figure 3-12 Analytical Models for Multi-stage Horizontal Shaft Pump

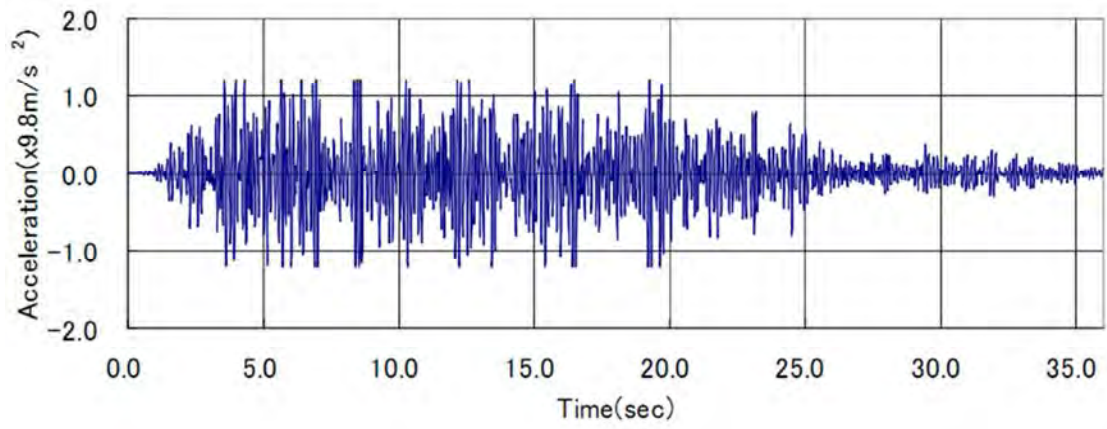
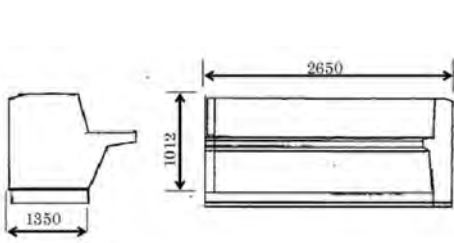
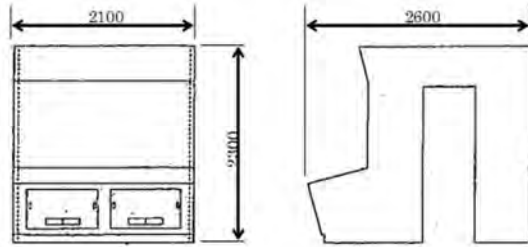


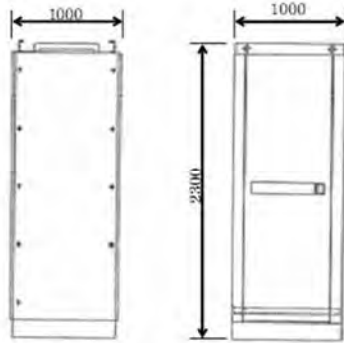
Figure 3-13 Basis Input Acceleration Time History for Electrical Panel Tests



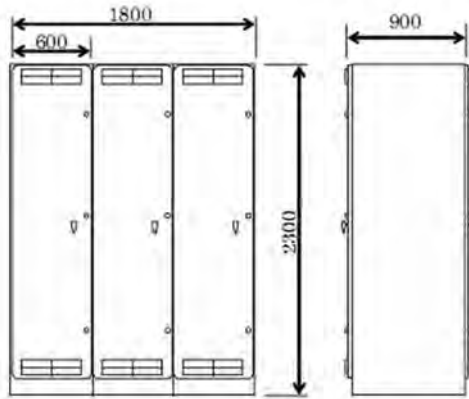
(A) Main Control Board



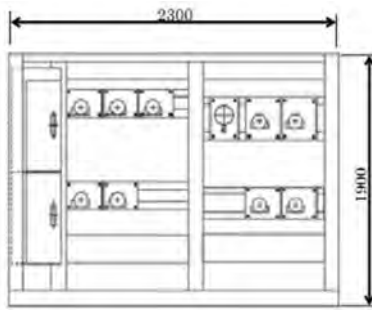
(B) Reactor Auxiliary Control Board



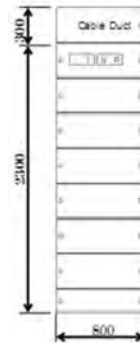
(C) Logic Circuit Control Panel



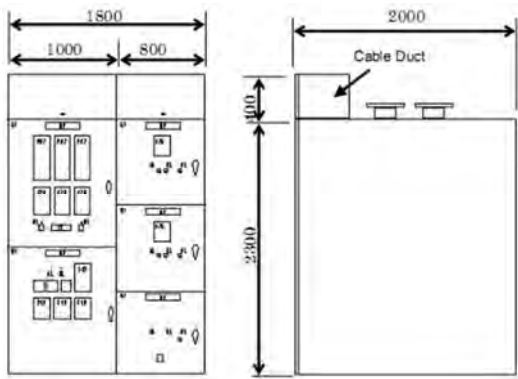
(D) Reactor Protection Rack



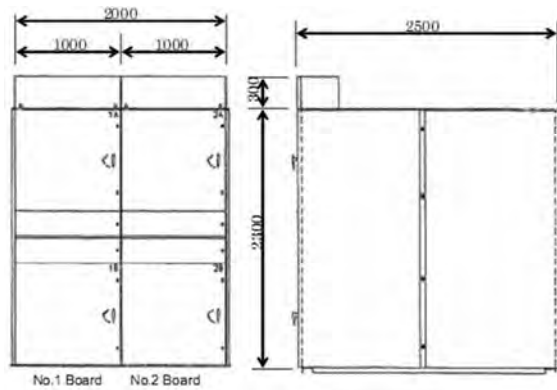
(E) Instrumentation Rack



(F) Reactor Control Center



(G) Power Center



(H) 6.8 kV Metal-Clad Switchgear

Figure 3-14 Illustration of Electrical Panels

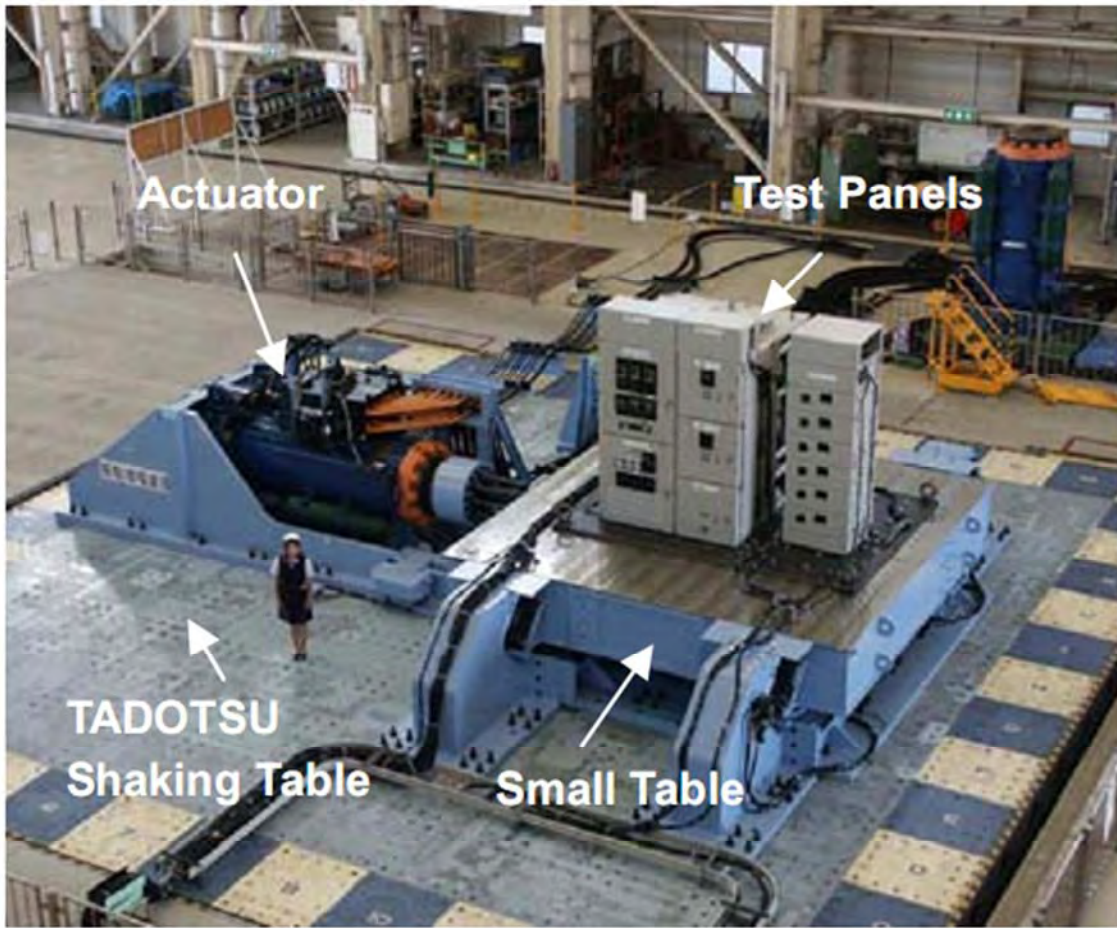


Figure 3-15 Test Setting for Electrical Panels

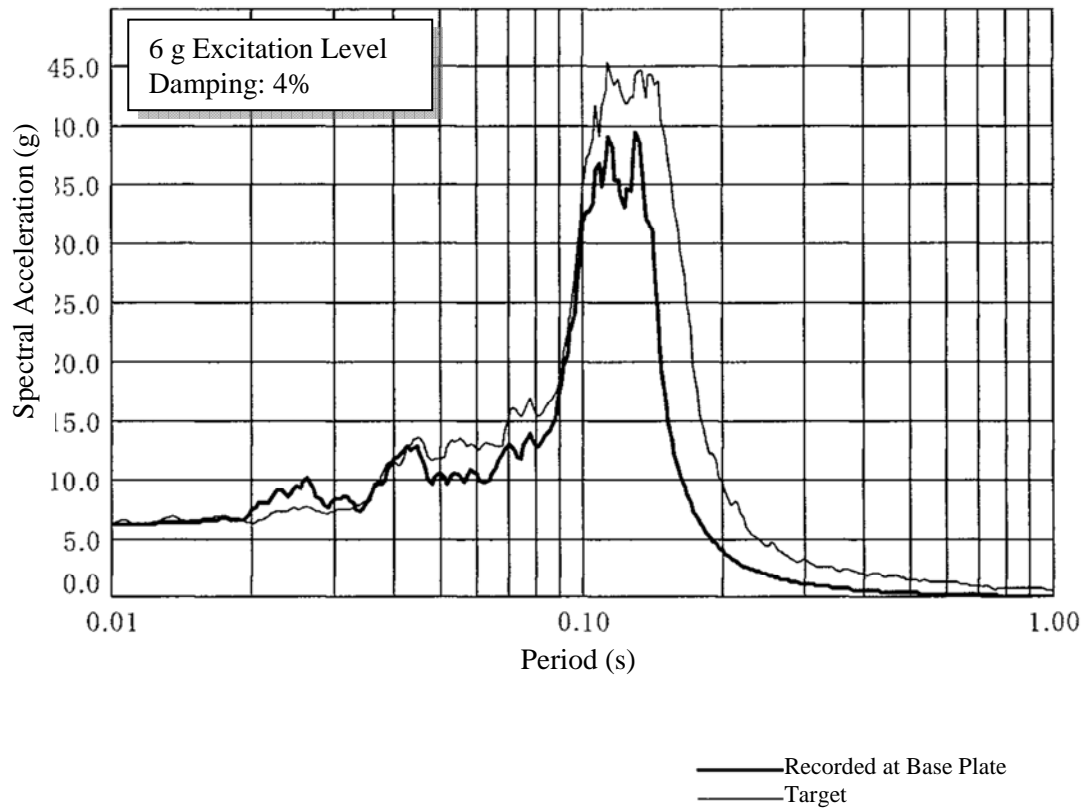


Figure 3-16 Comparison of Front-Back 6 g Level Response Spectra for Reactor Control Center Test

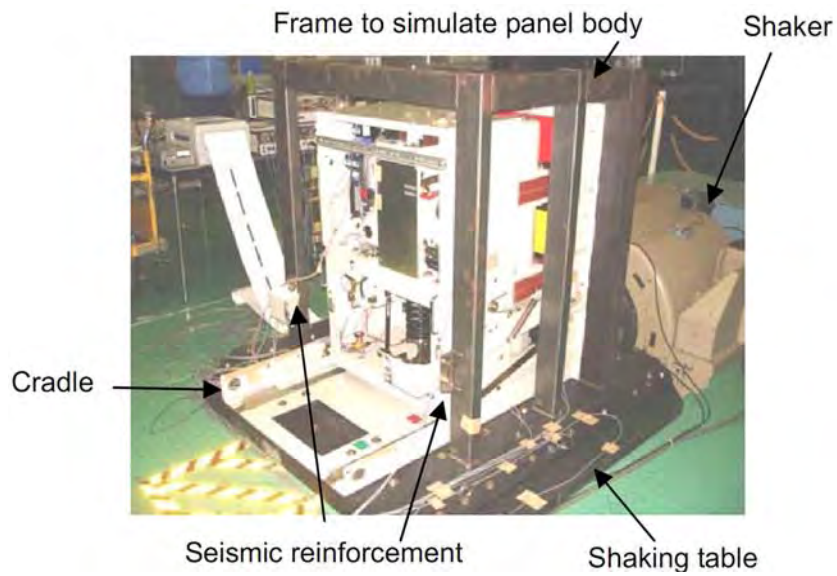
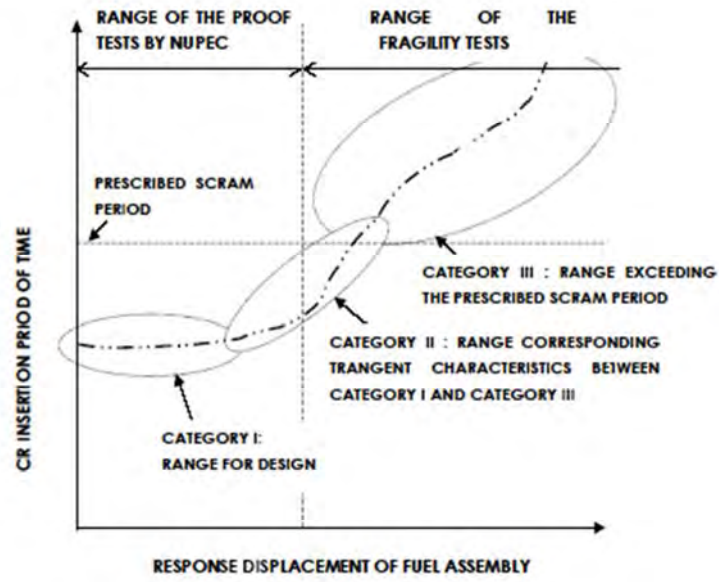


Figure 3-17 Gas Circuit Breaker Installed on a Support Frame in Element Test



FUNCTION OF CR INSERTION

Figure 3-18 JNES Target Range of the Fragility Tests



Figure 3-19 Test Setup for PWR Control Rod Insertion System



Figure 3-20 Mockup of A PWR Fuel Assembly

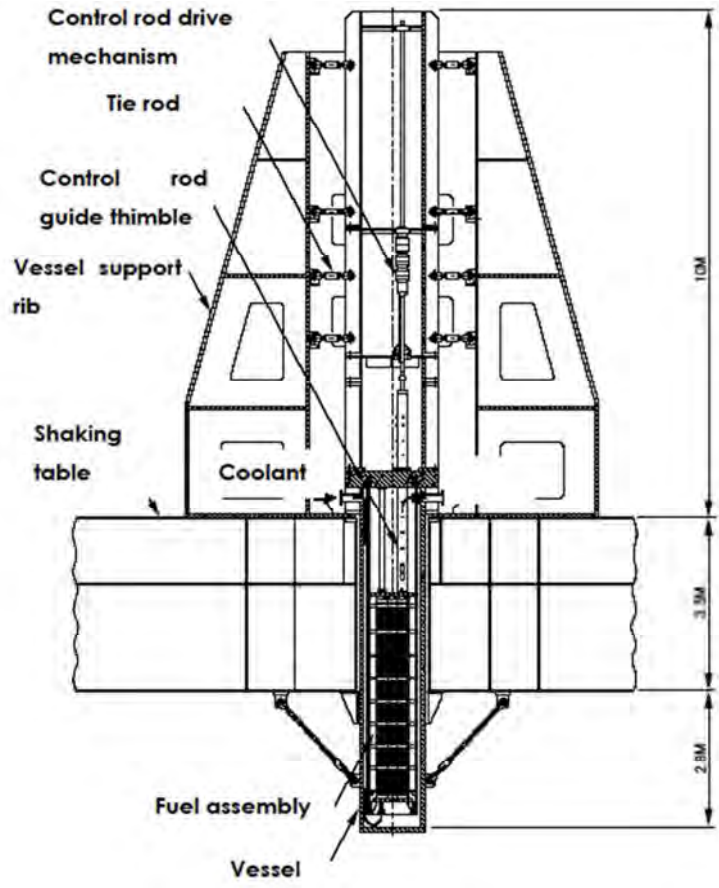


Figure 3-21 Section View of the Test Setup for PWR Control Rod Insertion System

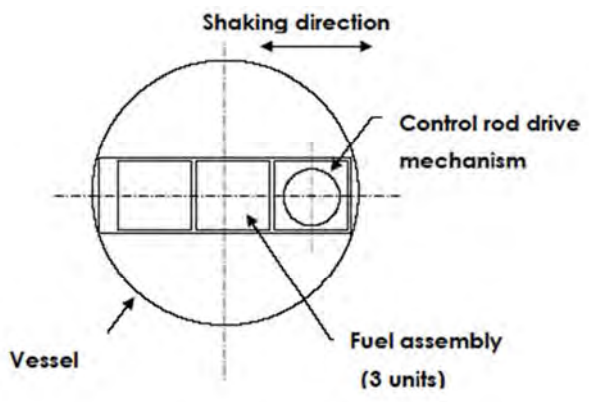


Figure 3-22 Layout of 3 PWR Fuel Assemblies

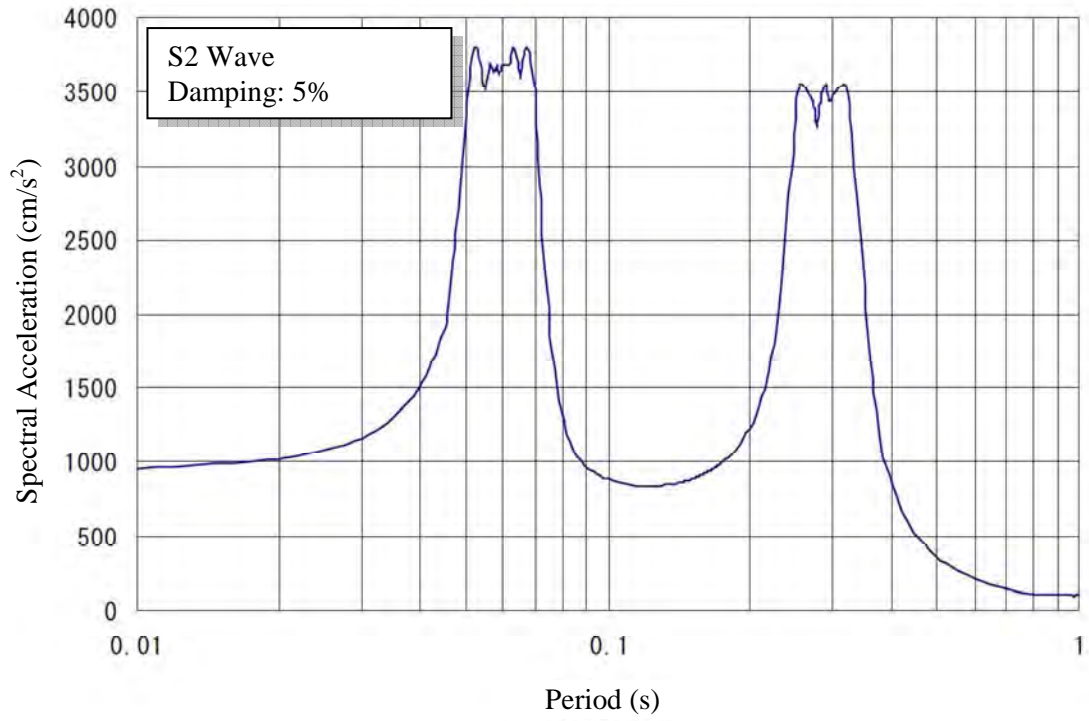


Figure 3-23 Synthesized Wave for Full-Scale Test of PWR CRDM

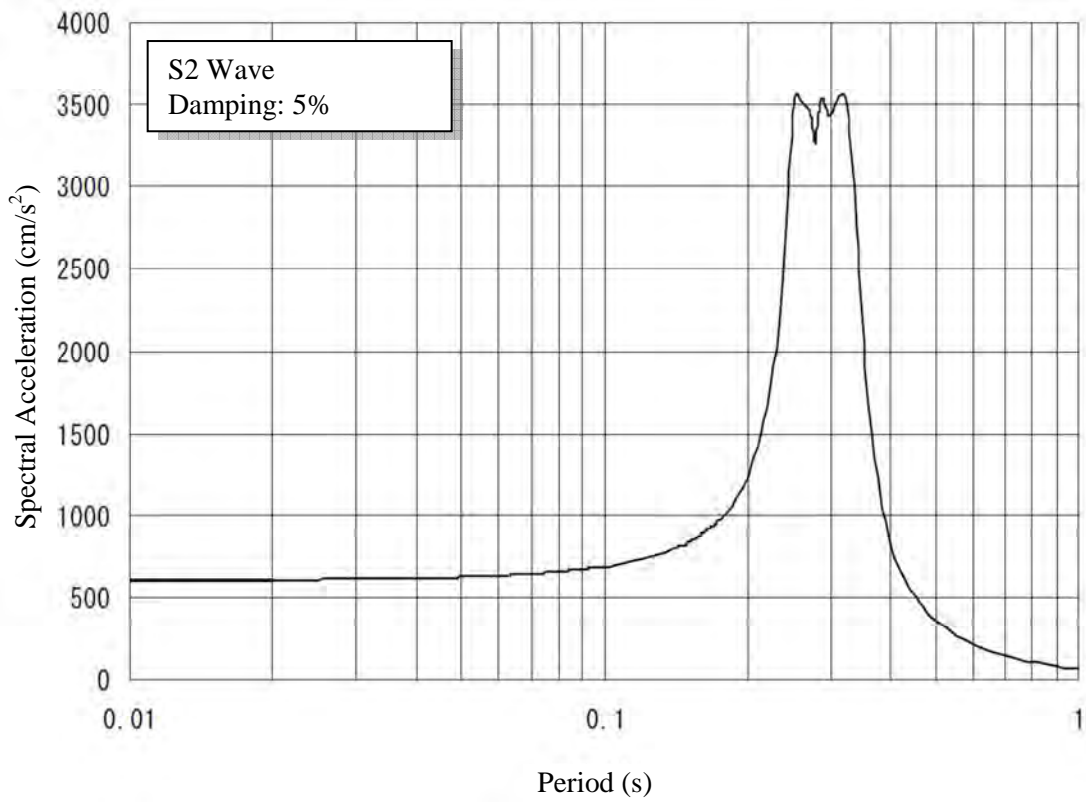


Figure 3-24 Filtered Wave for Fuel Excitation

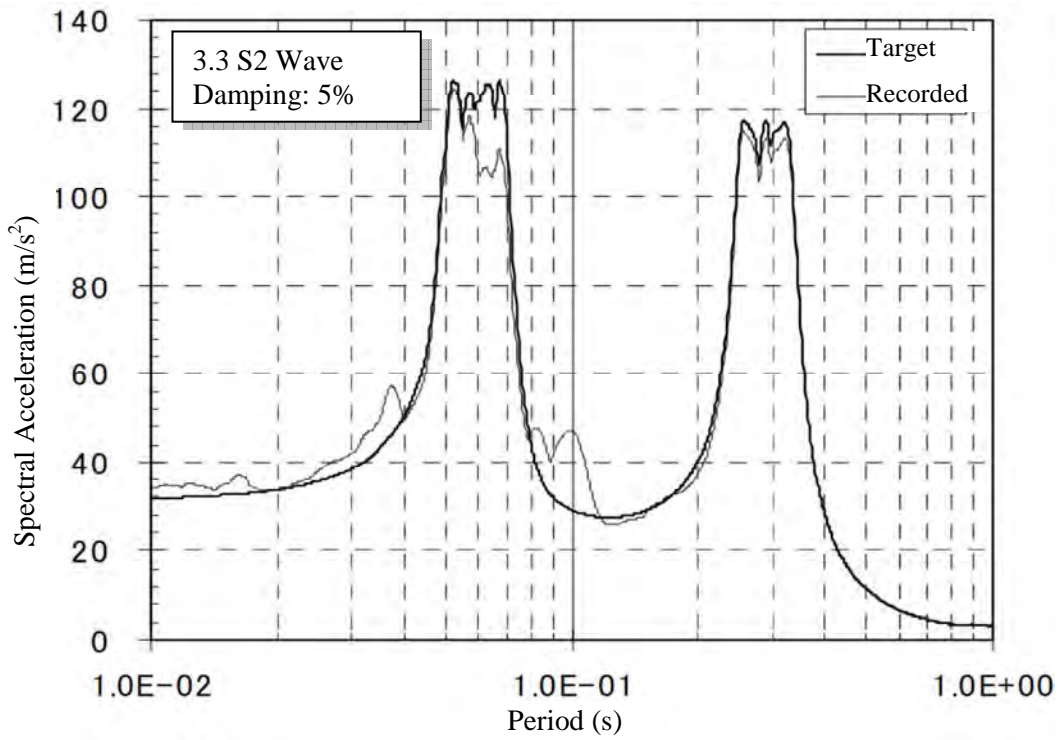


Figure 3-25 Comparison of PWR CRDM Target Input and Shaking Table Response (Still Water)

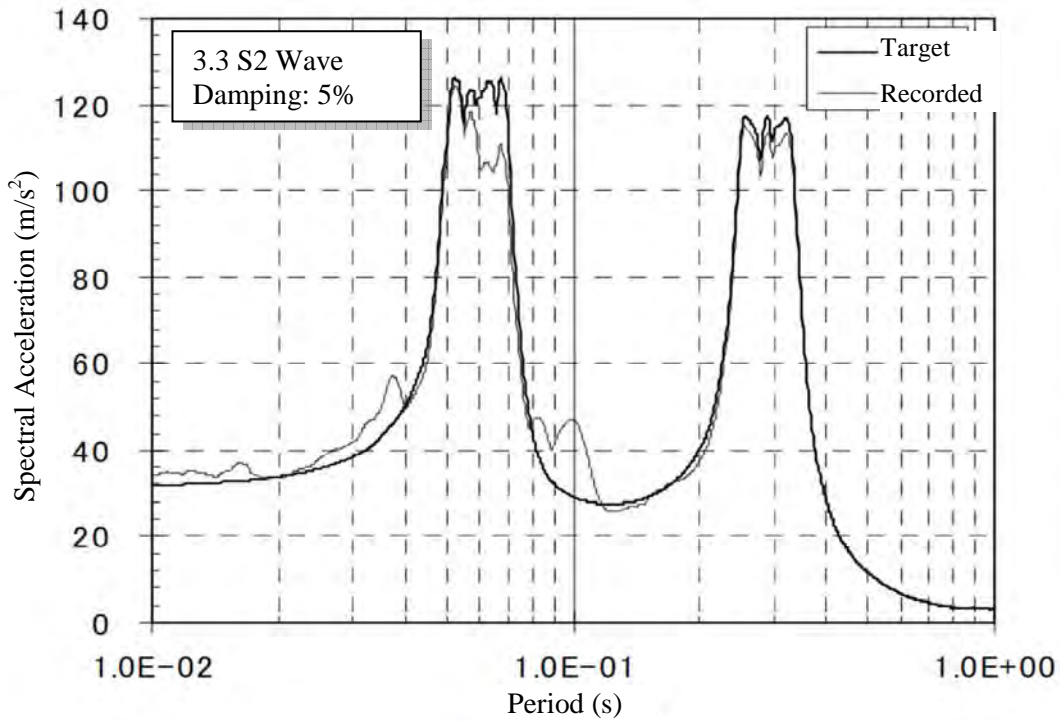


Figure 3-26 Comparison of PWR CRDM Target Input and Shaking Table Response (With Core Flow)

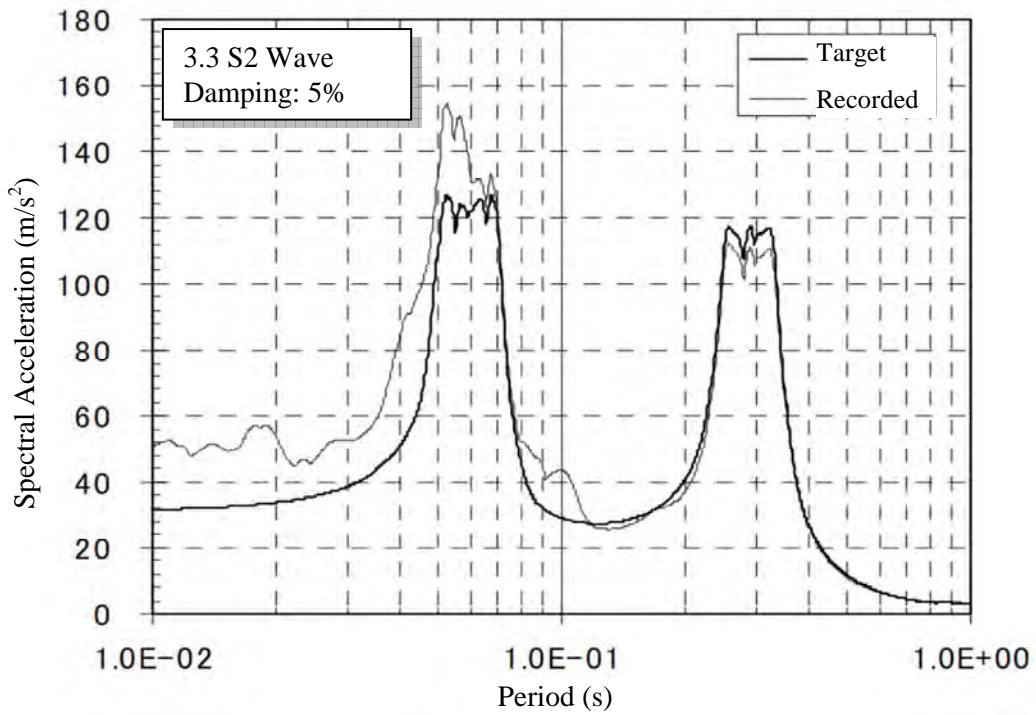


Figure 3-27 Comparison of PWR CRDM Target Input and Upper Core Plate Response (Still Water)

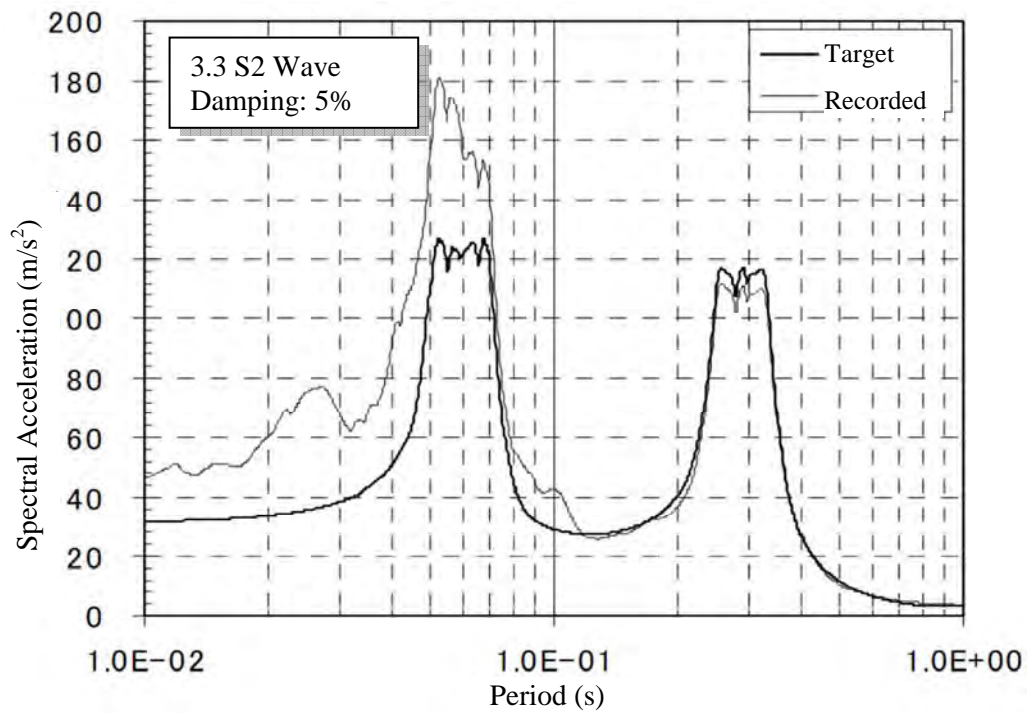


Figure 3-28 Comparison of PWR CRDM Target Input and Lower Core Plate Response (Still Water)

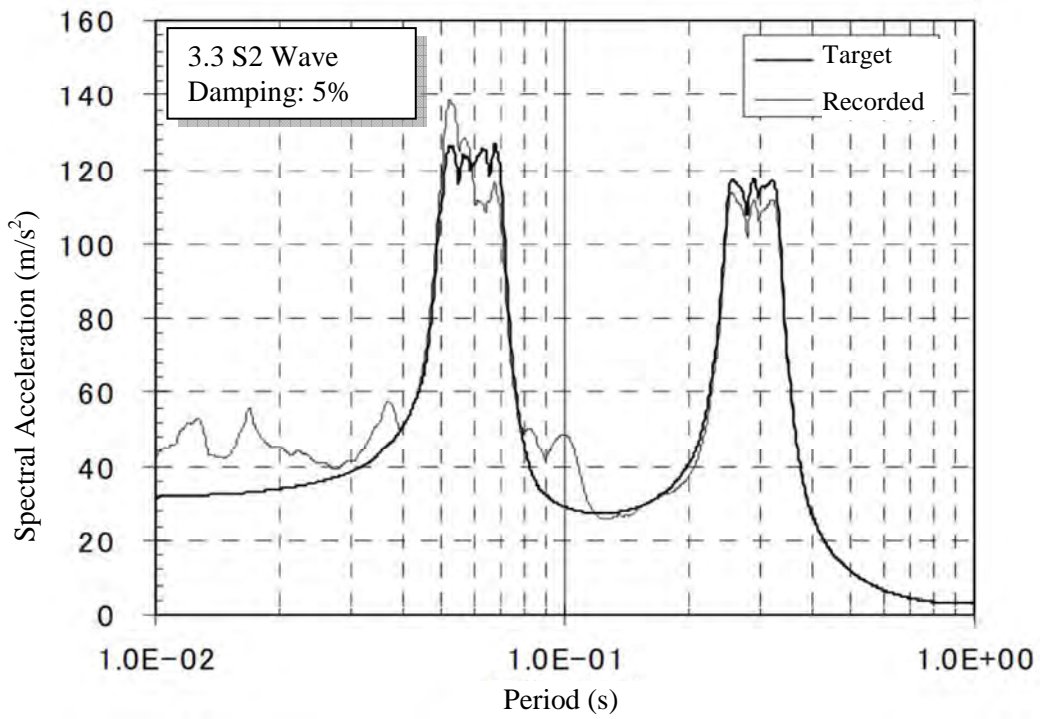


Figure 3-29 Comparison of PWR CRDM Target Input and CRDM Base Response (Still Water)

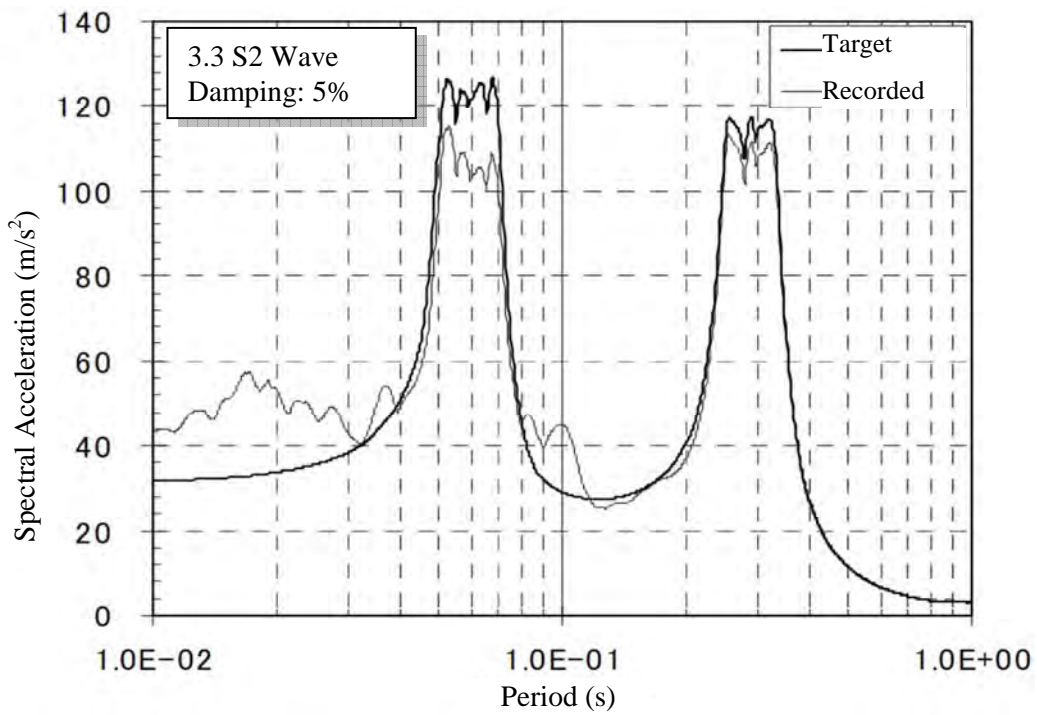
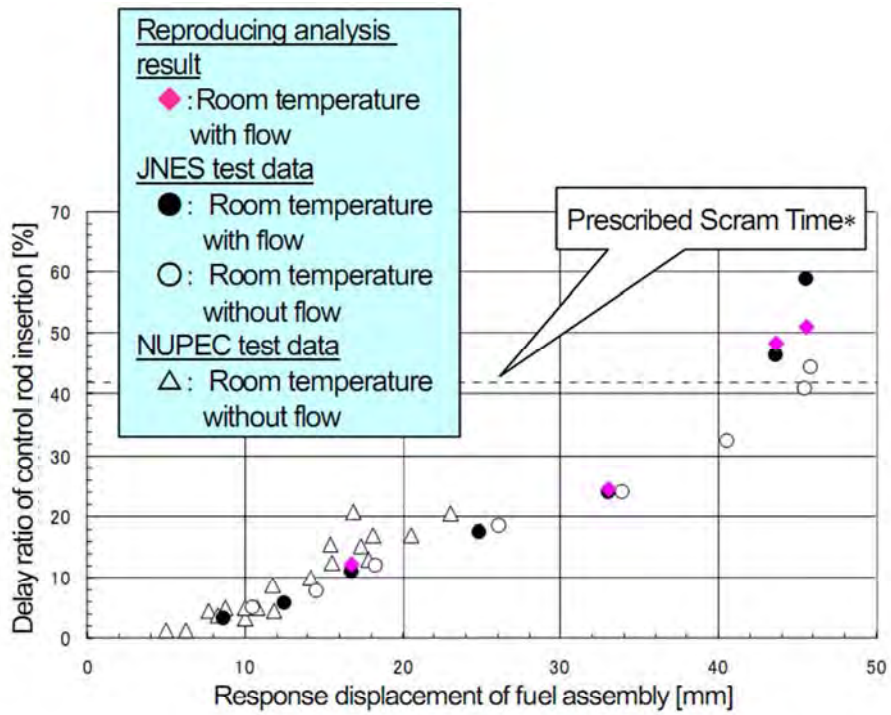


Figure 3-30 Comparison of PWR CRDM Target Input and Upper Core Support Plate Response (Still Water)



*: Prescribed time in safety evaluation: 2.2sec. (85% insertion time). Exceeding it does not directly result in a problem.

Figure 3-31 Delay Ratio of PWR Control Rod Insertion



Figure 3-32 Test Setup for BWR Control Rod Insertion System



Figure 3-33 Mockup of A BWR Fuel Assembly

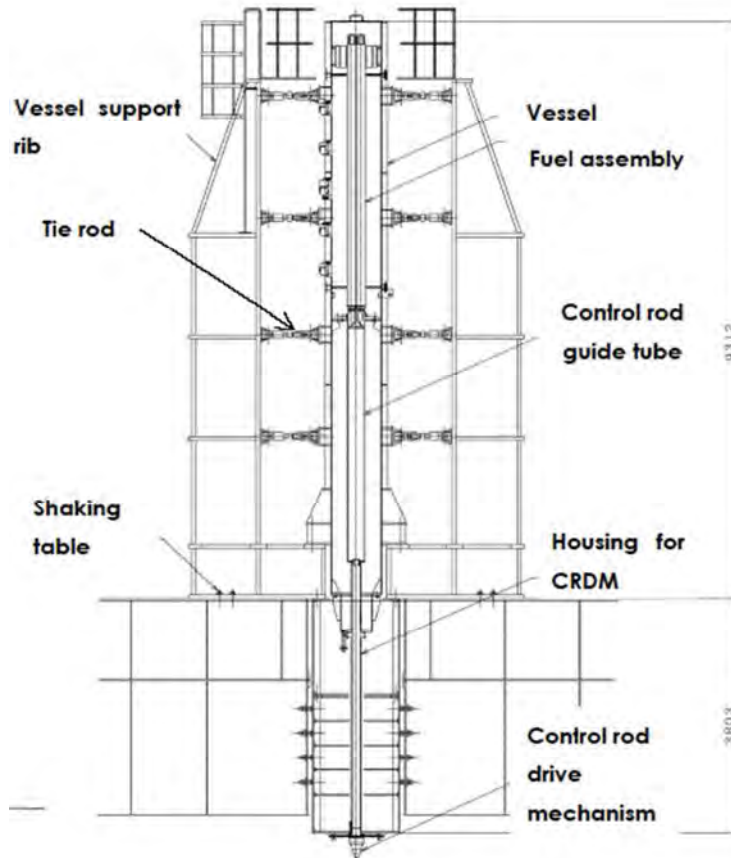


Figure 3-34 Section View of the Test Setup for BWR Control Rod Insertion System

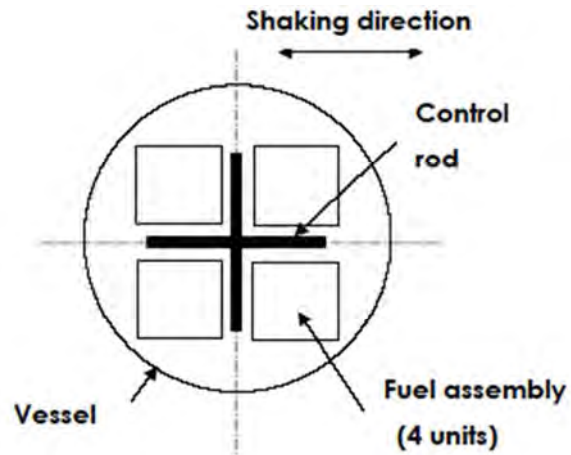


Figure 3-35 Layout of a BWR Fuel Assembly

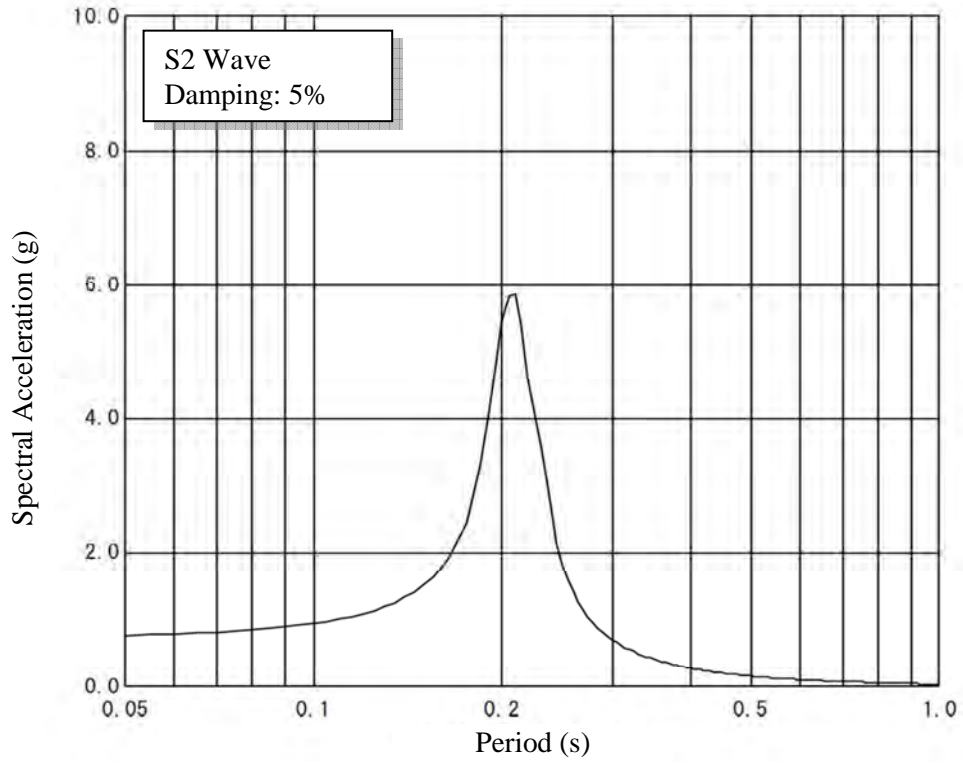


Figure 3-36 BWR CRDM Basis Input Wave C with Center Frequency 4.8 Hz

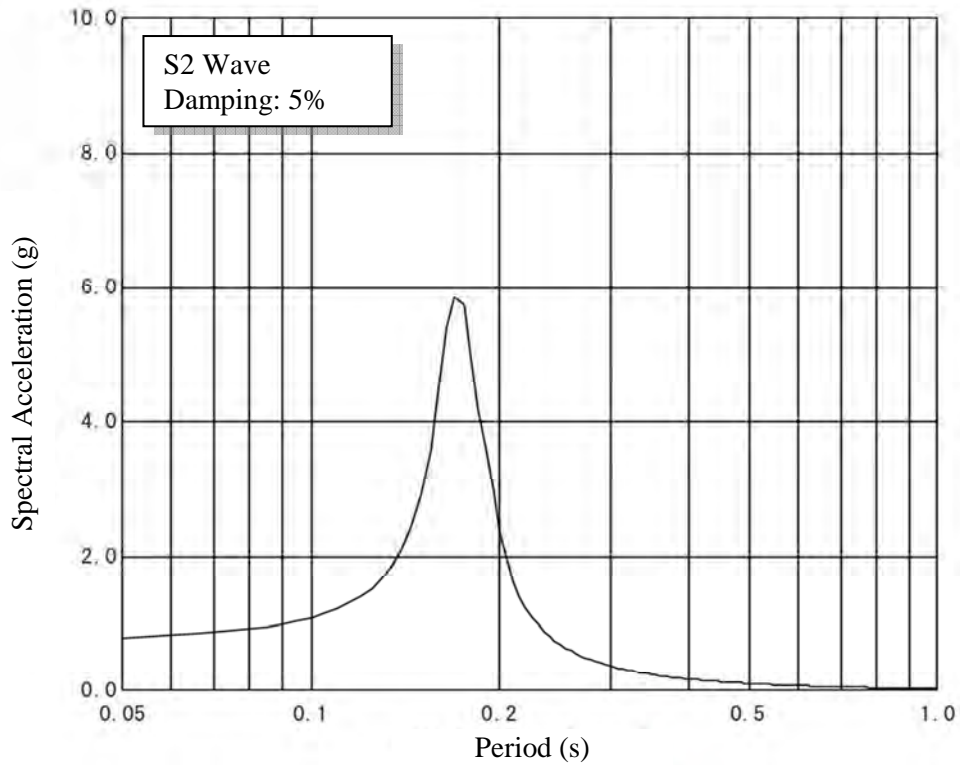


Figure 3-37 BWR CRDM Basis Input Wave C with Center Frequency 5.8 Hz and 10% broadening

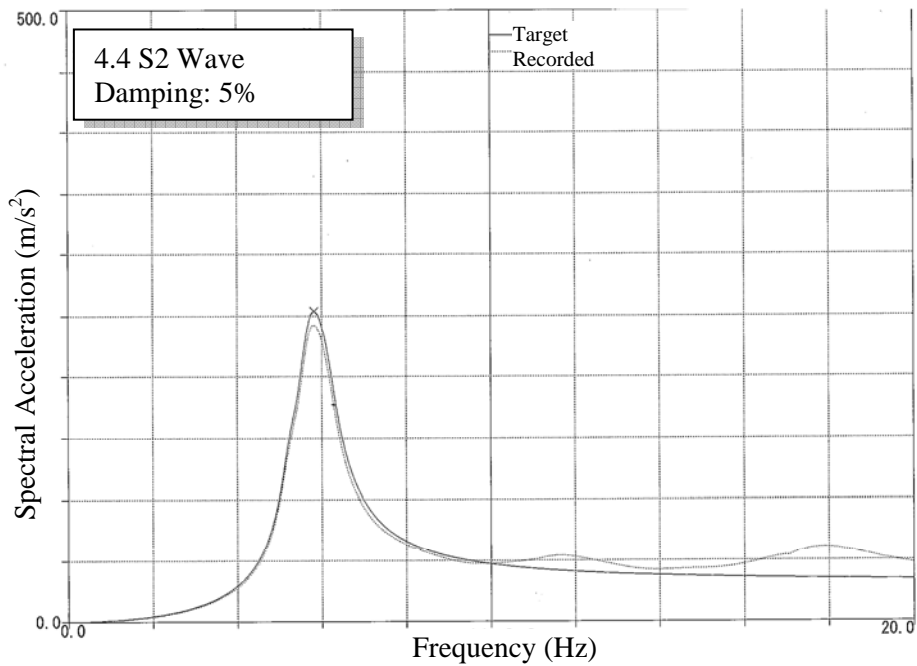
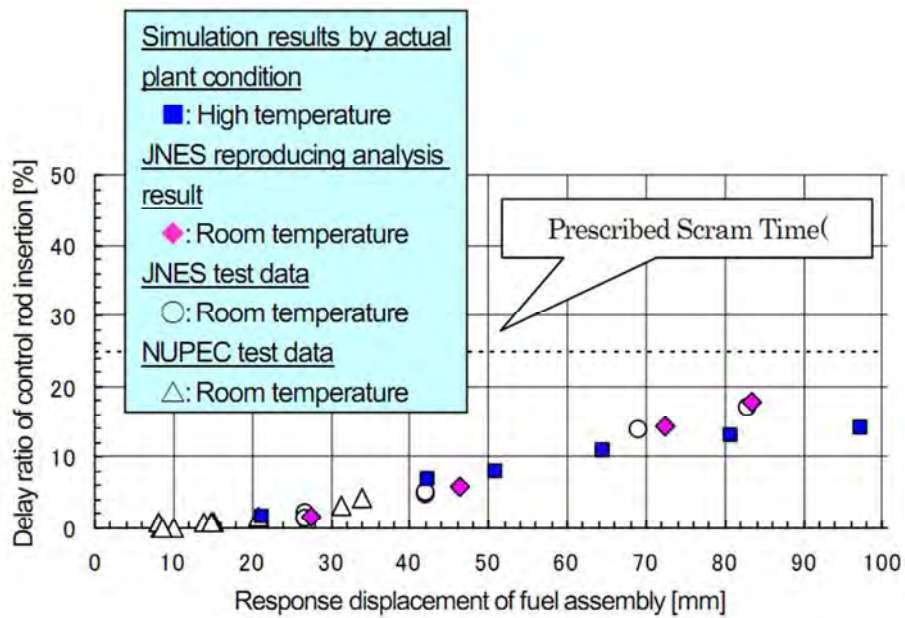


Figure 3-38 Comparison of BWR Target Input and Shaking Table Response



(: Prescribed time in safety evaluation: 1.62 sec. (75% insertion time). Exceeding it does not directly result in a problem.

Figure 3-39 Delay Ratio of BWR Control Rod Insertion

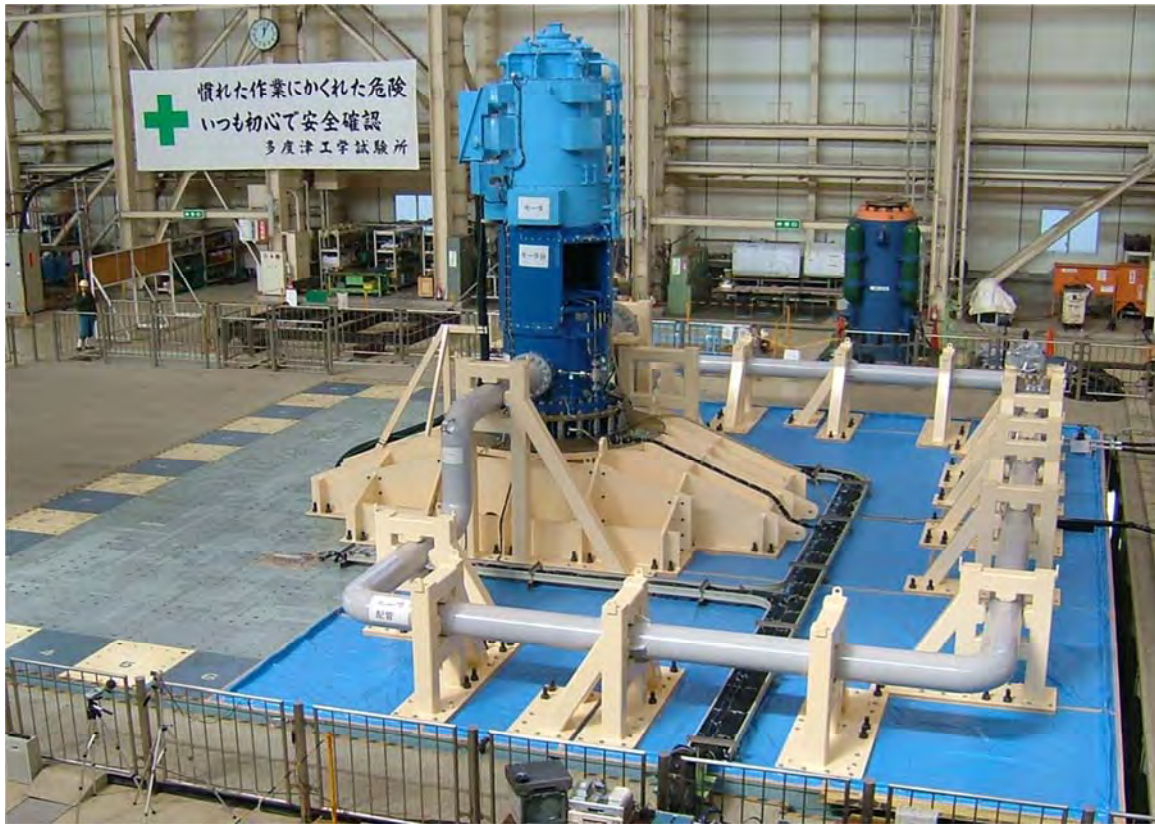


Figure 3-40 Test Setup for Vertical Shaft Pump

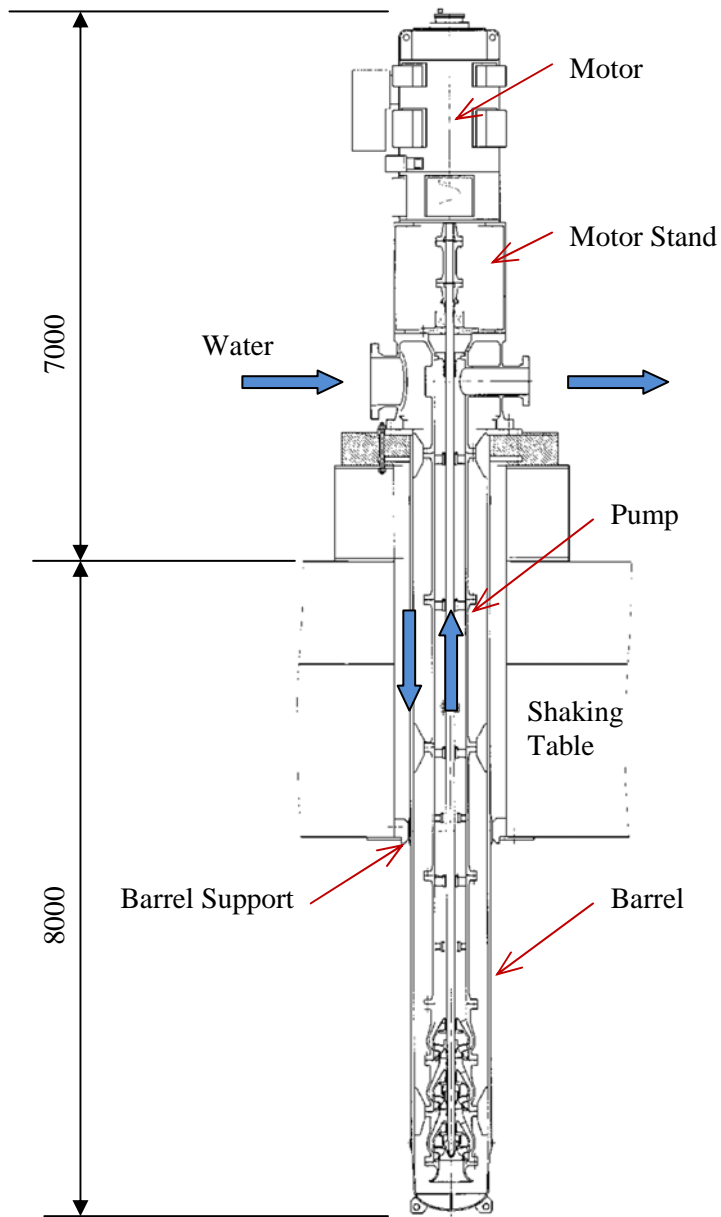


Figure 3-41 Section View of the Test Setup for Vertical Shaft Pump

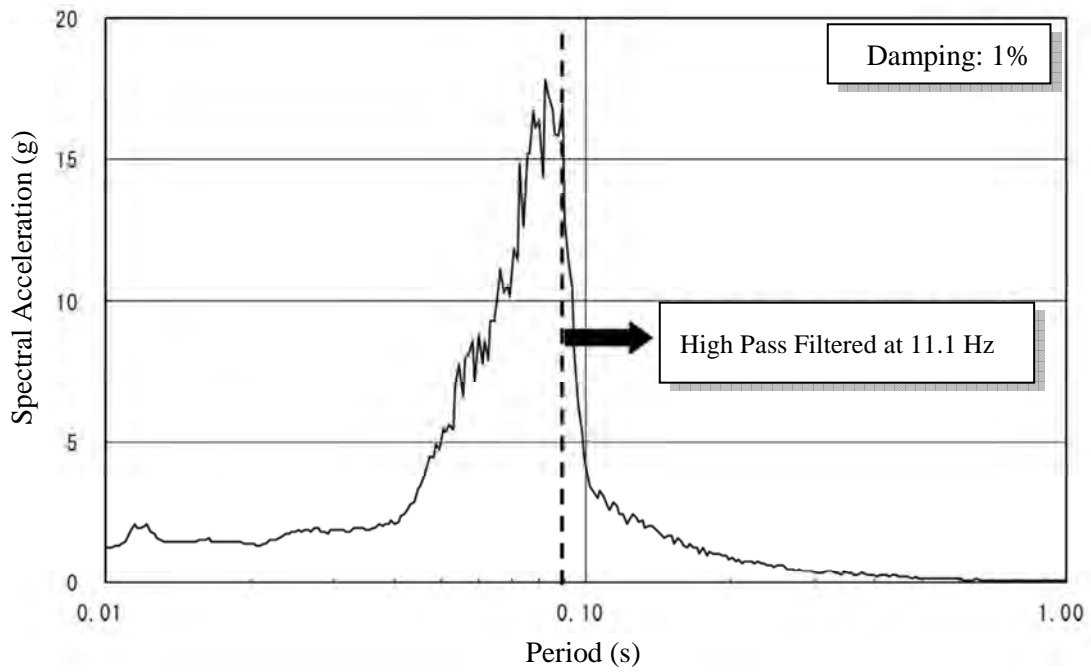


Figure 3-42 Response Spectrum for A-Wave

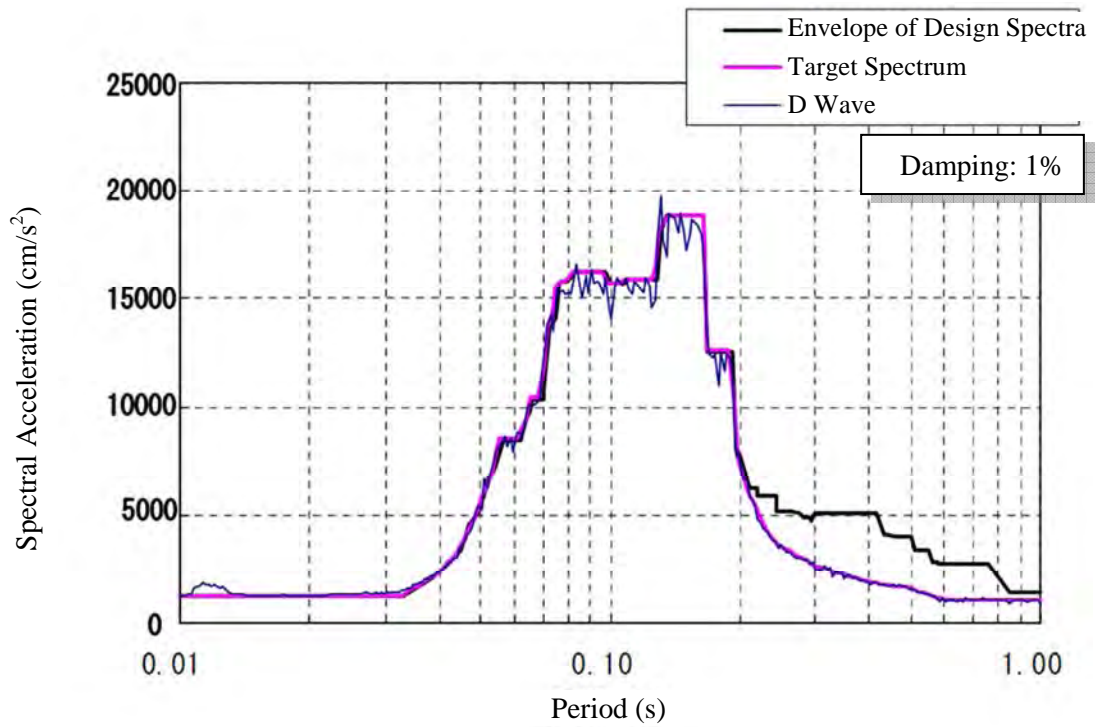


Figure 3-43 Response Spectra for D-Wave (Horizontal)

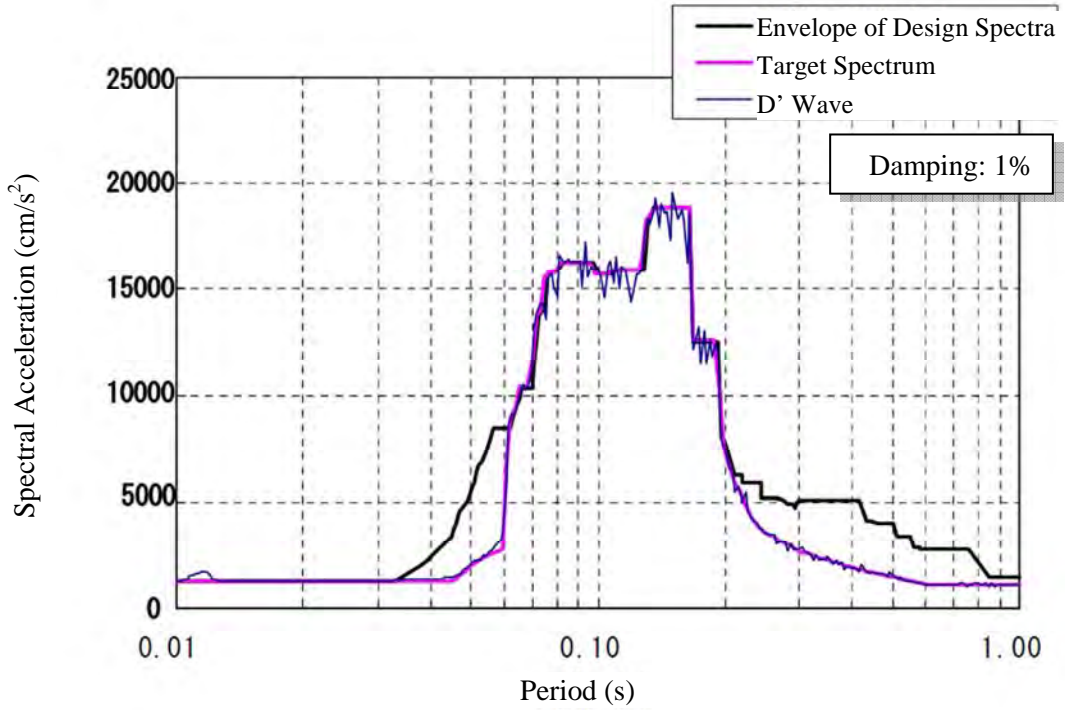


Figure 3-44 Response Spectra for D'-Wave (Horizontal)

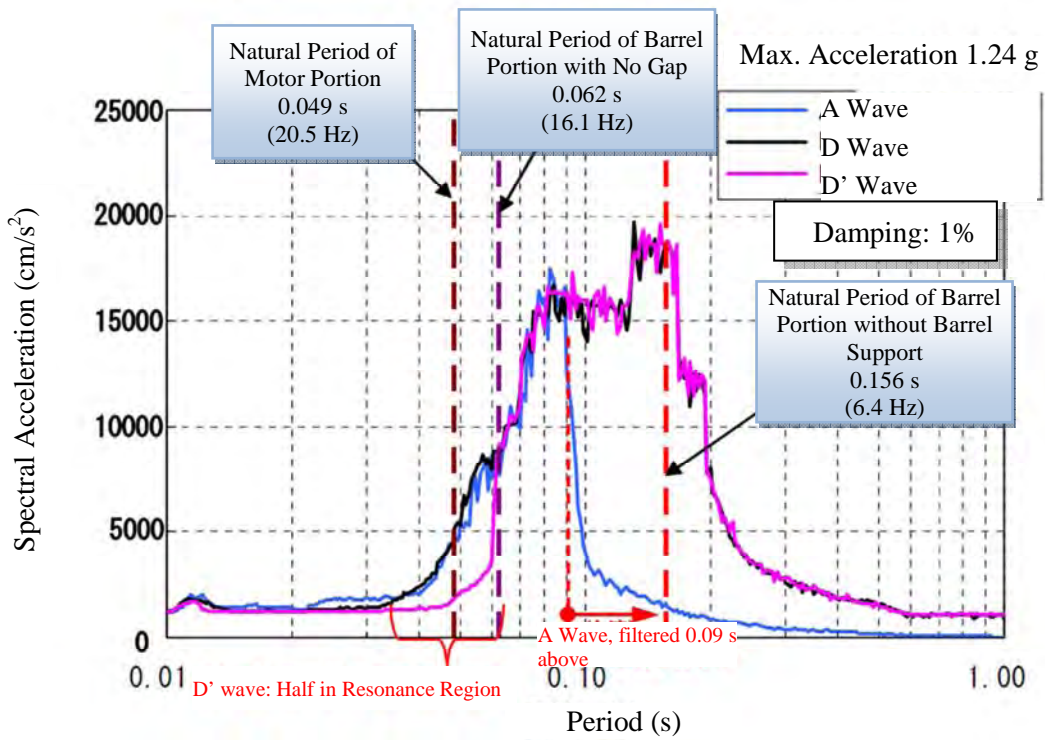


Figure 3-45 Comparison of A, D, and D' Waves

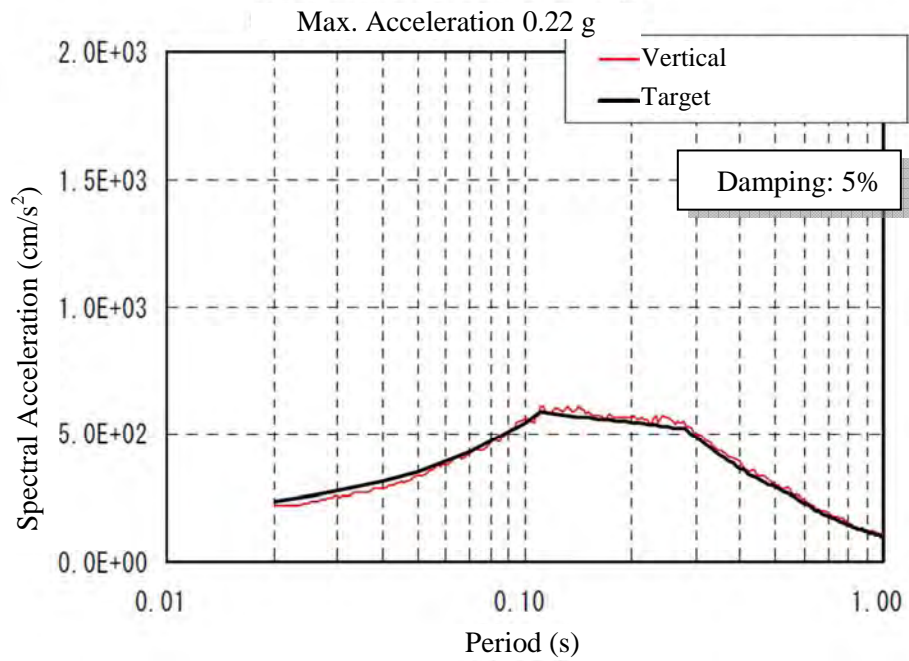


Figure 3-46 Response Spectra for Vertical Wave



Figure 3-47 Liner Ring and Shaft Bearing

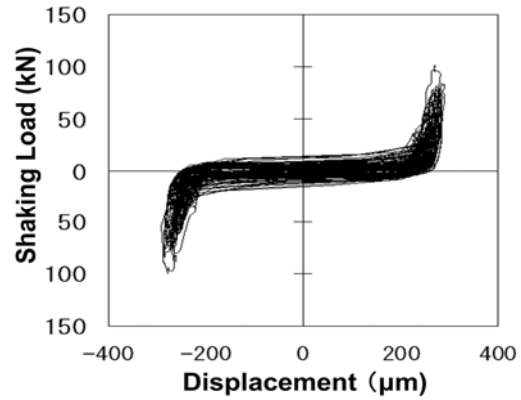
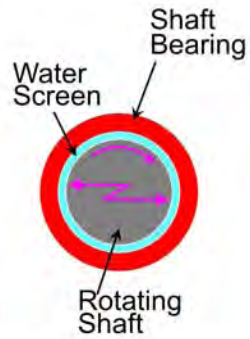


Figure 3-48 Illustration of Shaft Bearing and the Nonlinear Load-Displacement Behavior

(i) Pit barrel type (BWR)	(ii) Vertical mixed flow type (BWR/PWR)	(iii) Vertical single-stage floor type (BWR/PWR)
<p>500MW/800MW/1100MW</p> <ul style="list-style-type: none"> • Residual heat removal system (RHR) pump • LP core spray system pump • HP core spray system pump 	<ul style="list-style-type: none"> • Seawater pump (RSW/SWP) 	<p>500MW/800MW/</p> <ul style="list-style-type: none"> • Residual heat removal system pump • Core spray system pump

Figure 3-49 Structural Types of Large Size Vertical Shaft Pumps

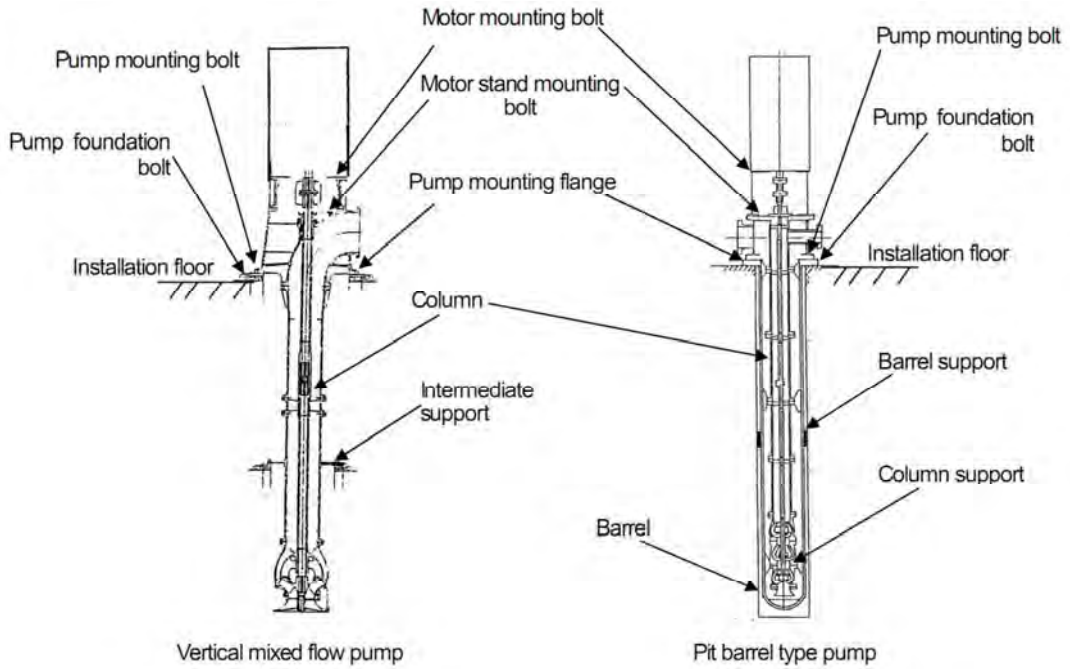
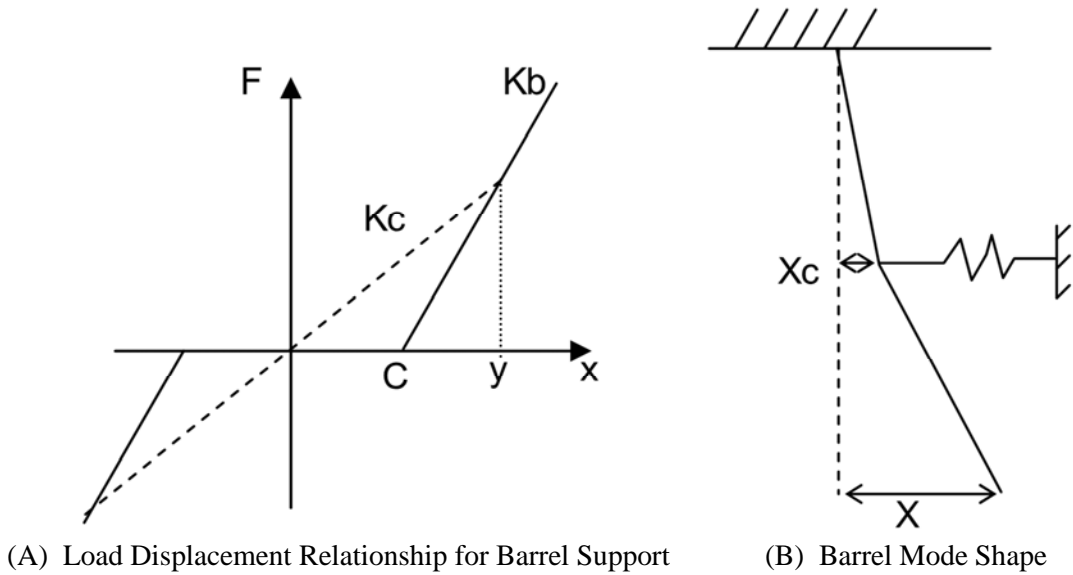


Figure 3-50 Similar Structural Features of Vertical Mixed Flow Pump and Pit Barrel Type Pump



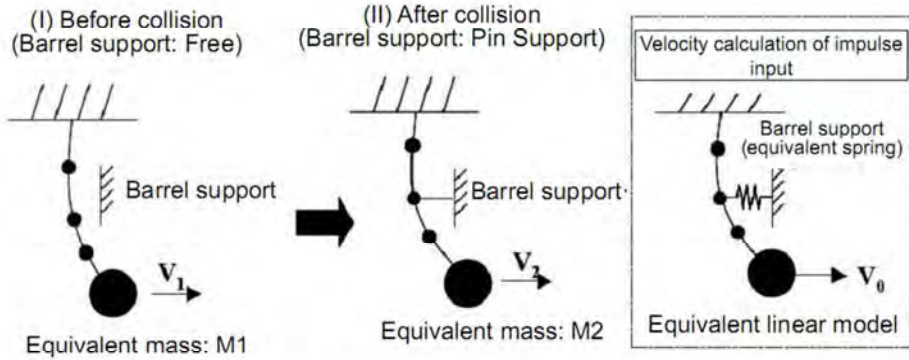
Note: K_b : barrel support stiffness
 K_c : Linearized stiffness for the equivalent linear analysis
 C : clearance of barrel support
 X and X_c : mode vector

Figure 3-51 Equivalent Linear Stiffness of Barrel Support

$$F\Delta t = M_1V_1 - M_2V_2$$

M_1, M_2 : Equivalent mass of fundamental vibration mode before and after collision

V_1, V_2 : Velocity before and after collision



(d) Momentum change of fundamental vibration mode before and after collision

Equivalent mass, M_1, M_2 : Calculated by eigenvalue analysis
 Velocity $V_1, V_2=V_0$: Assume that velocity is not change just before and just after collision. Use the velocity in response analysis using equivalent linear model.

Figure 3-52 Calculation of Impulsive Force

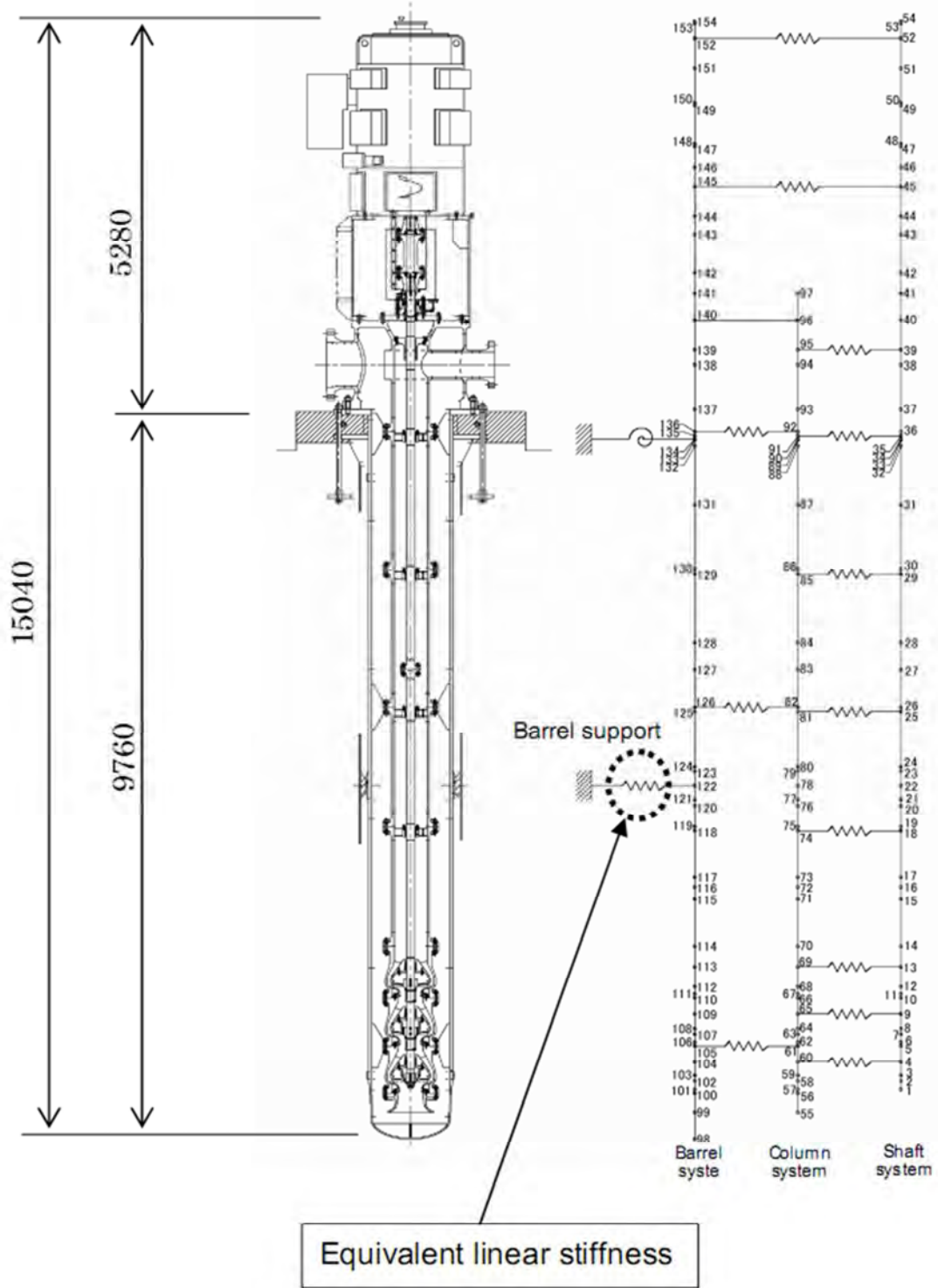


Figure 3-53 Stick Model for the Pit Barrel Type Pump

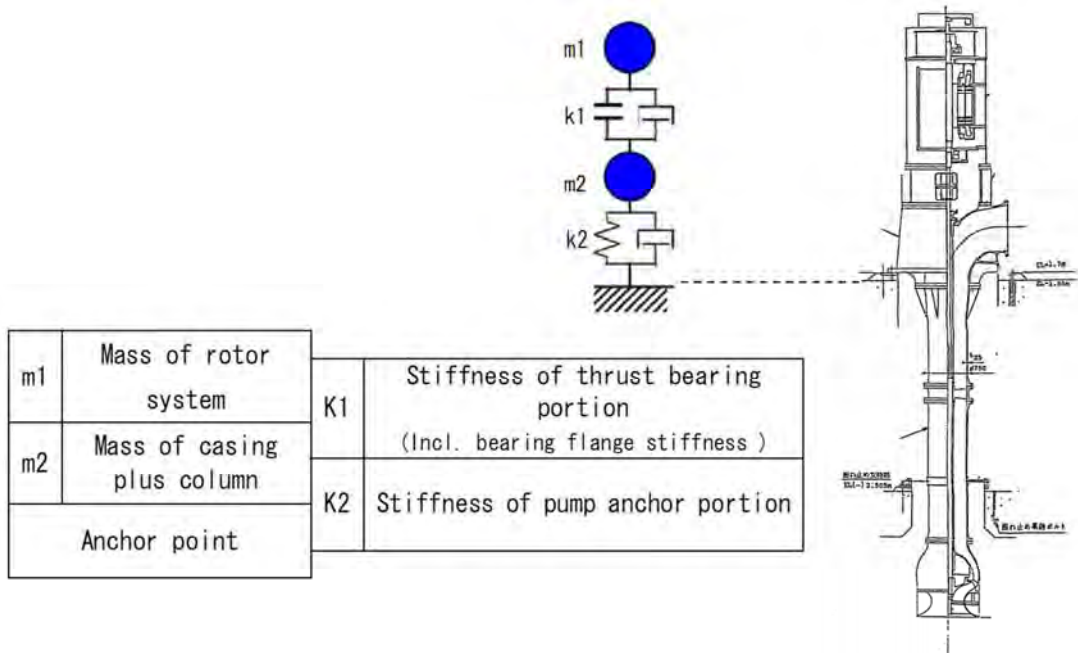


Figure 3-54 Two Mass Model for the Vertical Response Analysis for the Vertical Shaft Pumps

4 EVALUATION OF JNES EQUIPMENT FRAGILITY TEST DATA

4.1 Introduction

Review and evaluation of the JNES equipment test results are based on the JNES equipment fragility test report [JNES, 2009], which is included in Appendix A of this report, and the JNES status presentations [Uchiyama, 2008a, b]. The purpose of this evaluation is to:

- compare the JNES fragility results with the fragility data typically used in current U.S. seismic probabilistic risk assessments (SPRAs),
- assess the impact that the new test results may have on current SPRAs and how this data can be utilized for future SPRAs.

As described in the previous section, JNES has performed a series of high amplitude shake table tests on full-scale components supplemented by additional analyses. The purpose of these tests was to determine the functional seismic fragility levels during strong shaking (called herein “function during” fragility levels) for these components. These full-scale component tests were generally limited by the shake table capability to about 6.0g zero period acceleration (ZPA). If no functionality anomaly occurred prior to reaching the upper limit of the testing, a function confirmed (FC) capacity was reported. In this case, no fragility level was actually found, and the reported median fragility was set either at or only slightly above the FC capacity. For situations where a functional anomaly was observed, the reported median fragility was set midway between the highest ZPA level for which no functional anomaly occurred, and the ZPA level at which the anomaly occurred.

One of the primary objectives of these JNES tests was to test full-scale components at shaking levels significantly higher than the function confirmed qualification tests to which they had previously been subjected. Therefore, these tests greatly improve the median fragility estimates for the specific components tested. In this regard, they provide a very valuable addition to the available fragility data base for U.S. NPPs. However, an open question exists as to how well this JNES fragility data can be extrapolated to similar components in U.S. NPPs. This section of the report will be devoted to address this issue.

As discussed in Section 3, the JNES equipment fragility report presents detailed fragility information for the Phase I four classes of components:

- Electrical components and devices mounted therein
- Horizontal shaft pumps
- Large vertical shaft pumps
- Control rod insertion capability

The review of the JNES equipment fragility tests focused on these Phase I four classes of components. As additional information is provided by JNES, a supplement to this report will be prepared to address additional classes of equipment.

The bases presented in the JNES equipment fragility report were reviewed for the median fragilities reported therein for the specific components considered in the four classes. These reported fragilities are based on a combination of full-scale component shake table testing, device (element) shake table testing, and analyses. It can be stated categorically that a very comprehensive and conscientious effort appears to have been performed to develop realistic

median fragility estimates for the specific components being considered. Therefore, it can be concluded that the median fragilities reported in the JNES equipment fragility report [JNES, 2009] and summarized in this report are reasonable for the specific components considered in each of the four classes.

Therefore, the next four subsections will concentrate on (1) comparing the JNES fragility results with the fragility data typically used in current U.S. SPRAs and (2) assessing the impact that the new test results may have on current U.S. SPRAs and how this data can be utilized for future SPRAs. The purpose of this assessment is to provide comparisons and assessments of the applicability of the JNES equipment fragility information for similar components in existing U.S. NPPs.

For the purposes of making comparisons, Section 2 of this report presents a summary of common U.S. practice for estimating seismic fragilities for equipment that has been qualified by test. The emphasis of Section 2 is to present generic fragility estimates that are commonly used for Central and Eastern U.S. (CEUS) SPRAs. Examples of such fragility estimates are presented in Table 2-2 through Table 2-6. Of course, higher fragility capacities can generally be justified for any specific component by a detailed review of the qualification test data and/or stress analyses performed on that specific component. However, for many components included in CEUS SPRAs, this additional effort is not performed. Instead, generic fragilities similar to those summarized in Section 2 are used. For higher seismic sites, these generic fragilities are generally not used.

All of the generic fragilities summarized in Table 2-2 through Table 2-6 of Section 2 are defined in terms of a broad frequency 5% damped spectral acceleration SA at the base of the component. For these broad frequency generic fragilities summarized in Table 2-2 through Table 2-6 of Section 2, the relationship between the broad frequency 5% damped spectral acceleration SA and the zero period acceleration (ZPA) can be approximated by:

$$SA \approx 2.4 * ZPA \quad (4-1)$$

The JNES fragilities reported in the JNES equipment fragility test report and summarized in Section 3 of this report are commonly defined in terms of ZPA . However, the response spectrum shape used in the JNES tests was very different from the broad frequency response spectrum shape used to define the Section 2 U.S. generic fragilities. As noted in Section 3, the JNES tests typically had more highly amplified and narrower frequency response spectrum shapes. In the JNES tests, the response spectra typically peaked in the 7 to 10 Hz frequency range. Over this narrower frequency range, the ratio of 4% damped spectral acceleration SA to ZPA was about 3.0.

Therefore, between about 7 to 10 Hz, the ratio of SA/ZPA for the JNES tests was higher than the 2.4 ratio defined by Eqn. (4-1) for the U.S. generic fragilities. However, below about 7 Hz and between about 10 to 20 Hz, the SA/ZPA for the JNES tests was lower than the SA/ZPA ratio appropriate for the U.S. generic fragilities summarized in Section 2. This difference in spectra shapes makes it more difficult to make an appropriate comparison between the JNES test results and the U.S. generic fragilities reported in Section 2. It was considered to be most appropriate, on average, to convert the JNES reported ZPA fragilities to equivalent broad frequency 5% damped SA fragilities by the use of Eqn. (4-1) for the purpose of these comparisons.

4.2 Electrical Component Fragilities

For this section, the term “component” is used to define a complete piece of equipment such as a motor control center or control cabinet, and “device” to define an individual element such as a relay within a component.

JNES fragility results are reported in Section 3 and the JNES equipment fragility test report [JNES, 2009] for eight different electrical components. These fragility results are summarized herein in Table 4-1. The reported *ZPA* capacities are directly from the JNES equipment fragility test report. The corresponding 5% damped spectral acceleration *SA* capacities in Table 4-1 have been estimated by Equation 4-1. Reported fragilities followed by (FC) indicate that no anomaly occurred at the highest test level. Therefore these reported values are actually function confirmed qualification values; the actual fragility level is higher than these FC levels.

The fragility levels reported in Table 4-1 for anomalies lie midway between the highest test level for which the function was confirmed and the test level at which the anomaly occurred, which is in accordance with the criteria specified in the JNES equipment fragility test report.

The median *SA*_{50%} fragility levels reported in Table 4-1 based on JNES test data for electrical components range between 5.5g and 14.2g. Generic median *SA*_{50%} fragilities reported in Table 2-2, Table 2-4, and Table 2-5 for similar electrical components range between 2.2g and 5.1g. This comparison indicates that generic fragilities commonly used in U.S. SPRAs for existing CEUS plants might be conservatively biased by more than a factor of two. The JNES test data median *SA*_{50%} fragility levels for electrical components are comparable to the ALWR “achievable” fragilities from EPRI TR-016780 [1999] shown in Table 2-7.

However, considerable caution must be exercised before extending the use of these JNES median fragilities for electrical components to existing electrical components in the U.S. plants. The natural frequencies reported in the JNES equipment fragility test report for all eight tested electrical components ranged between 20 Hz and greater than 50 Hz. All of these electrical components tested by JNES were very stiff and not representative of most similar existing electrical components in U.S. plants. Most of these electrical components in U.S. plants exhibit local panel mode frequencies in the 4 Hz to 15 Hz range when tested at higher shaking levels.

Cabinet response amplification factors AF_C (called *k* in the JNES equipment fragility test report [JNES, 2009]) were reported for representative device mounting locations in each of the eight electrical components considered. For the JNES tested components, these reported response amplification factors ranged between:

JNES Cabinets

$$AF_C = 1.0 \text{ to } 2.5 \quad (4-2)$$

These very low cabinet response amplification factors AF_C for the JNES tested components are not surprising considering that:

- (1) the JNES tested components had natural frequencies in excess of 20 HZ, and
- (2) the JNES test input had very little frequency content in excess of about 12 Hz.

For comparison, Table 2-3 reports generic median AF_C values recommended for use in representative existing U.S. electrical components. These recommended median AF_C values range between:

Existing U.S. Cabinets

$$AF_C = 2.8 \text{ to } 4.4 \quad (4-3)$$

It should be noted that the values in Table 2-3 are median response amplification factors for the worst location in the cabinet whereas the JNES reported values are for representative mounting locations. Even so, the differences are substantial.

Based both on the natural frequency comparisons, and the response amplification comparisons, it appears that the JNES tested electrical components are much stiffer than most electrical components in existing U.S. plants. However, they might be representative of electrical components to be used in new U.S. standard plants not yet built.

Therefore, the JNES reported median fragilities shown herein in Table 4-1 should not be used for U.S. electrical components unless it can be shown that the component has stiffnesses similar to those tested by JNES. In particular, the minimum natural frequency at high shaking levels should be in excess of 20 Hz before using the median fragility levels shown in Table 4-1 for an electrical component.

In addition to full-scale electrical component testing, the JNES equipment fragility test report also presents either function confirmed data or fragility data on 37 types of devices (elements) mounted within electrical components. Each type of device included a number of individual devices in the test. Seismic time history tests were conducted up to a $ZPA=10g$ level or slightly higher. Therefore, this data provides very high amplitude fragility data for these 37 tested devices. This data is directly usable for future U.S. SPRAs because the tested devices are identified by manufacturer and model number (see Table 3-9 for a summary of the fragility data for electrical parts, and pages A-64 through A-78 of Appendix A for details).

Fragility data is provided on:

- 3 protective relays
- 3 auxiliary relays
- 1 timing device
- 12 control equipment devices
- 4 pressure transmitters
- 2 magnetic contactors
- 3 molded case circuit breakers
- 3 switches
- 3 air circuit breakers
- 1 vacuum circuit breaker
- 1 gas circuit breaker
- 1 grounded potential transformer

All but 8 of these 37 types of devices had function confirmed (FC) at *ZPA* of about 10g or slightly higher. Thus, their device fragility level is even higher than *ZPA* of 10g for seismic input at the device mounting location.

The eight types of devices for which loss of function occurred were:

- 1 protective relay: *ZPA* \approx 9.0g
- 1 auxiliary relay: *ZPA* \approx 5.9g
- 1 AC controller card: *ZPA* \approx 7.0g
- 2 air circuit breakers: *ZPA* \approx 3.5g*
- 1 vacuum circuit breaker: *ZPA* \approx 4.4g
- 1 gas circuit breaker: *ZPA* \approx 3.5g*
- 1 grounded potential transformer: *ZPA* \approx 2.5g*

Subsequent to the initial test, additional seismic reinforcement was added to the devices identified above with an asterisk (*) and their capacities were increased. It should be noted that for these loss of function device types, the capacities listed above represent the smallest; the other specimens in the same device group exhibited higher capacities, for example, one protective relay succeeded at a *ZPA* of 10.9g in the test.

With the exception of the air and gas circuit breakers, and the grounded potential transformer, all of these device fragilities exceed the median fragility level used for similar devices in existing U.S. SPRAs which have often been based on EPRI NP-7147 [Merz, 1991b]. The circuit breaker and transformer capacities are consistent with those used in existing U.S. SPRAs.

The JNES electrical equipment device fragility data is a highly valuable resource for future SPRAs.

4.3 Large Horizontal Shaft Pumps

As described in Section 3, JNES performed a full-scale test on one reactor building closed cooling water (RCW) pump (single stage centrifugal type) that was 9-feet long by 4.4-feet high. This tested pump appears to be very similar to RCW pumps in U.S. nuclear plants. Therefore, it is judged that this test result could be used to estimate the median fragility of RCW pumps in U.S. plants.

For the tested pump, function was confirmed at:

$$\begin{array}{ll} \text{RCW Pump} & \\ & \text{ZPA} \approx 6.0\text{g (FC)} \end{array} \quad (4-4)$$

which indicates that the median fragility level should be set at a *ZPA* level somewhat higher than 6.0g.

JNES also performed fragility tests on two sizes of deep groove ball bearings and one type of angular ball bearing. The load to generate sufficient friction to result in a decrease of bearing operating life was confirmed to exceed 20 kN (4.4 kips) in the thrust direction and somewhat higher in the radial direction for deep groove ball bearings. The function confirmed load for the tested angular ball bearing was 60 kN (13.5 kips) in the thrust direction.

JNES performed analyses to compute the *ZPA* levels at which bearing wear would result in decreased operating life. These analyses were performed for two different size RCW pumps and one Charging High Pressure Injection pump (multi-stage centrifugal type). Based on these analyses, the following median bearing wear functionality limits were computed by JNES:

Bearing Wear Median Fragility

$$\begin{aligned} \text{Tested RCW Pump: } ZPA_{50\%} &= 8.4\text{g} \\ \text{Larger RCW Pump: } ZPA_{50\%} &= 8.6\text{g} \\ \text{Charging Injection Pump: } ZPA_{50\%} &= 17.3\text{g} \end{aligned} \tag{4-5}$$

JNES also calculated the median capacity of the pump frame anchorage to the foundation and the capacity at which the motor might slip on the pump frame potentially resulting in damage to the pump shaft and/or bearings. The pump frame to foundation anchorage median capacities reported in the JNES equipment fragility test report for the three evaluated pumps ranged between $ZPA=11.0\text{g}$ to 28.5g and were not controlling.

The potentially controlling fragility appears to be slip of the motor on the pump frame due to inadequate torqueing of the mounting bolts and oversize bolt holes. The JNES equipment fragility test report calls the computed fragility for this onset of motor slip failure mode a reference fragility. The reported computed values for this onset of motor slip reference fragility are:

Motor Slip Reference Fragility

$$\begin{aligned} \text{Tested RCW Pump: } ZPA &= 6.1\text{g} \\ \text{Larger RCW Pump: } ZPA &= 5.3\text{g} \\ \text{Charging Injection Pump: } ZPA &= 2.6\text{g} \end{aligned} \tag{4-6}$$

The onset of motor slip reference fragilities were based on a coefficient of friction of 0.3. It is not reported what bolt tightening force was assumed in these slip calculations.

There is considerable uncertainty in the coefficient of friction that should be used in these slip calculations. For a specified minimum bolt torque applied to the mounting bolts, there is significant variability in the bolt tension preload. There are limits as to how far the motor might slip due to oversized or slotted bolt holes. It is also not known how much motor slip is likely to damage the pump shaft and/or bearings. It would be highly desirable to have additional testing performed to address the topic of horizontal pump functionality limits associated with motor slip on pump frames. This mode may be a controlling functionality failure mode for large horizontal pumps.

For large and critical horizontal pumps such as RCW pumps and Charging High Pressure Injection pumps, it has been common U.S. fragility practice to base their fragility estimate on a review and scaling of the qualification stress report for the specific pump involved. In addition, the anchorage of the pump frame to the foundation and the capacity of the motor mounting to pump frame are evaluated. The degree of rigor with which motor slip has been assessed, and the parameters used in this assessment have likely varied among fragility analysts.

For lower CEUS seismic regions, and for less critical horizontal pumps, horizontal pumps have often been assigned a ground motion screening level spectral acceleration of $SA_{SL} = 1.2\text{g}$ based on EPRI NP-6041-SL [1991] screening tables as discussed in Section 2.3. Thus, from Table 2-5, the

median spectral acceleration capacity at the base of the pump frame would be about $SA_{50\%} = 4.8g$ which, based on the approximation of Equation 4-1, would correspond to a median ZPA capacity of only about:

$$ZPA_{50\%} \approx 4.8g/2.4 = 2.0g \quad (4-7)$$

which is much less than the function confirmed $ZPA = 6.0g$ obtained in the JNES RCW pump full-scale test. These screening level based fragility estimates are exceedingly conservative for horizontal pumps within our experience. This screening level approach should not be used for risk important horizontal pumps.

4.4 Large Vertical Shaft Pump

JNES performed a full-scale test on a large Residual Heat Removal System (RHR) pump of the pit barrel type. The barrel extended 32-ft below the top of the pump base but was intermediately supported at about mid-depth. The motor extended 17.3-ft above the top of the pump base. Function was confirmed separately for the Barrel/Column portion of the pump and for the Motor portion. Results are reported both in terms of the input ZPA and the response ZPA .

No loss of function was confirmed at the following horizontal input and response ZPA levels:

Function Confirmed

Motor (4-8)

Input $ZPA = 1.6g$
Top of Motor $ZPA = 14.0 g$

Barrel/Column (4-9)

Input $ZPA = 2.8g$
Bottom of Barrel $ZPA = 31g$
Bottom of Column $ZPA = 35 g$

The JNES equipment fragility test report indicates that yielding of the motor mounting bolts was confirmed at an input ZPA of 1.5g (top of motor ZPA of 12.0g) and that yielding of the barrel was confirmed at a bottom of barrel ZPA of 31.0. However, there was no loss of function.

In higher quality fragility analyses, the median fragility of vertical pumps is typically determined by analysis in which median capacities are based on 90% of the fully plastic moment capacity for each of the following elements:

- Motor mounting bolts
- Lower motor stand
- Pump barrel, casing, column, or shaft

whichever controls when compared to the estimated moment demand. The JNES large vertical pump test results seem to confirm the reasonableness of this approach.

For low seismic CEUS sites and for less critical vertical pumps, the screening levels reported in Table 2-4 of EPRI NP-6041-SL [1991] have often been used as discussed in Section 2.3. For vertical pumps with unsupported barrel or casing lengths less than 20-feet, as is the case for the

JNES tested pump, the spectral acceleration screening level is $SA_{SL} = 1.2g$. As shown in the last paragraph of Section 4.3, this screening level corresponds to a median ZPA capacity of about:

$$ZPA_{50\%} \approx 2.0g \quad (4-10)$$

This value should not be used for large critical vertical pumps. Instead, the fragility should be based on pump specific analysis.

Median loss of function fragility evaluations are also reported in the JNES equipment fragility test report for four large vertical pumps including the full-scale tested pump discussed above. These fragility evaluations are based on analysis. Similarly as for the large horizontal pumps, the lowest reported fragility is a motor slip reference fragility reported in terms of top of motor ZPA response (ZPA_{TOM})

For the four analyzed pumps:

$$\underline{\text{Motor Slip Reference Fragility}} \quad (4-11)$$

$$\begin{aligned} \text{Tested Pump: } ZPA_{TOM} &= 3.6g \\ \text{Other Three Pumps: } ZPA_{TOM} &= 2.8g-6.2g \end{aligned}$$

The JNES equipment fragility test report states on Page A-41 that there was no slip during the full-scale test. However, a footnote on Page A-84 indicates that the motor mounting on the pump base was strengthened prior to the function confirmed test for which Equation 4-8 summarizes the results.

The comments in Section 4.3 about motor slip for large horizontal pumps equally apply to large vertical pumps. This issue deserves further investigation, including testing.

Element testing was performed on submerged bearings. Results are reported in Table 3.4-4 of the JNES equipment fragility test report. Capacities are reported in terms of bearing surface pressure times rotating velocity on the bearing, i.e., PV value. The median PV fragility levels reported for bulging and cracking of resin and rubber bearings are approximately 60 MPa-m/s and 70 MP-m/s, respectively. Function was confirmed at a PV level of at least 70 MPa-m/s for carbon bearings and solid lubricant distributed oil-less bearings. Based on these bearing capacities and seismic analyses of the pump shafts, the following median loss of submerged bearing function limits are reported in terms of the bottom of barrel (casing) acceleration ZPA_{BOB} :

Submerged Bearing Functional Limit

$$\begin{aligned} \text{Tested Pump: } ZPA_{BOB} &= 37.1g \\ \text{Other Three Pumps: } ZPA_{BOB} &= 14.6g-96.9g \end{aligned} \quad (4-12)$$

For the tested pump, this computed submerged bearing functional limit was 20% higher than the highest test level. Therefore, this computed functional limit was not confirmed in the full-scale test.

To the best knowledge of the authors, the functional failure of submerged bearings has not been considered in U.S. fragility analyses of vertical pumps. The JNES data on bearings should be considered in future U.S. practice. Clearly JNES is concerned about these potential failure modes. However, in the JNES data, the submerged bearing functional limit data does not seem to control the pump fragilities since these fragilities are controlled by other failure modes.

Lastly, JNES performed a vertical input seismic shaking on the RHR Pump. The concern is with vertical loads being imposed on the motor thrust bearing, and with lifting the shaft more than the clearance that exists between the impeller and the lower liner ring. For the tested pump, no loss of function was confirmed for a vertical *ZPA* level of 1.9g.

To the best knowledge of the authors, this potential for failure to function of the motor thrust bearing or exceedance of vertical clearance due to vertical shaking has also not been considered in U.S. fragility analyses of vertical pumps. The reported thrust bearing capacity and vertical clearance capacity were Function Confirmed capacities since no loss of function occurred at a vertical *ZPA* of 1.9g. Therefore, the actual vertical *ZPA* fragility level is unknown. The importance of this JNES concern is unknown. No guidance can be given for future U.S. practice.

4.5 Control Rod Insertion Capability

4.5.1 PWR Plants

JNES conducted a full-scale test on a control rod drive mechanism, control rod, and fuel bundle assembly representative of 3 and 4 loop PWR plants. The fuel assembly was the 17x17 type. The input motion and resulting maximum fuel assembly displacement were:

$$\begin{aligned} ZPA &= 3.2g \\ \text{Displacement} &= 48\text{mm} \end{aligned} \quad (4-13)$$

Control rod insertion simulation analyses were performed and JNES estimated the following median value and composite variability β_C for functionality limit on control rod insertion:

PWR (3 and 4 Loop) Functional Limit Fuel Assembly Displacement

Median	β_C
77mm	0.19

(4-14)

No input motion level corresponding to the 77mm fuel assembly displacement was explicitly defined in the JNES equipment fragility test report. However, on Page A-28 of the JNES report it is stated that the full-scale test was conducted at 3.3 times the S_2 input. Later on Page A-28, it is reported that the 77mm displacement corresponds to 4 times the S_2 input. On this basis, the median *ZPA* fragility is estimated to be:

PWR (3 and 4 loop)

$$ZPA_{50\%} \approx (4.0/3.3) * 3.2g = 3.9g \quad (4-15)$$

Based on simulation analysis, the JNES report also reports a median functional limit displacement $\delta_{50\%}$ of 66mm for PWR (2 loop) plants with 14x14 type fuel assembly. Based on scaling, the median fragilities for the 2 loop PWR plants can be estimated as:

PWR (2 loop)

$$\begin{aligned} \delta_{50\%} &= 69\text{m} \\ ZPA_{50\%} &\approx 3.7g \end{aligned} \quad (4-16)$$

4.5.2 BWR Plants

JNES also conducted a full-scale test on a control rod drive mechanism, control rod, and fuel bundle assembly representative of a BWR5 plant with a high speed scram type control rod drive mechanism. The full-scale test had a 100 mil thick channel box. However, JNES has estimated that the same fragility estimates are applicable for 80 mil and 120 mil channel boxes. For the full-scale test the input motion and resulting fuel assembly displacement were:

$$\begin{aligned} ZPA &= 3.0g \\ \text{Displacement} &= 83\text{mm} \end{aligned} \quad (4-17)$$

JNES considered that the critical damage state was reached when the fuel bundle collided with the shroud. They estimated a 5% probability of damage at 83mm displacement, and 95% probability of damage at 100mm displacement. Based on these estimates, JNES reports the following fuel assembly displacement fragility:

BWR5 Fuel Assembly Displacement Fragility

Median	β_C
91mm	0.10

(4-18)

The basis for β_C is not clear. With 83mm displacement at the 5% probability level and 100mm displacement at the 95% probability level, a β_C can be computed as:

$$\beta_C = \frac{\ln[100/83]}{2 * 1.645} = 0.06 \quad (4-19)$$

However, a β_C of 0.10 already seems to be very low for this complex of a phenomena, therefore it is not recommended that the JNES $\beta_C=0.10$ be further reduced for U.S. NPP applications without further information.

No median $ZPA_{50\%}$ corresponding to a 91mm fuel assembly displacement is reported. However, since an 83mm displacement corresponds to a $ZPA=3.0g$, the median fragility is estimated as:

BWR5

$$ZPA_{50\%} = 3.1g - 3.3g \quad (4-20)$$

4.5.3 Applicability of Results for U.S. Fragility Assessments

The JNES fragility results are applicable for failure modes associated with fuel assembly displacements. However, these results do not address structural failure modes since the entire assembly was supported by very stiff frames in the test.

Within the U.S., control rod insertion fragilities are generally derived based on a detailed review and scaling of Nuclear Steam Supply System (NSSS) vendor submitted qualification reported results. For PWR plants, the derived fragilities are generally controlled by the supports of the control rod drive mechanism. During the JNES test, the control rod drive mechanism was very substantially supported by a very rigid frame. The failure modes that have typically been considered to be controlling in U.S. fragility assessments for control rod insertion could not have

occurred during these tests. Fragilities for control rod insertion need to be primarily addressed by the NSSS vendors.

Table 4-1 JNES Fragilities for Electrical Components

Component	ZPA (g)	SA (g)	
BWR Main Control Board	5.7	13.7	(FC)
PWR Reactor Auxiliary Board	5.9	14.2	(FC)
BWR Logic Circuit Control Cabinet	5.9	14.2	(FC)
PWR Reactor Protection Instrumentation Rack (malfunction of a miniature relay in AC controller card)	3.7	8.9	
BWR Instrument Rack	5.7	13.7	(FC)
PWR Reactor Control Center (error of magnetic contactor caused by auxiliary relay chatter)	5.5	13.2	
PWR Power Center (receiving circuit breaker misclosed)	3.3	7.9	
(air circuit breaker broke)	4.3	10.3	
69kV Metal Clad Switchgear (fallout of fuses from GPT instrument transformer)	2.3	5.5	
(damage to vacuum circuit breaker)	3.8	9.1	

5 CONCLUSIONS

This report presents an assessment of the equipment fragility test program performed by the Japan Nuclear Energy Safety Organization (JNES). The goal of this assessment was to compare the JNES fragility results with the fragility data typically used in current U.S. SPRAs and assess the impact that the new test results may have on current SPRAs and how this data can be utilized for future SPRAs. The JNES fragility results are also useful for seismic margin analyses (SMAs), which are important in design certification (DC) or combined license (COL) applications because of the lack of full SPRAs at the DC or COL stage. This report includes a brief overview of the current U.S. SPRA practices, a description of the JNES equipment fragility test program, and an evaluation of the JNES fragility data. This section presents the major findings and insights on whether and how the JNES fragility data can be applied to the U.S. SPRA practices.

The JNES equipment fragility test program started in 2002 and is planned to continue until 2012. The tests of the safety significant active equipment in the JNES equipment fragility test program were scheduled into two phases. In the phase I program, the tested equipment included horizontal shaft pumps, electrical panels, control rod insertion capability, and large size vertical shaft pumps. The phase II program included fans, valves, tanks, support structures, and overhead cranes. This report documents the evaluation of the fragility data for the JNES phase I equipment. As additional information is made available by JNES for the phase II equipment, a supplement to this report will be prepared to document the corresponding evaluation results.

The seismic fragility data described in the JNES equipment fragility test report 08TAIHATV-0027, also reproduced as Appendix A to this report, was developed based on high level shaking table tests of full-scale equipment, element tests, and analyses. In the full-scale tests, actual equipment as used in typical BWR and PWR nuclear power plants in Japan were shaken under excitations much larger than the design basis earthquakes which have been used in previous equipment qualification tests and design proving tests. The purpose of the full-scale tests was to identify critical acceleration levels and failure modes of the equipment. The element tests were conducted with multiple samples for each element type, and therefore their median capacity and the associated variation were able to be determined statistically. The purpose of the element tests was to evaluate threshold acceleration levels of parts and to assess median capacities and the associated uncertainties. The purpose of the various analyses was to estimate the seismic fragility capacities of the equipment based on the element fragility data and numerical models representing the appropriate failure modes as determined from the full-scale tests.

The JNES fragilities were commonly defined in terms of the zero period acceleration (*ZPA*) at the top of the shaking table, and some were reported as the response accelerations/displacements. However, all of the generic fragilities in the U.S. SPRA practices are defined in terms of a broad frequency 5% damped spectral acceleration (*SA*) at the base of the component. A reasonable relationship between *ZPA* and *SA*, $SA \approx 2.4 \times ZPA$, has been used to convert the JNES fragilities for the purpose of comparison (see Section 4.1).

Specific insights on the JNES equipment fragility tests and the corresponding evaluation results are summarized below. It should be emphasized that an analysis of the component anchorage and support fragility needs to be performed as a necessary supplement to the equipment fragility data for a proper application.

5.1 Horizontal Shaft Pumps

The horizontal shaft pump in the full-scale test was a reactor building closed cooling water (RCW) pump used in Japan BWR plants, which appears to be very similar to RCW pumps in U.S.

nuclear plants. Therefore, it is judged that this test result could be used to estimate the median fragility of RCW pumps in U.S. plants. The function of the RCW pump was confirmed at a *ZPA* of 6.0 g in the full-scale test. The median functional fragilities of the tested RCW pump, a larger RCW pump, and a charging injection pump were estimated to be 8.4 g, 8.6 g, and 17.3 g, respectively, based on the results of the bearing tests.

The potentially controlling fragility appears to be slip of the motor on the pump frame. As large uncertainties exist for the slip phenomenon, the calculated fragilities were designated as *reference* fragilities. The reference fragilities for the tested RCW pump, the larger RCW pump, and the charging injection pump were reported to be 6.1 g, 5.3 g, and 2.6 g. A coefficient of friction of 0.3 was used in the reference slip fragility calculation. The bolt tightening force used in the fragility calculation was not reported; however in the large size vertical shaft pump fragility analysis, an internal force coefficient was conservatively set to 0.5 in the bolt tensile stress calculation.

For large and critical horizontal pumps such as RCW pumps and Charging High Pressure Injection pumps, it has been common U.S. fragility practice to base their fragility estimate on a review and scaling of the qualification stress report for the specific pump involved. For lower Central and Eastern U.S. (CEUS) seismic regions, and for less critical horizontal pumps, based on a screening level spectral acceleration of 1.2 g, the median *ZPA* capacity of horizontal pumps can be estimated to be about 2.0 g, which is much less than the function confirmed *ZPA* = 6.0 g obtained in the JNES RCW pump full-scale test. The JNES tests demonstrate that these screening level based fragility estimates are exceedingly conservative for horizontal pumps, and thus confirm the judgment that the screening level approach should not be used for risk important horizontal pumps.

5.2 Electrical Panels

Eight electrical panels were selected for the JNES full-scale tests:

- Main control board (BWR)
- Reactor auxiliary control board (PWR)
- Logic circuit control panel (BWR)
- Instrumentation rack (BWR)
- Reactor protection rack (PWR)
- Reactor control center (PWR)
- Power center (PWR)
- 6.9 kV Metal-clad switchgear (BWR).

The median spectral fragilities for these panels, converted from the JNES test data, range between 5.5 g and 14.2 g; while the generic median fragilities in the U.S. SPRA practice range between 2.2 g and 5.1 g. This comparison indicates that generic fragilities commonly used in U.S. SPRAs for existing CEUS plants might be conservatively biased by more than a factor of two. The JNES test data median fragility levels for electrical components are comparable to the ALWR “achievable” fragilities, which are in the range of 8.3 g to 9.8 g.

However, the natural frequencies for all eight tested electrical components ranged between 21 Hz and 44 Hz. Most of these electrical components in U.S. plants exhibit local panel mode frequencies in the 4 Hz to 15 Hz range when tested at higher shaking levels. Cabinet response amplification factors AF_C were reported for representative device mounting locations in the JNES tested components to be 1.0 to 2.5; while the recommended median AF_C values at the worst

location for the existing U.S. cabinets range between 2.8 to 4.4. Based both on the natural frequency comparisons and the response amplification comparisons, it appears that the JNES tested electrical components are much stiffer than most electrical components in existing U.S. plants. The JNES reported median fragilities should not be used for U.S. electrical components unless it can be shown that the component has stiffnesses similar to those tested by JNES. However, they might be representative of electrical components to be used in new U.S. standard plants not yet built.

Electrical element tests included 37 types of devices:

- 3 protective relays
- 3 auxiliary relays
- 1 timing device
- 12 control equipment devices
- 4 pressure transmitters
- 2 magnetic contactors
- 3 molded case circuit breakers
- 3 switches
- 3 air circuit breakers
- 1 vacuum circuit breaker
- 1 gas circuit breaker
- 1 grounded potential transformer.

Seismic time history tests were conducted up to a $ZPA=10g$ level or slightly higher. All but 8 of these 37 types of devices had function confirmed at ZPA levels of about 10g or slightly higher. The smallest ZPA at which loss of function occurred for eight types of devices was 2.5 g. Additional seismic reinforcement to some of the devices increased the fragility level. With the exception of the air and gas circuit breakers, and the grounded potential transformer, all of these device fragilities exceed the median fragility level used for similar devices in existing U.S. SPRAs. The circuit breaker and transformer capacities are consistent with those used in existing U.S. SPRAs. Because the tested devices are identified by manufacturer and model number, the JNES electrical equipment device fragility data is a highly valuable resource for future SPRAs.

5.3 Control Rod Insertion Capability

JNES performed a full-scale test on a control rod drive mechanism, control rod, and fuel bundle assembly representative of 3 and 4 loop PWR plants. The fuel assembly was the 17x17 type. The input motion and resulting maximum fuel assembly displacement were 3.2 g (ZPA) and 48 mm, respectively. The reported computed median fragility for fuel assembly displacement is 77 mm. The median ZPA fragility for 3 and 4 loop PWR plants is estimated as 3.9 g in this report.

Based on simulation analysis, the JNES report also reports a median functional limit displacement of 66 mm for 2 loop PWR plants with 14x14 type fuel assembly. The median ZPA and displacement fragilities are estimated in this report as 3.7 g and 69 mm, respectively.

JNES also conducted a full-scale test on a control rod drive mechanism, control rod, and fuel bundle assembly representative of a BWR5 plant with a high speed scram type control rod drive mechanism. JNES estimated that the same fragility estimates were applicable for 80 mil and 120 mil channel boxes. The input motion and resulting maximum fuel bundle assembly displacement were 3.0 g (ZPA) and 83 mm, respectively. JNES estimated the median fragility for the fuel

bundle displacement was 91 mm. The corresponding median ZPA fragility is estimated as 3.1 g to 3.3 g.

The JNES fragility results are applicable for failure modes associated with fuel assembly displacements. Within the U.S., control rod insertion fragilities are generally derived based on a detailed review and scaling of NSSS vendor submitted qualification reported results. For PWR plants, the derived fragilities are generally controlled by the supports of the control rod drive mechanism. The failure modes that have typically been considered to be controlling in U.S. fragility assessments for control rod insertion could not have occurred during these tests because the entire fuel assembly was supported by very stiff frames in the JNES tests.

5.4 Large Size Vertical Shaft Pumps

The large size vertical shaft pump in the full-scale test was a pit barrel type pump in the reactor residual heat removal system (RHR). Function was confirmed at an input ZPA of 1.6 g and a corresponding response ZPA of 14.0 g at the top of motor, and separately at an input ZPA of 2.8 g and a corresponding response ZPA of 31 g at the bottom of barrel. The JNES large vertical shaft pump test results seem to confirm the reasonableness of the U.S. fragility analysis method that determines the pump fragility as the minimum individual fragility capacity of the motor mounting bolts, lower motor stand, pump barrel, casing, column, and shaft.

For low seismic CEUS sites and for less critical vertical pumps, using a screening level of 1.2 g, a median ZPA capacity can be estimated to be 2.0 g for the JNES test pump. This value should not be used for large critical vertical pumps. Instead, the fragility should be based on pump specific analysis.

Similarly as for the large horizontal pumps, the lowest reported fragility is a motor slip reference fragility reported in terms of the top of the motor ZPA response. The computed slip reference fragility for the tested RHR pump, a high pressure core injection system pump, a component cooling seawater pump (PWR), and a component cooling seawater pump (BWR) was 3.6 g, 3.5 g, 6.2 g, and 2.8 g, respectively. However, a fragility capacity of 14 g at the top of motor was achieved in the full-scale test after tightening the anchor bolts, confirming that large uncertainties exist for the slip reference fragility.

Based on the test results of the submerged bearings, the functional fragilities in terms of the bottom of barrel were estimated to be 37.1 g for the tested RHR pump, and were between 14.6 g and 96.9 g for the other three pumps. For the tested pump, this computed submerged bearing functional limit was 20% higher than the highest test level. The functional failure of submerged bearings has not been considered in U.S. fragility analyses of vertical pumps. The JNES data on bearings should be considered in future U.S. practice; however, the submerged bearing functional limit data did not seem to control the pump fragilities.

5.5 Summary

The JNES tests make a valuable contribution to the overall state of knowledge of equipment fragility levels for use in SPRAs. The JNES fragility capacities were determined based on full-scale component tests and element tests under simulated seismic excitations that were much larger than the design basis earthquakes commonly used in previous qualification tests or design proving tests. The fragility levels found in the JNES tests are in general much higher than those used in current U.S. SPRAs. Additional failure modes, such as relative motor slip on pump frame and functional failure of submerged bearings, have been identified for consideration by fragility analysts. These test results should be considered by fragility analysts in performing future

SPRAs. However, caution must be applied to assess the applicability of the results to the specific equipment being considered. In particular, an analysis of the component anchorage and support fragility needs to be performed as a necessary supplement to the equipment fragility data for a proper application.

6 REFERENCES

Bandyopadhyay, K. and C.H. Hofmayer (1986). *Seismic Fragility of Nuclear Power Plant Components* (Phase I), NUREG/CR-4659, Vol. 1, Brookhaven National Laboratory.

Bandyopadhyay, K., C.H. Hofmayer, M.K. Kassir, and S.E. Pepper (1987). *Seismic Fragility of Nuclear Power Plant Components* (Phase II), Motor Control Center, Switchboard, Panelboard and Power Supply, NUREG/CR-4659, Vol. 2, Brookhaven National Laboratory.

Bandyopadhyay, K., C.H. Hofmayer, M.K. Kassir, and S.E. Pepper (1990). *Seismic Fragility of Nuclear Power Plant Components* (Phase II), Switchgear, I&C Panels (NSSS) and Relays, NUREG/CR-4659, Vol. 3, Brookhaven National Laboratory.

Bandyopadhyay, K., C.H. Hofmayer, M.K. Kassir, and S. Shteyngart (1991). *Seismic Fragility of Nuclear Power Plant Components* (Phase II), A Fragility Handbook on Eighteen Components, NUREG/CR-4659, Vol. 4, Brookhaven National Laboratory.

EPRI NP-6041-SL (1991). *A Methodology for Assessment of Nuclear Power Plant Seismic Margin*, Revision 1, Electric Power Research Institute.

EPRI TR-016780 (1999). *PRA Key Assumptions and Groundrules*, Advanced Light Water Reactor Utility Requirements Document, Vol. III, Rev. 8, Chapter 1, App. A, Section 3.3.6.6, Electric Power Research Institute.

EPRI 1019200 (2009). *Seismic Fragility Application Guide Update*, Electric Power Research Institute.

Fujita, T., Y. Sasaki, H. Abe, K. Kuroda, K. Kato, N. Yoshiga, N. Kojima, S. Asakura, and M. Nakamaru (1997). "NUPEC project: seismic proving test on reactor shutdown cooling systems – (summary of results)," K17/3, *Transactions of the 14th International Conference on Structural Mechanics in Reactor Technology*, SMiRT 14, Lyon, France.

Holman, G.S., C.K. Chou, G.D. Shipway, and V. Glozman (1987). *Component Fragility Research Program* (Phase I Demonstration Tests), NUREG/CR-4900, Vols. 1 and 2, Lawrence Livermore National Laboratory.

IEEE C37.98 (1984). *Seismic Testing of Relays*, ANSI/IEEE Standard C37.98-1984, Institute of Electrical and Electronic Engineers.

Iijima, T., H. Abe, and T. Fujita (2004). "Program outline of seismic fragility capacity tests on nuclear power plant equipment," *Proceedings of the 12th International Conference on Nuclear Engineering*, ICONE12, Virginia, USA.

Iijima, T., H. Abe, and K. Suzuki (2005). "Seismic fragility capacity of equipment – horizontal shaft pump test," *Proceedings of the 18th International Conference on Structural Mechanics in Reactor Technology*, SMiRT 18, Beijing, China.

Iijima, T., H. Abe, and K. Suzuki (2007). "Seismic fragility capacity of equipment – electric panel test," *Transactions of the 19th International Conference on Structural Mechanics in Reactor Technology*, SMiRT 19, Toronto, Canada.

Inagaki, M., K. Suzuki, and H. Abe (2006). "Overview of seismic fragility capacity test of PWR and BWR control rod insertion systems," Proceedings of *the 14th International Conference on Nuclear Engineering*, ICONE14, Florida, USA.

JNES (2009). Fragility Data of Equipment for Nuclear Facilities by Shaking Tests, 08TAIHATV-0027

McGuire, R.K., W.J. Silva, and C.J. Costantino (2001). Technical Basis for Revision of Regulatory Guidance on Design Ground Motions: Hazard- and Risk-consistent Ground Motion Spectra Guidelines, NUREG/CR-6728, Risk Engineering, Inc. for U.S. Nuclear Regulatory Commission, Washington, DC

Merz, K.L. (1991a). Generic Seismic Ruggedness of Power Plant Equipment, *EPRI NP-5223*, Rev. 1, Electric Power Research Institute, Palo Alto, California.

Merz, K.L. (1991b). Seismic Ruggedness of Relays, *EPRI NP-7147*, Electric Power Research Institute, Palo Alto, California.

Reed, J.W. and R.P. Kennedy (1994). Methodology for Developing Seismic Fragilities, *EPRI TR-103959*, Electric Power Research Institute, Palo Alto, California.

Tsai, N.C., G.L. Mochizuki, and G.S. Holman (1989). Component Fragility Research Program (Phase II Development of Seismic Fragilities from High-Level Qualification Data), NUREG/CR-5470, NCT Engineering, Inc. and Lawrence Livermore National Laboratory.

Uchiyama, Y. (2008a). Status of Fragility Tests in JNES (slides), July 17.

Uchiyama, Y. (2008b). Status of JNES Seismic Test Projects After September 2006 (slides), July 17.

**APPENDIX A JNES FRAGILITY DATA OF EQUIPMENT FOR NUCLEAR
FACILITIES BY SHAKING TESTS**

Fragility Data of Equipment for Nuclear Facilities by Shaking Tests

January 2009

Seismic Safety Division/Japan Nuclear Energy Safety Organization

This report is English version of Chapter IV “Development of Fragility Data” excerpted from the “Report of Fragility Tests of Equipment - Part 3 (Overall evaluation) - in FY 2005”, which was the outcome of the program conducted by Japan Nuclear Energy Safety Organization (JNES).

Table of content

Part-I Introduction	A-1
1. Background of study	A-3
1.1 Necessity of fragility data of equipment	A-3
1.2 Fragility capacity evaluation test of equipment and its progress, and positioning of the report	A-3
2. Evaluation process for fragility capacity of equipment	A-5
Part-II Development of fragility data	A-7
1. Outline	A-9
1.1 Outcome of fragility capacity tests for equipment	A-10
1.1.1 Horizontal shaft pump	A-10
1.1.2 Electrical equipment	A-11
1.1.3 Control rod inserting capability	A-12
1.1.4 Large size vertical shaft pump	A-14
2. Evaluation method of fragility capacity	A-17
2.1 Horizontal shaft pump	A-17
2.2 Electrical equipment	A-25
2.3 Control rod inserting capability	A-28
2.4 Large size vertical shaft pump	A-33
3. Fragility data	A-47
3.1 Horizontal shaft pump	A-48
3.2 Electrical equipment	A-55
3.3 Control rod inserting capability	A-79
3.4 Large size vertical shaft pump	A-83
4. Summary	A-93
Reference	A-95

Part-I

Introduction

1. Background of study

1.1 Necessity of fragility test of equipment

In safety assessment of nuclear power installation, probabilistic safety assessment (Seismic PSA) is studied to probabilistically evaluate possibility of core damage due to the earthquake movement exceeding the current design basis. Necessity and flow to improve seismic fragility evaluation is shown in Figure 1-1. In seismic PSA, as shown in the figure, responses of building and equipment are calculated using the ground movement by earthquake hazard evaluation, and equipment damage probability evaluation is performed using the above results and equipment fragility data, and core damage frequency is evaluated by accident sequence analysis. To evaluate equipment damage probability, fragility data of the equipment, i.e., data of function limit of equipment, are necessary. Test data are also important to adequately grasp seismic margin of equipment.

1.2 Fragility test of equipment in JNES and its progress, and positioning of the report

Fragility data for equipment having large contribution to core damage are one of the important items in performing seismic PSA. However, the existing knowledge is not enough to adequately specify fragility capacity for such equipment. Therefore, it is important issue for performing seismic PSA with high reliability to identify functional limit and damage mode of equipment by test, and to develop fragility data set.

Regarding objective equipment for fragility test, the following equipment having large influence were selected, referring seismic PSA trial analysis performed for BWR and PWR plants in Japan, and tests were performed to obtain fragility data as Part 1 to Part 3 test.

Fragility Test, Part 1: Horizontal shaft pump and electrical equipment

Fragility Test, Part 2: Equipment related to control rod inserting capability (PWR and BWR)

Fragility Test, Part 3: Large size vertical shaft pump

: Overall and comprehensive evaluation of Part 1 to Part 3

In comprehensive evaluation, the results obtained in the tests of Part 1 to Part 3 were summarized as fragility data set. Supplemental tests were also done at this stage. Major items of additional tests and evaluation performed in the summarization stage include the followings:

- Comprehensive evaluation of the fragility values obtained in the tests was performed considering element tests and analytical evaluation of critical portions.
- For the elements of electrical panels and others, in which abnormality occurred at relatively low acceleration, additional element tests were performed after the elements were improved.
- Fragility data after improvement were developed by combining the element test results and response analysis results of equipment body in which the element is installed.

This report is English version of Chapter IV “Development of Fragility Data” excerpted from the above mentioned comprehensive evaluation report.

Part 1 to Part 3 of Equipment Fragility Test were conducted in FY 2002 to 2005, and then Part 4 test (valve, tank) and Part 5 test (support structure and fan) were planned from FY 2005 to 2009 as the next object after them from viewpoint of importance on seismic PSA. However, they are not included in this report.

The JNES reports of this Fragility Test series are listed in reference and English reports presented at international conferences are attached to this report.

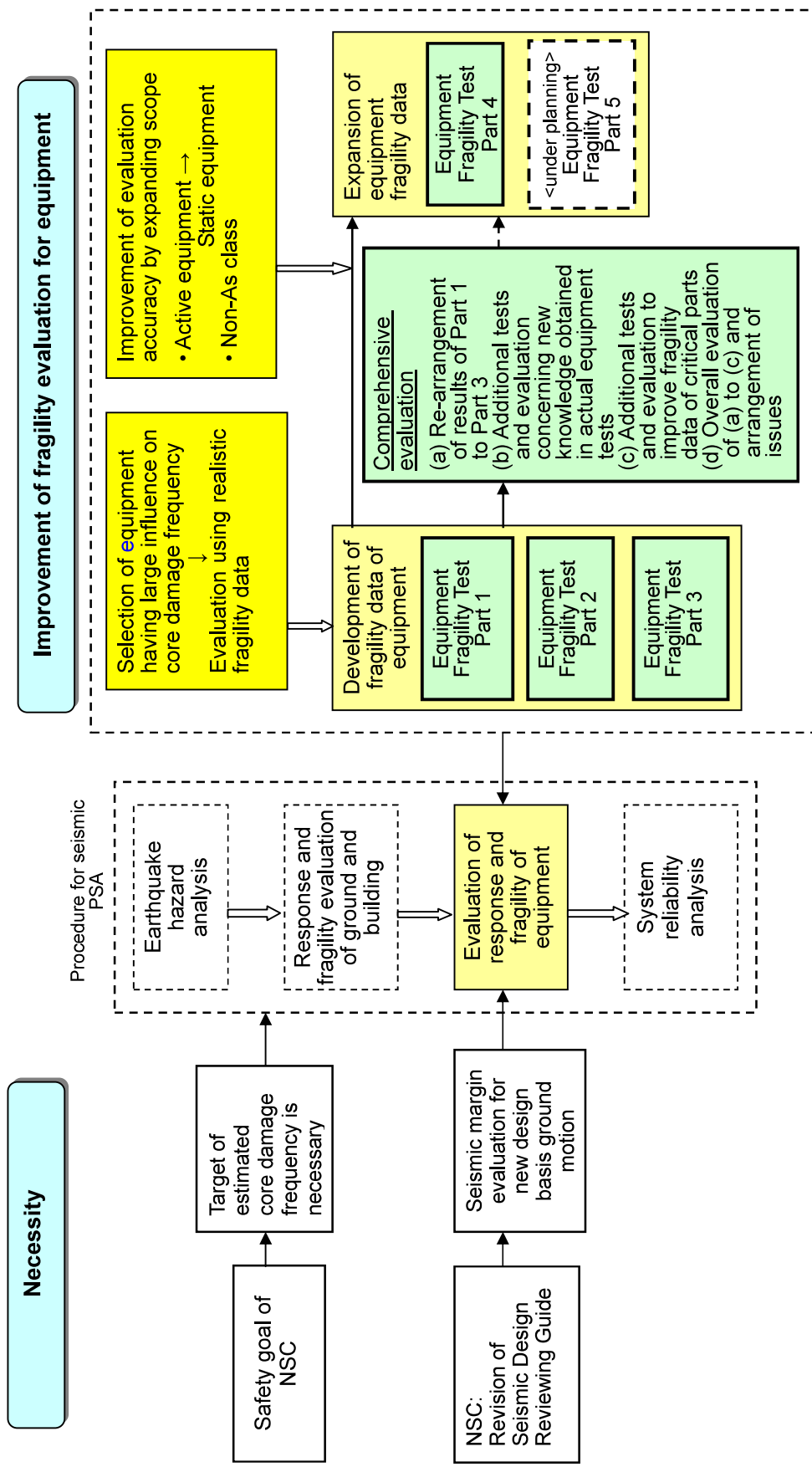


Figure 1-1 Necessity of Fragility Data and Sophistication of Equipment Fragility Evaluation

2. Evaluation process for equipment fragility capacity

Evaluation process in Part 1 to Part 3 of Fragility Capacity of Equipment is shown in Figure 2-1. In the fragility capacity tests of equipment, the tests are performed for the selected equipment, and it is examined whether structural damage and/or loss of active function occur, and if abnormality occurs, detailed analysis is performed for such abnormality. Various types of abnormality can be expected as abnormality of function, and some of fragility capacity could be improved by relatively simple measures, depending on such abnormality. Therefore, limits for maintaining function (acceleration, load, displacement, etc.) are evaluated, confirming how much fragility could be improved by reinforcement measures if necessary.

For establishment of fragility evaluation method, fragility of equipment is evaluated by combining seismic response analysis under large input earthquake conditions with fragility capacity of parts confirmed in the additional element tests. This method is expandable to equipment which has similar structure that was tested in Part 1 to 3 of this project. Fragility data of these kinds of equipment were also evaluated in the study of overall and comprehensive evaluation and included in the data table of this report.

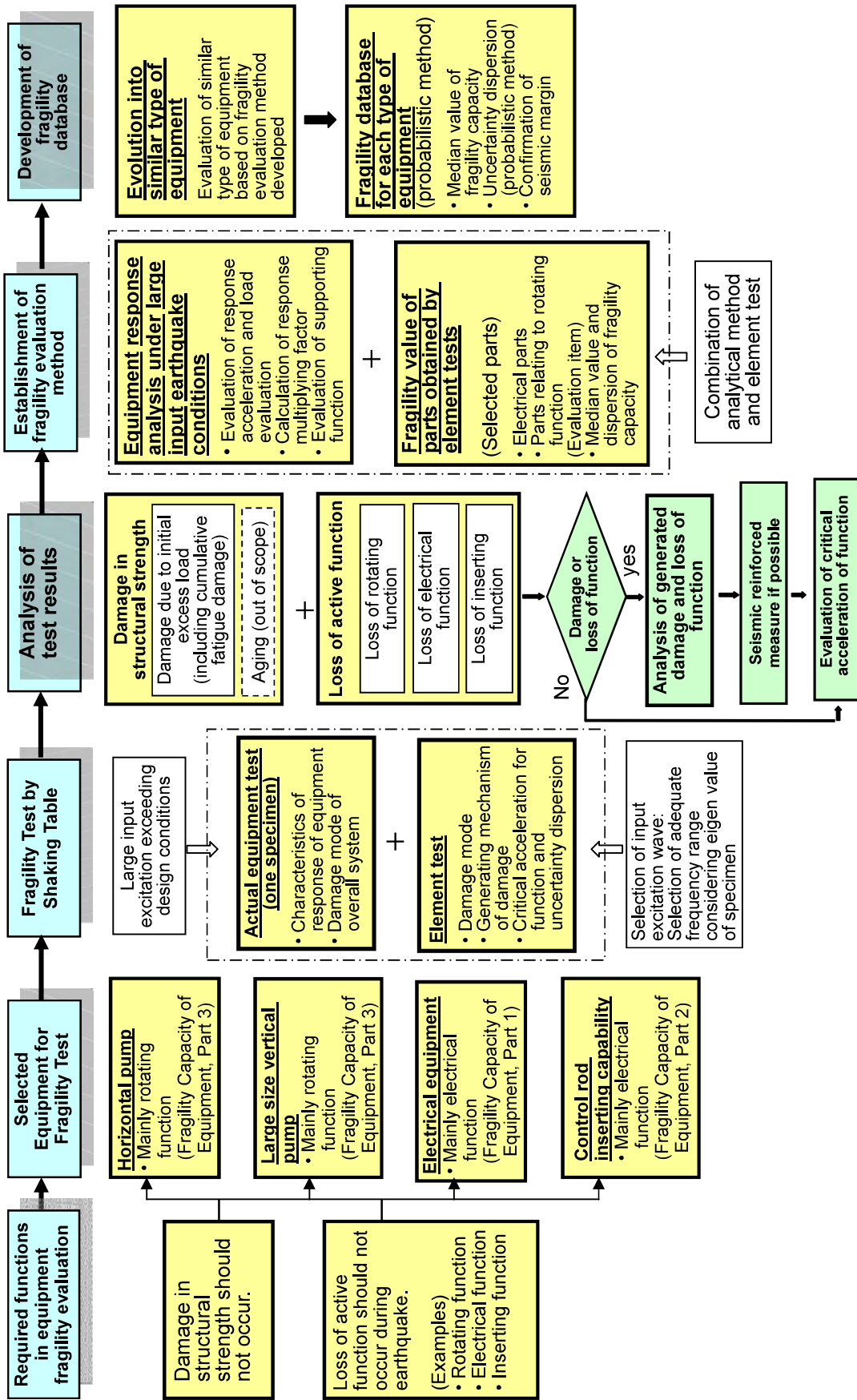


Figure 2-1 Evaluation Process for Fragility Capacity of Equipment

Part-II

Development of Fragility Capacity Data

1. Outline

In the Program on Equipment Fragility Test, fragility tests for horizontal shaft pump, electrical pannels, control rod insertion system and large size vertical shaft pump were performed with earthquake motion largely exceeding the design level, in order to obtain data on realistic fragility capacity of such components, as Part 1 to Part 3 of Equipment Fragility Test. In addition, the issues identified by these tests were studied by conducting additional tests and analysis, and fragility evaluation method was established based on the knowledge from these tests and analysis. Evaluation on fragility capacity of similar type equipment was performed using the method developed.

In this paper, as a summary of Part 1 to Part 3 of Equipment Fragility Test, the results of the Program and the evaluation method of fragility capacity are described, and fragility capacity data of equipment and their major parts are summarized.

1.1 Outcome of Fragility Capacity Tests for Equipment

Outline of Equipment Fragility Test results is described below for horizontal shaft pump, electrical equipment, control rod insertion system and large size vertical shaft pump.

1.1.1 Horizontal shaft pump

The fragility capacity tests for horizontal shaft pump consisting of two kinds of tests were performed. One is full-scale equipment test of reactor building closed cooling water (RCW) pump, and another is element test of bearings and liner rings. The full-scale equipment test was performed with up to the maximum acceleration of $6 \times 9.8 \text{ m/s}^2$, using simulated earthquake wave covering design floor response spectra of horizontal shaft pumps of BWR and PWR plants which are Seismic Class As and A and are important to safety. The pumps were vibrated in axial and lateral directions under operating and standby conditions respectively. In the tests, hydraulic characteristics of pump, load acting on bearing, acceleration due to rotation, water leakage, and strain generated on foundation bolts were measured and observed as well as seismic response. However, no abnormality was identified in active function and structural strength of the pump, and no abnormality was also found in disassembling inspection after the test.

In the element tests, in addition to the bearing and liner ring used in horizontal shaft single stage pump which were tested in the full-scale equipment test, bearings and liner rings used in horizontal shaft multi-stage pump were also selected for tests. Tests were performed with load corresponding to the seismic acceleration largely exceeding the one used for the full-scale equipment test. As the result, friction was generated among balls, inner and outer rings in the thrust direction loading test of deep groove ball bearing, and plastic flow was generated at white metal on inner side of bearing in the test of radial bearing which is one of slide bearings. Although such degradation of bearing would not immediately result in shutdown of the pump, it would cause decrease of bearing operating life. However, it should be noted that such phenomena were generated under extremely large load conditions greater than 10 to $20 \times 9.8 \text{ m/s}^2$ equivalent to acceleration on pump of actual plant.

Although no abnormality of pump function was identified in full-scale equipment test, degradation was identified in the element tests, which could result in decrease of operating life of bearing. Pumps related to safety function of nuclear power plants are required to be continuously operated for a certain period after occurrence of earthquake, and if operating life of bearing decreases, such requirement could not be satisfied. Therefore, critical load of the bearing is conservatively specified based on the load which would generate abnormality to cause decrease of operating life of bearing, or the maximum load under which function is identified to be maintained. In addition, model of response analysis was developed for horizontal shaft pump during large input earthquake. Using the earthquake response analysis, seismic force resulting in the critical load of the bearing was obtained and evaluation method of fragility capacity was developed to evaluate critical acceleration for active function of horizontal shaft pump. Furthermore, from viewpoint of structural strength, stress on bolt of pump and motor support and slip of installing portion were evaluated by simplified static analysis, and critical acceleration of structural strength was calculated.

Section 2.1 describes the evaluation method of fragility capacity of horizontal shaft pump established in the Part 1 of Equipment Fragility Test, and Section 3.1 shows fragility data of bearing and liner ring obtained by the element tests, and fragility data of horizontal shaft pump evaluated by applying fragility evaluation method.

1.1.2 Electrical equipment

In fragility test of electrical equipment, 8 kinds of representative electrical panels, i.e., a main control board, a reactor auxiliary control board, a logic circuit control panel, a reactor protection instrumentation rack, an instrumentation rack, a reactor control center, a power center and a metal-clad switchgear were selected to be tested for full-scale equipment test, as electrical equipment (panels) important to seismic PSA. In the full-scale equipment tests, tests were performed with up to the maximum acceleration of $6 \times 9.8 \text{ m/s}^2$, using simulated earthquake wave covering design floor response spectra of the above electrical equipment of BWR and PWR plants. In the test, electrical conditions during normal operation were simulated, and electrical equipment was vibrated in the direction of back and forth and from side to side, and then electric functional abnormality and structural damage were to be identified. As the results of the tests, no electrical nor structural abnormality was identified for a main control board, a reactor auxiliary control board, a logic circuit control panel and an instrumentation rack, and, however, abnormalities in electrical function or functional abnormalities due to structural damage were generated at electrical parts contained in a protection instrument rack, a reactor control center, a power center and a metal-clad switchgear.

In the element tests, based on the investigation of the full-scale test specimen and similar type elements used in similar panels, about 30 types of parts including relays, control devices, instrument equipment, electrical equipment and switches were selected from viewpoint of electrical functions and actuating mechanism, and shaking tests were performed for 3 to 6 specimens of each type in principle. Seismic response analysis of electrical equipment was performed using simulated earthquake waves developed for the full-scale equipment test, and response wave at the location mounting the part obtained by the analysis was used as an input wave. Input acceleration level was specified as about $10 \times 9.8 \text{ m/s}^2$ at the maximum, considering response amplification of panel and performance of the shaking table. In the tests, electrical parts were vibrated in the direction of back and forth and from side to side, under the electric conditions simulating normal operation, and were also vibrated by sine beat wave, back and forth, from side to side and vertically as a reference.

As the results of the tests, abnormalities in electrical function were identified in some of relays and control devices. However, most of other parts had no malfunction even though they were vibrated up to the performance limit of the shaking table.

It was considered to be necessary to improve fragility data of circuit breaker, because fragility capacity of breaker became critical for power center and metal-clad switchgear in the Part 1 of Equipment Fragility Test. Therefore, element test for breaker was performed and fragility data for breaker were reinforced. In addition, applicability of Bayes analysis was studied as an evaluation method for median value and dispersion concerning fragility of the parts.

As an evaluation method of fragility of electrical equipment, method to evaluate critical acceleration at panel foundation was established based on comparison between fragility data obtained by element tests and response multiplying factor at the location of mounting parts obtained by seismic response analysis of the panel. Both this critical acceleration of electrical function and critical acceleration of structural strength specified by stress limit of panel cabinet or anchor bolt were also to be evaluated as fragility capacity of electrical equipment.

Section 2.2 describes the method to evaluate fragility capacity of electrical equipment established in the Part 1 of Equipment Fragility Test, and Section 3.2 shows fragility data of electrical parts obtained by the element tests, and fragility data of electrical equipment evaluated by applying the fragility evaluation method.

1.1.3 Control rod inserting capability

Regarding control rod of PWR and BWR, control rod inserting capability tests were performed, covering up to the fuel response largely exceeding the one used in the past tests.

(1) Component related to PWR control rod inserting capability

In the element test for PWR control rod inserting capability, a test vessel containing one fuel assembly and filled with water was placed on the shaking table, and was vibrated totally. Through this test, vibration characteristic of fuel assembly in water was obtained for large amplitude region. Based on the test results, input data for beam element analysis were prepared, and analysis model of fuel assembly response which can reproduce vibration characteristics (natural frequency, amplitude dependency of damping factor) was established.

For the full-scale equipment test of PWR control rod insertion system (consisting of control rods, fuel assembly, control rod drive mechanism, etc.), design conditions of domestic PWR plants were investigated, and pre-analysis was performed using evaluation method verified by the past tests, and input wave for the test was developed to make responses of simulated fuel assembly and control rod drive mechanism the same as ones of actual plant. In the test, it was vibrated by 3.3 times of seismic force due to the extreme design earthquake ground motion S_2 , and no abnormality was identified to hinder control rod inserting function. Relation between displacement of fuel assembly and time delay ratio of control rod insertion was compared with the past data, and both test results were confirmed to be roughly identical within the fuel response displacement level of the past test.

Analytical method of control rod inserting capability during large input was established based on these test results, and reproduction analysis of full-scale equipment test results was performed. Then it was confirmed by the analysis result that seismic response of major equipment and control rod insertion time could be simulated. Functional limit was defined considering both structural and insertion aspects, i.e. the fuel response displacement was defined considering the application limit of evaluation method as functional limit (fragility capacity). Structural strength of major component is also in this consideration. Median value and dispersion (logarithmic standard deviation) of fragility were evaluated by performing analytical evaluation with additional consideration of actual plant conditions such as temperature and flow velocity.

Section 2.3 describes the fragility evaluation method of component related to PWR control rod inserting capability established in the Part 2 of Equipment Fragility Test, and Section 3.3 shows fragility data of representative actual plants evaluated by applying the fragility evaluation method.

(2) Component related to BWR control rod inserting capability

In the element test for BWR control rod inserting capability, critical strength tests (material test, buckling test, load-displacement history test, repeated loading test) were performed for channel box which was main structural member of fuel assembly, using quasi-dynamic displacement loading facility and critical strength of fuel assembly was obtained in large amplitude region. It was confirmed that behavior of plastic deformation at operating temperature of actual plant became larger than the one at room temperature. Analytical model was developed to reproduce behavior obtained in the element tests.

For the full-scale equipment test of BWR control rod insertion system, design conditions of domestic BWR plants were investigated, and pre-analysis was performed using the evaluation method verified by the past tests, and input wave for the test was developed to make responses of simulated fuel assembly the same level as actual plant. In the test, vibration tests were performed up to 4 times of seismic input corresponding to the design limit earthquake S_2 , and no abnormality was identified to hinder control rod inserting function. Relation between displacement of fuel assembly and time delay ratio of control rod insertion was compared with the past data, and both test results were confirmed to be roughly identical within the response displacement level of the past data.

Analytical method of control rod inserting capability under large input was established based on these test

results, and reproduction analysis of full-scale equipment test results was performed. It was confirmed by the analysis result that seismic response of major equipment and control rod insertion time could be simulated. Then, considering structural strength of related component and application limit of evaluation method etc., certain fuel response displacement was defined as fragility capacity limit. Median value and uncertainty dispersion of fragility (logarithmic standard deviation) were evaluated by performing analytical evaluation with additional consideration of actual plant conditions such as temperature etc.

Regarding BWR control rod inserting capability, effects of vertical earthquake ground motion exceeding gravity acceleration had not been confirmed only by the existing knowledge. Therefore, analytical investigation of the effect of vertical excitation was performed for the effects on control rod insertion time and up-lift of fuel assembly, and outlook that effects of vertical earthquake ground motion on control rod inserting capability are small was obtained.

Section 2.3 describes the fragility evaluation method of component related to BWR control rod inserting capability established in the Part 2 of Equipment Fragility Test, and Section 3.3 shows fragility data of representative actual plants evaluated by applying the fragility evaluation method.

1.1.4 Large size vertical shaft pump

In the fragility capacity test of large size vertical shaft pump, full-scale equipment test for pit barrel type pump of reactor residual heat removal system (RHR) and element test for submerged bearing, liner ring (austenite stainless steel), and thrust bearing, which are parts important to rotating function, were performed.

In full-scale equipment test, specimen was excited horizontally and vertically under the normal operating conditions and shutdown conditions of the pump respectively, using simulated earthquake wave enveloping design floor response spectra for large size vertical shaft pumps of BWR and PWR plants, in order to confirm function of pump. Test procedure and specimen of the full-scale equipment test are shown in Figure 1.1.4-1 and 2. As the results of the horizontal vibration test (fragility test (A) and (B)). It was confirmed that motor mounting bolt was yielded at $12.0 \times 9.8 \text{ m/s}^2$ of response acceleration at the top of motor (motor function of motor itself was maintained even at $14.0 \times 9.8 \text{ m/s}^2$ of response acceleration at the top of motor), and that barrel was yielded at $31.0 \times 9.8 \text{ m/s}^2$ of response acceleration at the bottom end of the barrel. Regarding non-linear response behavior caused by clearance of barrel support, relation between change of clearance (diametric clearance: 4.0 mm, 2.0 mm and 1.0 mm) and non-linear response was confirmed. As the results of vertical vibration tests (Step 3 and 4 of fragility capacity test (A)), it was confirmed that function of the pump was maintained even at $31.0 \times 9.8 \text{ m/s}^2$ of response acceleration at the bottom end of barrel and $12.0 \times 9.8 \text{ m/s}^2$ of response acceleration at the top of motor. No abnormality was also identified in operation and disassembling inspection after the test. The results of the full-scale equipment test are shown in Table 1.4-1.

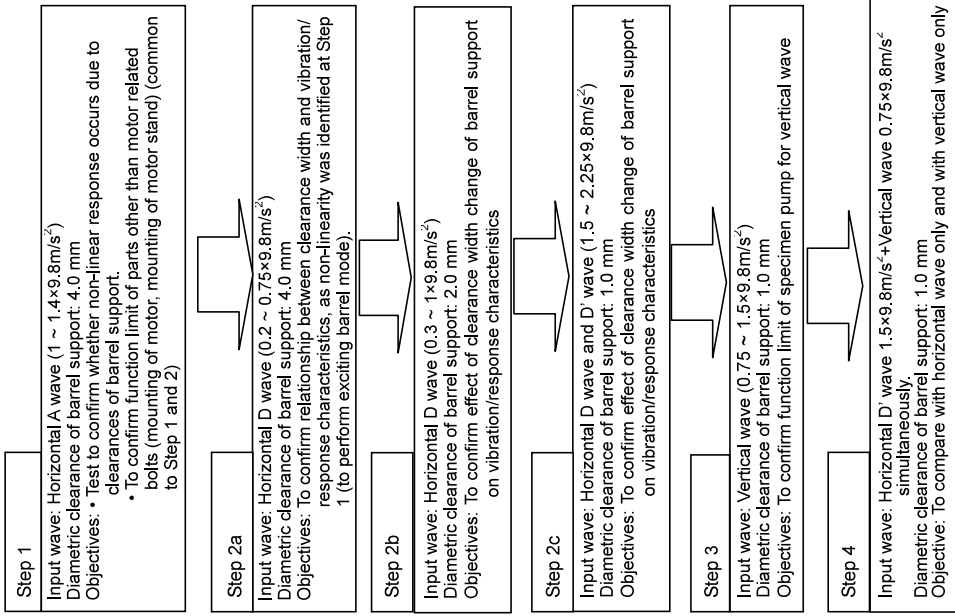
These results confirmed that pump function was maintained even at the response acceleration in horizontal direction which widely exceeded the function-confirmed response acceleration (bottom end of barrel column: $10.0 \times 9.8 \text{ m/s}^2$, top of motor (portion of bearing): $2.5 \times 9.8 \text{ m/s}^2$; JEAG4601) of each portion of vertical shaft pump obtained by Utilities Joint Research "Study on Maintaining Function of Active Component during Earthquake (ACT Joint Research)" conducted from FY 1980 to FY 1982, aiming at confirmation of maintaining function of active component during earthquake.

In the element test, specimen was vibrated with the load corresponding to the extremely greater seismic load than one in the full-scale equipment test, in order to confirm whether function of the part itself is lost, and to obtain dynamic characteristics (spring constant, damping factor, PV value (index for seizure limit of material: product of contact surface pressure P and slip speed V between two surfaces)) As the test results, it was confirmed for submerged bearing that rotating function of bearing was maintained with the surface pressure which was at least 5 times of allowable surface pressure considered in the design of actual plant (abnormality such as deformation, which was considered to be pre-indication of function limit, occurred after the maximum vibration for rubber and resin bearings among submerged bearings, and rotating function was, however, maintained.). For liner ring, it was confirmed that rotating function was maintained even under the maximum vibrating load of about 17.0 kN (equivalent to 3 times of S_2 ; S_2 is the wave enveloping design floor responses of BWR/PWR (ZPA: $1.24 \times 9.8 \text{ m/s}^2$)). For slide bearing among thrust bearings, up-lift analysis was performed using spring constant of bearing itself obtained by the test. Based on the analysis result, vertical acceleration of 1.3 to $1.5 \times 9.8 \text{ m/s}^2$ is evaluated as the acceleration where the bearing load reaches to the maximum load in element test or the acceleration where collision between liner ring and impeller occurs. The latter is conservatively defined as uplift limit of vertical pump shaft. The evaluated acceleration correspond to about six times of S_2 which is vertical ground motion (ZPA : $0.22 \times 9.8 \text{ m/s}^2$) tentatively used in the Improvement and Standardization Program.

Simulation analysis was performed for the full-scale equipment test using the above test results, and simplified evaluation method (equivalent linear analysis and impulse response analysis method) capable of fragility evaluation for large size vertical shaft pump of actual plant was established.

Section 2.4 describes the fragility evaluation method of large size vertical shaft pump of actual plant established in the Part 3 of Equipment Fragility Test, and Section 3.4 shows fragility data of bearings, liner rings and thrust bearings obtained by the element tests, and fragility data of representative pump of actual plants evaluated by applying the fragility evaluation method.

Fragility Capacity Test (A)



Fragility Capacity Test (B)

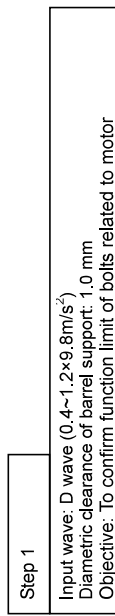


Figure 1.1.4-1 Procedure to Perform Actual Equipment Test

Table 1.4-1 Results of Full-scale Equipment Tests

Viewpoint	Results of Tests
(Fragility Test A) Confirmation at larger level than existing test	[Step 2c: Diametric clearance of support: 1.0 mm, D' wave] Pump function was maintained for up to the following horizontal response (it was confirmed that design yield point was exceeded near barrel support). • Bottom of barrel: 31.0×9.8m/s ² (2.8×9.8m/s ² input)
Barrel Column (existing test shown in JEAG4601: 10.0×9.8m/s ² at bottom end of barrel column)	[Step 2c: Diametric clearance of support: 1.0 mm, D' wave] Pump function was maintained up to the following horizontal response • Bottom of column: 35.0×9.8m/s ² (2.8×9.8m/s ² input)
Motor Maintaining or Loss of Function	[Step 3: Diametric clearance of support: 1.0 mm, vertical wave] Pump function Motor Stand lined for up to the following vertical response (1.9×9.8m/s ² input) • Bottom of barrel: 2.2×9.8m/s ² • Bottom of column: 1.6×9.8m/s ²
Structure for mounting motor	[Step 1: Diametric clearance of support: 4.0 mm, A wave] Pump function is maintained for up to the following horizontal response Top of motor (upper bearing portion): 14.0×9.8m/s ² (1.6×9.8 m/s ² input) [Step 3: Diametric clearance of support: 1.0 mm, vertical wave] Pump function is maintained for up to the following vertical response Top of motor (upper bearing portion): 2.3×9.8m/s ² (1.9×9.8 m/s ² input)
Effect of clearance of barrel support on pump response	[Diametric clearance of support: 1.0 mm, D wave] Pump function is maintained up to the following horizontal response (it was confirmed that design yield point was exceeded at bolts for mounting motor). Top of motor (upper bearing portion): 12.0×9.8m/s ² (1.5×9.8 m/s ² input) Effect of response on horizontal input was obtained making diametric clearance of barrel support as parameters (4.0 mm⇒2.0 mm⇒1.0 mm)

A wave: Input wave including natural frequency constituent of barrel 16.1 Hz (analyzed value before test under the assumption that clearance of barrel support is negligible)
D wave: Input wave including natural frequency constituent of barrel body/6.4 Hz (analyzed value before test in the case that clearance of barrel support is assumed not to be negligible and is large enough to avoid collision)
D' wave: Spectrum obtained modifying D wave by reducing the acceleration spectrum by half in natural frequency region of motor (near 20 Hz, analyzed value before test) in order to suppress response of motor and particularly aiming to produce big response of barrel to investigate function limit of barrel system

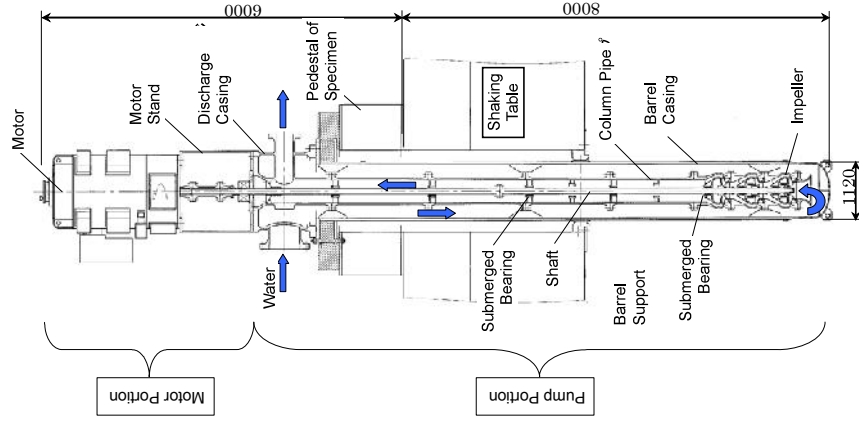


Figure 1.1.4-2 Outline of Structure of Actual Equipment Specimen

2. Evaluation method of fragility capacity

2.1 Horizontal shaft pump

The fragility evaluation method for horizontal shaft pump was discussed in “Report on Verification of Seismic Reliability of Nuclear Power Installations in FY 2004: Equipment Fragility Test: Part 1”.

Flow of fragility capacity evaluation for horizontal shaft pump is shown in Figure 2.1-1. Regarding fragility capacity tests for horizontal shaft pump, although no abnormality was identified for pumps in the full-scale equipment test, damages which would cause decrease of operating life of bearing were identified at some bearings in the element tests. Hence bearing load was chosen as indicator of fragility evaluation for conservative evaluation. To do this analytical model was developed for large input motion and bearing loads in axial and radial direction were derived by time history analysis. Input acceleration in which bearing load reaches to the limit is considered as dynamic function limit acceleration.

Simplified evaluation was performed to evaluate structural strength of foundation bolts and mounting bolts and slip of mounting portions of pump and motor, as items to be considered as critical in not only active function but also structural strength, and their critical accelerations were evaluated.

Critical portions extracted to evaluate critical acceleration of active function and critical acceleration of structural strength are shown in Table 2.1-1. Their values set for evaluation are also shown in the Table. Basic concept to evaluate critical components and setting of critical values of each component are shown in the table, and basic thought of analytical model making and evaluation are described below.

(1) Limit of active function

(i) Critical load of bearing

Critical load for fragility evaluation of bearing was specified based on the load under which abnormality occurred or function was confirmed to be maintained in the element tests. Concept of critical load setting for ball bearing and slide bearing are shown below. Critical load data (some of them are of function-confirmed load since no abnormality was found up to sufficiently large load) of each bearing are shown in Table 3.1-3 of Section 3.1. They were used as a basis for horizontal pump fragility evaluation.

a. Ball bearing

(a) Thrust load

In the element test, frictional wear was generated for deep groove ball bearing which could cause decrease of operating life of bearing. Therefore, critical load was specified as 1/3 times of run-onto static rated load C_{oa} based on the load which generated friction wear. For angular ball bearing, no significant damage other than friction wear was identified and its critical load was conservatively specified as run-onto static rated load C_{oa} .

(b) Radial load

No significant damage was identified in the element tests for deep groove ball bearing and angular ball bearing. However, as the maximum input load in the element tests was 1/1.5 times of basic static rated load, critical load was conservatively specified as 1/1.5 times of basic static rated load C_{or} .

b. Slide bearing

(a) Thrust bearing

In the element test, although specimen was loaded with the maximum load which test facility could impose, no significant damage was identified in the bearing. For thrust bearing, the maximum imposed load, under which function was confirmed to be maintained, is conservatively specified as critical load for fragility capacity evaluation of horizontal pumps. PV value (P: Surface pressure, V: Velocity) used as an index of contact pressure limit of slide bearing is specified as criterion of fragility capacity evaluation. As the range of bearing diameter was limited for horizontal shaft pump, evaluation is possible with the dimensions of the specimen. Therefore, the minimum PV value, under which function was confirmed to be maintained in the test, is used as representative critical value.

(b) Radial bearing

In the element tests, shaft torque gradually increased as increase of imposed load, and plastic flow, which could cause decrease of operating life of bearing, was identified on the surface of bearing in the inspection after the test. Although plastic flow was considered to be still small when change of shaft torque began, the load, at which shaft torque began to increase, is conservatively specified as critical load for fragility capacity evaluation of the bearing, and PV value calculated based on it is specified as criterion for fragility capacity evaluation and the minimum PV value, under which function was confirmed to be maintained in the test, is used the same as thrust bearing.

(ii) Median values and dispersion of fragility capacity

Critical acceleration of active function calculated based on preceding Item (i) is specified as median value of fragility capacity for active function of horizontal shaft pump. As the maximum logarithmic standard deviation of critical load obtained in the element test was 0.21 for deep groove ball bearing and 0.12 for slide (radial) bearing, these values are used as critical acceleration evaluation of active function for these bearings.

(iii) Analytical model

a. Horizontal shaft single stage pump

Object of tests and analysis was horizontal shaft single stage pump using ball bearing, and analytical model was made reflecting vibration characteristics of ball bearing in the large amplitude region obtained by the element tests. Analytical model in axial direction is one mass system model shown in Figure 2.1-2, and rotator mass including contained water M , stiffness of bearing box k_1 , stiffness of bearing k_2 , and damping factor of bearing portion c_1 are considered in the model. Regarding stiffness and damping factor, k_1 is determined from configuration of bearing box, and k_2 and c_1 are specified by the results of element test. Specifically, as the element test of bearing showed that load displacement characteristics of bearing can be simulated with high accuracy by Hertz formula, spring constant having non-linear characteristics obtained by Hertz formula is used as k_2 . The average value of damping factor obtained from the tests is used as c_1 , because there was no significant difference due to difference of bearing. Pump casing is treated as rigid and is not included in the model.

Analytical model in lateral direction is to be multi-mass system shown in Figure 2.1-3. Bearing is reflected in the analytical model using spring constant with non-linear characteristic obtained from Hertz formula, and liner ring is reflected in the analytical model as non-linear spring consisting of average spring constants in water film region and contact region respectively obtained in the element tests.

Damping factor used in seismic response analysis is specified as the damping factor, 1%, for design of

pumps, etc. given in the Japan Electric Association "Technical Guidelines For Seismic Design of Nuclear Power Plants" (JEAG 4601), excluding bearing and liner ring.

b. Horizontal shaft multi-stage pump

Object of tests and analysis was horizontal shaft multi-stage pump using slide bearing, and analytical model was made reflecting vibration characteristics of ball slide bearing in the large amplitude region obtained by the element tests. Analytical model in axial direction is one mass system model shown in Figure 2.1-4, and rotator mass including contained water M , stiffness of bearing bracket (considering stiffness of mounting flange and mounting bolt) k_1 , stiffness of thrust bearing k_2 , and damping factor of bearing portion c_1 are considered in the model. The average value of spring constants in water film region and contact region respectively obtained in the element test is used as spring constant of thrust bearing k_2 in the analytical model. Damping factor c_1 is derived from dimensionless factor obtained in the element test using load, rotating speed and representative dimensions.

As shown in Figure 2.1-5, vibration model in lateral direction is multi mass model that mass of rotating shaft system is supported at bearing portion by springs of radial bearing and bearing bracket (considering stiffness of mounting flange and mounting bolt), and liner ring portion is supported by spring of liner ring portion. Spring constants of radial bearing and liner ring are to be non-linear spring consisting of average spring constants in water film region and contact region respectively obtained in the element tests. The dimensional value of damping factor, which is derived from dimensionless damping factor obtained in the element test using load, rotating speed and representative dimensions, is used as damping factor.

Damping factor used in seismic response analysis is specified as the damping factor, 1%, for design of pumps, etc. given in JEAG 4601, excluding bearing and liner ring.

(iv) Input earthquake

Acceleration time historical response wave on mounting floor of horizontal shaft pump is used as input earthquake motion to evaluate critical value for active function.

(2) Structural strength limit

(i) Items to be evaluated

Horizontal shaft pump fundamentally has rigid structure and has no local response. Therefore, following portions, which are considered to be critical in structural strength, are evaluated. In the evaluation, simple static analysis method is used. The seismic acceleration used in the static analysis is 1.2 times of floor response acceleration (ZPA).

a. Evaluation of bolt strength

Study in Part 1 of Equipment Fragility Test indicated that the portions, where seismic margin was smallest among strength members, were foundation bolt and mounting bolt of supporting portion, and strength evaluation is, therefore, to be performed for them. Stress calculation of bolt is to be performed using static analysis described in JEAG4601-1991.

b. Slip evaluation for mounting portion

Pump and motor are mounted on a common foundation and there is possibility of relative slip by seismic force between pump and motor. This slip could cause abnormality in rotating function of pump.

However, relation between seismic force and slip is unknown, and detailed analysis is difficult. Therefore,

acceleration to generate slip is to be evaluated by simplified static analysis using magnitude of frictional force at mounting portion of pump and motor.

There are many uncertain factors for slip of mounting portion, and detailed study is necessary to obtain the actual critical value. As slip of mounting portion depends on tightening condition of the relevant portion, fragility capacity would be improved by relatively simplified measures such as reinforcement of anchor portion. Therefore, acceleration to generate slip is treated as reference.

(ii) Evaluation method

a. Evaluation of bolt strength

Stresses of foundation bolt and mounting bolt are calculated for lateral and axial directions, and are compared with critical stress, and fragility capacity is evaluated. Critical stress is to be as follows based on "FY 2002, Report on Development of Evaluation Method of Probabilistic Seismic Safety - Development of Fragility Data of Component - " (March, 2003, NUPEC INS/M02-22):

- For critical tensile stress, design tensile stress (S_u) described in Japan Society of Mechanical Engineers (JSME) "Standards for Nuclear Power Generation Equipment: Design and Construction Standards" is specified as the lower limit, and the value obtained dividing it by confidence coefficient η is specified as median value of critical stress (η : 0.856 for general steel materials and 0.885 for stainless steel). Critical tensile stress for screw portion of bolt is specified as 0.75 times of critical tensile stress of bolt, using ratio of cross section of root diameter/cross section of nominal diameter of bolt.
- Critical stress for shear is specified as $1/\sqrt{3}$ times of critical stress for tensile, based on theory of shear-strain stress.

b. Slip evaluation of mounting portion (as reference)

Frictional force is calculated for pump body and motor, and then critical acceleration of slip is to be calculated from comparison with earthquake load in horizontal direction. For frictional force, tightening force by mounting bolt and mass of equipment is considered.

(iii) Median value and dispersion of fragility capacity

Bolt strength calculated from the above evaluation and critical acceleration for slip of mounting portion are specified as median value of fragility capacity for structural strength. Regarding dispersion of bolt strength evaluation, $0.75S_u$ is treated as 1%, and $0.75S_u/0.856$ as median value in the distribution of tensile strength of material, and logarithmic standard deviation β becomes as $\beta = -1/2.326 \times \text{LN}(0.856) = 0.07$.

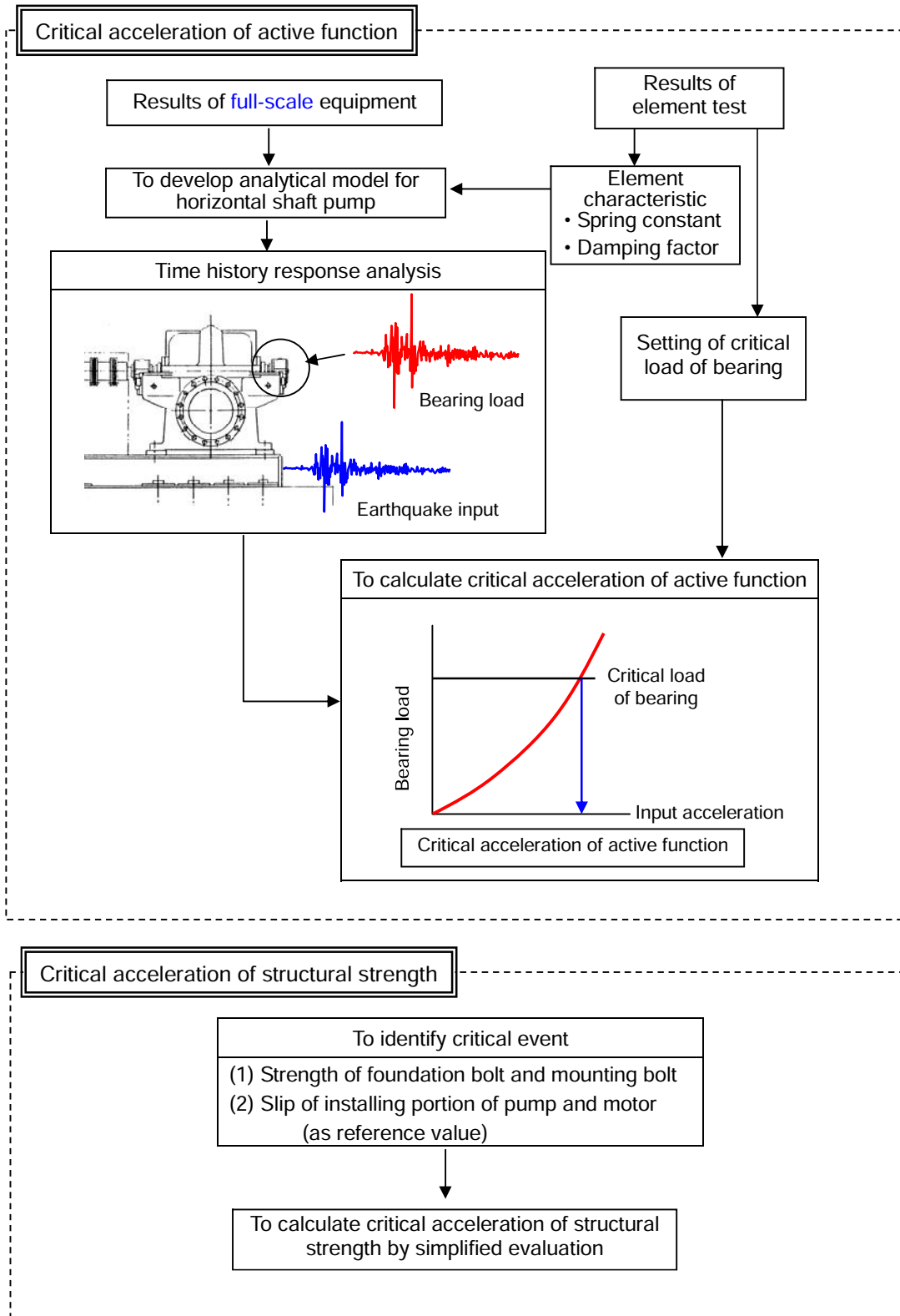
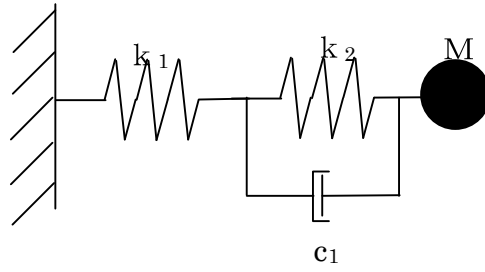


Figure 2.1-1 Flow of Fragility Evaluation of Horizontal Shaft Pump

Table 2.1-1 Portion for Fragility Evaluation of Horizontal Shaft Pump and Set Values

Function	Direction	Critical portion	Fragility evaluation item		Description	
			Item	Set value*		
Active function	Axial	Deep groove ball bearing	Bearing load	Coa×1/3	<ul style="list-style-type: none"> • Coa: Run-onto static rated load of bearing • To be set based on friction generation load which could cause decrease of operating life of bearing, using the element test results 	
		Angular ball bearing		Coa	<ul style="list-style-type: none"> • To be more conservatively set than function-confirmed load in the element test 	
		Slide bearing	PV value	129MPa·m/s	<ul style="list-style-type: none"> • Minimum value of function-confirmed load in the element test 	
	Lateral	Deep groove ball bearing	Bearing load		Cor×1/1.5	<ul style="list-style-type: none"> • Cor: Basic static rated load of bearing • To be more conservatively set than function-confirmed load in the element test
		Angular ball bearing				
		Slide bearing	PV value	121MPa·m/s	<ul style="list-style-type: none"> • To be set based on the minimum value of load due to shaft torque change, considering generation of plastic flow which could cause decrease of operating life of bearing 	
Structural strength	Axial/ Lateral	Foundation bolt Mounting bolt	Tensile stress	0.75Su/η	<ul style="list-style-type: none"> • Su: Design tensile stress η: Confidence coefficient (general steel product: 0.856, stainless steel: 0.885) 	
			Shear stress	(Su/√3)/η	<ul style="list-style-type: none"> • Simplified evaluation for bolt strength 	
	Axial/ Lateral	Mounting bolt	Horizontal load	μ·(F+W) (As reference value)	<ul style="list-style-type: none"> • μ: Friction coefficient (0.3) F: Sum of bolt tightening forces W: Dead load of pump or motor 	
					<ul style="list-style-type: none"> • Simplified evaluation for slip of mounting portion 	

* Set value: Reference value used for fragility evaluation in this report



M: Mass of rotor system (including additional mass of water)
 k_1 : Spring constant of bearing box (linear)
 k_2 : Spring constant of bearing (non-linear)
 c_1 : Damping of bearing

Figure 2.1-2 Analytical Model of Horizontal Shaft Single Stage Pump in Axial Direction

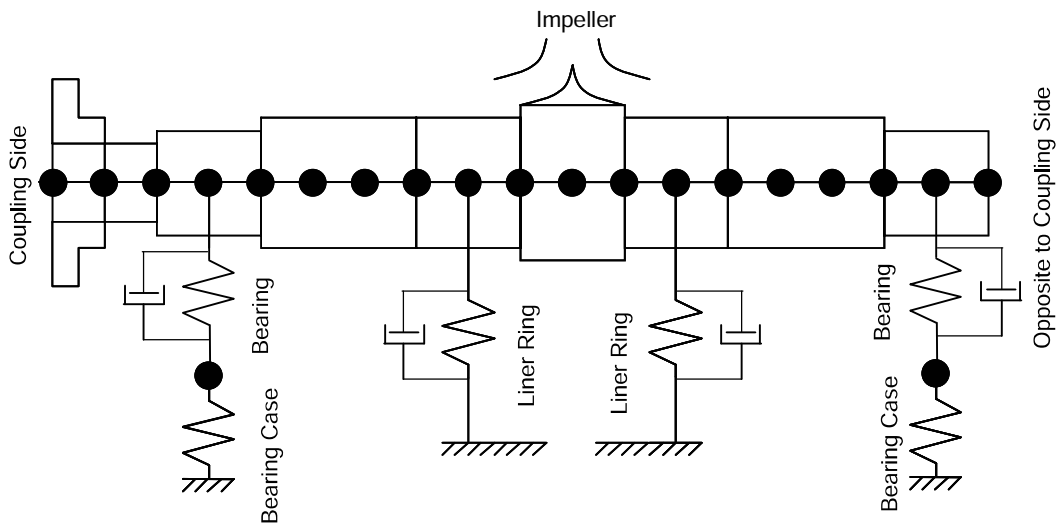
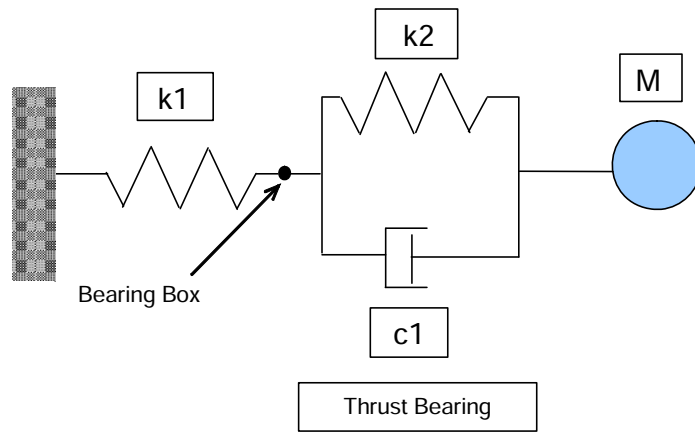


Figure 2.1-3 Analytical Model of Horizontal Shaft Single Stage Pump in Lateral Direction



M: Mass of rotating shaft system (including additional mass of water)
 K1: Spring constant of bearing bracket (linear)
 K2: Spring constant of thrust bearing (non-linear)
 c1: Damping factor of thrust bearing

Figure 2.1-4 Analytical Model of Horizontal Shaft Multi-Stage Pump in Axial Direction

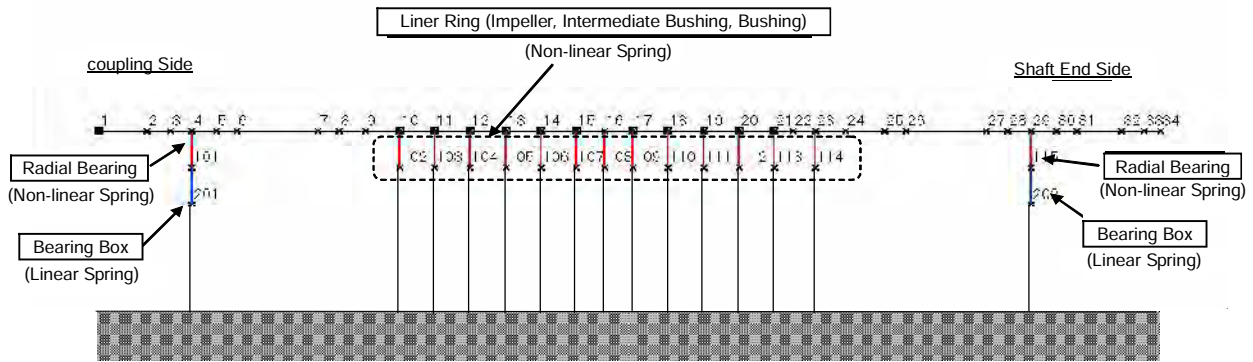


Figure 2.1-5 Analytical Model of Horizontal Shaft Multi-Stage Pump in Lateral Direction

2.2 Electrical equipment

Outline of fragility evaluation method of electrical equipment (panels) is shown below.

(1) Basic concept to specify fragility capacity

Critical acceleration of electrical function and critical acceleration of structural strength are to be calculated as fragility capacity of electrical equipment. Fragility capacity is generally calculated as response at arbitrary point of equipment. However, as mounting position of parts critical in response properties or electrical function is various, fragility capacity is specified by acceleration at foundation portion of panel because of easy use and understandability.

Fragility capacity of electrical parts is specified by input acceleration (i.e. acceleration at mounting position of the relevant part) in the element test.

(2) To specify fragility capacity of electrical equipment (panels)

(i) Critical acceleration for electrical function

Critical acceleration for electrical function is calculated by $A=m/k$ using median value (m) of critical acceleration for function of critical part specified from the element test results and response amplification factor (k) at mounting position of the relevant part to the equipment base. Multiplying factor is calculated from time historical response analysis using analysis model capable of simulating response characteristics of electrical equipment during large input vibration (Figure 2.2-1).

(ii) Critical acceleration for structural strength

Critical acceleration for structural strength is specified by performing stress evaluation of foundation bolt and housing. Response spectrum analysis using analysis model during large input vibration is applied as evaluation method. However, for critical tensile stress, which is a basis for evaluation, design tensile stress (S_u) described in JSME "Standards for Nuclear Power Generation Equipment: Design and Construction Standards" is specified as the lower limit, and the value obtained by dividing the calculated value by confidence coefficient η (0.856 for general steel) is used.

(iii) Dispersion

Dispersion of critical acceleration of function for electrical parts or critical stress of structural member, which becomes critical in fragility evaluation, is made to represent dispersion of electrical equipment.

(3) To specify fragility capacity of electrical parts

Fragility capacity of electrical parts is specified using the results of element tests.

Fragility capacity of each part was evaluated as follows.

(i) In case when loss-of-function occurred

For calculation of critical acceleration of function for each part, the average value of loss-of-function-acceleration, under which loss of function was identified in the test, and function-maintained-acceleration, under which function was confirmed to be maintained at one step before loss of function, is specified as critical acceleration of function.

(ii) In case when function was maintained

If loss of function never occurred even at the maximum test acceleration, loss of function is assumed to occur at the next step, i.e. the average value of the acceleration one step larger and the maximum test acceleration is specified as function-maintained acceleration.

Assuming that data of critical acceleration of function has logarithmic normal distribution, logarithmic average value of critical accelerations of function for each part obtained by the above is specified as median value of critical acceleration of function.

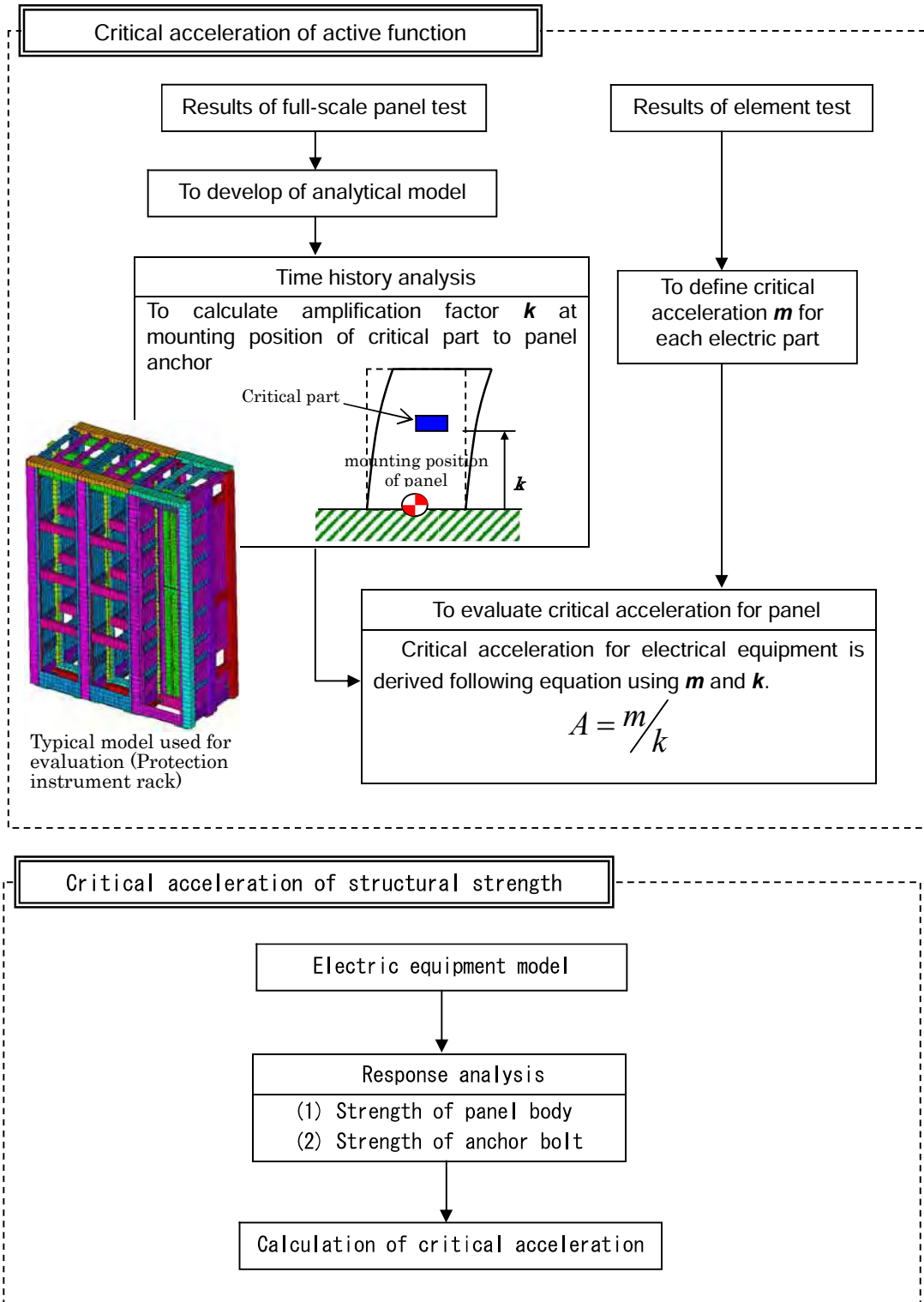


Figure 2.2-1 Flow of Fragility Evaluation of Electric Equipment

2.3. Control rod inserting capability

(1) PWR control rod inserting capability

Fragility evaluation for PWR control rod inserting capability was studied in "FY 2005, Report of Tests and Investigation on Technology of Seismic Resistance Evaluation for Nuclear Installations, Equipment Fragility Test, Part 2 (PWR Control Rod Inserting Capability)". Outline of the report is described below.

(i) Fragility evaluation method

In fragility evaluation of control rod inserting capability, response displacement of fuel assembly was used as evaluation index, based on the results of Seismic Verification Test of PWR Core Internals previously performed by NUPEC (1981 to 1985), and tests and evaluation recently performed by JNES.

As element tests, test vessel containing one fuel assembly with filled water was placed on shaking table and was wholly vibrated, and in-water vibration characteristics of fuel assembly in large amplitude region (fuel response displacement: about 80 mm) were obtained.

In full-scale equipment test simulating PWR control rod insertion system, specimen was vibrated with up to 3.3 times of seismic force due to design basis extreme earthquake S_2 , and test data up to about 45 mm of fuel response displacement were obtained, largely exceeding the past test data (fuel response displacement: about 22 mm). Simulation analysis was performed for control rod insertion, reflecting the data obtained in these tests, and analytical method of control rod inserting capability during large input was established by confirming that seismic responses of the major portions of the specimen and control rod insertion time can be simulated. (Refer to Figure 2.3-1).

In the past fragility evaluation, prescribed scram time (the prescribed time in safety evaluation was applied as target of control rod insertion time during earthquake) was defined as 2.2 seconds (85% insertion time), and this insertion time, where control rod insertion time reached to the prescribed scram time as the result that fuel response displacement became large with increase of earthquake input, was defined as fragility capacity limit. In Part 2 (PWR control rod inserting capability) of Equipment Fragility Test, the state, where guide thimble was damaged due to excess increase of fuel response displacement, was treated as critical event, and analysis and evaluation were performed under the actual plant circumstances considering actual plant conditions such as temperature and flow rate. As the result, displacement of fuel assembly of 77 mm, generated by seismic force which was 4 times of design basis extreme earthquake S_2 was specified as median value of fragility capacity. In specifying median value of fragility capacity, fuel response displacement confirmed in the element tests was considered as the limit of application of this evaluation method.

Regarding this fuel displacement, it was confirmed by simulation analysis that control rod insertion time was less than newly specified insertion target time (refer to Item (ii)).

(ii) Prescribed scram time

Although prescribed scram time scram is defined to be 2.2 second in the past fragility capacity evaluation, exceeding the prescribed value does not directly result in a problem. Regarding possibility of core damage in case of exceeding the prescribed scram time, referring to NUPEC Report (INS/M03-05) "FY 2003, Report on Development of Probabilistic Safety Evaluation Method for Earthquake, Part III, Sophistication of Evaluation Method (In-core Thermal Hydraulic Analysis for Time Delay of Control Rod Insertion in PWR)", it was determined that core damage would not occur if control rod can be inserted by the time of initial actuation of pressurizer safety valve (about 8 sec.), and this time is specified as new target of control rod insertion time used in fragility capacity evaluation.

(iii) Dispersion

Dispersion is specified as 0.19, considering dispersions of tensile strength and dimensional tolerance of guide thimble of fuel assembly, and dispersions of response confirmed in the full-scale equipment test.

(2) BWR control rod inserting capability

Fragility capacity evaluation for BWR control rod inserting capability was studied in "FY 2005, Report of Tests and Investigation on Technology of Seismic Resistance Evaluation for Nuclear Installations, Equipment Fragility Test, Part 2 (BWR Control Rod Inserting Capability)". Outline of the report is described below.

(i) Fragility evaluation method

In fragility evaluation of control rod inserting capability, response displacement of fuel assembly was used as evaluation index, based on the results of Seismic Verification Test of BWR In-core Structure previously performed by NUPEC (1982 to 1987), and the results of tests and evaluation recently performed by JNES.

As element tests, critical strength test was performed for channel box which is major structural strength members of BWR fuel assembly, and mechanical behavior of fuel assembly in large amplitude region (fuel response displacement: up to about 100 mm) was obtained. In full-scale equipment test simulating BWR control rod insertion system, specimen was vibrated with up to 4 times of seismic force due to design basis extreme earthquake S_2 , and test data up to about 83 mm of fuel response displacement were obtained, largely exceeding the past test data (fuel response displacement: about 34 mm). Simulation analysis was performed for control rod insertion during large input, reflecting the data obtained in these tests, and analytical method of control rod inserting capability during large input was established by confirming that seismic response of the major portions of the specimen and control rod insertion time can be simulated (refer to Figure 2.3-2).

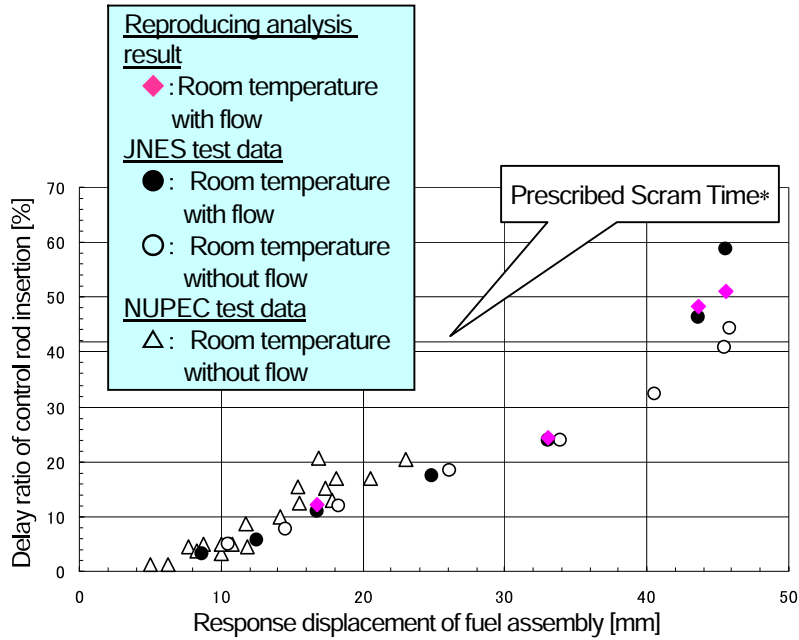
In the past fragility evaluation, prescribed scram time (the prescribed time in safety evaluation was applied as target of control rod insertion time during earthquake) was defined as 1.62 seconds (75% insertion time), and this insertion time, where control rod insertion time reached to the prescribed scram time as the result that fuel response displacement became large with increase of earthquake input, was defined as fragility capacity limit. In Part 2 (BWR control rod inserting capability) of Equipment Fragility Test the critical state, where collision of fuel bundle with shroud was initiated due to excess increase of fuel response displacement, was newly defined as fragility capacity limit. Analysis and evaluation were performed under the actual plant circumstances considering actual plant conditions such as temperature, and fragility value was defined as follows. 5% damage probability value was defined as 83mm (maximum response displacement in the full-scale equipment test), 95% damage probability value was defined as 100mm (response displacement to initiate collision with shroud), median value of fragility capacity was defined as 91 mm assuming logarithmic normal distribution from 5% and 95% values.

(ii) Prescribed scram time

Although prescribed scram time was defined to be 1.62 second in the past fragility capacity evaluation, exceeding the prescribed value does not directly result in a problem. In this evaluation, the prescribed scram time is made as it is, because it was confirmed by analysis that scram time was still below the prescribed time even when fuel assembly response reaches 100mm where it will initiate collision with shroud. (Figure 2.3-2)

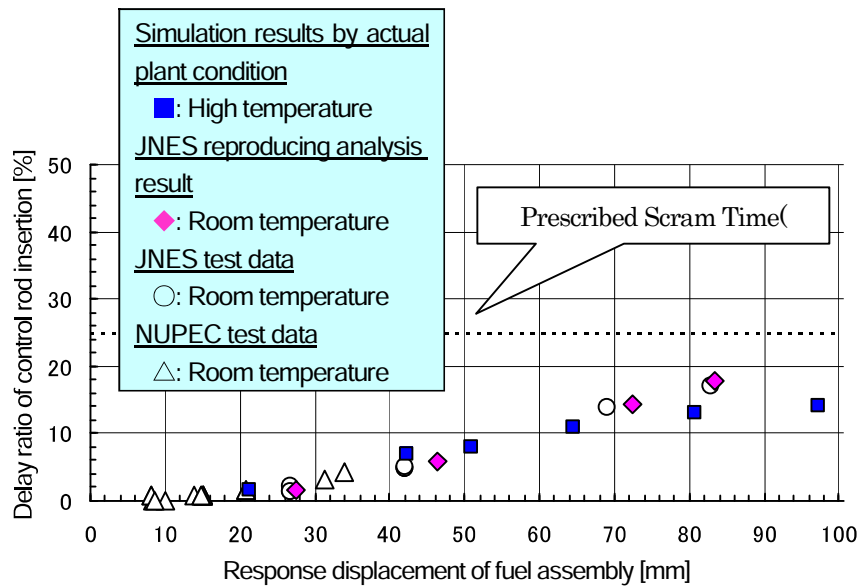
(iii) Dispersion

Dispersion is specified as 0.1 based on the damage probability assumption described above item (i), i.e. the 5% damage probability is 85mm (maximum fuel displacement achieved in full-scale equipment test) and 95% damage probability is 100mm (where fuel bundle initiate to collision with shroud).



*: Prescribed time in safety evaluation: 2.2sec. (85% insertion time). Exceeding it does not directly result in a problem.

Figure 2.3-2 Data of Delay Ratio of PWR Control Rod Insertion



(: Prescribed time in safety evaluation: 1.62 sec. (75% insertion time). Exceeding it does not directly result in a problem.

Figure 2.3-2 Data of Delay Ratio of BWR Control Rod Insertion

2.4 Large size horizontal shaft pump

(1) Pump to be evaluated

Fragility evaluation for large size horizontal shaft pump was studied in "FY 2005, Report of Tests and Investigation on Technology of Seismic Resistance Evaluation for Nuclear Installations, Equipment Fragility Test, Part 3 (Large Size Horizontal Shaft Pump)".

Simplified evaluation method to evaluate fragility capacity of various types of large size vertical shaft pump of actual plant, was developed using analytical method to simulate the results of full-scale equipment tests (in particular, the maximum response value).

Large size vertical shaft pump can be classified into 3 categories according to their structural types, that is, pit barrel type pump, vertical mixed flow type pump and vertical single-stage floor type pump, as shown in Figure 2.4-1. Considering that vertical single-stage floor type pump has a structure only above the floor, and its structure is the nearly same as structures above installation floor of other two types of pumps, and that it was confirmed by the results of full-scale equipment tests that response evaluations for portion above installation floor (motor portion) and portion below installation floor (pump portion) could be separately performed, pit barrel type pump and vertical mixed flow type pump were selected as the object of the fragility evaluation method.

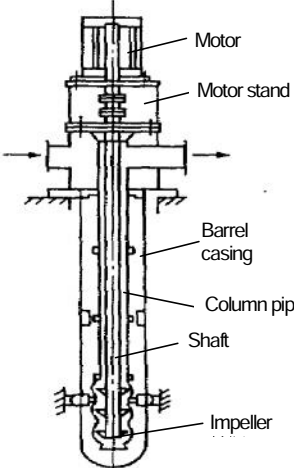
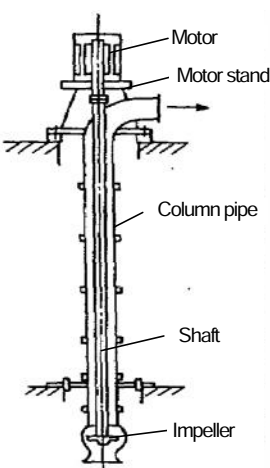
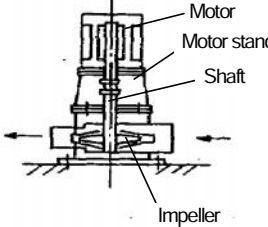
(i) Pit barrel type (BWR)	(ii) Vertical mixed flow type (BWR/PWR)	(iii) Vertical single-stage floor type (BWR/PWR)
		
<p>500MW/800MW/1100MW • Residual heat removal system (RHR) pump • LP core spray system pump • HP core spray system pump</p>	<p>• Seawater pump (RSW/SWP)</p>	<p>500MW/800MW/ • Residual heat removal system pump • Core spray system pump</p>

Figure 2.4-1 Structural Types of Large Size Vertical Shaft Pump

Pit barrel type pump has lateral supports between barrel and barrel pit and between column and barrel. There are clearances of several millimeters in each support portion. Vertical shaft mixed flow pump has no barrel, but normally it has a support between column and installed structure called intermediate support. And this support has two types, that is, the one with clearance and the other without clearance.

Name of each part of pump in this Section is shown in Figure 2.4-2.

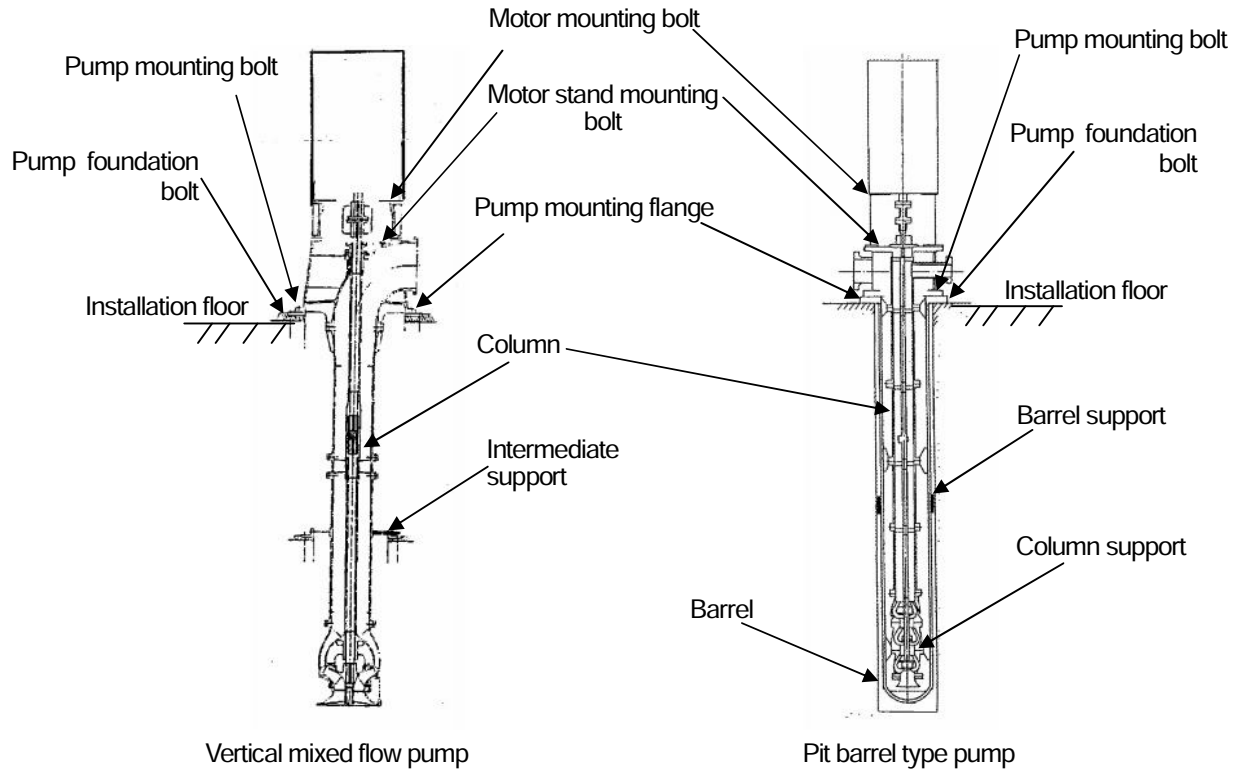


Figure 2.4-2 Names of Each Parts of Pump

(2) Calculation method of seismic load for fragility evaluation

Pump for full-scale equipment test is pit barrel type pump of reactor residual heat removal system (RHR). It was confirmed from the test results that response of pump portion (barrel, column and shaft) included high frequency component due to collision at clearance of barrel support portion, as well as fundamental wave component (primary mode of barrel). On the other hand, it was confirmed that response of motor portion almost had no high frequency component response and evaluation can be performed only with fundamental frequency component.

Therefore, for calculation of seismic load on pump portion having clearance at support portion (pit barrel type pump and vertical mixed flow pump having clearance at intermediate support portion), equivalent linear analysis to calculate fundamental frequency component response and impulse response analysis to calculate high frequency component response are performed, and the seismic load is evaluated by summing the both results. Seismic load at motor portion is evaluated using only the results of linear analysis (analytical model is identical to equivalent linear analysis model) for calculation of fundamental frequency component response. For pump without clearance at support portion (vertical mixed flow type pump without clearance at intermediate support), the seismic load can be calculated by linear response analysis using stiffness of intermediate support, because of no generation of high frequency component response due to collision.

(i) Method of equivalent linear analysis

Modeling of equivalent linear analysis and analysis method are described below. Outline of equivalent linear analysis model is shown in Table 2.4-1.

a. Number of dimensions to be considered

Structures such as barrel, column and rotating shaft are simulated by one dimensional multi-mass bending shear beam model.

b. Modeling

(a) Modeling of barrel system and barrel support portion (intermediate support portion)

Equivalent damping factor of barrel system is specified as 2.5%. Spring constant, which depends on input level and clearance width, is calculated using "Method to specify equivalent linear stiffness" shown in the next page.

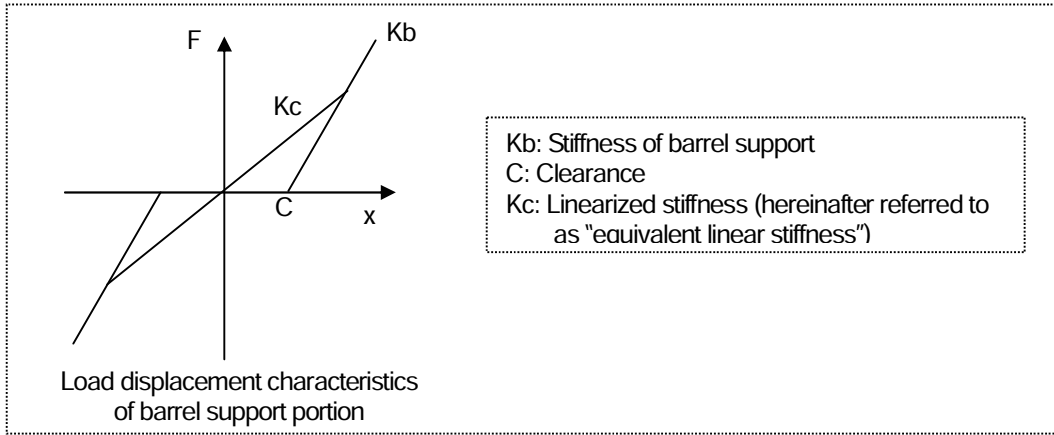
If clearance exists in intermediate support portion of vertical mixed flow pump, damping factor of support portion is specified as 2.5%, and in case of without clearance, it is specified as 1.0%, because damping effect of collision cannot be expected.

(b) Modeling of column support

Spring constant is specified as compression stiffness of column support portion, and damping factor is specified as 1.0%.

[Method to specify equivalent linear stiffness]

Equivalent linear stiffness is obtained as linear stiffness which can simulate the maximum load and displacement in nonlinear hysteresis. If this specifying method is applied to vertical mixed flow type pump, "barrel" is replaced by "column", and "barrel support" is replaced by "intermediate support".



If the maximum displacement at barrel support portion in nonlinear hysteresis is designated as y , then y can be expressed by the following equation using K_b , K_c and C :

$$y = \frac{K_b}{K_b - K_c} C$$

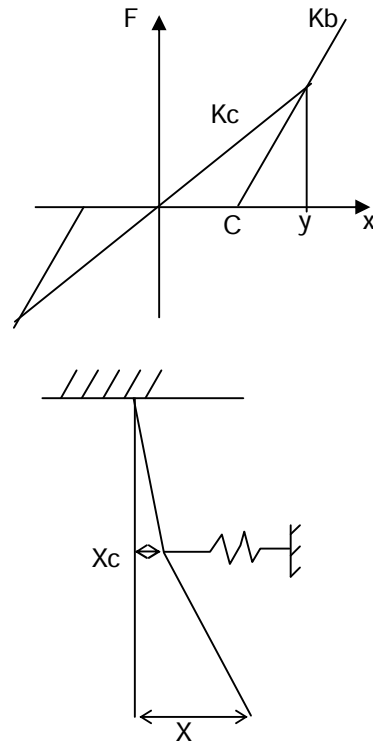
On the other hand, mode vector obtained by eigenvalue analysis is placed in the way shown in the figure below for barrel support portion and representative point of mode (location where mode vector becomes the maximum. In case of the figure below, bottom position).

As ratio of both mode vectors is equal to ratio of displacements, following relation is obtained if displacement of representative point of mode is designated as δ :

$$X_c : X = y : \delta = \frac{K_b}{K_b - K_c} C : \delta$$

Therefore, δ can be expressed by

$$\delta = \frac{K_b}{K_b - K_c} C \frac{X}{X_c}$$



That means, if eigenvalue analysis is performed using K_c as parameter and X/X_c is obtained, then, displacement of representative point of mode, δ , corresponding to equivalent linear stiffness, K_c , can be obtained because K_b and C are known.

Seismic response analysis is performed using this equivalent linear stiffness, and the input acceleration used in such analysis is required to be the acceleration where representative point of mode, δ , corresponding to equivalent linear stiffness, K_c , is calculated as a result of seismic response analysis.

(c) Modelling of submerged bearing

Spring constant in water film region (non-contact region) obtained by the element test of submerged bearing is used.

(d) Modeling of liner ring

Stiffness and damping are not considered within the range where contact of impeller with liner ring does not occur. Within the range where such contact occurs, spring constant of contact region for liner ring obtained in the element tests of liner ring is used.

(e) Modeling of motor system

Damping factor of motor casing system is specified as 3.0%. Stiffness of pump mounting flange portion is considered as rotating spring. Cross sectional defect of opening for coupling adjustment at motor stand, and rotating stiffness of tightening portions of motor mounting bolt and motor stand mounting bolt are considered only if the effects of their existence on vibration response could not be neglected.

(ii) Method of impulse response analysis

For pump having clearance at intermediate support portion among bit barrel type pump and vertical mixed flow pump, higher wave component response due to collision at the relevant clearance portion is obtained using impulse response analysis. Method of impulse response analysis is described below. The analysis model used in impulse response analysis is a model constructed by removing model of barrel support portion from equivalent linear analysis model described in Item (i).

[Impulse response analysis method]

a. Impulse response analysis for pit barrel type pump

As shown in Figure 2.4-3 (e), momentum change of pump system before and after collision between barrel and barrel support is calculated. Mass of pump system in the calculation is specified as equivalent mass at fundamental vibration mode, and velocity is specified as the velocity at the lumped mass where response velocity becomes the maximum among masses of barrel system. Momentum change is inputted to barrel support portion as impulse, $F \cdot \Delta t$, and higher wave response is obtained.

$F \Delta t = M_1 V_1 - M_2 V_2$	
M_1, M_2	: Equivalent mass of fundamental vibration mode before and after collision
V_1, V_2	: Velocity before and after collision

Δt here is to be 1/600 sec. as sufficiently fine time step compared with main component of bearing load (below 100 Hz) in the full-scale equipment test (the same for the case of vertical mixed flow pump).

b. Impulse response analysis for vertical mixed flow pump

If intermediate support portion of vertical mixed flow pump has clearance, high frequency response component due to collision of support portion is calculated, replacing barrel by column and barrel support by intermediate support, according to the calculation of component due to collision of barrel support shown in the above item. If intermediate support of vertical mixed flow pump has no clearance, impulse response analysis is not performed.

(iii) Response evaluation method

Excluding the case that intermediate support portion of vertical mixed flow pump has no clearance, response of each under-floor portion of pump (acceleration, load, etc.) is obtained by adding the results of equivalent linear analysis in the above Item (i) to the results of impulse response analysis in Item (ii).

Response of above-floor portion is obtained only by the results of equivalent linear analysis, because it is not affected by collision at under-floor portion of pump.

If intermediate support of vertical mixed flow pump has no clearance, the result of linear response analysis is used as response for each portion of pump.

Response of under-floor portions of pit barrel type and vertical mixed flow pumps (if intermediate support has clearance)

(Seismic load for evaluation) = (Equivalent linear response analysis) + (Impulse response analysis)

Response of above-floor portions of pit barrel type and vertical mixed flow pumps (if intermediate support has clearance)

(Seismic load for evaluation) = (Equivalent linear response analysis)

Response of vertical mixed flow pumps (if intermediate support has no clearance)

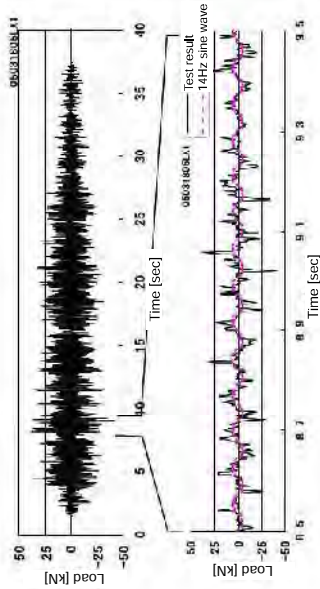
(Seismic load for evaluation) = (Linear response analysis)

Table 2.4-1 Analytical Model for Fragility Evaluation

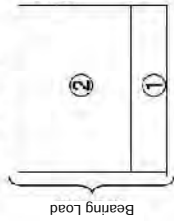
Model	Barrel support equivalent linear and bearing linear (Column support linear)
(1) System of barrel, column and rotating shaft	Multi-mass linear beam model
(2) Stiffness of barrel support portion	Equivalent linear spring (refer to item (ii) of 2.4(2) (i)) To give it so as to simulate the maximum of load-displacement relation for stiffness of barrel support portion according to input acceleration level
(3) Stiffness of column support portion	Linear spring stiffness: compression stiffness of column support portion
(4) Stiffness of submerged bearing portion	Water film stiffness obtained by the element test for pit barrel type pump and vertical mixed flow pump with clearance at intermediate support Contact region stiffness obtained by the element test for vertical mixed flow pump without clearance at intermediate support
(5) Stiffness of liner ring portion	Not considered, in case of no contact between liner ring and impeller
(6) Stiffness of pump foundation	Barrel flange portion (fixed portion) is considered as rotating spring stiffness Installation floor (concrete) is treated as rigid
(7) Damping of barrel, column and rotating shaft system	Damping factor of barrel: 2.5% Damping factor of rotating shaft and column: 1.0%
(8) Damping of barrel support portion	Damping factor: 2.5%
(9) Damping of column support portion	Damping factor: 1.0%
(10) Damping of submerged bearing portion	Not considered
(11) Damping of liner ring portion	Not considered
(12) Damping of pump foundation	Damping factor: 1.0%
(13) Modeling of motor casing system	Multi-mass linear beam model (Reduction of stiffness due to cross section defect of motor foundation opening is not considered)
(14) Modeling of motor rotating shaft system	Multi-mass linear beam model
(15) Damping of motor casing system	Damping factor: 3.0%
(16) Damping of motor rotating shaft system	Damping factor: 1.0%

(a) Bearing load time history by test

High frequency component is found other than fundamental wave component of barrel in bearing load time history wave form. The maximum value of bearing load is greatly affected by the high frequency component.

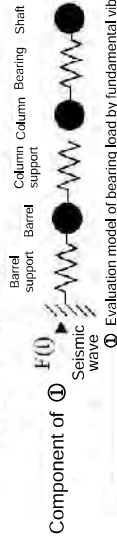


(b) Component of bearing load



① is reproduced by simulating fundamental wave component of barrel

(c) Concept of load transfer

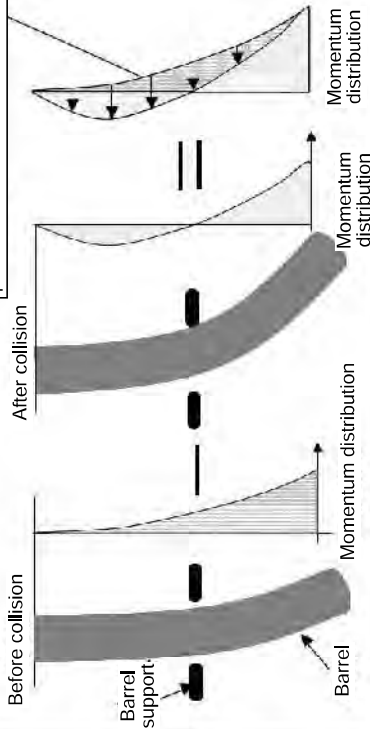


Component of ①

Component of ②

② Evaluation model for collision force of barrel support portion

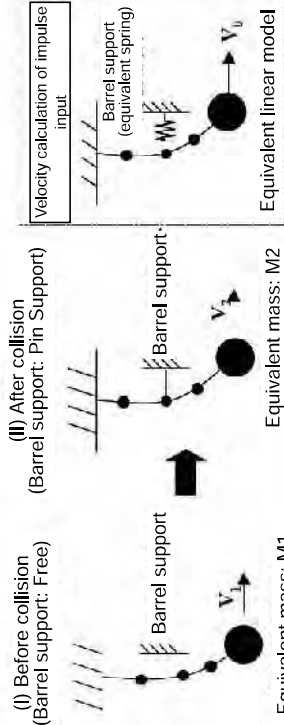
(d) Concept of calculation of collision component at barrel support portion



(e) Calculation of collision component at barrel support portion by analysis

$$F\Delta t = M1V_1 - M2V_2$$

M1, M2: Equivalent mass of fundamental vibration mode before and after collision
 V_1, V_2 : Velocity before and after collision



(d) Momentum change of fundamental vibration mode before and after collision

Equivalent mass, M1, M2 : Calculated by eigenvalue analysis
 Velocity $V_1, V_2 = V_0$: Assume that velocity is not change just before and just after collision. Use the velocity in response analysis using equivalent linear model.

(f) Impulse response analysis

For barrel support portion of the model without barrel support spring, impulse obtained in Item (e) is given as input.

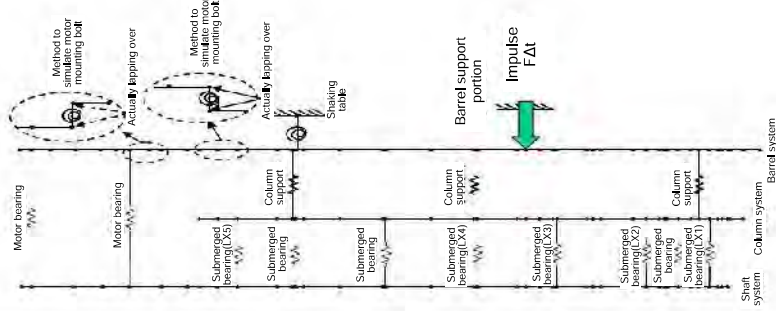


Figure 2.4-3 Evaluation Method of Collision Load at Barrel Support Portion Using Equivalent Linear Analysis Model

(3) Evaluation method of fragility capacity

(i) Evaluation items

Fragility capacity evaluation for horizontal earthquake is to be performed, focusing on the following portions which would result in function limit (evaluation of rotating function) and structural strength limit of pump based on the results of full-scale equipment test and element tests.

[Evaluation of rotating function]	[Evaluation of structural strength]
<ul style="list-style-type: none">• Motor body• Submerged bearing• Liner ring	<ul style="list-style-type: none">• Pump foundation bolt• Pump mounting bolt, motor mounting bolt, motor stand mounting bolt• Barrel• Column

(ii) Structural strength limit

a. Concept of structural strength limit

Evaluation of structural strength limit is performed using critical stress. The critical stress is specified according to "FY 2002, Report on Development of Evaluation Method of Probabilistic Safety for Earthquake - Development of Equipment Fragility Data -".

In evaluation of tensile stress of bolt, tensile stress due to earthquake and tensile stress due to initial tightening force are considered. In order to conservatively evaluate tensile stress due to earthquake, the internal force coefficient in the evaluation is conservatively specified as 0.5, based on ratio of internal and external forces, Φ , of normal bolt – narrow cylinder – described in "Quick Calculation Table of Internal and External Force Ratio, Φ " (Figure C-1 of Attachment C-2) of "Mechanical Engineering Handbook" (edited by Japan Society of Mechanical Engineers).

Regarding slip evaluation for bolt tightening surface, slip was not identified in the full-scale equipment tests, but active function of pump could not be maintained if center of motor was shifted from center of pump. Therefore, slip evaluation is to be performed for bolt tightening surface. Examples of bolt tightening portion, where slip evaluation is to be performed, are shown below:

- Tightening surface of motor mounting bolt
- Tightening surface of motor stand mounting bolt

Regarding dispersion of torque constant, median value and standard deviation of torque constant for M20 bolt shown in Japanese Industrial Standards(JIS), How to Use Series, "Points of Screw Tightening Mechanism Design" (Japanese Standards Association) (Figure C-2 in Attachment C-2) are used as a reference. As a result, logarithmic standard deviation, β , is $\beta=0.250$.

Furthermore, 0.3, which is conventionally used as friction coefficient for general steel, is used as friction coefficient of mounting surface necessary for slip evaluation. Regarding dispersion of friction coefficient, median value and logarithmic standard deviation in "slip coefficient shown in slip test results for sheet steel without treatment" described in "SI Unit Version, Guide for Design and Construction of Lightweight Steel Structure, and its Interpretation" are used for a reference. As a result, logarithmic standard deviation, β , becomes $\beta=0.123$.

However, slip evaluation method was studied as reference, because slip behavior on bolt tightening surface has many uncertain factors such as effect of rotating shaft system. Regarding slip on tightening surface, fragility capacity would be improved by relatively simple method such as increasing tightening bolt size.

b. Structural strength evaluation criteria

(a) Bolt

Critical stress for bolt is as follows:

- a) Tightening bolt where center shift due to slip on tightening surface does not become problem in rotating function of pump
- Regarding critical stress for tensile, design tensile strength (S_u) described in JSME, "Standards for Nuclear Power Generation Equipment: Design and Construction Standards" is specified as lower limit, and the value divided by confidence coefficient, η , indicated in the Standards is specified as median value of critical stress. ($\eta=0.856$ for general steel and $\eta=0.885$ for stainless steel)
 - Based on shear strain stress theory, $1/\sqrt{3}$ times of critical stress for tensile is specified as critical stress for shear stress.
 - If calculation of stress is performed using nominal diameter, critical stress is to be 0.75 times of critical stress for tensile of bolt, using ratio of root diameter cross section/nominal diameter cross section of bolt.
 - Dispersion of critical stress is 0.07 for general steel and 0.05 for stainless steel.
- b) Tightening bolt where center shift due to slip on tightening surface becomes problem in rotating function of pump

As slip evaluation is needed to be performed for these bolts, critical stress for bolt is as follows:

- Regarding critical stress for tensile, design yield stress (S_y) described in JSME, "Standards for Nuclear Power Generation Equipment: Design and Construction Standards" is specified as lower limit, and the value divided by confidence coefficient, η , indicated in the Standards is specified as median value of critical stress. ($\eta=0.856$ for general steel and $\eta=0.885$ for stainless steel)
- According to shear strain stress theory, $1/\sqrt{3}$ times of critical stress for tensile based on the above lower limit is specified as critical stress for shear stress. If calculation of stress is performed using nominal diameter, critical stress is to be 0.75 times of critical stress for tensile of bolt, using ratio of root diameter cross section/nominal diameter cross section of bolt.
- Dispersion of critical stress is 0.09 for general steel and 0.07 for stainless steel.

(b) Barrel and column

Critical stresses for barrel and column are as follows:

- Regarding critical stress at primary general membrane, design tensile strength (S_u) described in JSME, "Standards for Nuclear Power Generation Equipment: Design and Construction Standards" is specified as lower limit, and the value divided by confidence coefficient, η , indicated in the Standards is specified as median value. ($\eta: 0.856$ for general steel and 0.885 for stainless steel)
- Dispersion of critical stress is 0.07 for general steel and 0.05 for stainless steel.

c. Evaluation method of structural strength

Strength evaluation of each portion during earthquake is performed as follows:

(a) Tensile stress evaluation for bolt

Tensile stress generated at bolt is calculated by overturning moment. Internal force coefficient (conservatively 0.5) is considered in tensile stress calculation.

(b) Evaluation for shearing of bolt

Shearing force is obtained assuming that shearing force during earthquake is received by all of bolts.

(c) Evaluation for slip on bolt tightening surface (as a reference)

Evaluation for slip is performed based on comparison of friction force with shearing force of bolt portion.

(d) Evaluation of barrel and column

Strength of barrel and column is evaluated using primary general membrane stress. Primary general membrane stress is either axial stress or circumferential stress, whichever is greater. Axial stress is the sum of stress due to bending moment, stress due to internal pressure, and stress due to own weight and water weight in the barrel, and circumferential stress is stress due to internal pressure.

(iii) Rotating function limit

Loss of rotating function of pump did not occur in the element tests for submerged bearing and liner ring. Therefore, in principle, PV value where function was confirmed to be maintained by the element tests is specified as limit of rotating function regarding function limit of submerged bearing and liner ring in the evaluation. In the calculation of PV value, PV value should be calculated at rated operation state of pump. Data of function-confirmed PV value of bearing are shown in Section 3.4.

The maximum response acceleration at top of motor obtained by the full-scale equipment test ($14.0 \times 9.8 \text{ m/s}^2$) is considered to be function-confirmed response acceleration, and it should be treated as index for rotating function limit.

a. Carbon bearing and solid lubricant distributed non-lubricated bearing

Element test was performed up to vibration limit load of the test facility, and it was considered that there was sufficient margin because no loss of rotating function was identified. Therefore, function-confirmed PV value was specified, without calculating median value and logarithmic standard deviation of fragility capacity. Conservative evaluation is performed, using, as function-confirmed PV value, the minimum PV value obtained by the tests performed under the same conditions. In order to make the evaluation conservative, velocity during rated operation is used as the velocity, V, by which surface pressure during earthquake (P) is multiplied.

b. Rubber bearing and resin bearing

As the results of element tests up to the vibration limit of test facility, loss of rotating function did not occur. Therefore, it is not necessary to calculate median value and logarithmic standard deviation of fragility capacity, in the same way as the above Item a. However, from the fact that end surface of bearing was identified to be deformed at the maximum vibration load, it could be considered that it would be initiation indication of rotating function limit. Therefore, median value and logarithmic standard deviation are to be calculated based on PV value at the maximum bearing load, as a reference, and these values were conservatively considered in the subsequent fragility capacity evaluation for similar type of equipment.

c. Liner ring

As the results of performing tests up to the excitation limit of test facility for liner ring portion, loss of rotating function did not occur. Consequently, it is considered that there was sufficient margin. Therefore, function-confirmed PV value was specified without calculation of median value and logarithmic standard deviation of fragility capacity. For liner ring using martensitic stainless steel, PV value was specified based on the study results of Part 1 (horizontal shaft pump and electrical equipment); Equipment Fragility Test. Fragility evaluation for liner ring is to be performed if liner ring contacts with impeller.

(4) Analytical model for the pump to be evaluated for fragility capacity

Analytical model for large size vertical shaft pump is developed according to the modeling method shown in Section 2.4-1. For representative example, analytical model of pit barrel type pump (long size) is shown in Figure 2.4-4. In the same way, other types of pump are also modeled using one dimensional bending shear beam multi-mass.

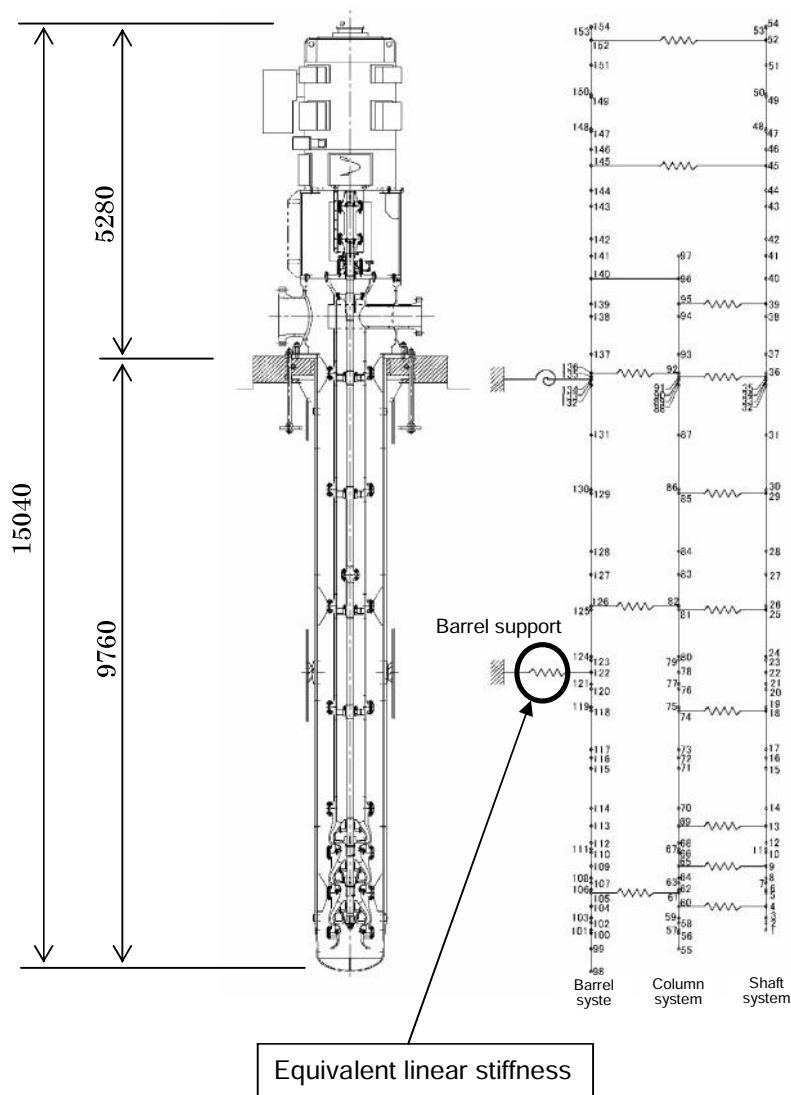


Figure 2.4-4 Analytical Model Diagram of Pit Barrel Type Pump (Long Size)

(5) Evaluation method for vertical fragility capacity

For vertical fragility evaluation, lifting analysis using spring-mass model of 2 mass system (Figure 2.4-5), which simulates shaft system of large size vertical shaft pump, is performed. In the model nonlinear behavior by up-lift at thrust bearing portion is considered. Evaluation is conducted using the following load and displacement as criteria:

- In the element test performed for Kingsbury and parallel plane bearings, thrust load was imposed up to the maximum load of 1500 kN (static load), and then rotating function of bearing was confirmed to be maintained for normal operation after removing the load. Consequently, it can be considered that bearing function is maintained with up to 1500 kN for collision load during lifting and getting down. Therefore, median value and logarithmic standard deviation are not calculated, and 1500 kN is specified as function-confirmed thrust load during getting down of rotating shaft system during vertical seismic motion.
- For amount of lifting, design clearance between liner ring and impeller is conservatively specified as evaluation criterion for vertical fragility capacity.

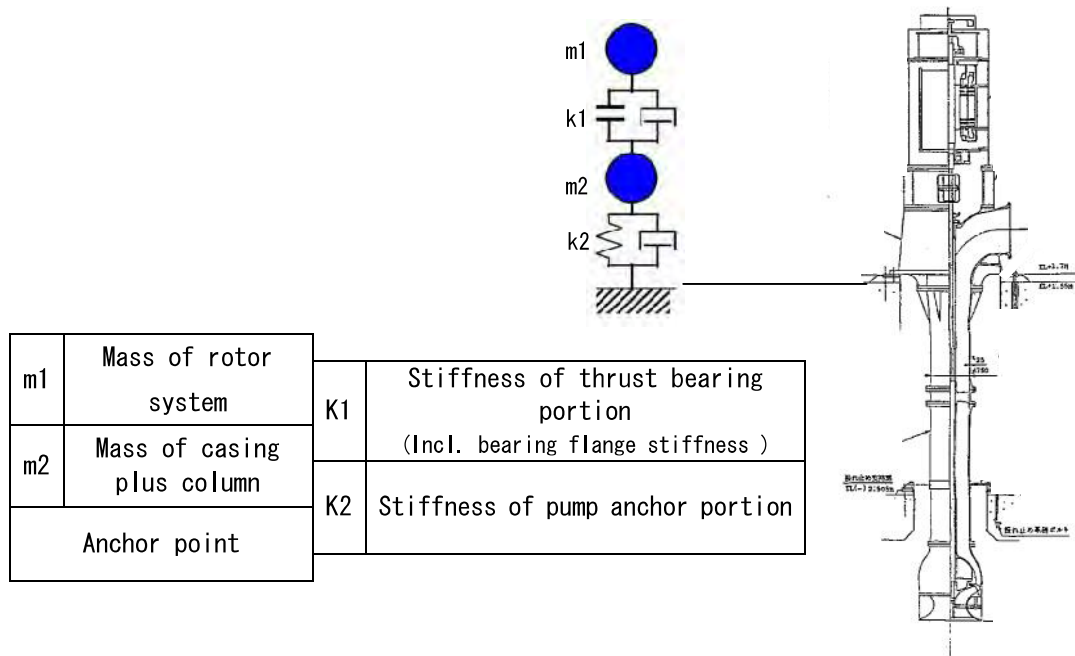


Figure 2.4-5 Two mass model for vertical direction response analysis of vertical shaft pump

3. Fragility data

Fragility evaluation results performed in Part 1 to Part 3 of Equipment Fragility Test for horizontal shaft pump, electrical equipment, control rod inserting capability and large size vertical shaft pump are summarized in this section.

In general, fragility capacity is expressed by response at a given point of equipment or facility. For the above equipments, point for defining fragility capacity is adequately specified for each equipment, and fragility data are processed. As shown in the previous section, it is fundamental to specify critical mode of function for each equipment, and analytically to calculate acceleration or displacement, by which response of equipment would reach to such state. Fragility capacity shown in this section is presented as response acceleration or response displacement or a set of response multiplying factor with input acceleration, and they are based on the vibration tests which use simulated earthquake wave enveloping earthquake conditions of the site where the objective equipment is installed. Relation between input earthquake motion and response of equipment depends on vibration characteristics of the relevant equipment and earthquake conditions of each site, and response of equipment would differ even if earthquake motion with the same maximum acceleration is imposed. Therefore, if more rigorous fragility capacity of equipment is required, evaluation is needed to be performed using earthquake conditions of each site, according to the fragility evaluation method of each equipment.

3.1 Horizontal shaft pump

Among fragility data studied in Part 1 of Equipment Fragility Test, fragility data related to horizontal shaft pump shown below are given in Table 3.1-2 to 3.1-4.

Table 3.1-1 Fragility Data related to Horizontal Shaft Pump

Equipment	Name	Table
Full-scale pump	RCW pump	Table 3.1-2
	Charging/HP injection pump	
Parts	Ball bearing	Table 3.1-3
	Slide bearing	
	Liner ring	Table 3.1-4

Table 3.1-2 Summary Table of Fragility Data (1/3)

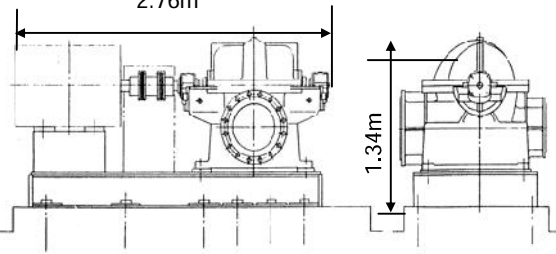
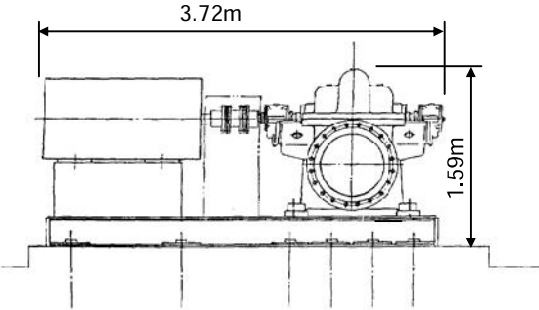
Equipment/ Facility	Horizontal shaft pump															
Type of objective equipment	Name: reactor building closed cooling water (RCW) pump Type: Single stage centrifugal type 2.76m 															
			<table border="1"> <thead> <tr> <th>Item</th> <th>Specification</th> </tr> </thead> <tbody> <tr> <td>Total pump head (m)</td> <td>55</td> </tr> <tr> <td>Flow rate (m³/h)</td> <td>1250</td> </tr> <tr> <td>Rotating speed (rpm)</td> <td>1800</td> </tr> <tr> <td>Motor output (kW)</td> <td>255</td> </tr> <tr> <td>Mass (ton) (including motor and contained water)</td> <td>5.7</td> </tr> </tbody> </table>			Item	Specification	Total pump head (m)	55	Flow rate (m ³ /h)	1250	Rotating speed (rpm)	1800	Motor output (kW)	255	Mass (ton) (including motor and contained water)
Item	Specification															
Total pump head (m)	55															
Flow rate (m ³ /h)	1250															
Rotating speed (rpm)	1800															
Motor output (kW)	255															
Mass (ton) (including motor and contained water)	5.7															
Test results and evaluation results of fragility capacity • Full-scale test • Element test • No test																
Outline of test results																
Vibration direction	Pump status	Maximum input acceleration (m/s ²)	Maximum response acceleration (m/s ²)		Abnormality of function											
			Top of motor Housing	Top of motor												
Axial	Operation	59.9	67.8	100.0	No abnormality											
	Shutdown	59.6	68.2	97.9	No abnormality											
Lateral	Operation	57.5	67.1	75.4	No abnormality											
	Shutdown	58.4	72.6	78.0	No abnormality											
Fragility evaluation																
Function	Direction	Median value of fragility	Log standard deviation	Failure mode	Evaluation method											
Limit of active function	Axial	8.4×9.8m/s ²	0.21	Wearing at ball bearing which would result in decrease of operating life	<ul style="list-style-type: none"> To calculate from critical load of bearing and pump response analysis Logarithmic standard deviation is calculated based on element test. 											
Limit of structural strength	Lateral	28.5×9.8m/s ²	0.07	Damage at pump foundation bolt	<ul style="list-style-type: none"> To calculate stress generated at foundation bolt by simplified method Logarithmic standard deviation is calculated using distribution of tensile strength of material. 											
	Axial/ lateral	<Reference> 6.1×9.8m/s ²	—	Slip of motor (relative shift between pump and motor)	<ul style="list-style-type: none"> To calculate acceleration exceeding friction force at motor mounting portion by simplified method 											
Remarks	<ul style="list-style-type: none"> Refer to Section 2.1 regarding fragility evaluation method. Median value of fragility capacity is acceleration at pump mounting floor slip is treated as a reference. 															

Table 3.1-2 Summary Table of Fragility Data (2/3)

Equipment/ Facility	Horizontal shaft pump								
Type of objective equipment	Name: reactor building closed cooling water (RCW) pump Type: Single stage centrifugal type								
		<table border="1"> <thead> <tr> <th>Item</th> <th>Specification</th> </tr> </thead> <tbody> <tr> <td>Flow rate (m³/h)</td> <td>2050</td> </tr> <tr> <td>Motor output (kW)</td> <td>440</td> </tr> <tr> <td>Mass (ton) (including motor and contained water)</td> <td>8.2</td> </tr> </tbody> </table>	Item	Specification	Flow rate (m ³ /h)	2050	Motor output (kW)	440	Mass (ton) (including motor and contained water)
Item	Specification								
Flow rate (m ³ /h)	2050								
Motor output (kW)	440								
Mass (ton) (including motor and contained water)	8.2								

Test results and evaluation results of fragility capacity • Full-scale test • Element test • **No test**

Results of fragility evaluation					
Function	Direction	Median value of fragility	Logarithmic standard deviation	Failure mode	Evaluation method
Limit of active function	Axial	8.6×9.8m/s ²	—	—	• To calculate from critical load of bearing and pump response analysis
Limit of structural strength	Lateral	23.5×9.8m/s ²	0.07	Damage at pump foundation bolt	• To calculate stress generated at foundation bolt by simplified method • Logarithmic standard deviation is calculated using distribution of tensile strength of material.
	Axial/ lateral	<reference> 5.3×9.8m/s ²	—	Slip of motor (relative shift between pump and motor)	• To calculate acceleration exceeding friction force at motor mounting portion by simplified method
Remarks	<ul style="list-style-type: none"> • Refer to Section 2.1 regarding fragility evaluation method. • Median value of fragility capacity is acceleration at pump mounting floor • Slip is treated as a reference. 				

Table 3.1-2 Summary Table of Fragility Data (3/3)

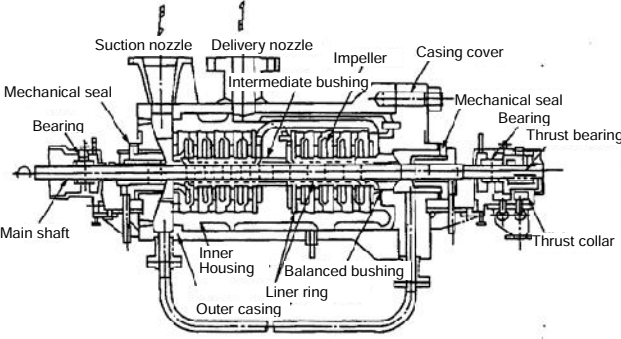
Equipment/ Facility	Horizontal shaft pump														
Type of objective equipment	Name: Charging/HP injection pump Type: Multi-stage centrifugal type		<table border="1"> <thead> <tr> <th>Item</th> <th>Specification</th> </tr> </thead> <tbody> <tr> <td>Total pump head (m)</td> <td>1770/732</td> </tr> <tr> <td>Flow rate (m³/h)</td> <td>34.1/147</td> </tr> <tr> <td>Motor output (kW)</td> <td>670</td> </tr> <tr> <td>Mass (ton)</td> <td>6.05</td> </tr> </tbody> </table>			Item	Specification	Total pump head (m)	1770/732	Flow rate (m ³ /h)	34.1/147	Motor output (kW)	670	Mass (ton)	6.05
	Item	Specification													
Total pump head (m)	1770/732														
Flow rate (m ³ /h)	34.1/147														
Motor output (kW)	670														
Mass (ton)	6.05														
	Dimension: 2.6m (length)×1.5m (width)×1.5m (height)														
Test results and evaluation results of fragility capacity • Full-scale test • Element test • No test															
Results of fragility evaluation															
Function	Direction	Median value of fragility	Logarithmic standard deviation	Failure mode	Evaluation method										
Limit of active function	Axial	17.3×9.8m/s ²	—	—	• To calculate from critical load of bearing and pump response analysis										
Limit of structural strength	Lateral	11×9.8m/s ²	0.07	Damage at pump foundation bolt	• To calculate stress generated at foundation bolt by simplified method • Logarithmic standard deviation is calculated using distribution of tensile strength of material.										
	Axial/ lateral	<reference> 2.6×9.8m/s ²	—	Slip of motor (relative shift between pump and motor)	• To calculate acceleration exceeding friction force at motor mounting portion by simplified method										
Remarks	<ul style="list-style-type: none"> • Refer to Section 2.1 regarding fragility evaluation method. • Median value of fragility capacity is acceleration at pump mounting floor • Slip is treated as a reference. 														

Table 3.1-3 Summary Table of Fragility Data (1/2)

Equipment/ Facility	Ball bearing for horizontal shaft pump						
Type of objective equipment	Type	Model number	Diameter of shaft (mm)	Outer diameter of outer ring (mm)	Basic static rated load (kN)	Run-onto static rated load (kN)	Number of specimens
	Deep groove ball bearing	6310	50	110	38.5	25	3
	Deep groove ball bearing	6316	80	170	86.5	56.8	3
	Angular ball bearing	7316B	80	170	109	26.4	3
Test results and evaluation results of fragility capacity • Full-scale test • Element test • No test							
Thrust load test							
Model number	Specimen No.	Test results		Fragility evaluation			
		Function-confirmed load (kN)	Load to generate friction (kN)	Function critical load (kN)	Median value (kN)	Log standard deviation	
6310	1	20	24	22.0	24.0	0.21	
	2	27	—	30.5			
	3	19	23	21.0			
				Bearing critical load for fragility evaluation (Coa/3) (kN)			
				8.3			
6316	1	20	31	25.5	25.3	0.01	
	2	21	29	25.0			
	3	22	29	25.5			
				Bearing critical load for fragility evaluation (Coa/3) (kN)			
				18.9			
7316B	1	62	—	—	—	—	
	2	61	—	—			
	3	59	—	—			
				Bearing critical load for fragility evaluation (Coa)			
				26.4			
Remarks	<ul style="list-style-type: none"> • Friction, which would result in decrease of bearing operating life, was generated on the surfaces of rotating body, and inner and outer ring of 6310 and 6316. • No abnormality for 7316B 			<ul style="list-style-type: none"> • Refer to Section 2.1 for fragility evaluation method • Coa: Run-onto static rated load 			
Radial load test							
Model number	Specimen No.	Test results		Fragility evaluation			
		Function-confirmed load (kN)	Load to generate friction (kN)	Function critical load (kN)	Median value (kN)	Log standard deviation	
6310	1	26	—	—	—	—	
	2	26	—	—			
	3	26	—	—			
				Bearing critical load for fragility evaluation (Cor/1.5)			
				25.7			
6316	1	33	—	—	—	—	
	2	31	—	—			
	3	33	—	—			
				Bearing critical load for fragility evaluation (Cor/1.5)			
				57.7			
Remarks	No abnormality in bearing			<ul style="list-style-type: none"> • Refer to Section 2.1 for specifying bearing critical load • Cor: Basic static rated load 			

Table 3.1-3 Summary Table of Fragility Data (2/2)

Equipment/ Facility	Slide bearing for horizontal shaft pump							
Type of objective equipment	Type	Inner diameter (mm)	Outer diameter (mm)	Length (mm)	Number of specimens	Remarks		
	Radial bearing	80	121	80	3	Sleeve type		
	Radial bearing	60	85	60	4	Sleeve type		
	Thrust bearing	67	127	44.5	4	Kingsbury type		
Test results and evaluation results of fragility capacity • Full-scale test • Element test • No test								
Radial bearing test								
Inner diameter (mm)	Specimen No.	Test results		Fragility evaluation				
		Function- confirmed load (kN)	Load to generate torque change (kN)	Function critical load (kN)	Median value		Log standard deviation	
80	1	40.0	42.5	41.3	42.9	8.9		134
	2	42.5	45.0	43.8				
	3	42.5	45.0	43.8				
					Critical PV value for fragility evaluation (MPa·m/s) 121			
60	1	17.5	20.0	18.8	21.2	8.0	121	0.12
	2	20.0	22.5	21.3				
	3	22.5	25.0	23.8				
	4	75	—	—	—		—	—
				Critical PV value for fragility evaluation (MPa·m/s) 121				
Remarks	<ul style="list-style-type: none"> • Generation of plastic flow of white metal on inner surface of bearing was identified by the inspection after the test. • For No. 4 specimen with inner diameter of 60 mm, vibration test was performed during shutdown, and no abnormality was identified. 			<ul style="list-style-type: none"> • Fragility evaluation was performed for the bearing where plastic flow of white metal was generated. • Refer to Section 2.1 for fragility evaluation method. 				
Thrust bearing test								
Outer diameter (mm)	Specimen No.	Test results				Fragility evaluation		
		Function- confirmed load (kN)	Maximum surface pressure (MPa)	Function critical PV value (MPa·m/s)	Load to generate abnormality (kN)	Median value	Log standard deviation	
127	1	45	5.24	129	—	—	—	
	2	45	5.24	129	—			
	3	45	5.24	129	—			
	4	45	—	—	—	—	—	
						Critical PV value for fragility evaluation (MPa·m/s) 129		
Remarks	<ul style="list-style-type: none"> • No abnormality in bearing • For No. 4 specimen with inner diameter of 60 mm, vibration test was performed during shutdown, and no abnormality was identified. 							

Table 3.1-4 Summary Table of Fragility Data

Equipment/ Facility	Liner ring for horizontal shaft pump						
Type of objective equipment	Inner diameter (mm)	Diametrical clearance (mm)	Length (mm)	Number of specimen	Remarks		
	270	0.56	41	3	Flat type		
	175	0.5	28	3	Flat type		
	267	1.1	40	3	Flat type		
	88	0.3	98	3	Flat type		
	195	0.38	19	3	Flat type		
	95.5	0.254	90	3	Thread groove type		
Test results and evaluation results of fragility capacity • Full-scale test • Element test • No test							
Liner ring test							
Inner diameter (mm)	Specimen No.	Test results				Fragility evaluation	
		Function-confirmed load (kN)	Maximum surface pressure (MPa)	Function-confirmed PV value (MPa·m/s)	Load to generate abnormality (kN)	Median value	Log standard deviation
270	1	20.9	1.9	47.9	—	—	—
	2	22.8	2.1	52.4	—		
	3	24.0	2.2	55.1	—		
175	1	6.0	1.2	20.1	—	—	—
	2	7.3	1.5	24.5	—		
	3	18.4	3.8	61.8	—		
267	1	24.9	2.3	58.4	—	—	—
	2	23.1	2.2	54.2	—		
	3	20.9	2.0	49.0	—		
88	1	12	1.39	31	—	—	—
	2	11	1.28	28	—		
	3	13	1.51	33	—		
195	1	8	2.16	66	—	—	—
	2	9	2.43	74	—		
	3	7	1.89	58	—		
95.5	1	5	0.58	10	—	—	—
	2	5	0.58	10	—		
	3	6	0.70	13	—		
Remarks		• No abnormality in liner ring					

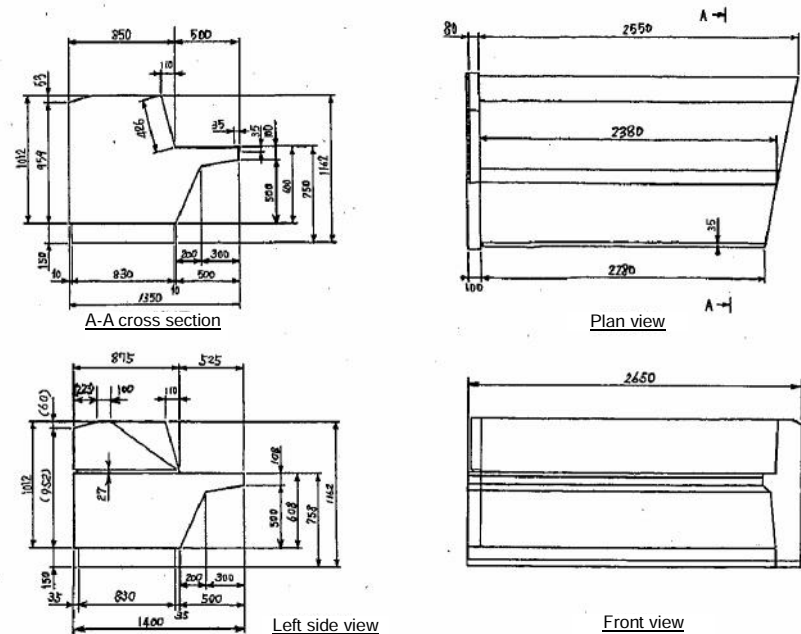
3.2 Electrical equipment

Among fragility data studied in Part 1 of Equipment Fragility Test, fragility data related to electrical equipment shown in the table below are presented in Table3.2-2 to Table3.2-8.

Table3.2-1 Fragility Data related to Electrical Equipment

Equipment	Name	Table
Electrical equipment (panels)	Main control board	Table3.2-2
	Reactor auxiliary panel	
	Logic control panel	
	Protection instrument rack	
	Instrument rack	
	Reactor control center	
	Power center	
	Metalclad switchgear	
Parts	Relays	Table 3.2-3
	Control devices	Table 3.2-4
	Instrument devices	Table 3.2-5
	Electric apparatus	Table 3.2-6
	Switches	Table 3.2-7
	Breakers, instrument transformers	Table 3.2-8

Table 3.2-2 Summary Table of Fragility Data (1/8)

Equipment/ Facility	Electrical equipment (panel)
Type of objective equipment	<p>Name: main control board Outside dimension: 2650W×1350D×1012H Mass: About 1010kg Reactor type: BWR</p>  <p>The drawings show a rectangular panel with a depth of 1012 mm. The A-A cross section shows a top width of 1350 mm and a bottom width of 1400 mm. The plan view shows a top width of 2650 mm and a bottom width of 2700 mm. The left side view shows a top width of 1400 mm and a bottom width of 1400 mm. The front view shows a top width of 2650 mm and a bottom width of 2650 mm.</p>

Test results and evaluation results of fragility capacity • Full-scale test • Element test • No test

Characteristic test	Natural frequency (Hz)	From side to side	43.8		
		Back and forth	Greater than 50		
Fragility test	Vibrating direction	Input acceleration		Abnormality in function	
		Function-confirmed acceleration ($\times 9.8\text{m/s}^2$)	Acceleration to generate abnormality ($\times 9.8\text{m/s}^2$)		
	From side to side	5.69	—		No abnormality
	Back and forth	5.71	—		No abnormality

Fragility evaluation						
Function type	Direction	Median value of fragility capacity ($\times 9.8\text{m/s}^2$)	Log standard deviation	Response amplification factor	Critical parts	Evaluation method
Electrical function limit	Side to side	5.6	—	1.7	Flat display	<ul style="list-style-type: none"> Calculated based on function critical acceleration of flat display. Amplification factor is value at mounting position of flat display to the board base.
Structural strength limit	Side to side	42.2	0.07	—	Foundation bolt	<ul style="list-style-type: none"> Log standard deviation is calculated based on distribution of tensile strength of material.

Remarks

- Refer to Section 2.2, Figure 2.2-1 for fragility evaluation method
- Median value of fragility capacity is acceleration on mounting floor of electrical equipment.

Table 3.2-2 Summary Table of Fragility Data (2/8)

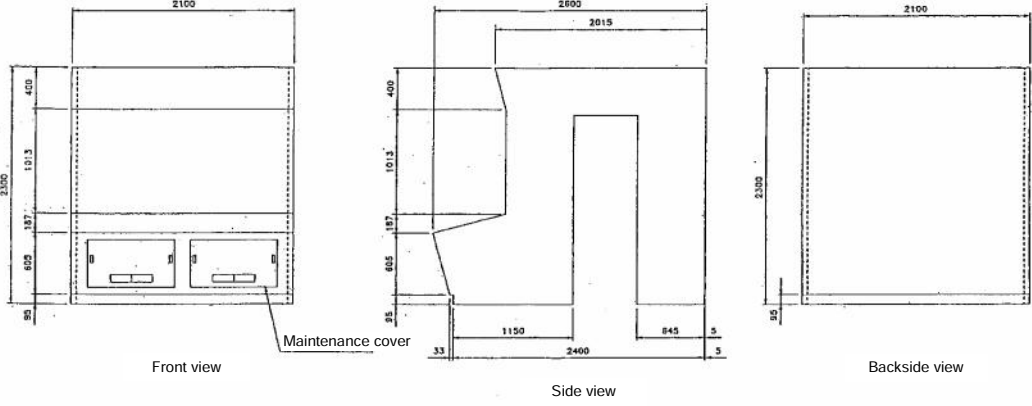
Equipment/ Facility	Electrical equipment (panel)								
Type of objective equipment	<p>Name: Reactor auxiliary panel Outer dimension: 2100W×2600D×2300H Mass: about 2580kg Reactor type: PWR</p>  <p>Front view Maintenance cover Side view Backside view</p>								
Test results and evaluation results of fragility capacity • Full-scale test • Element test • No test									
Characteristic test	Natural frequency (Hz)	Side to side	30.7						
		Back and forth	31.2						
Fragility test	Vibration direction	Input acceleration		Abnormality in function					
		Function- confirmed acceleration (×9.8m/s ²)	Acceleration to generate abnormality (×9.8m/s ²)						
	Side to side	6.19	—				No abnormality		
	Back and forth	5.9	—	No abnormality					
Fragility evaluation									
Function type	Direction	Median value of fragility capacity (×9.8m/s ²)	Log standard deviation	Response multiplying factor	Critical parts	Evaluation method			
Electrical function limit	Back and forth	9.8	0.02	1.1	Module switch	<ul style="list-style-type: none"> • Calculated based on function critical acceleration of module switch. • Log standard deviation is calculated based on element test result of module switch. • Response multiplying factor is the value at mounting position of module switch. 			
Structural strength limit	From side to side	82.4	0.07	—	Cabinet	<ul style="list-style-type: none"> • Log standard deviation is calculated based on distribution of tensile strength of material. 			
Remarks	<ul style="list-style-type: none"> • Refer to Section 2.2, Figure 2.2-1 for fragility evaluation method • Median value of fragility capacity is acceleration on mounting floor of electrical equipment. 								

Table 3.2-2 Summary Table of Fragility Data (4/8)

Equipment/ Facility	Electrical equipment (panel)
Type of objective equipment	Name: Protection instrumentation rack Outer dimension: 1800W×900D×2300H (3-panel structure) Mass: About 2160kg Reactor type: PWR

Test results and evaluation results of fragility capacity • Full-scale test • Element test • No test

Characteristic test	Natural frequency (Hz)	Side to side	29.0		
		Back and forth	44.9		
Fragility test	Vibration direction	Input acceleration		Abnormality in function	
		Function-confirmed acceleration ($\times 9.8\text{m/s}^2$)	Acceleration to generate abnormality ($\times 9.8\text{m/s}^2$)		
	Side to side	3.19	4.28		Malfunction of miniature relay in card
			5.42		Same as above
Back and forth	5.88	6.29	Same as above		
		—	No abnormality		

Fragility evaluation

Function type	Direction	Median value of fragility capacity ($\times 9.8\text{m/s}^2$)	Log standard deviation	Response multiplying factor	Critical parts	Evaluation method
Electrical function limit	Side to side	4.4	0.166	1.9	AC controller card	<ul style="list-style-type: none"> Calculated based on function critical acceleration of AC controller card. Log standard deviation is calculated based on element test result of AC controller card. Response multiplying factor is the value at mounting position of AC controller card.
Structural strength limit	Side to side	15.8	0.07	—	Anchor bolt	<ul style="list-style-type: none"> Log standard deviation is calculated based on distribution of tensile strength of material.
Remarks	<ul style="list-style-type: none"> Refer to Section 2.2, Figure 2.2-1 for fragility evaluation method Median value of fragility capacity is acceleration on mounting floor of electrical equipment. 					

Table 3.2-2 Summary Table of Fragility Data (5/8)

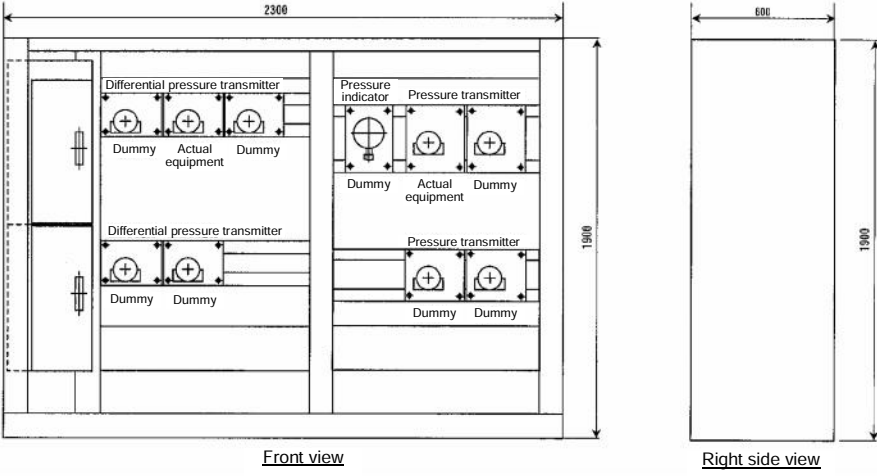
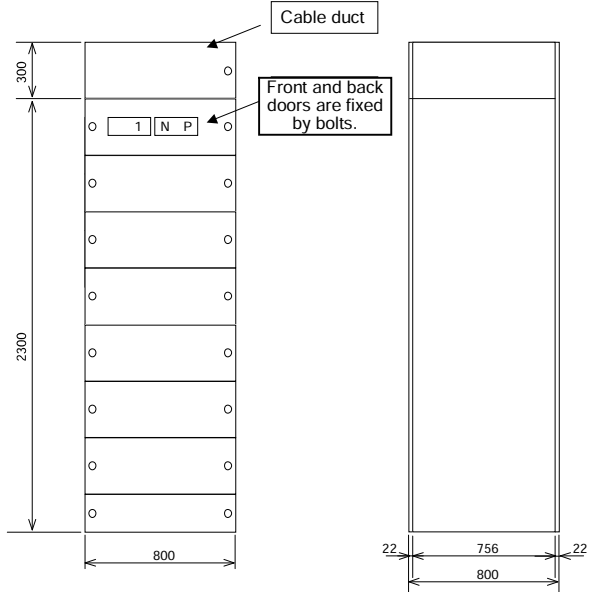
Equipment/ Facility	Electrical equipment (panel)					
Type of objective equipment	<p>Name: Instrument rack Outer dimension: 2300W×600D×1900H Mass: About 670kg Reactor type: BWR</p>  <p style="text-align: center;">Front view Right side view</p>					
Test results and evaluation results of fragility capacity • Full-scale test • Element test • No test						
Characteristic test	Natural frequency (Hz)	From side to side	32.7			
		Back and forth	43.8			
Fragility test	Vibration direction	Input acceleration		Abnormality in function		
		Function- confirmed acceleration (×9.8m/s ²)	Acceleration to generate abnormality (×9.8m/s ²)			
	Side to side	5.69	—			
	Back and forth	5.71	—	No abnormality		
Fragility evaluation						
Function type	Direction	Median value of fragility capacity	Log standard deviation	Response multiplying factor	Damage mode	Evaluation method
Electrical function limit	Side to side	4.2	—	2.5	Differential pressure transmitter	<ul style="list-style-type: none"> Calculated based on function critical acceleration of differential pressure transmitter. Response multiplying factor is the value at mounting position of differential pressure transmitter..
Structural strength limit	Back and forth	18.2	0.07	—	Anchor bolt	<ul style="list-style-type: none"> Log standard deviation is calculated based on distribution of tensile strength of material.
Remarks	<ul style="list-style-type: none"> Refer to Section 2.2, Figure 2.2-1 for fragility evaluation method Median value of fragility capacity is acceleration on mounting floor of electrical equipment. 					

Table 3.2-2 Summary Table of Fragility Data (6/8)

Equipment/ Facility	Electrical equipment (panel)
Type of objective equipment	<p>Name: Reactor Control center Outer dimension: 800W×800D×2300H Mass: About 640kg Reactor type: PWR</p> 

Test results and evaluation results of fragility capacity •Full-scale test • Element test • No test

Characteristic test	Natural frequency (Hz)	Side to side	37.6			
		Back and forth	35.8			
Fragility test	Vibration direction	Input acceleration		Abnormality in function		
		Function-confirmed acceleration ($\times 9.8\text{m/s}^2$)	Acceleration to generate abnormality ($\times 9.8\text{m/s}^2$)			
	Side to side	5.83	—	No abnormality		
Back and forth	4.93	6.12	Malfunction of auxiliary relay			
Fragility evaluation						
Function type	Direction	Median value of fragility capacity ($\times 9.8\text{m/s}^2$)	Log standard deviation	Response multiplying factor	Critical parts	Evaluation method
Electrical function limit	Back and forth	4.5	—	1.3	auxiliary relay	<ul style="list-style-type: none"> • Calculated based on function critical acceleration of auxiliary relay. • Response multiplying factor is the value at mounting position of auxiliary relay.
Structural strength limit	Side to side	22.6	0.07	—	Foundation bolt	<ul style="list-style-type: none"> • Log standard deviation is calculated based on distribution of tensile strength of material.
Remarks	<ul style="list-style-type: none"> • Refer to Section 2.2, Figure 2.2-1 for fragility evaluation method • Median value of fragility capacity is acceleration on mounting floor of electrical equipment (panel). 					

Table 3.2-2 Summary Table of Fragility Data (7/8)

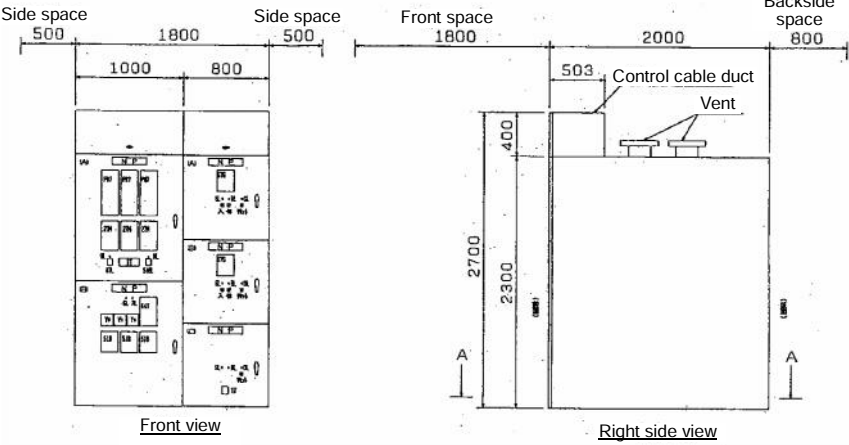
Equipment/ Facility	Electrical equipment (panel)					
Type of objective equipment	<p>Name: Power center Outer dimension: 1000+800W×2000D×2300H (two panel structure) Mass: About 4050kg (Total of 2 panels) Reactor type: PWR</p> 					
Test results and evaluation results of fragility capacity						<input checked="" type="radio"/> Full-scale test • Element test • No test
Characteristic test	Natural frequency (Hz)	Side to side	24.2			
		Back and forth	32.3			
Fragility test	Vibration direction	Input acceleration		Abnormality in function		
		Function- confirmed acceleration (×9.8m/s ²)	Acceleration to generate abnormality (×9.8m/s ²)			
	Side to side	3.91	—	No abnormality		
		5.03	—	No abnormality (however, circuit breaker was broken by back and forth excitation, and test was performed fixing circuit breaker, therefore, these data were as a reference)		
		5.83	—			
	Back and forth	2.82	3.72	Receiving circuit breaker was mis-closed. (however, functional limit can be increased by simple strengthening)		
4.96			Receiving circuit breaker was broken.			
6.05			Receiving circuit breaker was mis-opened. Receiving circuit breaker was mis-closed and mis-opened.			
Fragility evaluation						
Function	Direction	Median value of fragility capacity (×9.8m/s ²)	Log standard deviation	Response multiplying factor	Critical parts	Evaluation method
Electrical function limit	Back and forth	4.4	—	1.0	Receiving circuit breaker	<ul style="list-style-type: none"> • Calculated based on function critical acceleration of receiving circuit breaker. • Response multiplying factor is the value at mounting position of receiving circuit breaker.
Structural strength limit	Side to side	8.1	0.07	—	Housing	<ul style="list-style-type: none"> • Log standard deviation is calculated based on distribution of tensile strength of material.
Remarks	<ul style="list-style-type: none"> • Refer to Section 2.2, Figure 2.2-1 for fragility evaluation method • Median value of fragility capacity is acceleration on mounting floor of electrical equipment. 					

Table 3.2-2 Summary Table of Fragility Data (8/8)

Equipment/ Facility	Electrical equipment (panel)
Type of objective equipment	Name: Metal clad switchgear Outer dimension: 1000+1000W×2500D×2300H (+Control duct 300) Mass: about 5600kg Reactor type: BWR

Test results and evaluation results of fragility capacity • Full-scale test • Element test • No test

Characteristic test	Natural frequency (Hz)	Side to side	21.2		
		Back and forth	Greater than 50		
Fragility test	Vibration direction	Input acceleration		Abnormality in function	
		Function-confirmed acceleration (×9.8m/s ²)	Acceleration to generate abnormality (×9.8m/s ²)		
	Side to side	2.98	3.70		GPT (instrument transformer) moved toward disconnection. (however, functional limit can be increased by simple strengthening)
			4.10		Circuit breaker control circuit in upper shelf was deformed.
	Back and forth	2.04	2.52		Fuse of GPT was dropped out. (however, functional limit can be increased by simple strengthening)
			3.03		GPT moved toward disconnection. (however, functional limit can be increased by simple strengthening)
4.65			Circuit breaker in upper shelf moved.		

Fragility evaluation

Function type	Direction	Median value of fragility capacity (×9.8m/s ²)	Log standard deviation	Response multiplying factor	Critical parts	Evaluation method
Electrical function limit	Side to side	4.2	—	2.0	Circuit breaker	<ul style="list-style-type: none"> Calculated based on function critical acceleration of circuit breaker. Response multiplying factor is the value at mounting position of circuit breaker.
Structural strength limit	Side to side	8.6	0.07	—	Foundation bolt	<ul style="list-style-type: none"> Log standard deviation is calculated based on distribution of tensile strength of material.

Remarks

- Refer to Section 2.2, Figure 2.2-1 for fragility evaluation method
- Median value of fragility capacity is acceleration on mounting floor of electrical equipment.

Table 3.2-3 Summary Table of Fragility Data (1/3)

Equipment/ Facility	Electrical parts (relays)								
Type of objective equipment	Name of apparatus	Type	Manufacturer	Number of specimen	Remarks				
	Protection relay (ratio-differential relay)	TUB-2-D	MELCO	3	SS type				
	Protection relay (overcurrent relay)	CO-18-D	MELCO	9	Inductive disk type				
	Protection relay (overcurrent relay)	VCR62D	TMT&D	3	Digital type				
	auxiliary relay	NRD-81	MELCO	9					
	auxiliary relay	UP3A	TMT&D	9					
	auxiliary relay	MY4Z	Omron	9					
	Timer	H3M	Omron	9					
Test results and evaluation results of fragility capacity • Full-scale test • Element test • No test									
Name of apparatus	Type	Input wave	Direction	Specimen No.	Test result		Fragility evaluation		
					Function- confirmed acceleration ($\times 9.8\text{m/s}^2$)	Acceleration for loss of function ($\times 9.8\text{m/s}^2$)	Critical acceleration for function ($\times 9.8\text{m/s}^2$)	Median value ($\times 9.8\text{m/s}^2$)	Log standard deviation
Protection relay (ratio differential relay)	TUB-2-D	Seismic wave	Back and forth	1	8.7	9.0	8.85	9.54	0.131
				2	10.9	—	11.1		
				3	8.7	9.0	8.85		
			Side to side	1	10.0	—	10.05	10.05	0
				2	10.0	—	10.05		
				3	10.0	—	10.05		
Protection relay (overcurrent relay)	CO-18-D	Seismic wave	Back and forth	1	10.6	—	10.75	10.75	0
				2	10.6	—	10.75		
				3	10.6	—	10.75		
				4	10.6	—	10.75		
				5	10.6	—	10.75		
				6	10.6	—	10.75		
			Side to side	1	10.0	—	10.2	10.2	0
				2	10.0	—	10.2		
				3	10.0	—	10.2		
				4	10.0	—	10.2		
				5	10.0	—	10.2		
				6	10.0	—	10.2		
		Sine beat wave	Back and forth	7	10.3	—	10.65	10.65	0
				8	10.3	—	10.65		
				9	10.3	—	10.65		
			Side to side	7	10.1	—	11.1	11.1	0
				8	10.1	—	11.1		
				9	10.1	—	11.1		
Vertical	7~9	3.0	—	—	—	—			
Protection relay (overcurrent relay)	VCR62D	Seismic wave	Back and forth	1	12.2	—	13.55	13.4	0.013
				2	12.1	—	13.45		
				3	12.0	—	13.2		
			Side to side	1	14.2	—	15.2	14.06	0.068
				2	12.7	—	13.65		
				3	12.7	—	13.4		
Remarks	• Abnormality in function occurred for TUB-2-D.					• Refer to Section 2.2 for fragility evaluation method.			

Table 3.2-3 Summary Table of Fragility Data (2/3)

Test results and evaluation results of fragility capacity									
• Full-scale test • <u>Element test</u> • No test									
Name of apparatus	Type	Input wave	Direction	Specimen No.	Test result		Fragility evaluation		
					Function-confirmed acceleration ($\times 9.8\text{m/s}^2$)	Acceleration for loss of function ($\times 9.8\text{m/s}^2$)	Critical acceleration for function ($\times 9.8\text{m/s}^2$)	Median value ($\times 9.8\text{m/s}^2$)	Log standard deviation
Auxiliary relay	NRD-81	Seismic wave	Back and forth	1	5.8	6.0	5.9	5.9	0
				2	5.8	6.0	5.9		
				3	5.8	6.0	5.9		
				4	5.8	6.0	5.9		
				5	5.8	6.0	5.9		
				6	5.8	6.0	5.9		
			Side to side	1	10.6	—	10.85	10.85	0
				2	10.6	—	10.85		
				3	10.6	—	10.85		
				4	10.6	—	10.85		
				5	10.6	—	10.85		
				6	10.6	—	10.85		
		Sine beat wave	Back and forth	7	5.5	5.7	5.6	5.6	0
				8	5.5	5.7	5.6		
				9	5.5	5.7	5.6		
			Side to side	7	7.6	—	7.75	7.75	0
				8	7.6	—	7.75		
				9	7.6	—	7.75		
Vertical	7~9	4.1	—	—	—	—			
Auxiliary relay	UP3A	Seismic wave	Back and forth	1	11.0	—	11.75	11.85	0.009
				2	11.0	—	11.75		
				3	11.0	—	11.75		
				4	11.2	—	11.95		
				5	11.2	—	11.95		
				6	11.2	—	11.95		
			Side to side	1	11.5	—	12.25	12.76	0.045
				2	11.5	—	12.25		
				3	11.5	—	12.25		
				4	12.4	—	13.3		
				5	12.4	—	13.3		
				6	12.4	—	13.3		
		Sine beat wave	Back and forth	7	10.6	—	11.15	11.15	0
				8	10.6	—	11.15		
				9	10.6	—	11.15		
			Side to side	7	10.5	11.0	10.75	9.02	0.157
				8	7.6	8.3	7.95		
				9	8.3	8.9	8.6		
Vertical	7	2.9	—	—	—	—			
Remarks	<ul style="list-style-type: none"> • Abnormality in function occurred for NDR-81. • Abnormality in function occurred in sine beat test for UP3A. 					<ul style="list-style-type: none"> • Refer to Section 2.2 for fragility evaluation method.. 			

Table 3.2-3 Summary Table of Fragility Data (3/3)

Test results and evaluation results of fragility capacity									
• Full-scale test • Element test • No test									
Name of apparatus	Type	Input wave	Direction	Specimen No.	Test result		Fragility evaluation		
					Function-confirmed acceleration ($\times 9.8\text{m/s}^2$)	Acceleration for loss of function ($\times 9.8\text{m/s}^2$)	Critical acceleration for function ($\times 9.8\text{m/s}^2$)	Median value ($\times 9.8\text{m/s}^2$)	Log standard deviation
Auxiliary relay	MY4Z	Seismic wave	Back and forth	1	10.1	—	10.65	10.65	0
				2	10.1	—	10.65		
				3	10.1	—	10.65		
				4	10.1	—	10.65		
				5	10.1	—	10.65		
				6	10.1	—	10.65		
			Side to side	1	10.0	—	10.45	10.45	0
				2	10.0	—	10.45		
				3	10.0	—	10.45		
				4	10.0	—	10.45		
				5	10.0	—	10.45		
				6	10.0	—	10.45		
		Sine beat wave	Back and forth	7	10.1	—	10.55	10.55	0
				8	10.1	—	10.55		
				9	10.1	—	10.55		
Side to side	7		10.1	—	10.6	10.6	0		
	8		10.1	—	10.6				
	9		10.1	—	10.6				
Vertical	7	3.1	—	—	—	—			
Timer	H3M	Seismic wave	Back and forth	1	10.1	—	10.65	10.65	0
				2	10.1	—	10.65		
				3	10.1	—	10.65		
				4	10.1	—	10.65		
				5	10.1	—	10.65		
				6	10.1	—	10.65		
			Side to side	1	10.0	—	10.45	10.45	0
				2	10.0	—	10.45		
				3	10.0	—	10.45		
				4	10.0	—	10.45		
				5	10.0	—	10.45		
				6	10.0	—	10.45		
		Sine beat wave	Back and forth	7	10.1	—	10.55	10.55	0
				8	10.1	—	10.55		
				9	10.1	—	10.55		
Side to side	7		10.1	—	10.6	10.6	0		
	8		10.1	—	10.6				
	9		10.1	—	10.6				
Vertical	7	3.1	—	—	—	—			
Remarks							• Refer to Section 2.2 for fragility evaluation method..		

Table 3.2-4 Summary Table of Fragility Data (1/2)

Equipment/ Facility	Electrical parts (control equipment)									
Type of objective equipment	Name of apparatus	Type	Manufacturer	Number of specimen	Remarks					
	Comparator card	HALN	MELCO	3						
	AC controller card	HASN	MELCO	3						
	Flat display	18 inch type	TOTOKU	3						
	Controller	18 inch type	Hitachi	3						
	Controller	TOSMAP	Toshiba	3						
	Input/output unit	TOSMAP	Toshiba	3						
	Test module	S9166AW	Yokogawa Electric	3						
	Power supply module	S9016AW	Yokogawa Electric	3						
	Monitor module	S9146AW	Yokogawa Electric	3						
	Power supply equipment	-	MELCO	3	Package rectification type					
	Power supply equipment	TFV	Densei Lambda	3	Switching control module					
	Power supply equipment	S9980UD	Yokokawa Electric	2 (1 set)						
	Test results and evaluation results of fragility capacity • Full-scale test • Element test • No test									
Name of apparatus	Type	Input wave	Direction	Specimen No.	Test result		Fragility evaluation			
					Function- confirmed acceleration ($\times 9.8\text{m/s}^2$)	Acceleration for loss of function ($\times 9.8\text{m/s}^2$)	Critical acceleration for function ($\times 9.8\text{m/s}^2$)	Median value ($\times 9.8\text{m/s}^2$)	Log standard deviation	
Comparator card	HALN	Seismic wave	Back and forth	1	9.9	—	10.1	10.1	0	
				2	9.9	—	10.1			
				3	9.9	—	10.1			
			Side to side	1	9.5	—	9.7	9.7	0	
				2	9.5	—	9.7			
				3	9.5	—	9.7			
AC controller card	HASN	Seismic wave	Back and forth	1	9.9	—	10.1	10.1	0	
				2	9.9	—	10.1			
				3	9.9	—	10.1			
			Side to side	1	9.5	—	9.7	8.26	0.166	
				1	7.0	7.1	7.05			
				2	9.5	—	9.7			
				2	7.0	7.1	7.05			
				3	9.3	9.5	9.4			
				3	7.1	7.3	7.2			
Flat display	18 inch type	Seismic wave	Back and forth	1	10.2	—	10.85	10.85	0	
				2	10.2	—	10.85			
				3	10.2	—	10.85			
			Side to side	1	9.5	—	9.55	9.55	0	
				2	9.5	—	9.55			
				3	9.5	—	9.55			
Controller	18 inch type	Seismic wave	Back and forth	1	10.4	—	10.9	10.9	0	
				2	10.4	—	10.9			
				3	10.4	—	10.9			
			Side to side	1	10.4	—	11.0	11.0	0	
				2	10.4	—	11.0			
				3	10.4	—	11.0			
Remarks	• Abnormality in function occurred at AC controller card.					• Refer to Section 2.2 for fragility evaluation method..				

Table 3.2-4 Summary Table of Fragility Data (2/2)

Test results and evaluation results of fragility capacity									
• Full-scale test • <u>Element test</u> • No test									
Name of apparatus	Type	Input wave	Direction	Specimen No.	Test result		Fragility evaluation		
					Function-confirmed acceleration ($\times 9.8\text{m/s}^2$)	Acceleration for loss of function ($\times 9.8\text{m/s}^2$)	Critical acceleration for function ($\times 9.8\text{m/s}^2$)	Median value ($\times 9.8\text{m/s}^2$)	Log standard deviation
Controller	TOSMAP	Seismic wave	Back and forth	1	12.6	—	13.2	12.06	0.079
				2	10.8	—	11.45		
				3	11.1	—	11.6		
			Side to side	1	12.0	—	12.8	12.09	0.05
				2	10.9	—	11.65		
				3	11.1	—	11.85		
Input/output unit	TOSMAP	Seismic wave	Back and forth	1	12.2	—	13.0	12.15	0.068
				2	10.6	—	11.35		
				3	11.3	—	12.15		
			Side to side	1	11.8	—	12.6	11.72	0.063
				2	10.6	—	11.25		
				3	10.7	—	11.35		
Test module	S9166AW	Seismic wave	Back and forth	1	10.5	—	11.15	11.15	0
				2	10.5	—	11.15		
				3	10.5	—	11.15		
			Side to side	1	10.1	—	10.6	10.6	0
				2	10.1	—	10.6		
				3	10.1	—	10.6		
Power supply module	S9016AW	Seismic wave	Back and forth	1	10.5	—	11.15	11.15	0
				2	10.5	—	11.15		
				3	10.5	—	11.15		
			Side to side	1	10.1	—	10.6	10.6	0
				2	10.1	—	10.6		
				3	10.1	—	10.6		
Monitor module	S9146AW	Seismic wave	Back and forth	1	10.5	—	11.15	11.15	0
				2	10.5	—	11.15		
				3	10.5	—	11.15		
			Side to side	1	10.1	—	10.6	10.6	0
				2	10.1	—	10.6		
				3	10.1	—	10.6		
Power supply equipment	—	Seismic wave	Back and forth	1	11.1	—	11.9	11.9	0
				2	11.1	—	11.9		
				3	11.1	—	11.9		
			Side to side	1	9.7	—	9.9	9.9	0
				2	9.7	—	9.9		
				3	9.7	—	9.9		
Power supply equipment	TFV	Seismic wave	Back and forth	1	12.6	—	13.6	12.61	0.071
				2	11.0	—	11.8		
				3	11.6	—	12.5		
			Side to side	1	10.7	—	11.7	11.36	0.027
				2	10.4	—	11.3		
				3	10.2	—	11.0		
Power supply equipment	S9980UD	Seismic wave	Back and forth	1	10.5	—	11.2	—	—
				2	10.5	—	11.2		
			Side to side	1	10.1	—	10.3	—	—
				2	10.1	—	10.3		
Remarks							• Refer to Section 2.2 for fragility evaluation method..		

Table 3.2-5 Summary Table of Fragility Data

Equipment/ Facility	Electrical parts (Instrument devices)								
Type of objective equipment	Name of apparatus		Type	Manufacturer	Number of specimen	Remarks			
	Differential pressure transmitter		EDR-N6L	Hitachi	4				
	Pressure transmitter		EPR-N6L	Hitachi	1				
	Differential pressure transmitter		AP3107	Toshiba	3				
	Differential pressure transmitter		UNE13	Yokogawa Electric	3				
Test results and evaluation results of fragility capacity • Full-scale test • Element test • No test									
Name of apparatus	Type	Input wave	Direction	Specimen No.	Test result		Fragility evaluation		
					Function- confirmed acceleration ($\times 9.8m/s^2$)	Acceleration for loss of function ($\times 9.8m/s^2$)	Critical acceleration for function ($\times 9.8m/s^2$)	Median value ($\times 9.8m/s^2$)	Log standard deviation
Differential pressure transmitter	EDR-N6L	Seismic wave	Back and forth	1	10.0	—	10.3	10.3	0
				2	10.0	—	10.3		
				3	10.0	—	10.3		
				4	10.0	—	10.3		
			Side to side	1	10.1	—	10.6	10.6	0
				2	10.1	—	10.6		
				3	10.1	—	10.6		
				4	10.1	—	10.6		
Pressure transmitter	EPR-N6L	Seismic wave	Back and forth	1	10.4	—	10.95	—	—
			Side to side	1	10.1	—	10.6	—	—
Differential pressure transmitter	AP3107	Seismic wave	Back and forth	1	10.5	—	11.4	11.68	0.022
				2	10.9	—	11.9		
				3	10.8	—	11.75		
			Side to side	1	10.6	—	11.55	11.48	0.007
				2	10.6	—	11.5		
				3	10.5	—	11.4		
Differential pressure transmitter	UNE13	Seismic wave	Back and forth	1	10.0	—	10.3	10.3	0
				2	10.0	—	10.3		
				3	10.0	—	10.3		
			Side to side	1	10.0	—	10.5	10.5	0
				2	10.0	—	10.5		
				3	10.0	—	10.5		
Remarks							• Refer to Section 2.2 for fragility evaluation method..		

Table 3.2-6 Summary Table of Fragility Data (1/3)

Equipment/ Facility	Electrical parts (electrical apparatus)								
Type of objective equipment	Name of apparatus	Type	Manufacture	Number of specimens	Remarks				
	Magnetic contactor	MSO-A80	MELCO	9					
	Magnetic contactor	C-20J T-20J	Toshiba SE	9					
	Molded case circuit breaker	NF100-SH	MELCO	9					
	Molded case circuit breaker	SH100	Toshiba SE	9					
	Molded case circuit breaker	F type	Hitachi	9					
Test results and evaluation results of fragility capacity • Full-scale test • Element test • No test									
Name of apparatus	Type	Input wave	Direction	Specimen No.	Test result		Fragility evaluation		
					Function- confirmed acceleration ($\times 9.8\text{m/s}^2$)	Acceleration for loss of function ($\times 9.8\text{m/s}^2$)	Critical acceleration for function ($\times 9.8\text{m/s}^2$)	Median value ($\times 9.8\text{m/s}^2$)	Log standard deviation
Magnetic contactor	MSO-A80	Seismic wave	Back and forth	1	9.7	—	9.9	9.9	0
				2	9.7	—	9.9		
				3	9.7	—	9.9		
				4	9.7	—	9.9		
				5	9.7	—	9.9		
				6	9.7	—	9.9		
		Side to side	1	10.1	—	10.35	10.35	0	
			2	10.1	—	10.35			
			3	10.1	—	10.35			
			4	10.1	—	10.35			
			5	10.1	—	10.35			
			6	10.1	—	10.35			
		Sine beat wave	Back and forth	7	7.9	8.3	8.1	8.1	0
				8	7.9	8.3	8.1		
				9	7.9	8.3	8.1		
Side to side	7		10.6	—	10.8	10.8	0		
	8		10.6	—	10.8				
	9		10.6	—	10.8				
Vertical	7~9	3.0	—	—	—	—			
Magnetic contactor	C-20J T-20J	Seismic wave	Back and front	1	10.4	—	11.1	11.03	0.009
				2	10.4	—	11.1		
				3	10.3	—	10.9		
				4	10.3	—	10.9		
				5	10.4	—	11.1		
				6	10.4	—	11.1		
		Side to side	1	10.0	—	10.7	10.7	0	
			2	10.0	—	10.7			
			3	10.0	—	10.7			
			4	10.0	—	10.7			
			5	10.0	—	10.7			
			6	10.0	—	10.7			
		Sine beat wave	Back and front	7	10.2	—	11.75	11.62	0.02
				8	10.2	—	11.75		
				9	9.9	—	11.35		
Side to side	7		7.8	—	8.3	8.25	0.011		
	8		7.8	—	8.3				
	9		7.7	—	8.15				
Vertical	9	2.9	—	—	—	—			
Remarks	• Function abnormality occurred in sine beat wave test for MSO-A80.					• Refer to Section 2.2 for fragility evaluation method.			

Table 3.2-6 Summary Table of Fragility Data (2/3)

Test results and evaluation results of fragility capacity									
• Full-scale test • Element test • No test									
Name of apparatus	Type	Input wave	Direction	Specimen No.	Test result		Fragility evaluation		
					Function-confirmed acceleration ($\times 9.8\text{m/s}^2$)	Acceleration for loss of function ($\times 9.8\text{m/s}^2$)	Critical acceleration for function ($\times 9.8\text{m/s}^2$)	Median value ($\times 9.8\text{m/s}^2$)	Log standard deviation
Molded case circuit breaker	NF100-SH	Seismic wave	Back and forth	1	9.8	—	10.0	10.0	0
				2	9.8	—	10.0		
				3	9.8	—	10.0		
				4	9.8	—	10.0		
				5	9.8	—	10.0		
				6	9.8	—	10.0		
			Side to side	1	9.6	—	9.85	9.85	0
				2	9.6	—	9.85		
				3	9.6	—	9.85		
				4	9.6	—	9.85		
				5	9.6	—	9.85		
				6	9.6	—	9.85		
		Sine beat wave	Back and forth	7	11.9	—	12.2	12.2	0
				8	11.9	—	12.2		
				9	11.9	—	12.2		
			Side to side	7	10.8	—	10.95	10.95	0
				8	10.8	—	10.95		
				9	10.8	—	10.95		
Vertical	7 ~ 9	3.0	—	—	—	—			
Molded case circuit breaker	SH100	Seismic wave	Back and forth	1	10.5	—	10.65	10.67	0.011
				2	10.5	—	10.65		
				3	10.5	—	10.8		
				4	10.5	—	10.8		
				5	10.4	—	10.55		
				6	10.4	—	10.55		
			Side to side	1	10.1	—	10.65	10.65	0
				2	10.1	—	10.65		
				3	10.1	—	10.65		
				4	10.1	—	10.65		
				5	10.1	—	10.65		
				6	10.1	—	10.65		
		Sine beat wave	Back and forth	7	10.7	—	12.6	12.33	0.038
				8	10.7	—	12.6		
				9	10.6	—	11.8		
			Side to side	7	10.2	—	11.95	11.95	0
				8	10.2	—	11.95		
				9	10.2	—	11.95		
Vertical	7	3.1	—	—	—	—			
Remarks							• Refer to Section 2.2 for fragility evaluation method..		

Table 3.2-6 Summary Table of Fragility Data (3/3)

Test results and evaluation results of fragility capacity									
• Full-scale test • Element test • No test									
Name of apparatus	Type	Input wave	Direction	Specimen No.	Test result		Fragility evaluation		
					Function-confirmed acceleration ($\times 9.8\text{m/s}^2$)	Acceleration for loss of function ($\times 9.8\text{m/s}^2$)	Critical acceleration for function ($\times 9.8\text{m/s}^2$)	Median value ($\times 9.8\text{m/s}^2$)	Log standard deviation
Molded case circuit breaker	F type	Seismic wave	Back and forth	1	10.1	—	10.65	10.65	0
				2	10.1	—	10.65		
				3	10.1	—	10.65		
				4	10.1	—	10.65		
				5	10.1	—	10.65		
				6	10.1	—	10.65		
		Side to side	1	10.0	—	10.45	10.45	0	
			2	10.0	—	10.45			
			3	10.0	—	10.45			
			4	10.0	—	10.45			
			5	10.0	—	10.45			
			6	10.0	—	10.45			
	Sine beat wave	Back and forth	7	10.1	—	10.55	10.55	0	
			8	10.1	—	10.55			
			9	10.1	—	10.55			
		Side to side	7	10.1	—	10.6	10.6	0	
8			10.1	—	10.6				
9			10.1	—	10.6				
Vertical	7	3.1	—	—	—	—			
	7	3.1	—	—	—	—			
Remarks								• Refer to Section 2.2 for fragility evaluation method..	

Table 3.2-7 Summary Table of Fragility Data (1/2)

Equipment/ Facility	Electrical parts (switches)								
Type of objective equipment	Name of apparatus		Type	Manufacturer	Number of specimen	Remarks			
	Module switch		SSA-SD3-53	MELCO	9				
	Cam type operation switch		MS type	Hitachi	9				
	Key switch		ACSNK type	Hitachi	9				
Test results and evaluation results of fragility capacity									• Full-scale test • Element test • No test
Name of apparatus	Type	Input wave	Direction	Specimen No.	Test result		Fragility evaluation		
					Function- confirmed acceleration ($\times 9.8\text{m/s}^2$)	Acceleration for loss of function ($\times 9.8\text{m/s}^2$)	Critical acceleration for function ($\times 9.8\text{m/s}^2$)	Median value ($\times 9.8\text{m/s}^2$)	Log standard deviation
Module switch	SSA-SD3-53	Seismic wave	Back and forth	1	10.7	—	10.95	10.75	0.02
				2	10.7	—	10.95		
				3	10.7	—	10.95		
				4	10.3	—	10.55		
				5	10.3	—	10.55		
				6	10.3	—	10.55		
		Side to side	1	10.6	—	10.85	10.49	0.037	
			2	10.6	—	10.85			
			3	10.6	—	10.85			
			4	9.9	—	10.15			
			5	9.9	—	10.15			
			6	9.9	—	10.15			
		Sine beat wave	Back and forth	7	10.9	—	11.1	10.83	0.021
				8	10.5	—	10.7		
				9	10.5	—	10.7		
Side to side	7		10.8	—	11.0	10.53	0.038		
	8		10.1	—	10.3				
Vertical	7~9	3.1	—	—	—	—			
Cam type operation switch	MS type	Seismic wave	Back and forth	1	10.1	—	10.65	10.65	0
				2	10.1	—	10.65		
				3	10.1	—	10.65		
				4	10.1	—	10.65		
				5	10.1	—	10.65		
				6	10.1	—	10.65		
		Side to side	1	10.0	—	10.45	10.52	0.008	
			2	10.0	—	10.45			
			3	10.0	—	10.45			
			4	10.1	—	10.6			
			5	10.1	—	10.6			
			6	10.1	—	10.6			
		Sine beat wave	Back and forth	7	10.1	—	10.6	10.6	0
				8	10.1	—	10.6		
				9	10.1	—	10.6		
Side to side	7		10.2	—	10.75	10.75	0		
	8		10.2	—	10.75				
Vertical	7	3.06	—	—	—	—			
Remarks							• Refer to Section 2.2 for fragility evaluation method..		

Table 3.2-7 Summary Table of Fragility Data(2/2)

Test results and evaluation results of fragility capacity									
• Full-scale test • Element test • No test									
Name of apparatus	Type	Input wave	Direction	Specimen No.	Test result		Fragility evaluation		
					Function-confirmed acceleration ($\times 9.8m/s^2$)	Acceleration for loss of function ($\times 9.8m/s^2$)	Critical acceleration for function ($\times 9.8m/s^2$)	Median value ($\times 9.8m/s^2$)	Log standard deviation
Key switch	ACSNK type	Seismic wave	Back and forth	1	10.1	—	10.65	10.65	0
				2	10.1	—	10.65		
				3	10.1	—	10.65		
				4	10.1	—	10.65		
				5	10.1	—	10.65		
				6	10.1	—	10.65		
			Side to side	1	10.0	—	10.45	10.52	0.008
				2	10.0	—	10.45		
				3	10.0	—	10.45		
				4	10.1	—	10.6		
				5	10.1	—	10.6		
				6	10.1	—	10.6		
		Sine beat wave	Back and forth	7	10.1	—	10.6	10.6	0
				8	10.1	—	10.6		
				9	10.1	—	10.6		
Side to side	7		10.2	—	10.75	10.75	0		
	8		10.2	—	10.75				
	9		10.2	—	10.75				
Vertical	7	3.06	—	—	—	—			
Remarks							• Refer to Section 2.2 for fragility evaluation method..		

Table3.2-8 Summary Table of Fragility Data

Equipment/ Facility	Electrical parts (circuit breaker, grounded potential transformer)								
Type of objective equipment	Name of apparatus		Type	Manufacturer	Number of specimen	Remarks			
	Air circuit breaker		B10-1	Toshiba	1	Element test			
	Air circuit breaker		DS-416	MELCO	1	Element test			
	Air circuit breaker		DS-840	MELCO	1	Full-scale equipment test			
	Vacuum circuit breaker		VF-6M63	Toshiba	1	Full-scale equipment test			
	Gas circuit breaker		6-SFG-40S	MELCO	1	Element test			
	Grounded potential transformer		VTZ-E6EP	Toshiba	1	Full-scale equipment test			
					1	Element test (with seismic reinforcement)			
Test results and evaluation results of fragility capacity					• Full-scale test	• Element test	• No test		
Name of apparatus	Type	Input wave	Direction	Specimen No.	Test result		Fragility evaluation		
					Function- confirmed acceleration (×9.8m/s ²)	Acceleration for loss of function (×9.8m/s ²)	Critical acceleration for function (×9.8m/s ²)	Median value (×9.8m/s ²)	Log standard deviation
Air circuit breaker	B10-1	Seismic wave	Back and forth	1	9.06	—	9.76	9.76	—
			Side to side	1	10.14	—	10.51	10.51	—
	DS-416	Seismic wave	Back and forth	1	3.4	4.2	3.8	3.8	—
			Back and forth	1	7.9	—	8.5	8.5	—
	DS-840	Seismic wave	Back and forth	1	2.82	3.72	3.27	3.27	—
			Back and forth	1	3.7	5.0	4.4	4.4	—
Vacuum circuit breaker	VF-6M63	Seismic wave	Back and forth	1	4.1	4.7	4.4	4.4	—
			Side to side	1	7.7	9.0	8.4	8.4	—
Gas circuit breaker	6-SFG-40S	Seismic wave	Back and forth	1	3.2	3.8	3.5	3.5	—
			Side to side	1	6.7	—	7.6	7.6	—
	6-SFG-40S ^{*3}	Seismic wave	Back and forth	1	Among excitations of 2.2 G – 7.2G, at 4G excitation generated abnormality in ⁵		11.4 ^{*5}	11.4 ^{*5}	—
			Side to side	1	5.9	—	6.4	6.4	—
Grounded potential transformer	VTZ-E6EP	Seismic wave	Back and forth	1	2.26	2.69	2.48	2.48	—
			Side to side	1	7.36	10.13	8.75	8.75	—
	VTZ-E6EP ^{*4}	Seismic wave	Back and forth	1	9.39	—	10.1	10.1	—
			Side to side	1	10.34	—	10.9	10.9	—
Remarks	*1 ~ *4: Cases with seismic reinforcement *5: See next page for detail						• Refer to Section 2.2 for fragility evaluation method..		

Element test result and evaluation of gas circuit breaker with reinforcement

(i) Outline of the element test of gas circuit breaker

Electrical failures due to the dislocation of the breaker body were observed as shown in Table 3.2-2(8/8) in relatively low excitation and it was found that side-to-side vibration of the breaker body appeared even when it was vibrated back-and-front direction. This vibration was greater than excitation direction.

Based on this finding, element tests of the breakers with/without seismic reinforcement shown in Figure 3.2-1 were carried out as shown in Table 3.2-8. This section shows outline of the test and its result for a gas circuit breaker 6-SFG-40S among them.

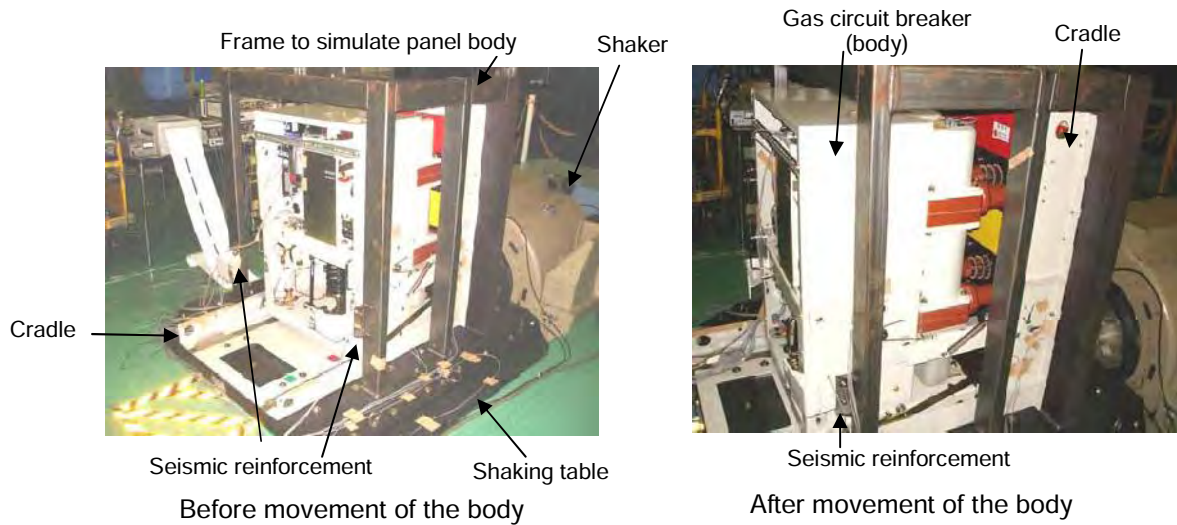


Figure 3.2-1 Element test of Gas circuit breaker with reinforcement

(ii) Test result

Test results are shown in Table 3.2-9 and 10. In the tests, excitations of several times for each level were carried out gradually increasing excitation level.

Table 3.2-9 Test results (with seismic reinforcement, Back and forth)

Excitation direction	Target acceleration ($\times 9.8\text{m/s}^2$)	Table acceleration ($\times 9.8\text{m/s}^2$)	Function	Note
With reinforcement, Back and forth	2.0	2.2	No abnormality	
	3.0	3.2	No abnormality	
	4.0	4.0	Fail to re-close (1-time in three excitations)	Due to chattering of auxiliary relay
	5.0	5.1	No abnormality (3-excitations)	
	6.0	7.2	No abnormality (3-excitations)	

Table 3.2-10 Test results (with seismic reinforcement, Side to side)

Excitation direction	Target acceleration ($\times 9.8\text{m/s}^2$)	Table acceleration ($\times 9.8\text{m/s}^2$)	Function	Note
With reinforcement, Side to side	4.0	4.2	No abnormality	
	5.0	4.9	No abnormality	
	6.0	5.9	No abnormality	

(iii) The cause of malfunction and its evaluation

a) Cause of failure of re-close at 4g back-and-forth test

This failure occurred only once among about 30 excitations in back-and-forth direction as shown in Table3.2-9. When chattering occurred in the auxiliary relay Y and contact "a" was set to ON, this relay is magnetized and self-hold circuit is made, and contact "b" keeps OFF state for about 15 to 20 milliseconds. During this state, if throw-in signal is issued, the breaker throw-in signal is blocked because contact "b" which provide throw-in coil current is OFF state, i.e. the breaker do not be thrown-in.

Further more this auxiliary relay Y is designed to maintain a magnetization state (hold state) if the throw-in command signal is continuing (200milliseconds). Therefore the sequence of malfunction was judged that chattering arose at contact "a" at first, immediately after that, throw-in signal was issued and self-holding circuits of the relay continued about 200 milliseconds but the throw-in command signal of a breaker was interrupted because contact "b" is kept in OFF during the command. This hold state of the relay resumes non-magnetized condition by OFF signal of throw-in command by the reset of self-hold circuit.

This sequence was confirmed by test records.

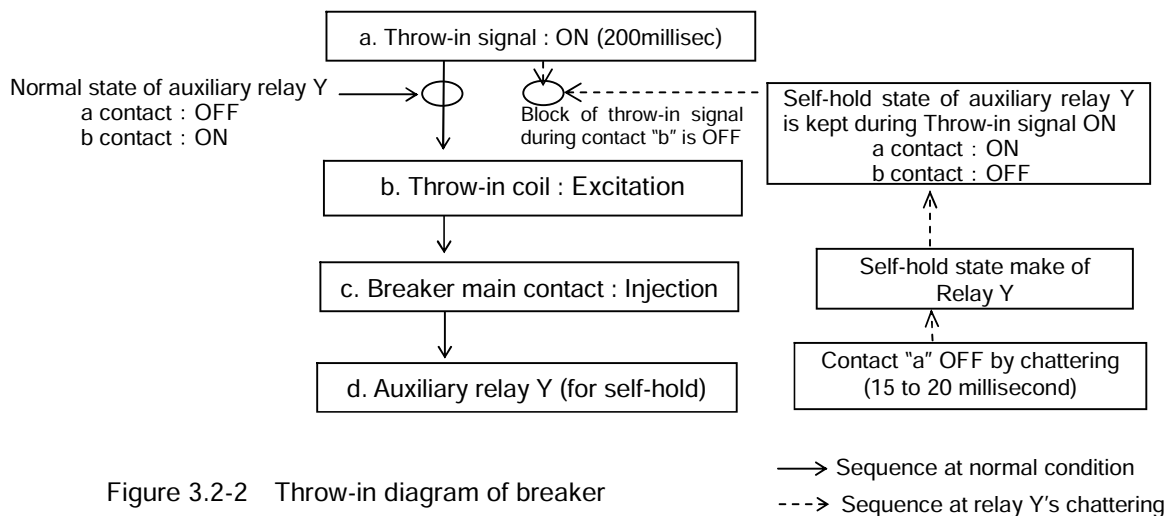


Figure 3.2-2 Throw-in diagram of breaker

This malfunction was occurred only once in about 30 throw-in tests under seismic excitation, so it is considered to be very rare phenomenon.

b) Evaluation of function limit acceleration

Assuming that probability of re-throw-in failure is increased with overlap time increase between chattering duration time and occurrence number. From this relation, it was examined to derive re-throw-in failure probability.

The number of times of occurrence of chattering and duration of fake contact time tend to increase with acceleration increase. The probability of re-throw-in failure is shown in Fig. 3.2-3.

The ratio of malfunction of the relay $\Delta t \cdot N/T$ is derived from the length of chattering Δt and occurrence number N during unit time. And the ratio of the chattering continuation time to unit time assumed to be equal to the probability of re-throw-in failure.

As shown in Figure 3.2-3, since chattering is not occurred by input acceleration less than $2.2 \times 9.8 \text{ m/s}^2$, the probability of re-throw-in failure is considered as zero for this level. In $6.0 \times 9.8 \text{ m/s}^2$, failure probability becomes about 0.2 and the failure occurs once to five trials.

From this figure, assuming failure probability as 4% for $3 \times 9.8 \text{ m/s}^2$ and 20% for $6 \times 9.8 \text{ m/s}^2$, and assuming log normal distribution, the median of fragility acceleration evaluated as $11.4 \times 9.8 \text{ m/s}^2$.

In addition, the breaker can be normally thrown in by re-inputting the throw-in signal even if the first throw-in is failed by the timing of throw-in command with chattering. Therefore, the influences on a real plant are considered to be small.

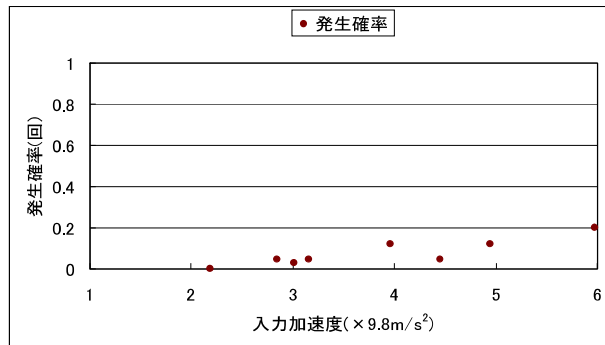


Figure 3.2-3 Re-throw-in failure probability (Gas circuit breaker with seismic reinforcement)

3.3 Control rod inserting capability

Among fragility data studied in Part 2 of Equipment Fragility Test, fragility data related to control rod inserting capability shown in the below table are given in Table 3.3-2 to 3.2-5.

Table3.3-1 Fragility Data related to Control Rod Inserting Capability

Objects of evaluation	Type	Table
PWR control rod inserting capability	Representative plants (3 loop, 4 loop)	Table 3.3-2
	Plants other than representative plants (2 loop)	Table 3.3-3
BWR control rod inserting capability	Representative plants (100mil channel box)	Table 3.3-4
	Plants other than representative plants (80mil and 120mil channel box)	Table 3.3-5

Table 3.3-2 Summary Table of Fragility Data (3 Loop and 4 Loop of PWR)

Equipment/ Facility	PWR control rod inserting capability		
Type of objective equipment	Name: Representative plants of PWR (3 loop, 4 loop) Type of fuel assembly: 17×17 type		
Test results and evaluation results of fragility capacity • Full-scale test • Element test • No test			
Results of full-scale equipment test			
Equipment		JNES test	NUPEC test ^{*1}
Maximum input acceleration (m/s ²)		About 3.2×9.8	About 1.1×9.8
Fuel assembly	Displacement (mm)	About 48	About 22
	Deformation of fuel assembly grid (mm) ^{*2}	About 3.5	About 1.3
CRDM	Displacement (mm)	About 17.2	About 3.3
*1: Results of test with vibration up to 1.5S ₂ in "Seismic Verification Test of In-Core Structure of PWR", (1985)			
*2: Deformation of support grid of fuel assembly in which control rod was inserted.			
Results of fragility evaluation			
Failure mode	Median value Response displacement of fuel assembly		Dispersion β _c
Excess response displacement of fuel assembly	77 mm ^{*3,*4}		0.19
*3: Although control rod insertion time exceeded the prescribed scram time, it has still safety margin.			
*4: This is a limit of application for control rod insertion analysis method, and it, therefore, has margin for structural damage.			

Table 3.3-3 Summary Table of Fragility Data (2 Loop of PWR)

Equipment/ Facility	PWR control rod inserting capability		
Type of objective equipment	Name: Plant other than representative plants of PWR (2 loop) Type of fuel assembly: 14×14 type		
Test results and evaluation results of fragility capacity • Full-scale test • Element test • No test			
Evaluation results of fragility			
Failure mode	Median value Response displacement of fuel assembly		Dispersion β _c
Excess response displacement of fuel assembly	69 mm ^{*1,*2}		0.19
*1: Although control rod insertion time exceeded the prescribed scram time, it has safety margin.			
*2: This is a limit of application for control rod insertion analysis method, and it, therefore, has margin for structural damage.			

Table 3.3-4 Summary Table of Fragility Data (BWR, 100 mil channel box)

Equipment/ Facility	BWR control rod inserting capability		
Type of objective equipment	Name: Representative plants of BWR (100 mil channel box) Wall thickness of channel box: 100 mil (about 2.5 mm) Reactor type: BWR5 (high speed scram type control rod drive mechanism)		
Test results and evaluation results of fragility capacity • Full-scale test • Element test • No test			
Results of actual equipment test			
Equipment		JNES test	NUPEC test ^{*1}
Maximum input acceleration (m/s ²)		About 3.0×9.8	About 1.5×9.8
Fuel assembly	Displacement (mm)	About 80	About 34
*1: Results of test with vibration up to 1.7S ₂ in "Seismic Verification Test of In-Core Structure of BWR", (1986)			
Results of fragility evaluation			
Failure mode	Median value Response displacement of fuel assembly		Dispersion β _c
Excess response displacement of fuel assembly	91 mm ^{*2,*3}		0.10
*2: Control rod insertion time was below the prescribed scram time, and it has still safety margin. *3: This is a limit of application for control rod insertion analysis method, and it, therefore, has margin for structural damage.			

Table 3.3-5 Summary Table of Fragility Data (BWR, 80 mil and 120 mil channel box)

Equipment/ Facility	BWR control rod inserting capability		
Type of objective equipment	Name: Representative plants of BWR (80 mil and 120 mil channel box) Wall thickness of channel box: 80 mil (about 2.0 mm) and 120 mil (about 3.0 mm) Reactor type: BWR5 (high speed scram type control rod drive mechanism)		
Test results and evaluation results of fragility capacity • Full-scale test • Element test • No test			
Evaluation results of fragility (80 mil)			
Type of channel box	Failure mode	Median value Response displacement of fuel assembly	Dispersion β _c
80 mil	Excess response displacement of fuel assembly	91 mm ^{*1,*2}	0.10
120 mil	Excess response displacement of fuel assembly	91 mm ^{*1,*2}	0.09
*1: Control rod insertion time was below the prescribed scram time, and it has safety margin. *2: This is a limit of application for control rod insertion analysis method, and it, therefore, has margin for structural damage.			

3.4 Large size vertical shaft pump

Among fragility data studied in Part 3 of Equipment Fragility Test, fragility data related to large size vertical shaft pump shown in the table below are given in Table 3.4-2 to 3.4-5.

Table 3.4-1 Fragility Data related to Large Size Vertical Shaft Pump

Equipment	Name	Direction of earthquake motion	Table
Pump	Residual heat removal system pump (full-scale specimen)	Horizontal	Table 3.4-2
	High pressure core injection system pump		
	Component cooling seawater pump (PWR)		
	Component cooling seawater pump (BWR)		
	Residual heat removal system pump	Vertical	Table 3.4-3
	Component cooling seawater system pump		
	High pressure core spray pump		
Parts	Submerged bearing	Horizontal	Table 3.4-4
	Liner ring		
	Thrust bearing	Vertical	Table 3.4-5

Table 3.4-2 Summary Table of Horizontal Fragility Data of Pump (1/4)

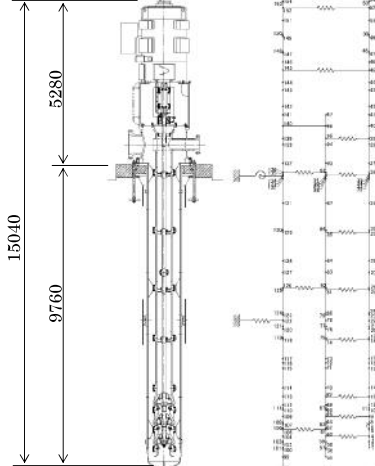
Equipment/ Facility	Large size vertical shaft pump															
Type of objective equipment	Name: Residual heat removal system pump Type: Pit barrel type pump (long size; full-scale specimen)															
		<table border="1"> <thead> <tr> <th>Item</th> <th>Specification</th> </tr> </thead> <tbody> <tr> <td>Total pump head (m)</td> <td>92</td> </tr> <tr> <td>Flow rate (m³/h)</td> <td>1691</td> </tr> <tr> <td>Rotating speed (rpm)</td> <td>1500</td> </tr> <tr> <td>Motor output (kW)</td> <td>750</td> </tr> <tr> <td>Mass (ton) (including motor and contained water)</td> <td>About 61 Pump portion (including motor stand): 49.0 Motor portion: 13.0</td> </tr> </tbody> </table>	Item	Specification	Total pump head (m)	92	Flow rate (m ³ /h)	1691	Rotating speed (rpm)	1500	Motor output (kW)	750	Mass (ton) (including motor and contained water)	About 61 Pump portion (including motor stand): 49.0 Motor portion: 13.0		
Item	Specification															
Total pump head (m)	92															
Flow rate (m ³ /h)	1691															
Rotating speed (rpm)	1500															
Motor output (kW)	750															
Mass (ton) (including motor and contained water)	About 61 Pump portion (including motor stand): 49.0 Motor portion: 13.0															
Test results and evaluation results of fragility capacity • Full-scale test • Element test • No test																
Outline of test results (Input wave: Wave enveloping response spectra at actual large size vertical shaft pump installing floor)																
Direction of vibration	Pump status	Focusing portion of response	Maximum response acceleration (×9.8m/s ²)	Event such as damage	Loss of function											
Horizontal	Operation	Bottom of barrel	31.0	Confirmed yield of barrel (near barrel support)	None											
		Top of motor	—	—	None											
	Shutdown	Bottom of barrel	31.0	Confirmed yield of barrel (near barrel support)	None											
		Top of motor	12.0	Confirmed yield of motor mounting bolt	None											
14.0	None (confirmed that function of motor body was maintained)		None													
Fragility evaluation (Input wave: Wave totally enveloping response spectra at actual pit barrel type pump installing floor)																
Function	Order of generation	Median value of fragility (×9.8m/s ²)	Log standard deviation	Damage mode	Evaluation method											
Function limit of pump system (below installing floor)	(1)	37.1 (response acceleration at bottom of barrel)	—	Loss of function of submerged bearing (carbon) (PV value)	• Acceleration where PV value of submerged bearing reaches to function-confirmed PV value obtained by element test is calculated by detailed analysis.											
Function limit of pump system (above installing floor)	(1)	<Reference> 3.6 ¹ (response acceleration at top of motor)	<Reference> 0.12 ¹	<Reference> Slip at tightening surface of motor mounting bolt	• Response acceleration where stress generated on foundation bolt reaches to design yield stress. • Log standard deviation is calculated based on distribution of friction factor of slip surface, torque constant of bolt and tensile strength of material.											
	(2)	14.0 ² (response acceleration at top of motor)	—	—	—											
Remarks	<ul style="list-style-type: none"> • Refer to Section 2.4 for fragility evaluation method. • Median value of fragility is response acceleration of each portion of pump. *1: Since the pump for an examination was the one designed by comparatively small load, a slide limit was produced at low acceleration. Since a motor mounting bolt was a portion designed according to earthquake load, it was presented as a reference value. *2: Fragility test was continued with reinforcing mounting bolt portion. This value was achieved by the test after reinforcing the motor mounting bolt. 															

Table 3.4-2 Summary Table of Horizontal Fragility Data of Pump (2/4)

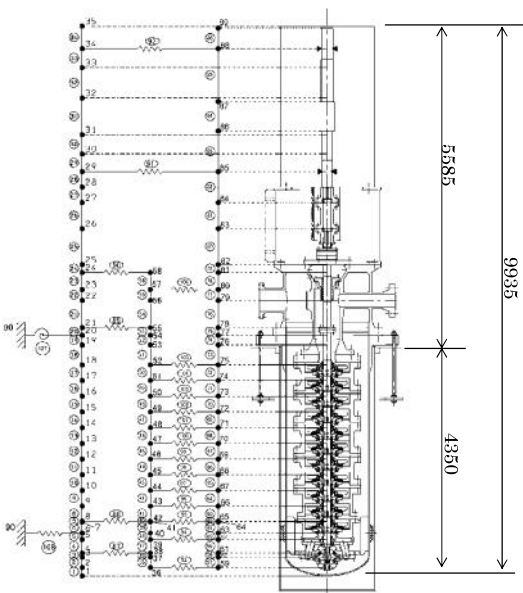
Equipment/ Facility	Large size vertical shaft pump															
Type of objective equipment	Name: High pressure core injection system pump Type: Pit barrel type pump (short size)															
		<table border="1"> <thead> <tr> <th>Item</th> <th>Specification</th> </tr> </thead> <tbody> <tr> <td>Total pump head (m)</td> <td>190</td> </tr> <tr> <td>Flow rate (m³/h)</td> <td>727</td> </tr> <tr> <td>Rotating speed (rpm)</td> <td>1500</td> </tr> <tr> <td>Motor output (kW)</td> <td>1400</td> </tr> <tr> <td>Mass (ton) (including motor and contained water)</td> <td>About 62 Pump portion (including motor stand): 52.5 Motor portion: 8.5</td> </tr> </tbody> </table>				Item	Specification	Total pump head (m)	190	Flow rate (m ³ /h)	727	Rotating speed (rpm)	1500	Motor output (kW)	1400	Mass (ton) (including motor and contained water)
Item	Specification															
Total pump head (m)	190															
Flow rate (m ³ /h)	727															
Rotating speed (rpm)	1500															
Motor output (kW)	1400															
Mass (ton) (including motor and contained water)	About 62 Pump portion (including motor stand): 52.5 Motor portion: 8.5															
Evaluation results of fragility capacity • Full-scale test • Element test • No test																
Fragility evaluation (Input wave: Wave totally enveloping response spectra at actual pit barrel type pump installing floor)																
Function	Order of generation	Median value of fragility (×9.8m/s ²)	Log standard deviation	Damage mode	Evaluation method											
Function limit of pump system (below installing floor)	(1)	17.7 (response acceleration at bottom of barrel)	—	Loss of function of submerged bearing (carbon) (PV value)	Acceleration where PV value of submerged bearing reaches to function-confirmed PV value obtained by element test is calculated by detailed analysis.											
Function limit of pump system (above installing floor)	(1)	<Reference> 3.5 (response acceleration at top of motor)	<Reference> 0.12	<Reference> Slip at tightening surface of motor mounting bolt	<ul style="list-style-type: none"> Response acceleration where shear force on tightening surface reaches to friction force. Log standard deviation is calculated based on distribution of friction factor of slip surface, torque constant of bolt and tensile strength of material. 											
	(2)	14.0 (response acceleration at top of motor)	—	—	—											
Remarks	<ul style="list-style-type: none"> Refer to Section 2.4 for fragility evaluation method. Median value of fragility is response acceleration of each portion of pump. Slip evaluation results is presented as a reference, because uncertainty factors such as effect of rotary shaft system are not considered. 															

Table 3.4-2 Summary Table of Horizontal Fragility Data of Pump (3/4)

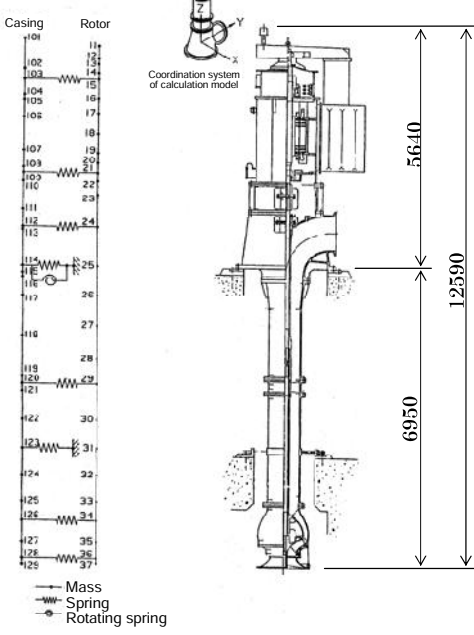
Equipment/ Facility	Large size vertical shaft pump															
Type of objective equipment	Name: Component cooling seawater pump Type: Vertical mixed flow pump (PWR)															
	 <p> Casing Rotor 108 11 102 12 103 13 104 14 105 15 106 16 102 17 107 18 108 19 109 20 110 21 110 22 111 23 112 24 115 25 116 26 117 26 116 27 115 28 120 29 121 30 122 30 124 32 125 33 126 34 127 35 128 36 129 37 → Mass ← Spring ○ Rotating spring </p>	<table border="1"> <thead> <tr> <th>Item</th> <th>Specification</th> </tr> </thead> <tbody> <tr> <td>Total pump head (m)</td> <td>48</td> </tr> <tr> <td>Flow rate (m³/h)</td> <td>5300</td> </tr> <tr> <td>Rotating speed (rpm)</td> <td>720</td> </tr> <tr> <td>Motor output (kW)</td> <td>980</td> </tr> <tr> <td>Mass (ton) (including motor and contained water)</td> <td>About 31 Pump portion: 17.8 Motor portion: 13.0</td> </tr> </tbody> </table>	Item	Specification	Total pump head (m)	48	Flow rate (m ³ /h)	5300	Rotating speed (rpm)	720	Motor output (kW)	980	Mass (ton) (including motor and contained water)	About 31 Pump portion: 17.8 Motor portion: 13.0		
Item	Specification															
Total pump head (m)	48															
Flow rate (m ³ /h)	5300															
Rotating speed (rpm)	720															
Motor output (kW)	980															
Mass (ton) (including motor and contained water)	About 31 Pump portion: 17.8 Motor portion: 13.0															
Evaluation results of fragility capacity • Full-scale test • Element test • No test																
Outline of test results (Input wave: Wave totally enveloping response spectra at actual vertical mixed flow pump installing floor)																
Function	Order of generation	Median value of fragility (×9.8m/s ²)	Log standard deviation	Damage mode	Evaluation method											
Function limit of pump system (below installing floor)	(1)	96.9 (response acceleration at bottom of barrel)	—	Loss of function of submerged bearing (carbon) (PV value)	• Acceleration where PV value of submerged bearing reaches to function-confirmed PV value obtained by element test is calculated by detailed analysis.											
Function limit of pump system (above installing floor)	(1)	<Reference> 6.2 (response acceleration at top of motor)	<Reference> 0.12	<Reference> Slip at tightening surface of motor mounting bolt	• Response acceleration where shear force on tightening surface reaches to friction force. • Log standard deviation is calculated based on distribution of friction factor of slip surface, torque constant of bolt and tensile strength of material.											
	(2)	6.3 (response acceleration at top of motor)	0.09	Yielded at mounting bolt of motor stand	• Response acceleration where stress generated on bolt reaches to design yield stress is calculated. • Log standard deviation is calculated based on distribution of tensile strength of material.											
Remarks	<ul style="list-style-type: none"> Refer to Section 2.4 for fragility evaluation method. Median value of fragility is response acceleration of each portion of pump. Slip evaluation results is presented as a reference, because uncertainty factors such as effect of rotary shaft system are not considered. 															

Table 3.4-2 Summary Table of Horizontal Fragility Data of Pump (4/4)

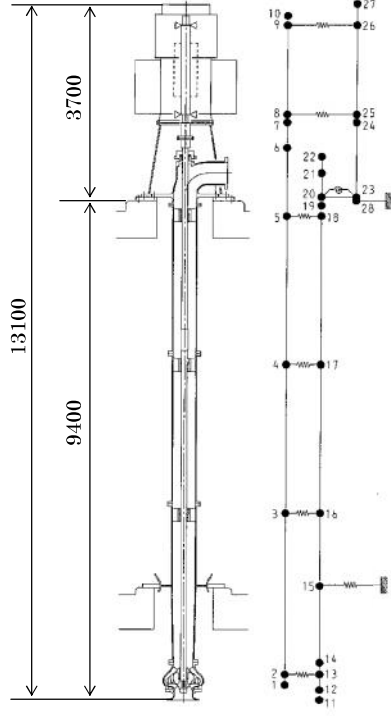
Equipment/ Facility	Large size vertical shaft pump															
Type of objective equipment	Name: Component cooling seawater pump Type: Vertical mixed flow pump (BWR)															
		<table border="1"> <thead> <tr> <th>Item</th> <th>Specification</th> </tr> </thead> <tbody> <tr> <td>Total pump head (m)</td> <td>40</td> </tr> <tr> <td>Flow rate (m³/h)</td> <td>1080</td> </tr> <tr> <td>Rotating speed (rpm)</td> <td>1200</td> </tr> <tr> <td>Motor output (kW)</td> <td>190</td> </tr> <tr> <td>Mass (ton) (including motor and contained water)</td> <td>About 15 Pump portion (including motor stand): 10.0 Motor portion: 5.0</td> </tr> </tbody> </table>				Item	Specification	Total pump head (m)	40	Flow rate (m ³ /h)	1080	Rotating speed (rpm)	1200	Motor output (kW)	190	Mass (ton) (including motor and contained water)
Item	Specification															
Total pump head (m)	40															
Flow rate (m ³ /h)	1080															
Rotating speed (rpm)	1200															
Motor output (kW)	190															
Mass (ton) (including motor and contained water)	About 15 Pump portion (including motor stand): 10.0 Motor portion: 5.0															
Evaluation results of fragility capacity • Full-scale test • Element test • No test																
Outline of test results (Input wave: Wave totally enveloping response spectra at actual vertical mixed flow pump installing floor)																
Function	Order of generation	Median value of fragility (×9.8m/s ²)	Log standard deviation	Damage mode	Evaluation method											
Function limit of pump system (below installing floor)	(1)	14.6 (response acceleration at bottom of barrel)	—	Loss of function of submerged bearing (carbon) (PV value)	• Acceleration where PV value of submerged bearing reaches to function-confirmed PV value obtained by element test is calculated by detailed analysis.											
Function limit of pump system (above installing floor)	(1)	<Reference> 2.8 (response acceleration at top of motor)	<Reference> 0.12	<Reference> Slip at tightening surface of motor mounting bolt	• Response acceleration where shear force on tightening surface reaches to friction force. • Log standard deviation is calculated based on distribution of friction factor of slip surface, torque constant of bolt and tensile strength of material.											
	(2)	4.3 (response acceleration at top of motor)	0.09	Yielded at mounting bolt of motor stand	• Response acceleration where stress generated on bolt reaches to design yield stress is calculated. • Log standard deviation is calculated based on distribution of tensile strength of material.											
Remarks	<ul style="list-style-type: none"> • Refer to Section 2.4 for fragility evaluation method. • Median value of fragility is response acceleration of each portion of pump. • Slip evaluation results is presented as a reference, because uncertainty factors such as effect of rotary shaft system are not considered. 															

Table 3.4-3 Summary Table of Vertical Fragility Data of Pump (1/2)

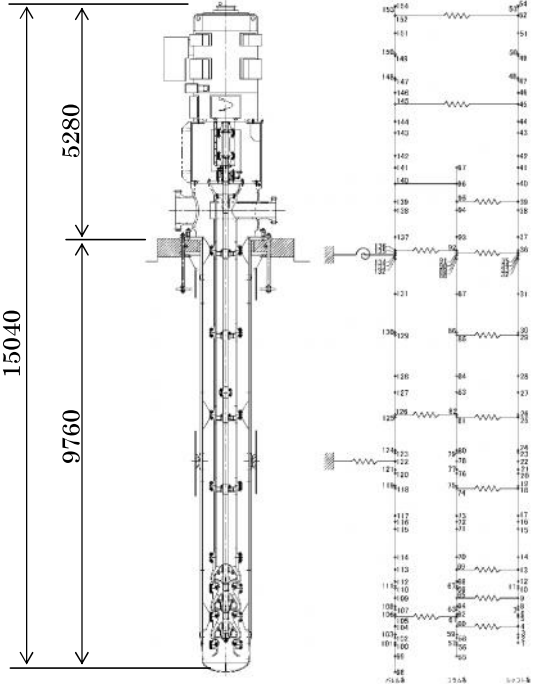
Equipment/ Facility	Large size vertical shaft pump																
Type of objective equipment	Name: High pressure core injection system pump Type: Pit barrel type pump (long size; Full-scale specimen) Motor thrust bearing: Ball bearing																
		<table border="1"> <thead> <tr> <th>Item</th> <th>Specification</th> </tr> </thead> <tbody> <tr> <td>Total pump head (m)</td> <td>92</td> </tr> <tr> <td>Flow rate (m³/h)</td> <td>1691</td> </tr> <tr> <td>Rotating speed (rpm)</td> <td>1500</td> </tr> <tr> <td>Motor output (kW)</td> <td>750</td> </tr> <tr> <td>Mass (ton) (including motor and contained water)</td> <td>About 61 Pump portion (including motor stand): 49.0 Motor portion: 13.0</td> </tr> </tbody> </table>					Item	Specification	Total pump head (m)	92	Flow rate (m ³ /h)	1691	Rotating speed (rpm)	1500	Motor output (kW)	750	Mass (ton) (including motor and contained water)
Item	Specification																
Total pump head (m)	92																
Flow rate (m ³ /h)	1691																
Rotating speed (rpm)	1500																
Motor output (kW)	750																
Mass (ton) (including motor and contained water)	About 61 Pump portion (including motor stand): 49.0 Motor portion: 13.0																
Evaluation results of fragility capacity • Full-scale test • Element test • No test																	
Direction of vibration	Pump status	Focusing portion of response	Maximum response acceleration (×9.8m/s ²)	Maximum input acceleration (×9.8m/s ²)	Event such as damage	Loss of function											
Vertical	Operation	Bottom of barrel		1.9	None	None											
		Top of motor	2.3		None	None											
	Shutdown	Bottom of barrel	2.2	1.9	None	None											
		Top of motor	2.3		None	None											
Horizontal + Vertical	Operation	Bottom of barrel	23.5 (horizontal) 2.1 (Vertical)	—	None	None											
		Top of motor	8.2 (horizontal) 2.2 (Vertical)	—	None	None											
	Shutdown	Bottom of barrel	23.5 (horizontal) 2.0 (Vertical)	—	None	None											
		Top of motor	8.2 (horizontal) 2.2 (Vertical)	—	None	None											
Remarks																	

Table 3.4-3 Summary Table of Vertical Fragility Data of Pump (2/2)

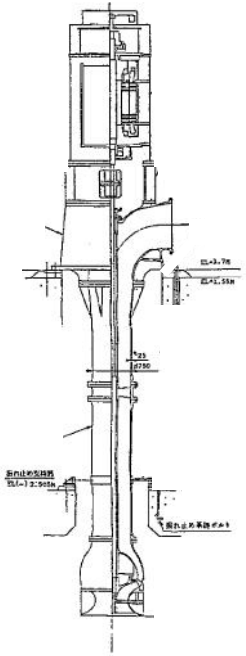
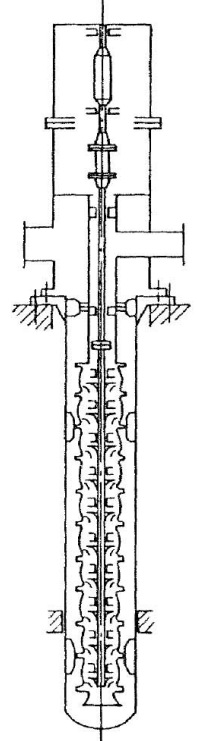
Equipment/ Facility	Large size vertical shaft pump						
Type of objective equipment	[A] Name: Component cooling seawater system pump Type: Vertical mixed flow pump (PWR) Thrust bearing: Kingsbury bearing		[B] Name: High pressure core spray pump Type: Pit barrel type pump Motor thrust bearing: Parallel plane bearing				
							
Evaluation results of fragility capacity • Full-scale test • Element test • No test							
Type	Order of occurrence	Critical value (Clearance between impeller and liner ring)		Analysis result		Fragility evaluation	
				Input acceleration to reach critical value ($\times 9.8\text{m/s}^2$)	Function- confirmed input acceleration ($\times 9.8\text{m/s}^2$)	Median value ($\times 9.8\text{m/s}^2$)	Log standard deviation
Kingsbury bearing	(1)	Lifting	13mm	1.5	1.5 ($6.7S_2$) (The minimum value of the left)	-	-
	(2)	Bearing load	1,500kN	1.6			
Parallel plane bearing	(1)	Lifting	20mm	1.3	1.3 ($5.7 S_2$) (The minimum value of the left)	-	-
	(2)	Bearing load	1,500kN	1.3			
Remarks	<ul style="list-style-type: none"> • For S_2, vertical simulated earthquake ground motion (ZPA: $0.22 \times 9.8\text{m/s}^2$) studied in Improvement and Standardization Program is specified as standard. • No abnormality in thrust bearing • Bearing load, 1,500 kN, is the thrust load where bearing function was confirmed to be maintained in element test. On the other hand, it was not confirmed whether function was maintained if lifting reached to the limit. Therefore, vertical input acceleration which results in the limit value calculated by analysis, is specified as input acceleration for maintaining function. 						

Table 3.4-4 Summary Table of Horizontal Fragility Data of Equipment (1/2)

Equipment/ Facility	Submerged bearing for large size vertical shaft pump						
Type of objective equipment	Type	Inner diameter (mm)	Bearing length (mm)	Diametric clearance (mm)	Allowable surface pressure of bearing (Mpa)	Number of specimens	Materials
	Carbon bearing (large)	100	115	0.41~0.48	1.47	3	Main component: graphite
	Carbon bearing (small)	55	50	0.41~0.48	1.47	3	Same as above
	Solid lubricant distributed oilless bearing	100	80	0.39~0.58	0.8	4	Sintered metal of lead bronze alloy and graphite
	Resin bearing	120	120	0.14~0.34	1.47	4	High polymer of fluorine and carbon
	Rubber bearing	100	120	0.14~0.34	1.47	4	Copolymer of butadiene and acrylonitrile
Test results and evaluation results of fragility capacity							• Full-scale test • Element test • No test
Load test for submerged bearing							
Type	Specimen No.	Test results			Fragility evaluation		
		Function- confirmed load (kN)	Function- confirmed surface pressure	Function- confirmed PV value (MPa · m/s)	Median value (kN)	Log standard deviation	
Carbon bearing (large)	1	95.9	8.3	65.2	-	-	
	2	100.4	8.7	68.2			
Carbon bearing (small)	3	101.0	8.7	68.6			
Carbon bearing (large)	1	51.9	18.7	80.9	-	-	
	2	54.7	19.8	85.3			
Carbon bearing (small)	3	56.4	20.3	87.8			
Carbon bearing (large)	1	98.8	12.3	77.1	-	-	
	2	109.5	13.6	—*			
	3	107.3	13.4	83.8			
	4	106.7	13.3	83.3			
Resin bearing	1	99.6	6.9	—*	<Reference> 61.1	<Reference> 0.06	
	2	123.6	8.6	64.6			
	3	117.6	8.2	61.4			
	4	110.0	7.6	57.5			
Rubber bearing	1	92.3	7.7	—*	<Reference> 69.8	<Reference> 0.03	
	2	104.2	8.7	68.0			
	3	109.9	9.1	71.7			
	4	107.0	8.9	69.8			
Remarks		<ul style="list-style-type: none"> Rotating function was maintained for all bearings after test. However, bulges and cracks were generated on edge of bearing for resin bearing and rubber bearing. * in the table means that result was not listed because of different test conditions. 			<ul style="list-style-type: none"> Bulge and crack of resin bearing and rubber bearing were considered as indication of loss of function, and their functions were conservatively assumed to be lost. Under such conditions, median value of fragility and log standard deviation were calculated as a reference. 		

Table 3.4-4 Summary Table of Horizontal Fragility Data of Equipment (2/2)

Equipment/ Facility	Liner ring for large size vertical shaft pump						
Type of objective equipment	Type	Inner diameter (mm)	Diametric clearance (mm)	Length (mm)	Number of specimens	Material	
	Flat type	355	0.53	50	3	Austenitic stainless steel	
	Flat type	550	1.17	45	3	Same as above	
Test results and evaluation results of fragility capacity • Full-scale test • <u>Element test</u> • No test							
Liner ring test							
Inner diameter (mm)	Specimen No.	Test result				Fragility evaluation	
		Function- confirmed load (kN)	Maximum surface pressure (MPa)	Function- confirmed PV value (MPa·m/s)	Load of abnormal occurrence (kN)	Median value	Log standard deviation
355	1	20.0	1.13	25	—	—	—
	2	22.5	1.27	28	—		
	3	21.7	1.22	27	—		
550	1	17.5	0.71	18	—	—	—
	2	17.5	0.71	18	—		
	3	17.5	0.71	18	—		
Remarks		• No abnormality in liner ring					

Table 3.4-5 Summary Table of Vertical Fragility Data of Equipment

Equipment/ Facility	Thrust bearing for large size vertical shaft pump																																				
Type of objective equipment	Type	Outer diameter of slide portion (mm)	Inner diameter of slide portion (mm)	Height (mm)	Number of specimens	Remarks																															
	Kingsbury type	540	270	270	3	Slide bearing																															
	Parallel plane type	470	250	184	3	Same as above																															
Test results and evaluation results of fragility capacity • Full-scale test • Element test • No test																																					
<p style="text-align: center;">Thrust bearing test</p> <table border="1" data-bbox="310 646 1338 1035"> <thead> <tr> <th data-bbox="315 646 532 751" rowspan="2">Outer diameter (mm)</th> <th data-bbox="537 646 680 751" rowspan="2">Specimen No.</th> <th data-bbox="685 646 1032 751">Test result</th> <th colspan="2" data-bbox="1037 646 1333 678">Fragility evaluation</th> </tr> <tr> <th data-bbox="685 684 1032 751">Function-confirmed load (static load) (kN)</th> <th data-bbox="1037 684 1167 751">Median value</th> <th data-bbox="1172 684 1333 751">Log standard deviation</th> </tr> </thead> <tbody> <tr> <td data-bbox="315 758 532 842" rowspan="3">Kingsbury type</td> <td data-bbox="537 758 680 789">1</td> <td data-bbox="685 758 1032 789">1,500</td> <td data-bbox="1037 758 1167 842" rowspan="3">-</td> <td data-bbox="1172 758 1333 842" rowspan="3">-</td> </tr> <tr> <td data-bbox="537 795 680 827">2</td> <td data-bbox="685 795 1032 827">1,500</td> </tr> <tr> <td data-bbox="537 833 680 865">3</td> <td data-bbox="685 833 1032 865">1,500</td> </tr> <tr> <td data-bbox="315 871 532 955" rowspan="3">Parallel plane type</td> <td data-bbox="537 871 680 903">1</td> <td data-bbox="685 871 1032 903">1,500</td> <td data-bbox="1037 871 1167 955" rowspan="3">-</td> <td data-bbox="1172 871 1333 955" rowspan="3">-</td> </tr> <tr> <td data-bbox="537 909 680 940">2</td> <td data-bbox="685 909 1032 940">1,500</td> </tr> <tr> <td data-bbox="537 947 680 978">3</td> <td data-bbox="685 947 1032 978">1,500</td> </tr> <tr> <td colspan="2" data-bbox="315 984 680 1035">Remarks</td> <td colspan="3" data-bbox="685 984 1333 1035">• No abnormality in thrust bearing</td> </tr> </tbody> </table>							Outer diameter (mm)	Specimen No.	Test result	Fragility evaluation		Function-confirmed load (static load) (kN)	Median value	Log standard deviation	Kingsbury type	1	1,500	-	-	2	1,500	3	1,500	Parallel plane type	1	1,500	-	-	2	1,500	3	1,500	Remarks		• No abnormality in thrust bearing		
Outer diameter (mm)	Specimen No.	Test result	Fragility evaluation																																		
		Function-confirmed load (static load) (kN)	Median value	Log standard deviation																																	
Kingsbury type	1	1,500	-	-																																	
	2	1,500																																			
	3	1,500																																			
Parallel plane type	1	1,500	-	-																																	
	2	1,500																																			
	3	1,500																																			
Remarks		• No abnormality in thrust bearing																																			

4. Summary

(1) Horizontal shaft pump

As fragility evaluation method for horizontal shaft pump, fragility evaluation method was established to obtain seismic force which reaches to critical load of bearing by seismic response analysis of horizontal shaft pump during large input earthquake, and to evaluate critical acceleration of active function. Regarding critical load of bearing, critical load and dispersion for fragility evaluation were developed according to the types of bearing, based on the element test results of bearing. Furthermore, mount bolts of motor and pump was evaluated by simplified static analysis from viewpoint of structural strength, and critical acceleration of structural strength was evaluated.

Critical accelerations of active function were evaluated for full-scale specimens (RCW pump), similar types of horizontal shaft single stage pump and multi stage pump. Accelerations obtained from the above evaluation exceeded function-confirmed acceleration ($6 \times 9.8 \text{ m/s}^2$) of actual equipment test.

(2) Electrical equipment

Regarding electrical equipment, fragility evaluation method was established to evaluate critical acceleration of electrical function for electrical equipment (panel) based on response multiplying factor of panel by analysis and function critical acceleration by parts tests. Regarding function critical accelerations of parts, median value and dispersion of fragility were developed based on the parts test results. From viewpoint of structural strength, stress evaluation was performed for cabinet body using response analysis of electrical equipment, and critical accelerations of structural strength were evaluated.

Critical accelerations of electrical function and critical accelerations of structural strength were evaluated for 8 type panel specimens and similar types of electrical panels. The results of evaluation revealed that electrical function is controlled by electrical fragility capacity for all electrical equipment, and fragility capacity obtained from the above evaluation results exceeded fragility capacity ($3.6 \times 9.8 \text{ m/s}^2$) used in the past seismic PSA.

(3) Control rod inserting capability

(i) PWR control rod inserting capability

Regarding PWR control rod inserting capability, structural fragility capacity and limit of control rod inserting capability were investigated by using analysis method, of which adequacy was verified by simulation analysis of actual equipment test. Seismic response analysis and strength analysis of fuel assembly, control rod drive mechanism and in-core structure for actual representative plant (4 loop) and plant other than representative (2 loop) were performed, and based on such evaluation results, fragility evaluation was performed.

As the results of fragility evaluation for actual representative plant (4 loop), fragility capacity was decided by excess response displacement of fuel assembly, and calculated median value of fragility capacity (77 mm) exceeded the median value of fragility (fuel response displacement: 36 mm) used in the past seismic PSA.

(ii) BWR control rod inserting capability

Regarding BWR control rod inserting capability, fragility capacity of equipment and limit of control rod inserting capability were investigated by using analysis method, of which adequacy was verified by simulation analysis of full-scale equipment test. Seismic response analysis and strength analysis of fuel assembly and in-core structure for standard plant (channel box type: 100 mil) and plant other than standard (channel box type: 80 mil and 120 mil) were performed, and based on such evaluation results, fragility evaluation was performed.

As the results of fragility evaluation for actual plant (channel box type: 100 mil), fragility capacity was decided by excess response displacement of fuel assembly, and calculated median value of fragility capacity (91 mm) exceeded the median value of fragility (fuel response displacement: 82 mm) used in the past seismic PSA.

(4) Large size vertical shaft pump

As fragility evaluation method for large size vertical shaft pump, seismic force, under which mounting bolts and barrel reached to yield, and seismic force, under which submerged bearing reached to function-confirmed PV value (index for seizing limit of material: product of contact surface pressure, P, by slip velocity between 2 surfaces, V), were obtained by seismic response analysis of large vertical shaft pump during earthquake, and fragility evaluation method was established to evaluate critical acceleration of active function. For active function limit of submerged bearing and liner ring, function-confirmed PV values were developed for fragility evaluation respectively based on element test results.

Evaluations of critical acceleration of active function for pit barrel type pumps (long size; full-scale test specimen, short size), vertical mixed flow pump (PWR, BWR) were performed. As the result, it was found that vertical mixed flow pump (BWR) has smallest fragility value, and median value of it is $14.6 \times 9.8 \text{m/s}^2$ for response acceleration at column bottom and $4.3 \times 9.8 \text{m/s}^2$ for response acceleration at motor top. These values exceed the function-confirmed horizontal response accelerations in former study^{note 1}, i.e., $10.0 \times 9.8 \text{m/s}^2$ and $2.5 \times 9.8 \text{m/s}^2$ respectively, which were obtained in the past study.

Note 1: Function-confirmed horizontal response accelerations for each portion of large size vertical shaft pump (RHR pit barrel type pump) which were obtained in the Utilities Research, "Study on Maintaining Function of Active Component during Earthquake (ACT Joint Study)" performed from 1980 to 1982, in order to confirm maintenance of function during earthquake for active component. (Study summary is described in JEAG4601-1991)

Reference

- JNES report (2006), 06 KIKOHO 0003, "Overall and comprehensive evaluation report of Equipment Fragility Test, Part 1 to Part 3" (in Japanese)
- JNES report (2005), 05 KIKOHO 0002, "Fragility Test, Part 1 : Horizontal shaft pump and electrical equipment" (in Japanese)
- JNES report (2004), 04 KIKOHO 0003, "Fragility Test, Part 1 : Horizontal shaft pump and electrical equipment" (in Japanese)
- JNES report (2006), 06 KIKOHO 0001, "Fragility Test, Part 2 : PWR control rod inserting capability" (in Japanese)
- JNES report (2006), 06 KIKOHO 0014, "Fragility Test, Part 2 : BWR control rod inserting capability" (in Japanese)
- JNES report (2005), 05 KIKOHO 0005, "Fragility Test, Part 2 : PWR and BWR control rod inserting capability"
- JNES report (2006), 06 KIKOHO 0002, "Fragility Test, Part 3 : Large size vertical shaft pump" (in Japanese)
- JNES report (2005), 05 KIKOHO 0004, "Fragility Test, Part 3 : Large size vertical shaft pump" (in Japanese)
- JNES report (2004), 04 KIKOHO 0004, "Fragility Test, Part 3 : Large size vertical shaft pump" (in Japanese)

APPENDIX B ELECTRICAL PANEL TEST RESPONSE SPECTRA

This appendix describes response spectra used in the JNES electrical panel tests and the electrical device tests. Response spectra for the horizontal shaft pump tests, the vertical shaft pump tests, and the control rod driven mechanism (CRDM) insertion capability tests are included in Section 3. These spectra were developed based on recorded time histories in the tests, or determined by analyses. JNES provided these spectra to NRC/BNL through its annotated fragility reports, which are in Japanese.

The annotations and labels in these spectra in this appendix are created based on the JNES annotations. The unit for the spectral acceleration in a spectrum plot may be g, gal (cm/s^2), or m/s^2 , as being consistent with the unit in the corresponding original spectrum plot in the JNES fragility reports. Similarly, the horizontal axis can be period (s) or frequency (Hz). The damping ratio for a response spectrum and the level of excitation are also indicated in the spectrum plots. The damping ratio for the electrical panels and the electrical devices is 4%. Other information useful in identifying the spectra is also presented as annotations or included in the captions.

The response spectra for the electrical panels and devices will be described in two sections of this appendix. The first section includes the spectra for the tests reported in September 2003. The zero period accelerations (ZPA) of these spectra are 5 g or smaller. The second section includes the spectra for the tests reported in July 2004 that have higher input ZPAs.

B.1 Response Spectra Reported in September 2003

These spectra were extracted from the JNES annotated fragility report dated September 2003. The title of that report in English is “Report on Seismic Reliability Proving Test, Vol. 2 – Equipment Fragility Vol. 1 (Horizontal Shaft Pump, Electrical Panels and Their Components).” A total of 36 figures are included in this section.

For device tests (i.e., component tests in JNES’s annotation), the input motions were developed based on analysis of the panels instead of recorded data in the tests, because the device tests were scheduled before the full scale panel tests. For a device that was installed in a tested panel, the input motion was the predicted response time history at its installation point; otherwise, the input motion was obtained from prior analysis of similar panels that included the subject device. The analytical input motions were further filtered by removing long period (< 8 Hz) components to consider the shaking table characteristics so that high acceleration was achieved in the concerned frequency range. The spectra for devices included in this section were extracted from Appendix C of the above mentioned proving test report.

B.1.1 Reactor Control Center

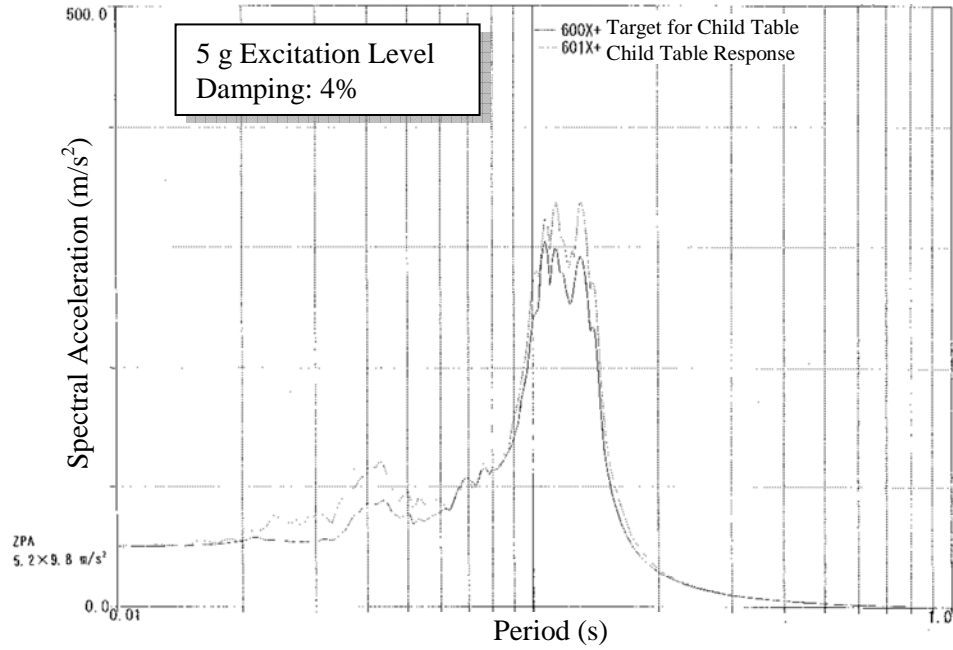


Figure B-1 Reactor Control Center Test – Child Table RS – 5 g (Side to Side)

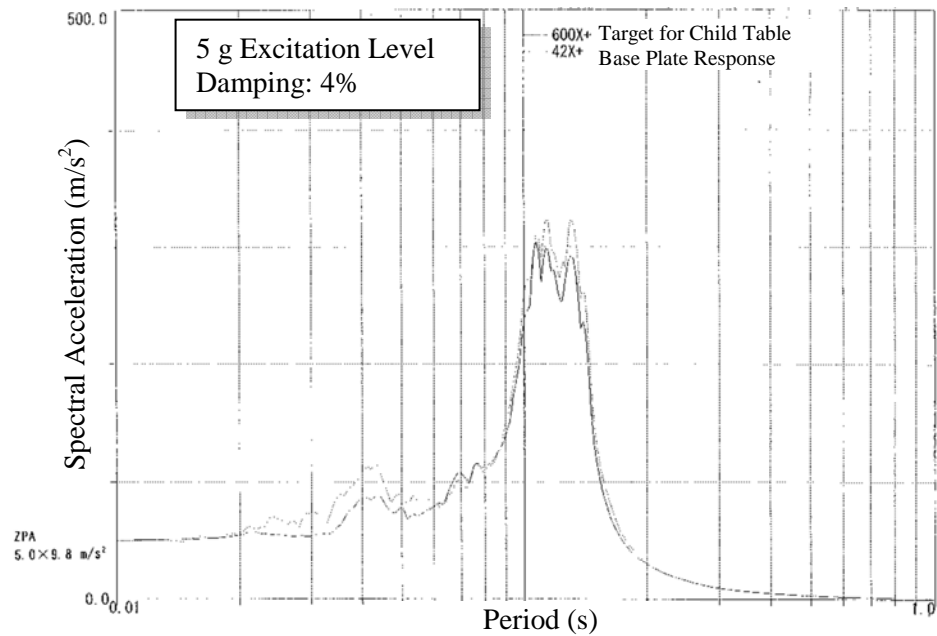


Figure B-2 Reactor Control Center Test – Base Plate RS – 5 g (Side to Side)

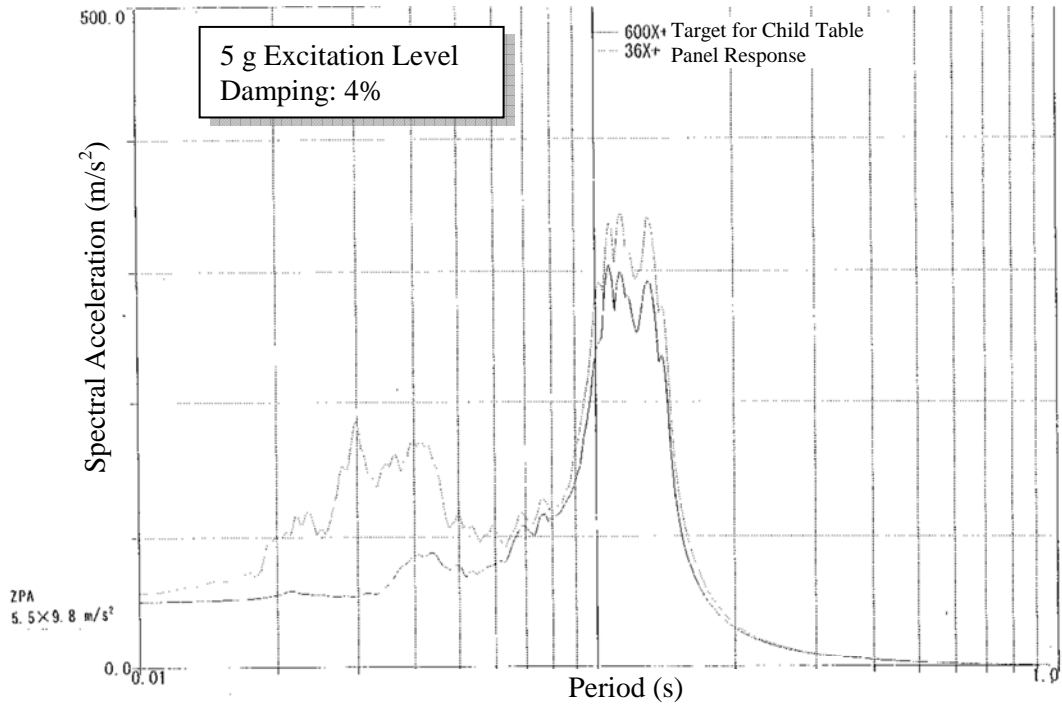


Figure B-3 Reactor Control Center Test – Panel RS at the Installation Point of Magnetic Contactor – 5 g (Side to Side)

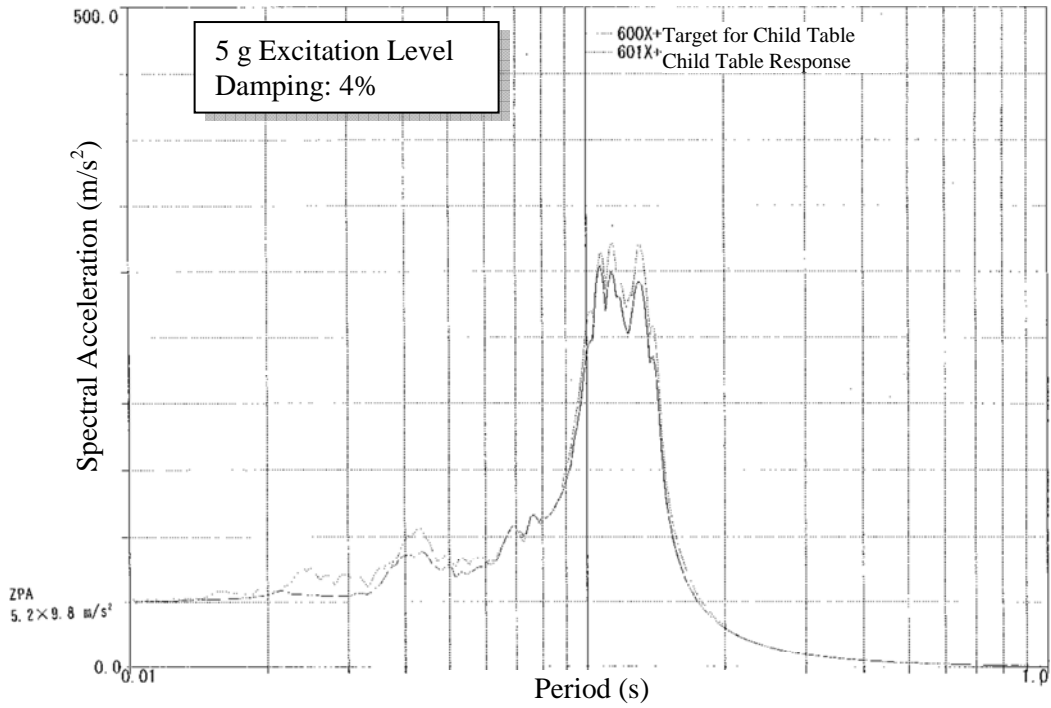


Figure B-4 Reactor Control Center Test – Child Table RS – 5 g (Back to Forth)

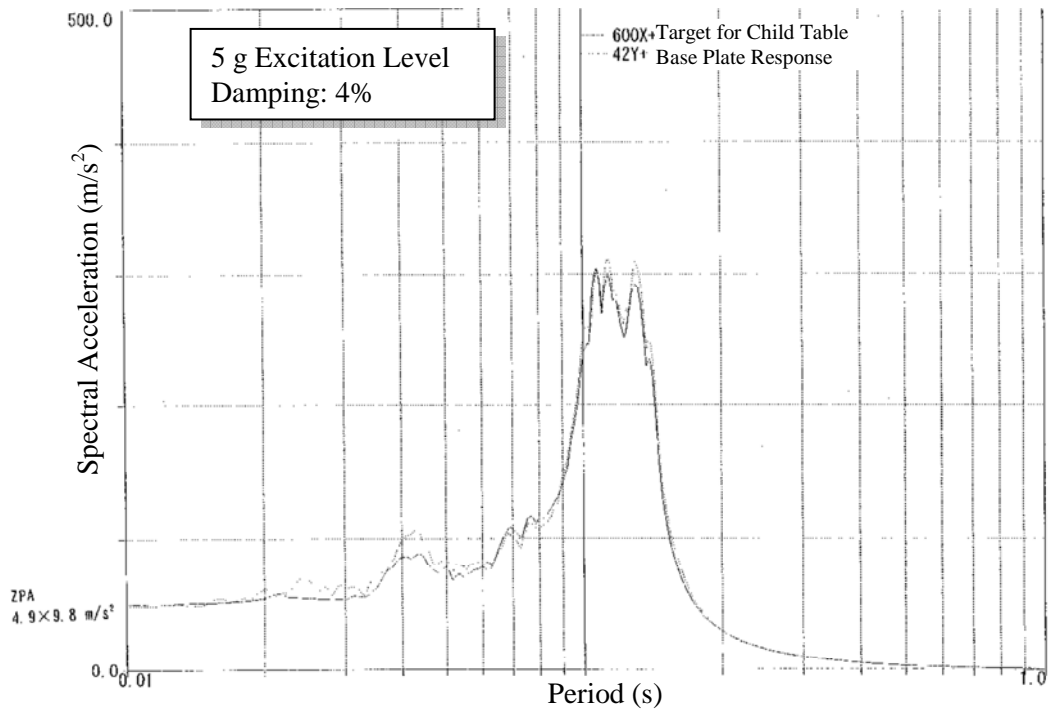


Figure B-5 Reactor Control Center Test – Base Plate RS – 5 g (Back to Forth)

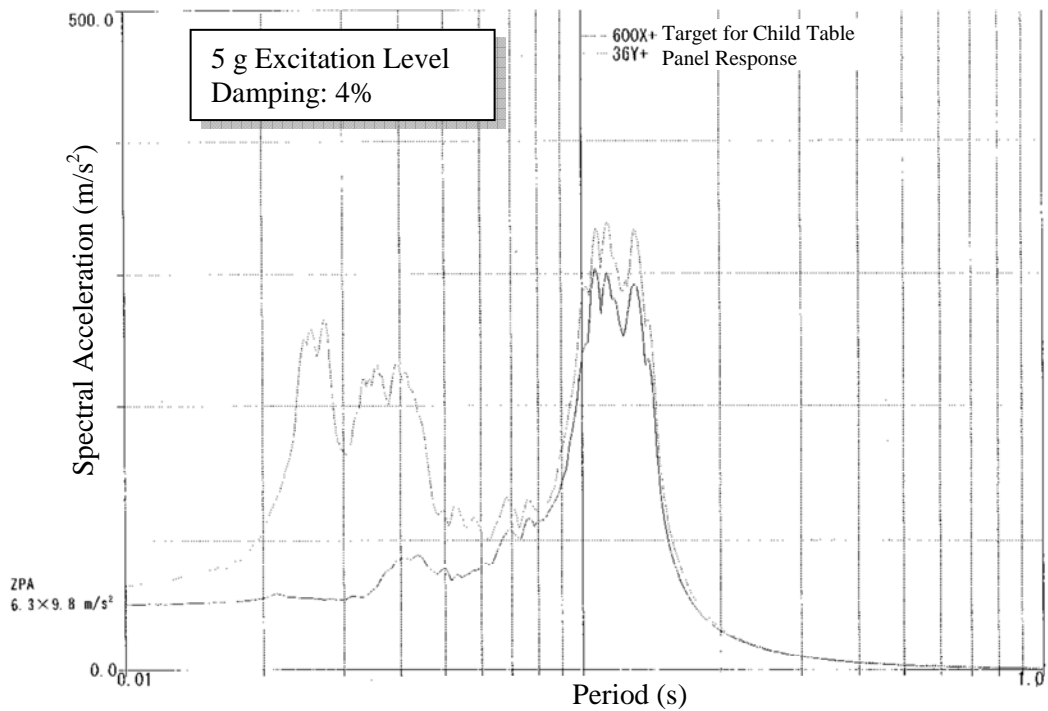


Figure B-6 Reactor Control Center Test – Panel RS at the Installation Point of Magnetic Contactor – 5 g (Back and Forth)

B.1.2 Power Center

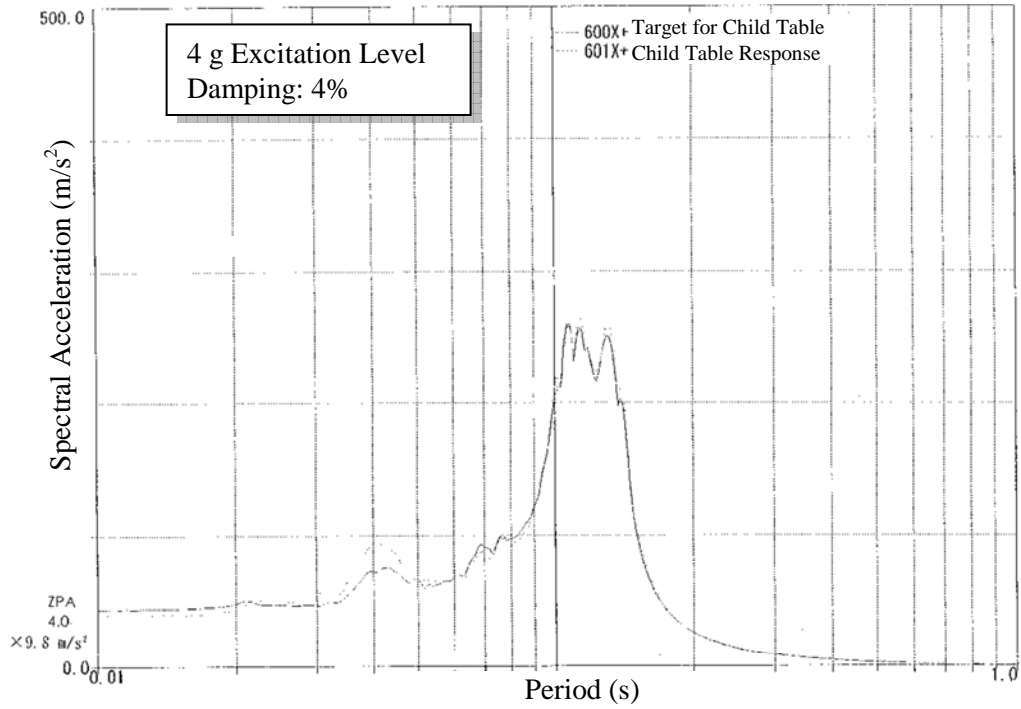


Figure B-7 Power Center Test – Child Table RS – 4 g (Side to Side)

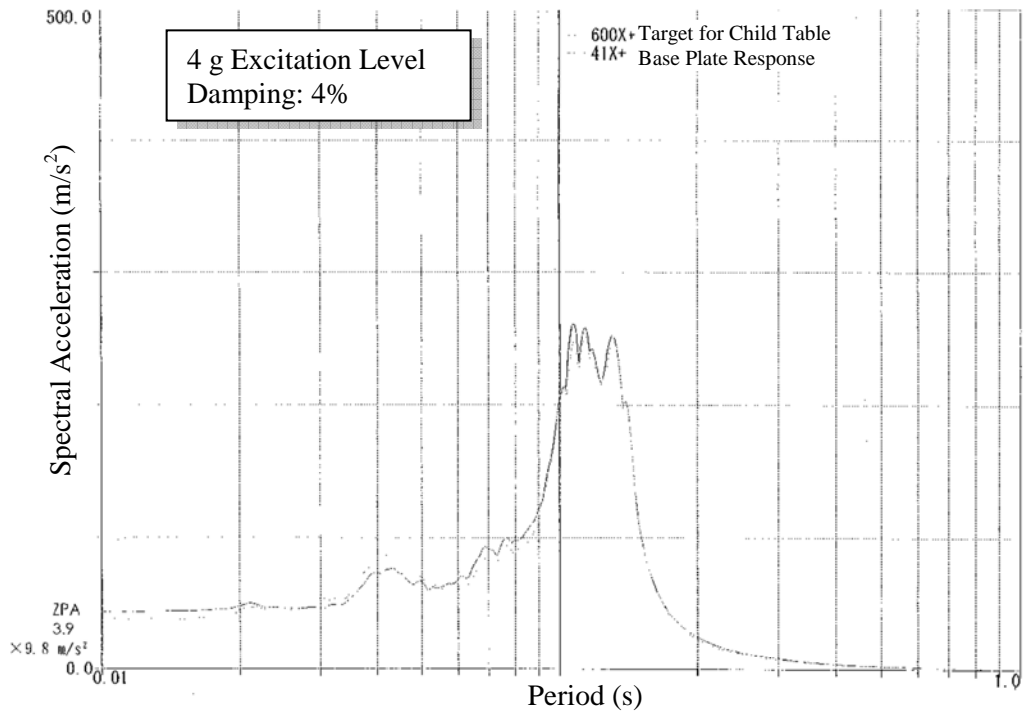


Figure B-8 Power Center Test – Base Plate RS – 4 g (Side to Side)

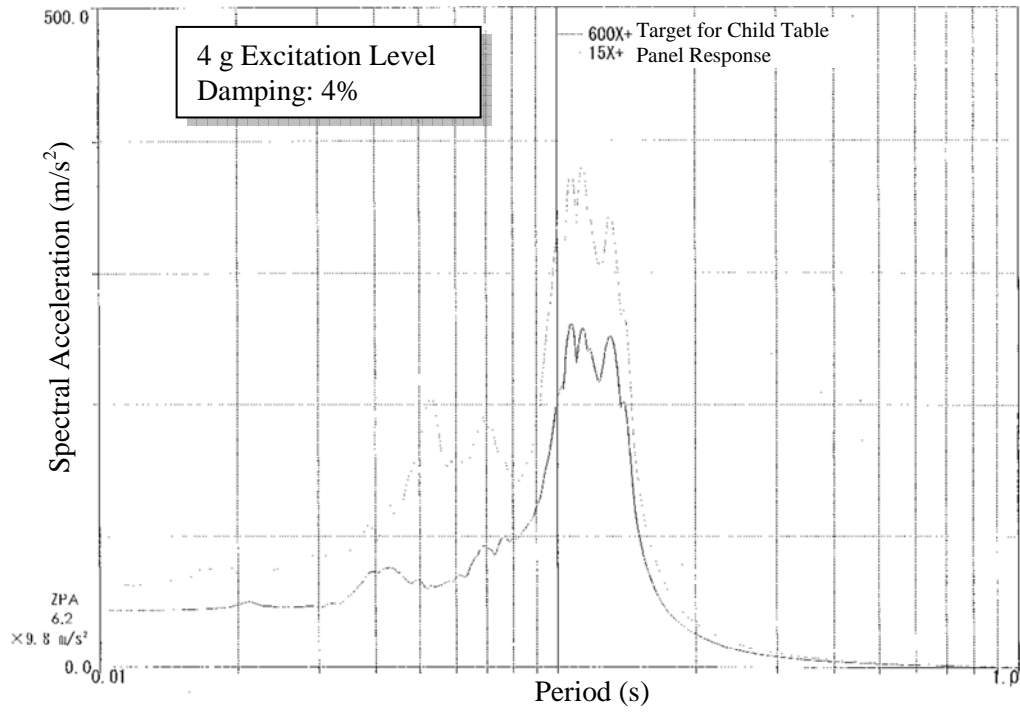


Figure B-9 Power Center Test – Panel RS at the Installation Point of the Ratio Differential Relay
– 4 g (Side to Side)

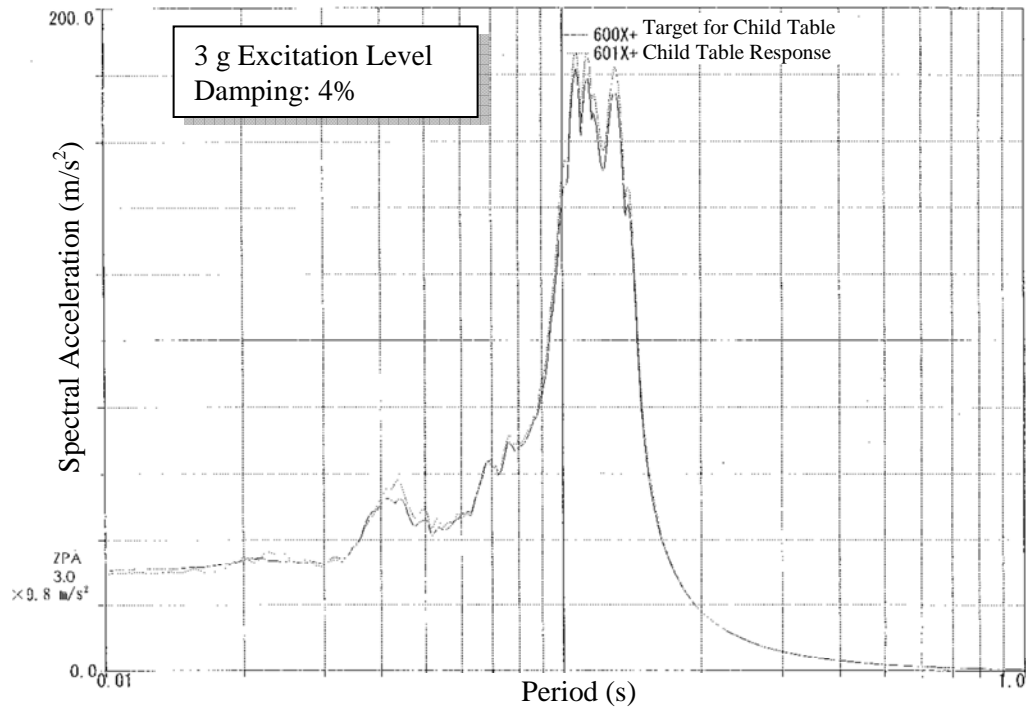


Figure B-10 Power Center Test – Child Table RS – 3 g (Back and Forth)

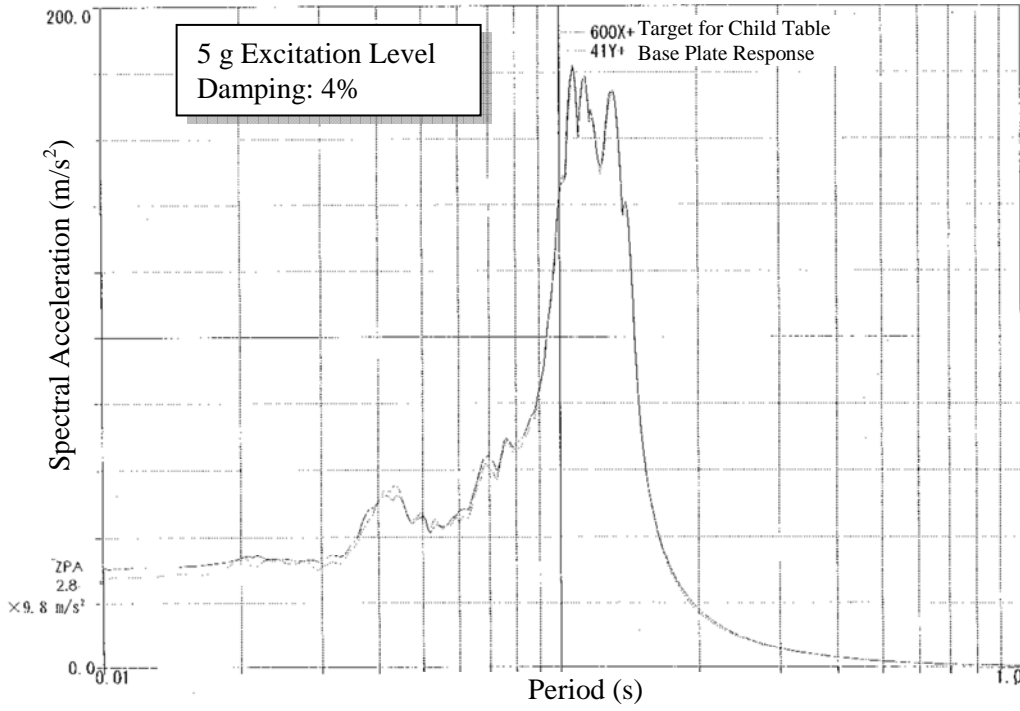


Figure B-11 Power Center Test – Base Plate RS – 3 g (Back and Forth)

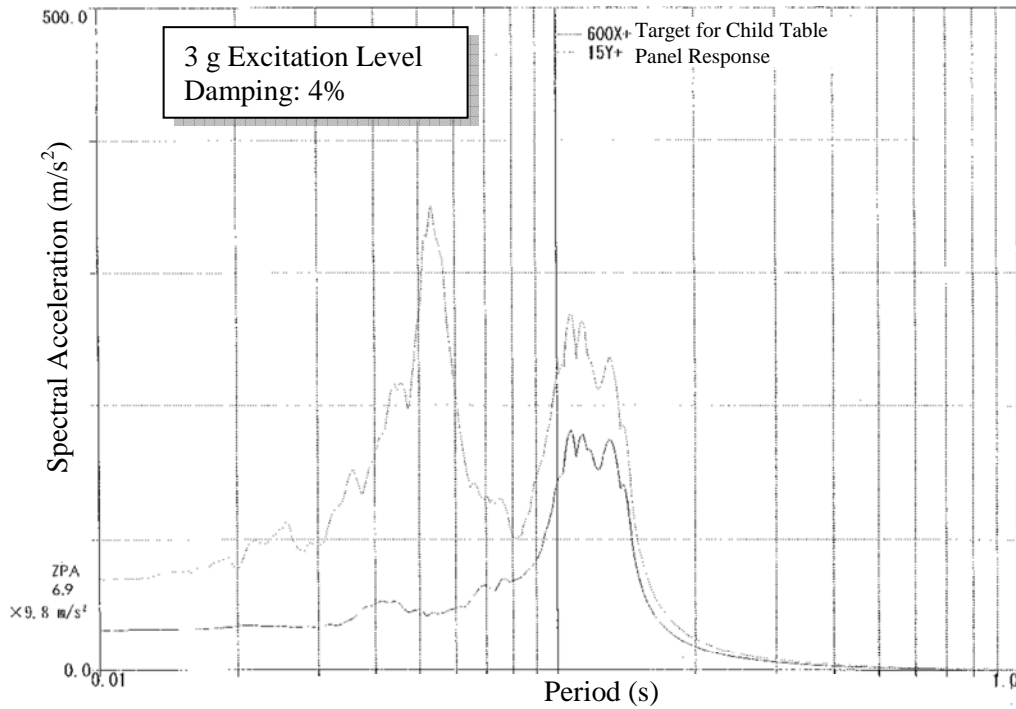


Figure B-12 Power Center Test – Panel RS at the Installation Point of the Ratio Differential Relay – 3 g (Back and Forth)

B.1.3 Device Tests

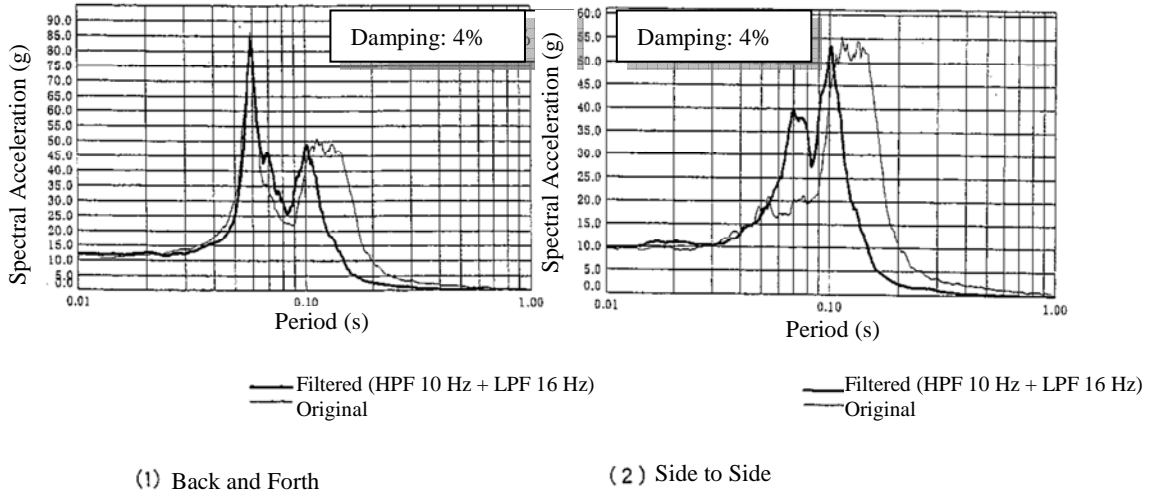


Figure B-13 Ratio Differential Relay (MELCO TUB-2-D)

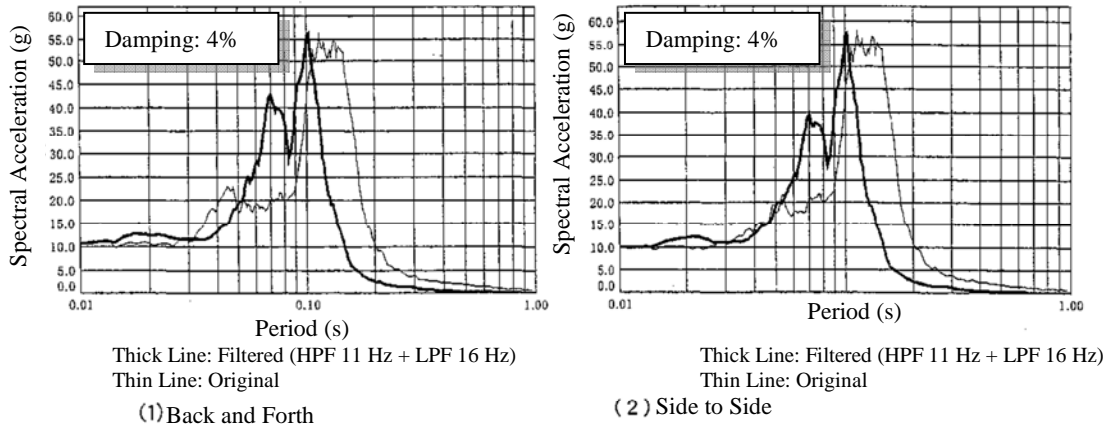
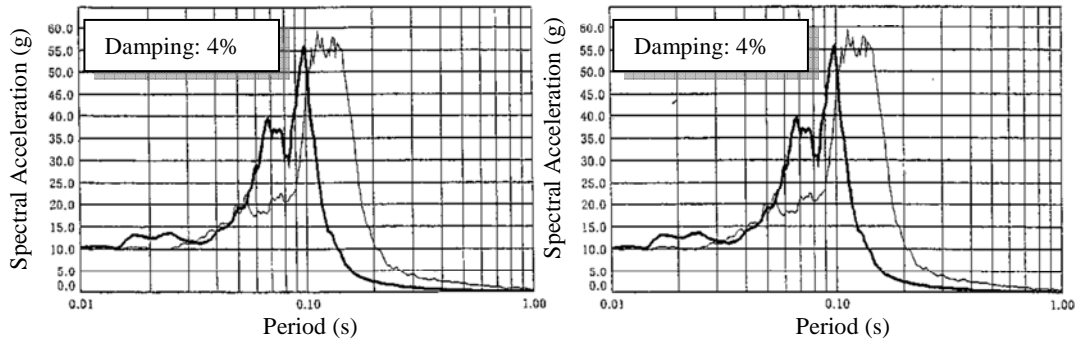


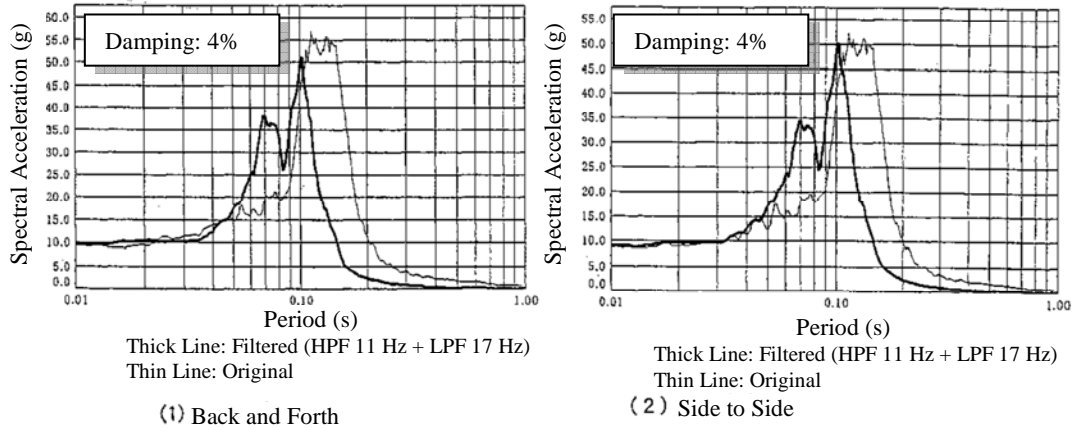
Figure B-14 Over Current Relay (MELCO CO-18-D)



(1) Back and Forth

(2) Side to Side

Figure B-15 Auxiliary Relay (MELCO NRD-81)



(1) Back and Forth

(2) Side to Side

Figure B-16 Comparator Card (MELCO HALN)

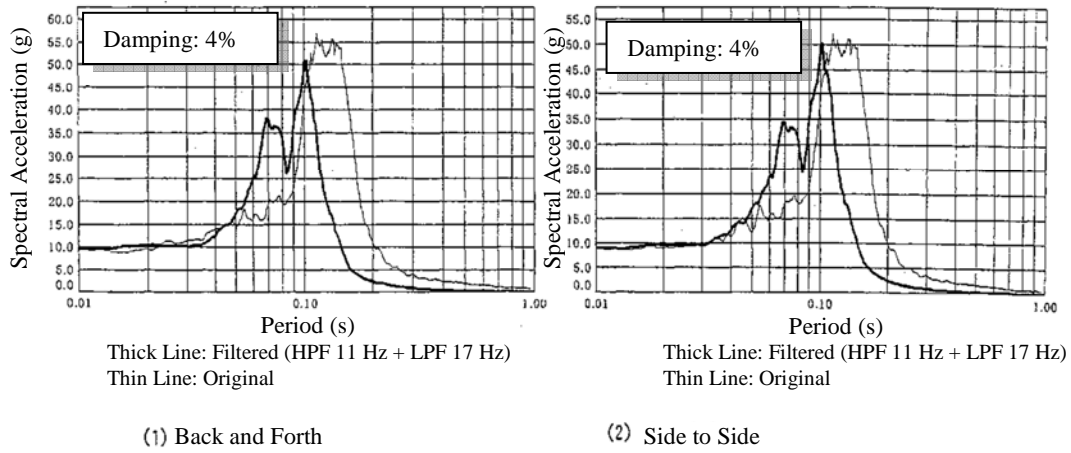


Figure B-17 AC Controller Card (MELCO HASN)

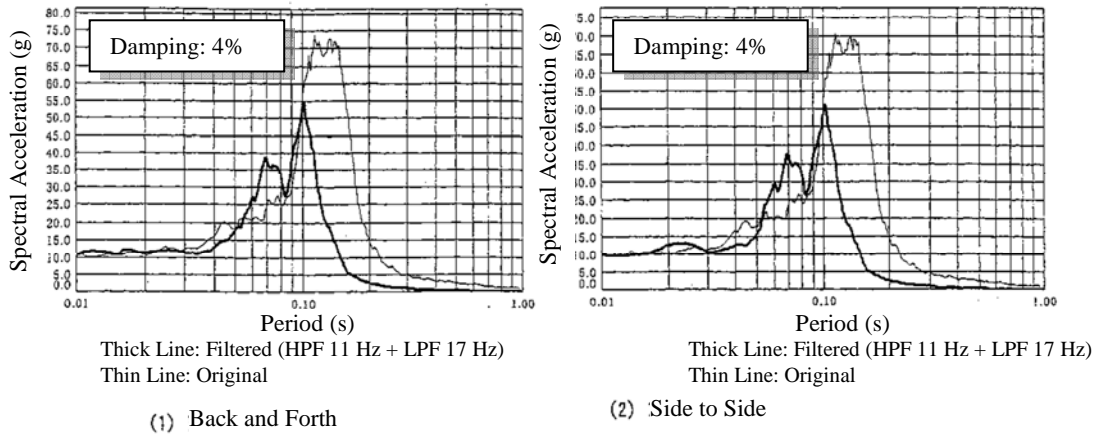
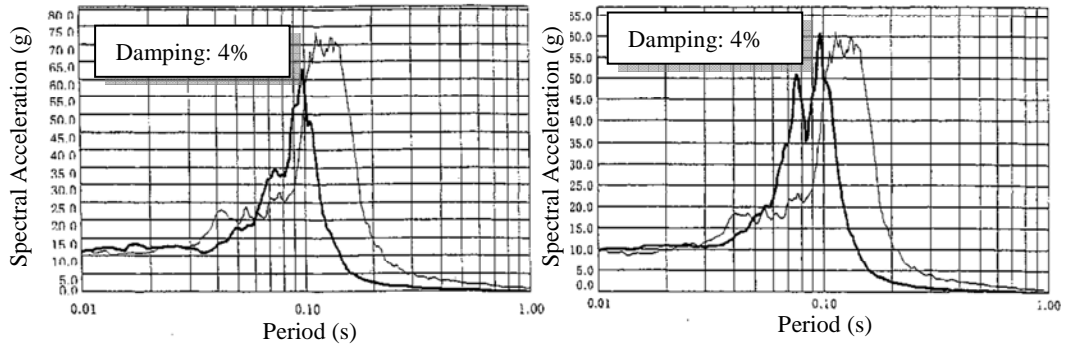


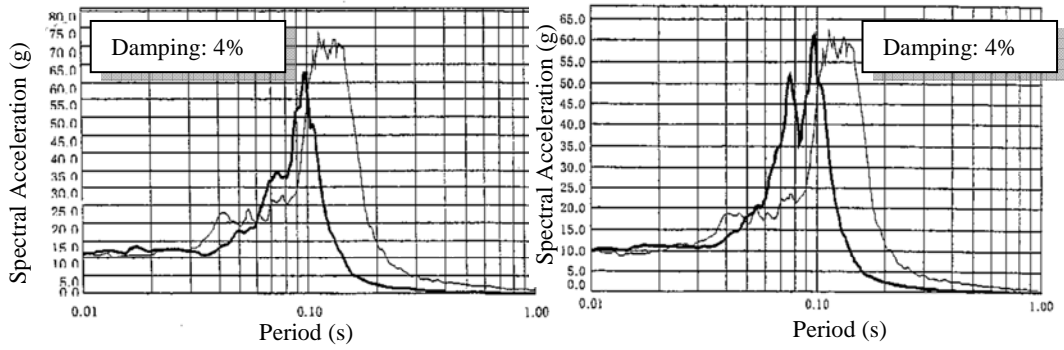
Figure B-18 Power Supply Equipment (MELCO -)



(1) Back and Forth

(2) Side to Side

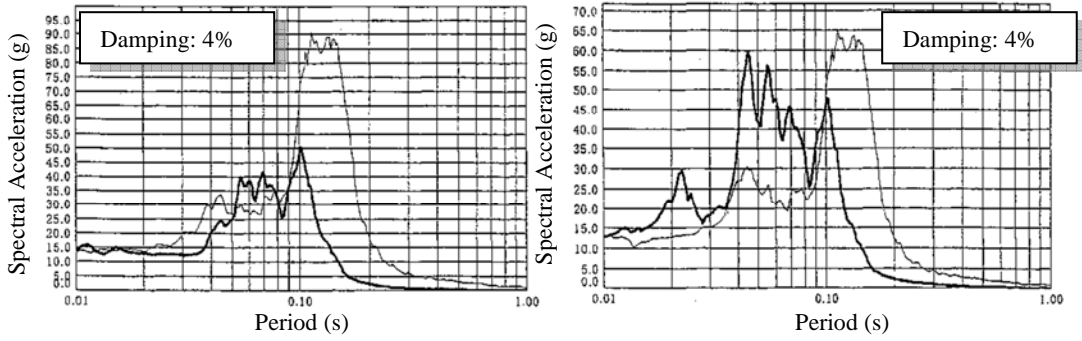
Figure B-19 Magnetic Contactor (MELCO MSO-A80)



(1) Back and Forth

(2) Side to Side

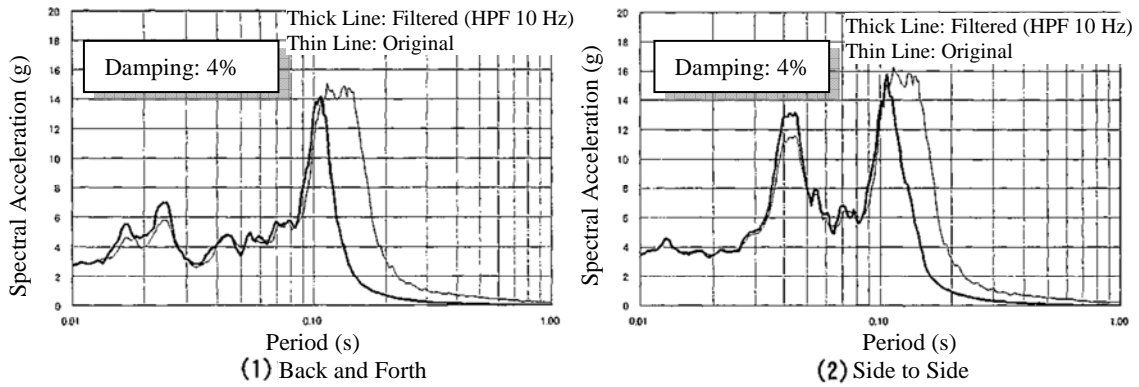
Figure B-20 Breaker for Wiring (MELCO NF-100-SH)



(1) Back and Forth

(2) Side to Side

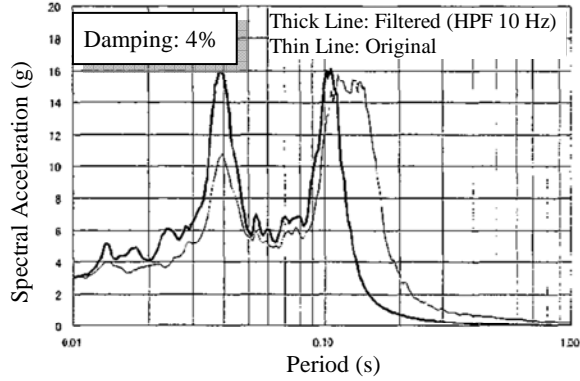
Figure B-21 Module Switch (MELCO SSA-SD3-53)



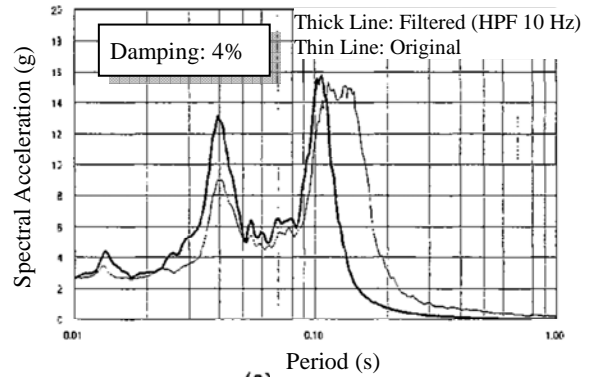
(1) Back and Forth

(2) Side to Side

Figure B-22 Over Current Relay (Toshiba VCR520) and Auxiliary Relay (Toshiba UP3A)

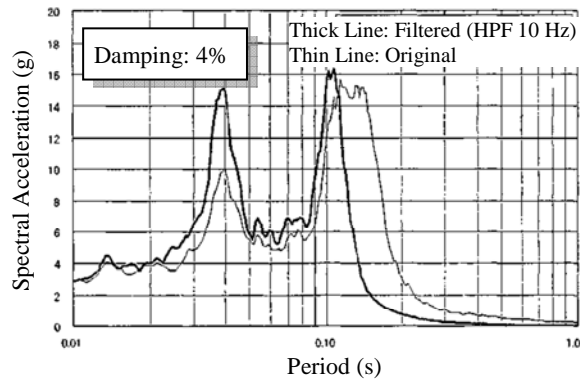


(1) Back and Forth

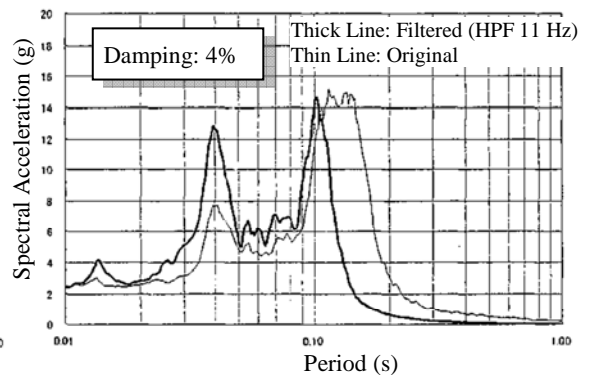


(2) Side to Side

Figure B-23 Controller (Toshiba TOSMAP)



(1) Back and Forth



(2) Side to Side

Figure B-24 I/O Unit (Toshiba TOSMAP)

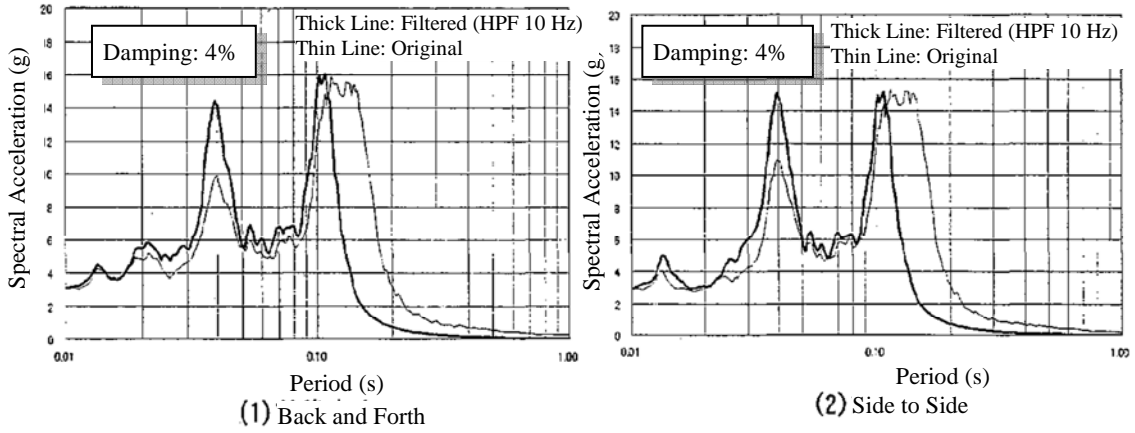


Figure B-25 Power Supply Equipment (Toshiba TFV)

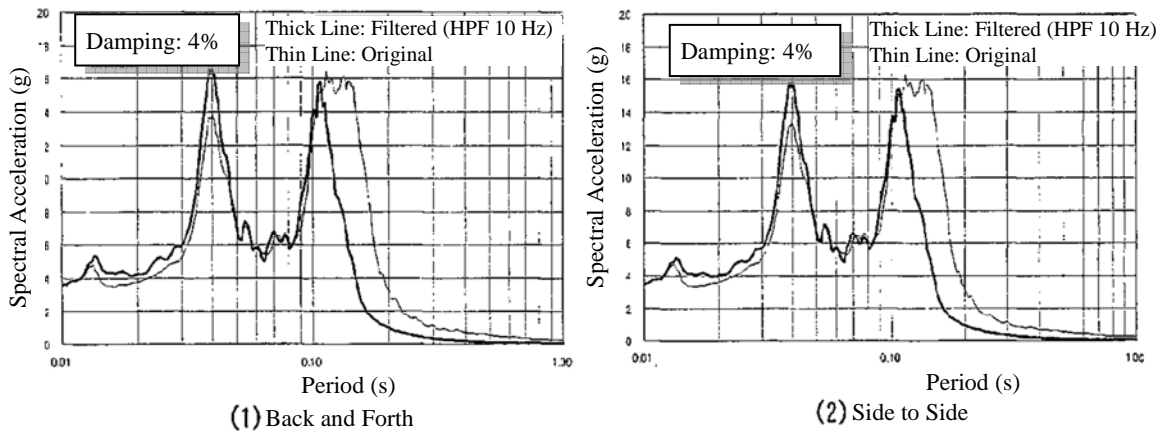


Figure B-26 Differential Pressure Transmitter (Toshiba AP3107)

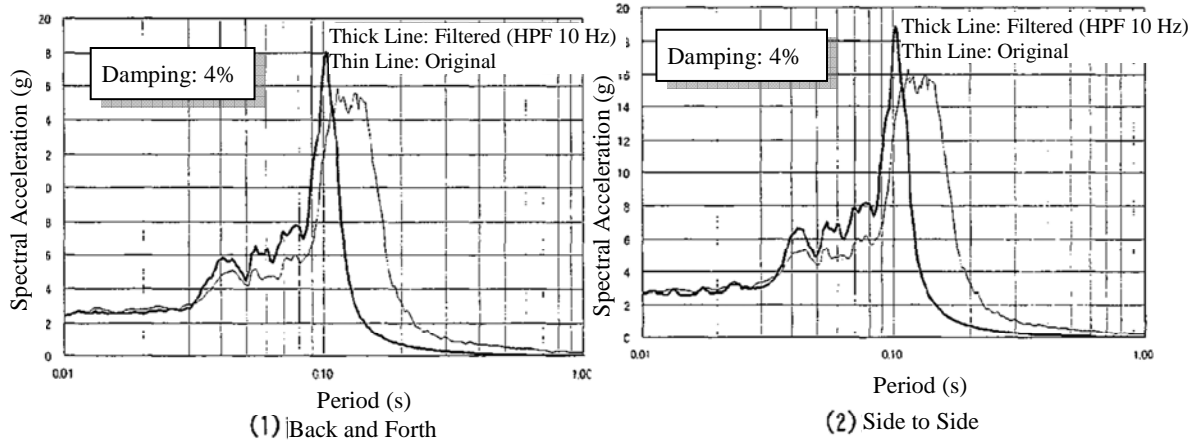


Figure B-27 Magnetic Contactor (Toshiba C-20J, T-20J) and Breaker for Wiring (Toshiba SH100)

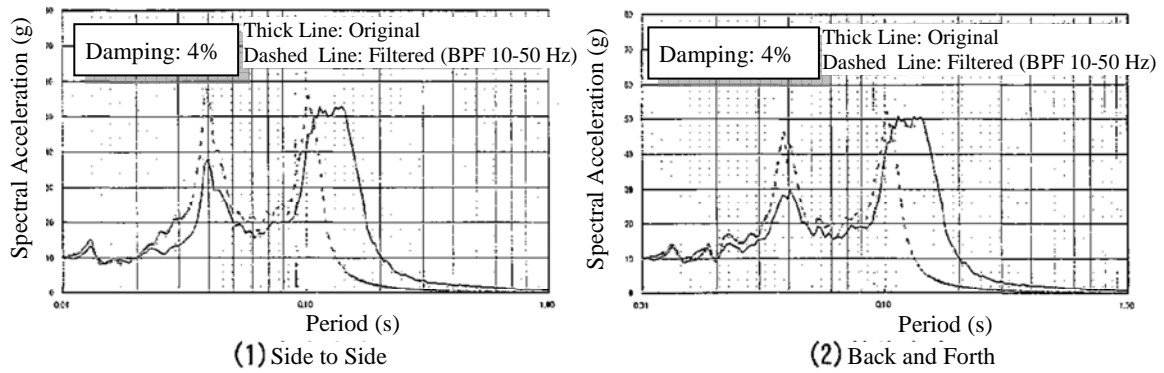


Figure B-28 Auxiliary Relay (HITACHI MY4Z), Timer (HITACHI H3M), and Breaker for Wiring (HITACHI F type)

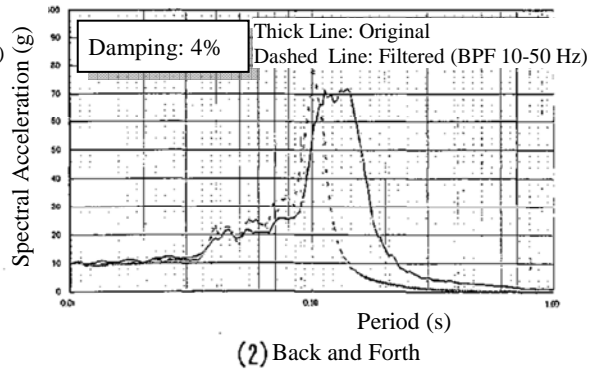
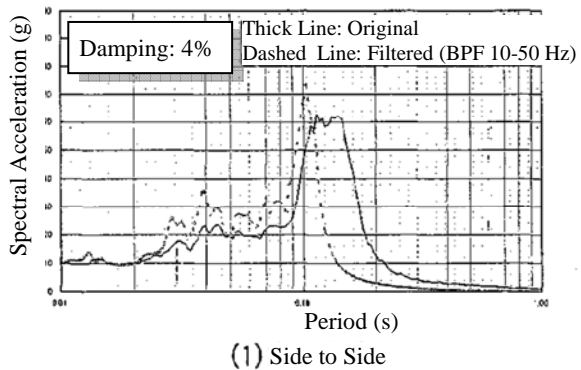


Figure B-29 Flat Display (HITACHI 18" type)

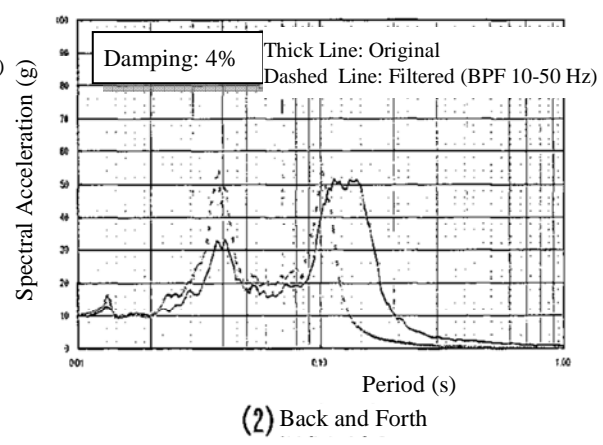
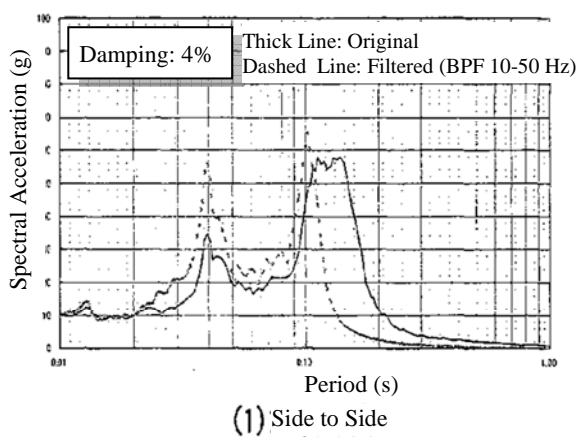
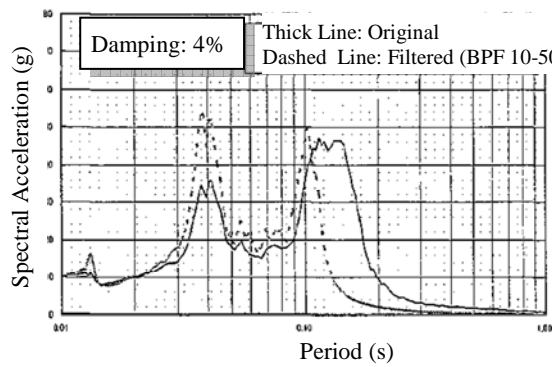
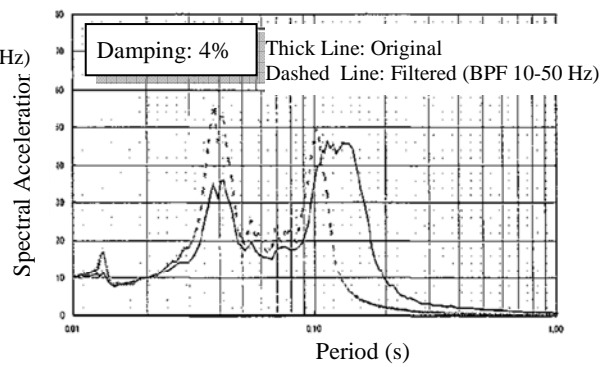


Figure B-30 Controller Display (HITACHI 18" type)

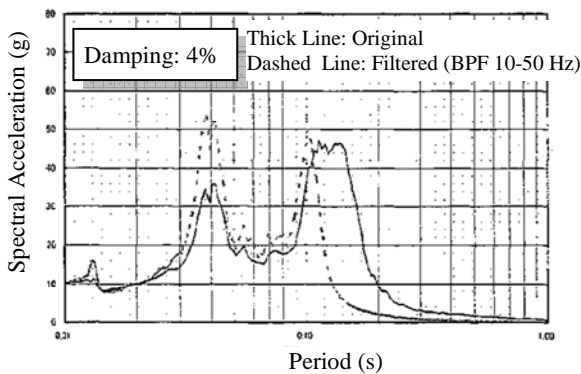


(1) Side to Side

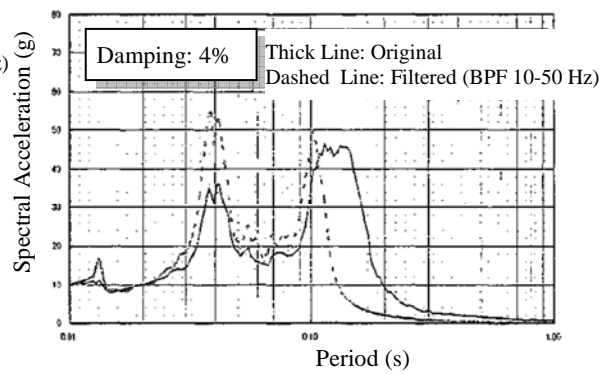


(2) Back and Forth

Figure B-31 Differential Pressure Transmitter (HITACHI EDR-N6)



(1) Side to Side



(2) Back and Forth

Figure B-32 Pressure Transmitter (HITACHI EPR-N6)

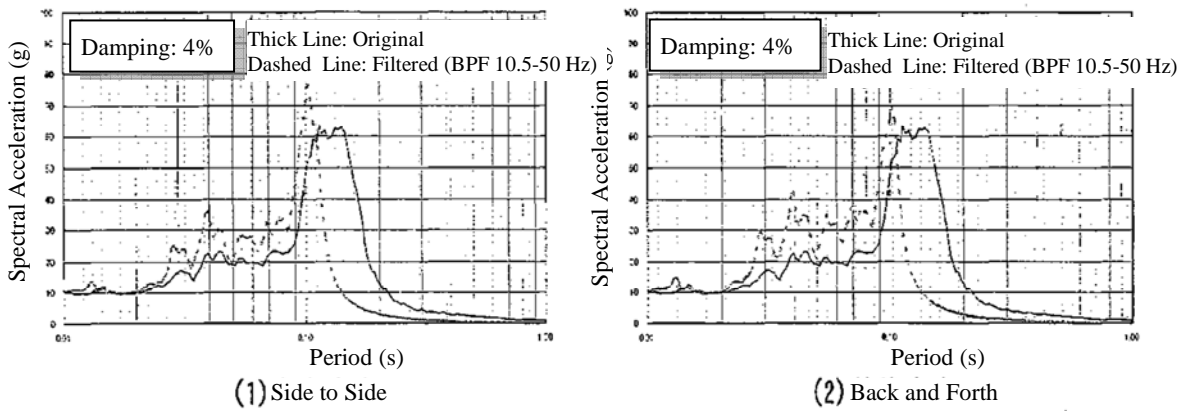


Figure B-33 Cam Type Switch (HITACHI MS type) and Key Switch (HITACHI ACSNK type)

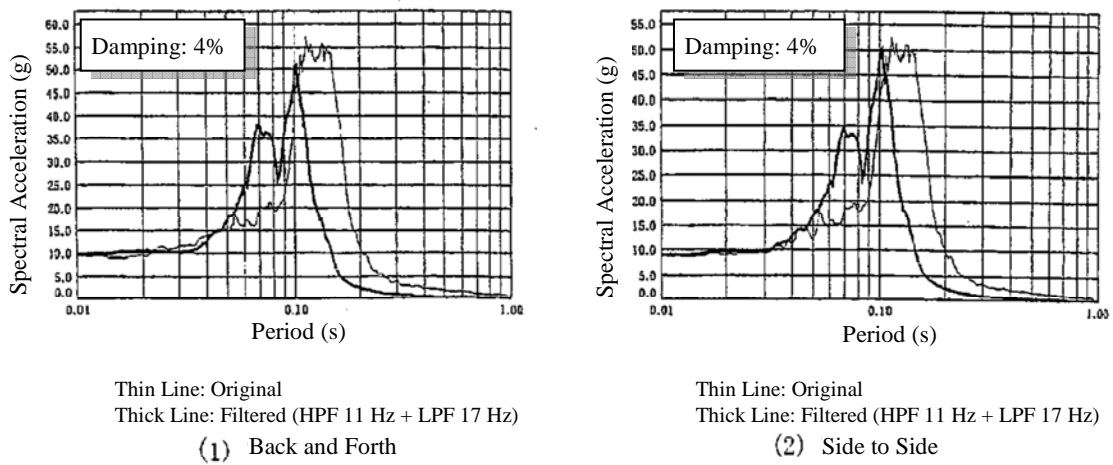
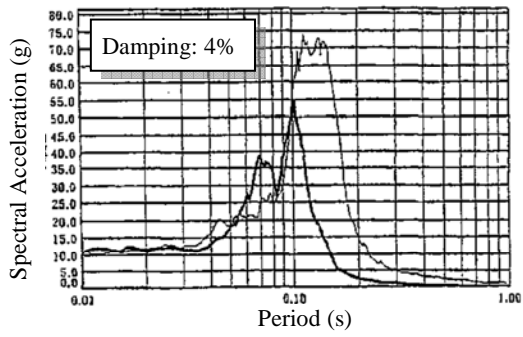
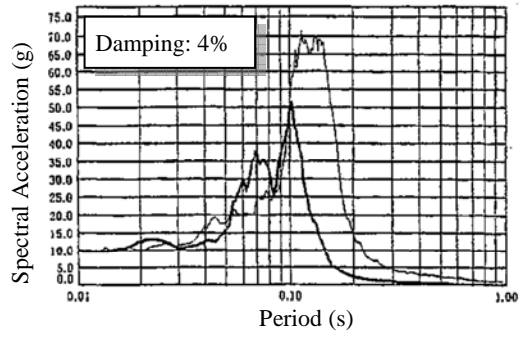


Figure B-34 Test Module (S9186AW), Power Supply Module (S9016AW), and Monitor Module (S9146AW), All Produced by Yokogawa Electric Co.



Thin Line: Original
 Thick Line: Filtered (HPF 11 Hz + LPF 17 Hz)

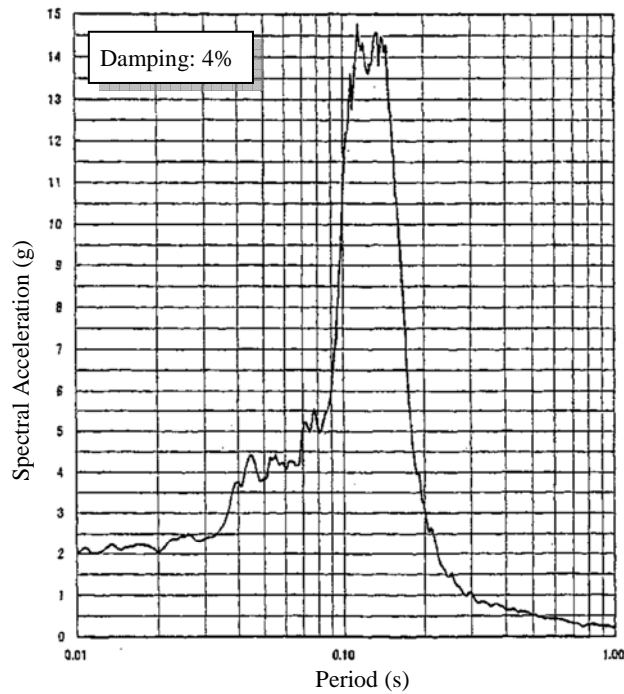
(1) Back and Forth



Thin Line: Original
 Thick Line: Filtered (HPF 11 Hz + LPF 18 Hz)

(2) Side to Side

Figure B-35 Power Supply Module (S9980UD), Produced by Yokogawa Electric Co.



Back and Forth / Side to side

This test was implemented later as reported in July 2004.

Figure B-36 Differential Pressure Transmitter (UNE13), Produced by Yokogawa Electric Co.

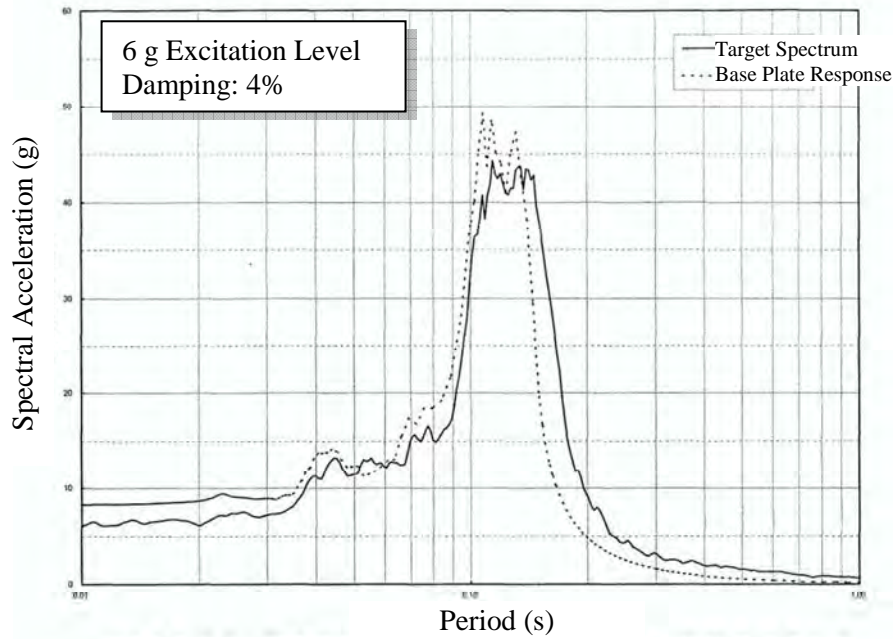
B.2 Response Spectra Reported in July 2004

These spectra were extracted from the JNES annotated fragility report dated July 2004. The title of that report in English is “Seismic Proving Test – Equipment Fragility Vol. 1 (Horizontal Shaft Pump and Electric Panels).” A total of 42 figures are included in this section.

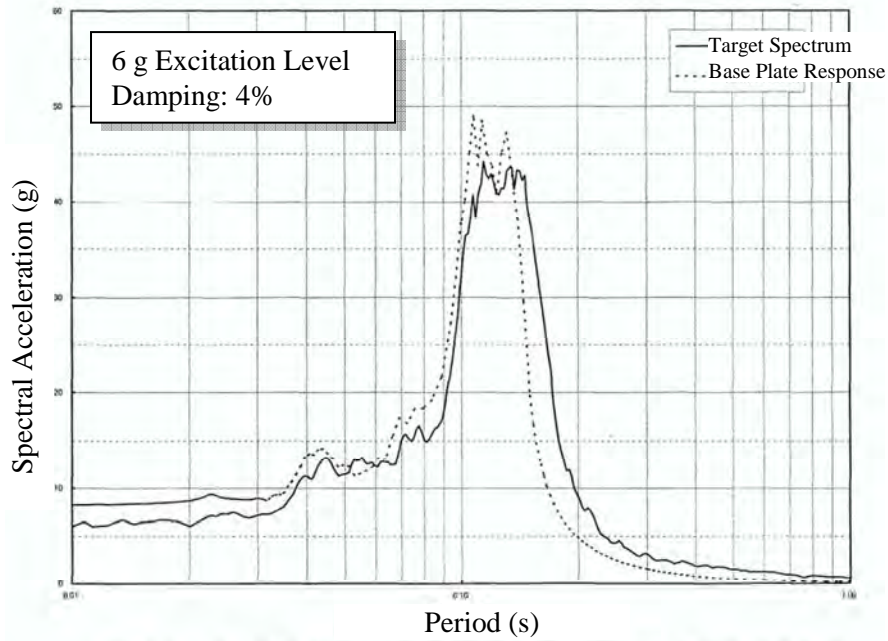
In the full scale tests of the electrical panels, the target spectrum was developed by enveloping Japanese PWR and BWR spectra. The synthesized input time history was adjusted by filtering out long period components (period > 0.14 s).

For device tests, both time histories obtained from the full scale panel/rack tests and time histories obtained from analysis were used.

B.2.1 Main Control Board

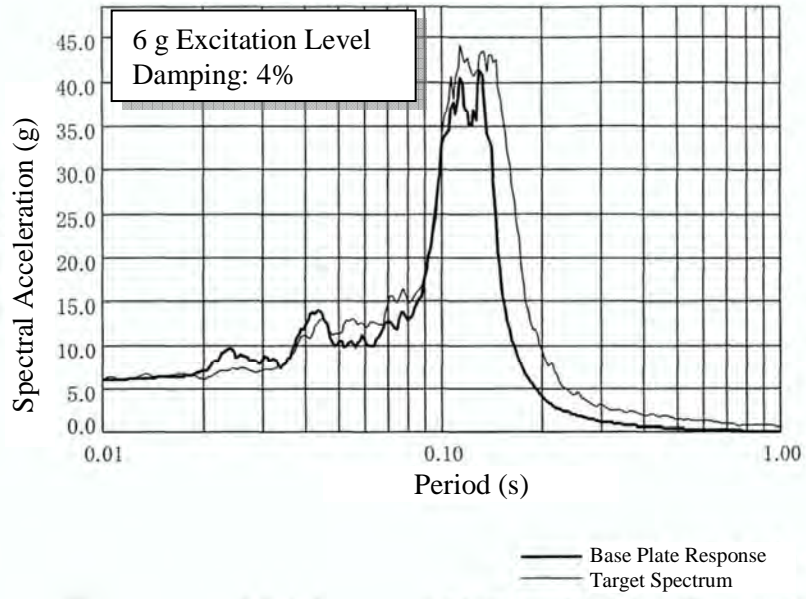


(A) Side to Side Direction

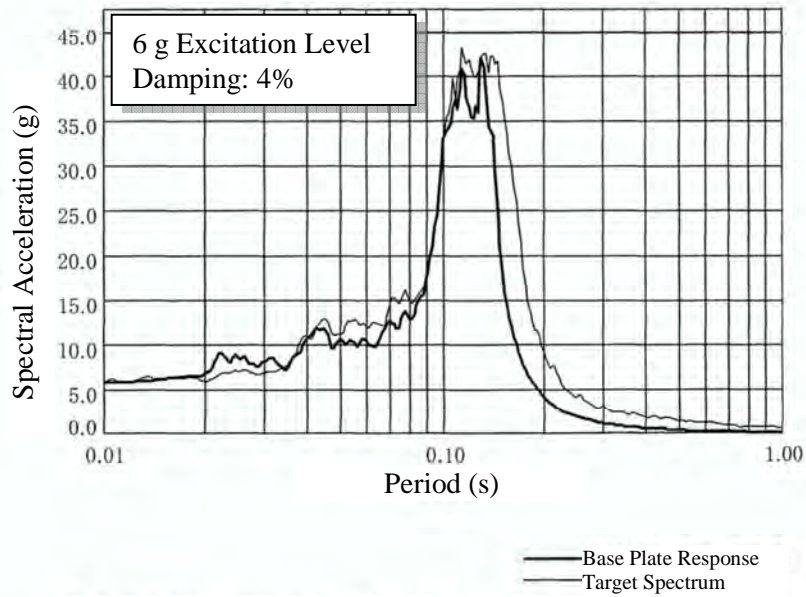


(B) Back and Forth Direction

Figure B-37 Main Control Board Test – Base Plate RS – 6 g



(A) Side to Side Direction



(B) Back and Forth Direction

Figure B-38 Reactor Auxiliary Panel – Base Plate RS – 6g

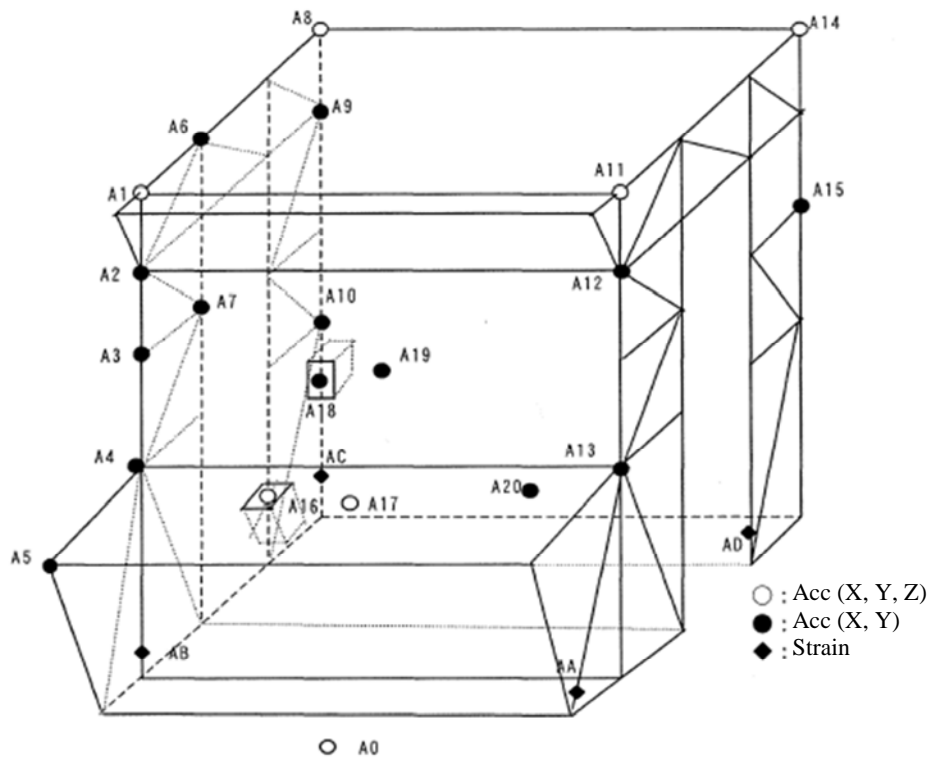


Figure B-39 Reactor Auxiliary Panel Sensor Location

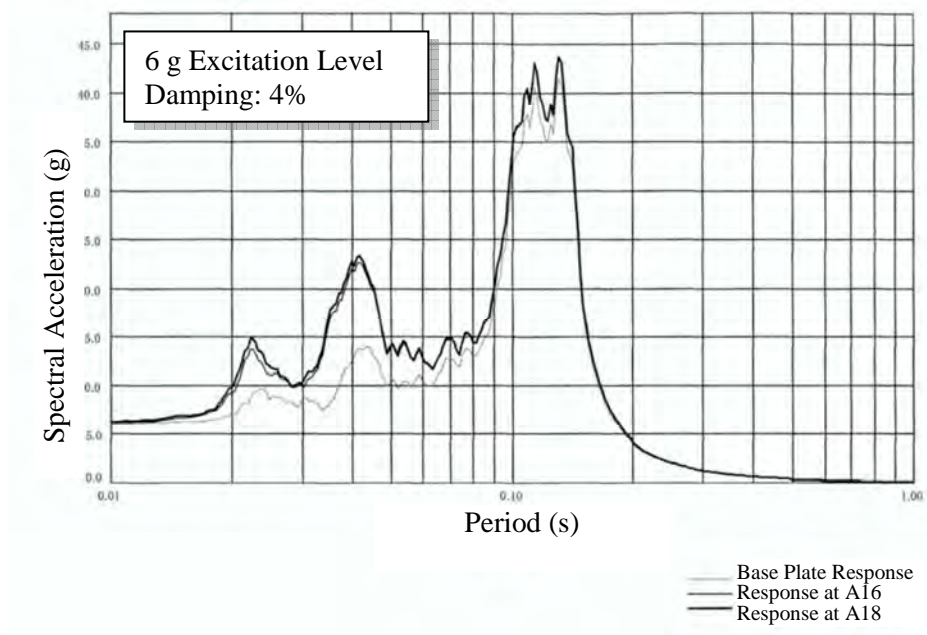


Figure B-40 Reactor Auxiliary Panel – Panel RS – 6 g (Side to Side)

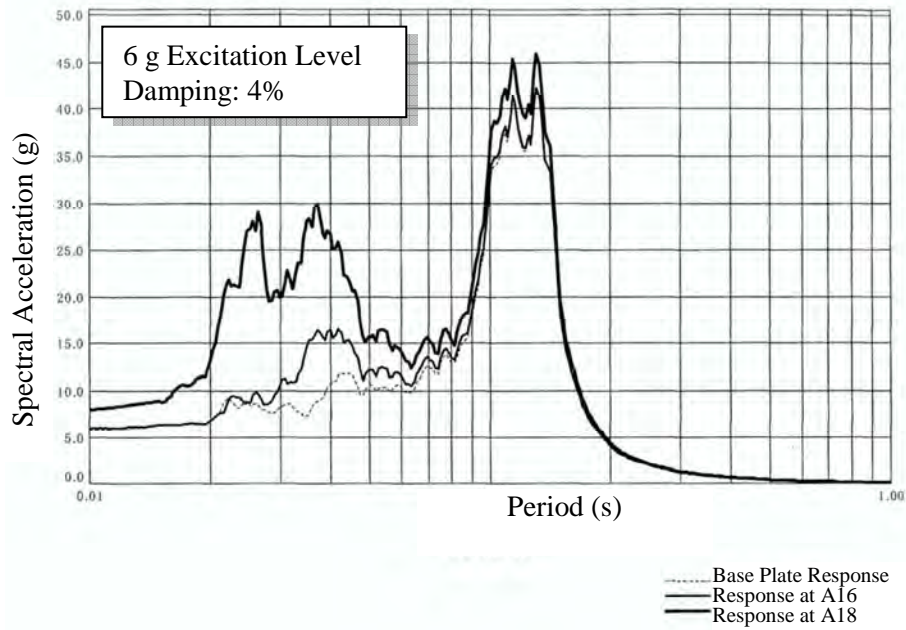
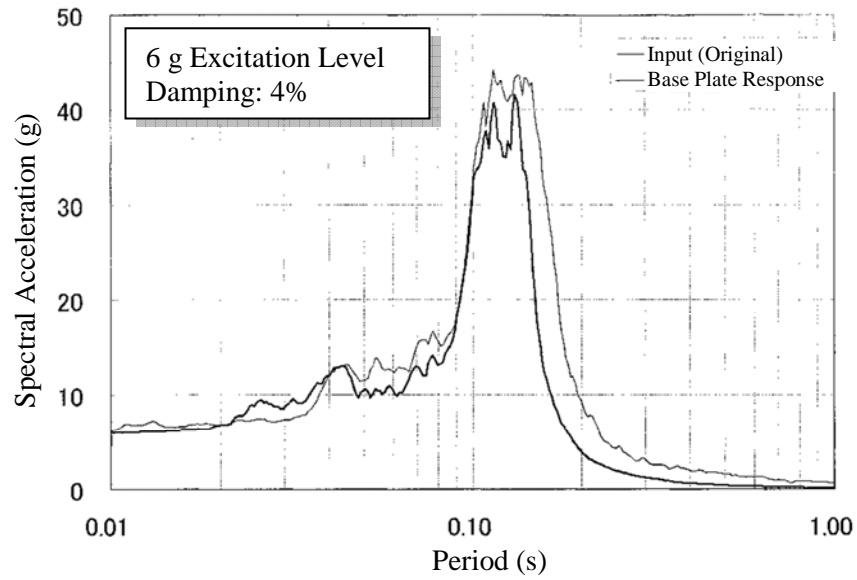
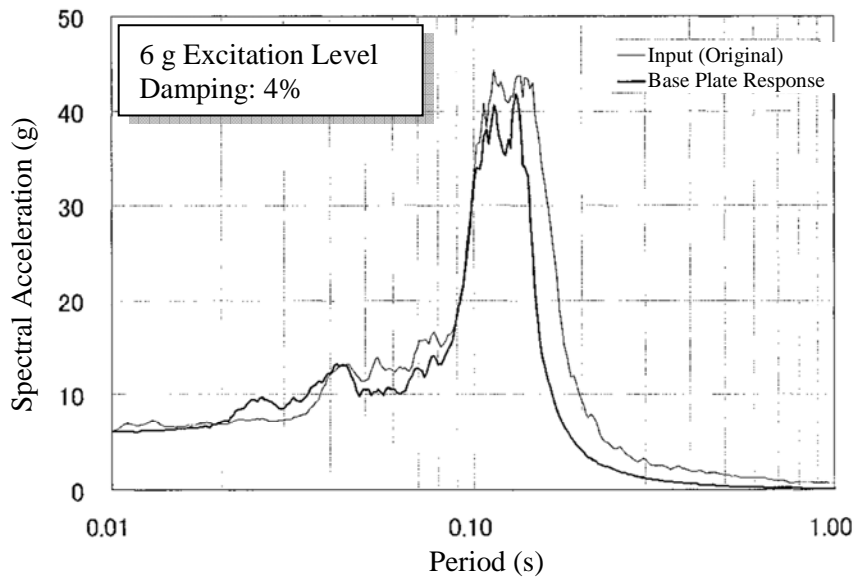


Figure B-41 Reactor Auxiliary Panel – Panel RS – 6 g (Back and Forth)

B.2.2 Logic Control Panel



(A) Back and Forth Direction



(B) Side to Side Direction

Figure B-42 Logic Control Panel – Base Plate RS – 6 g

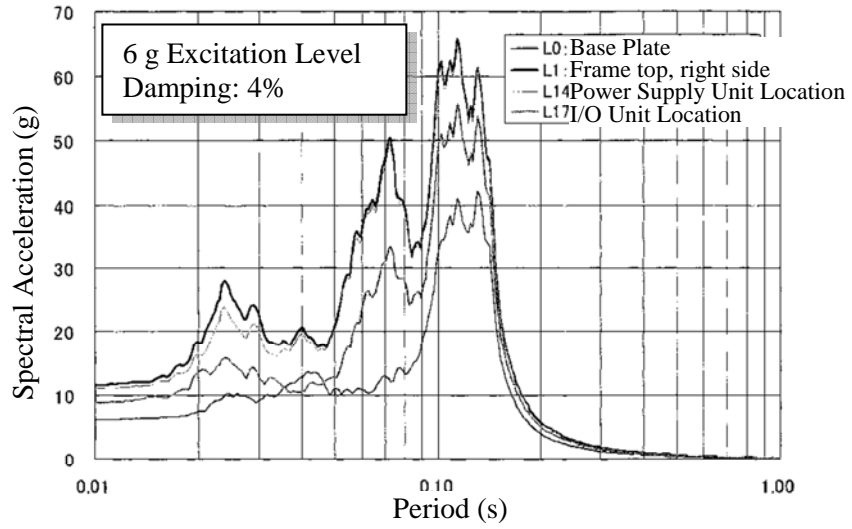


Figure B-43 Logic Control Panel – Panel RS – 6 g (Side to Side)

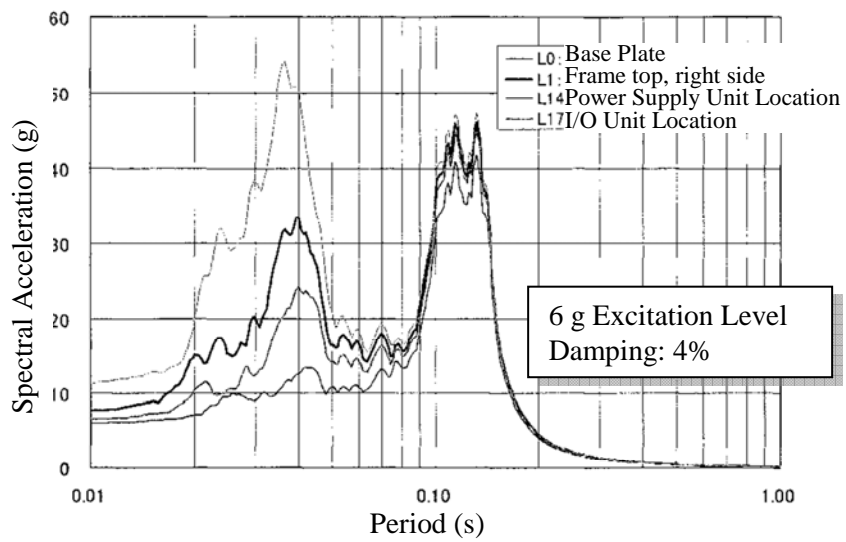


Figure B-44 Logic Control Panel – Panel RS – 6 g (Back and Forth)

B.2.3 Protection Instrument Rack

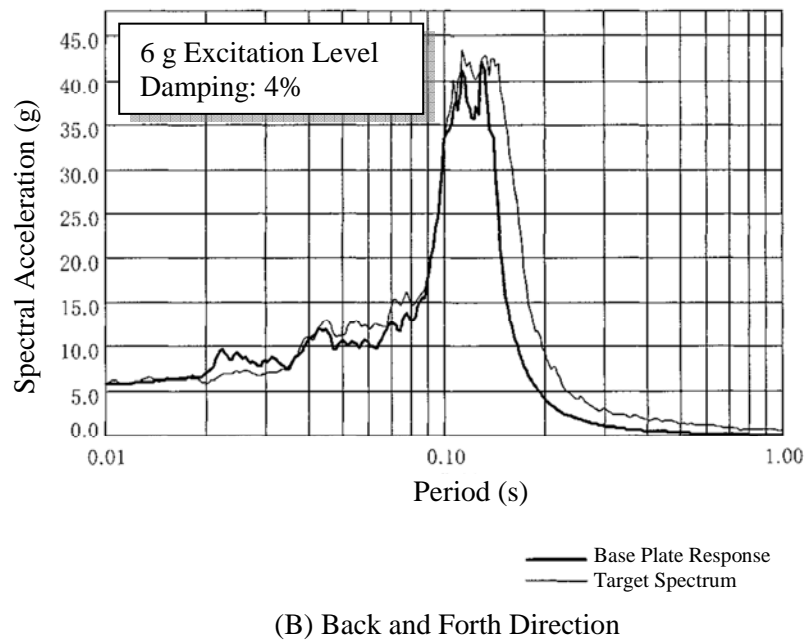
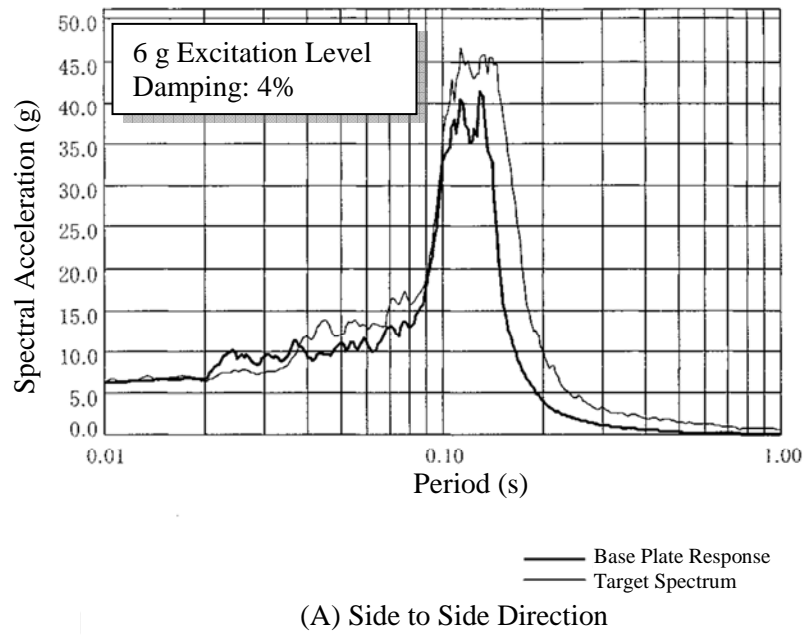


Figure B-45 Protection Instrument Rack – Base Plate RS – 6 g

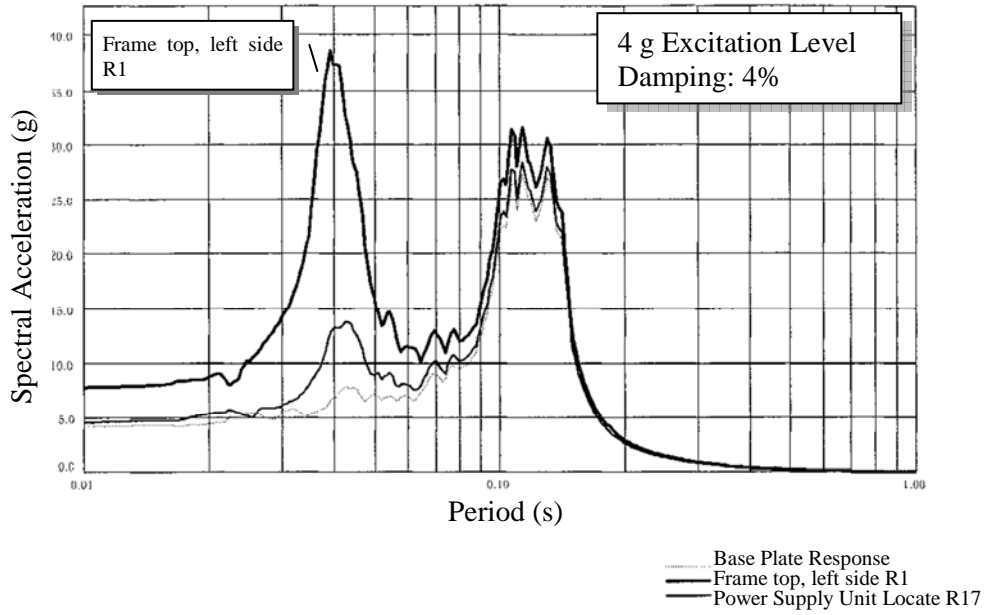


Figure B-46 Protection Instrument Rack – Rack RS – 4 g (Side to Side)

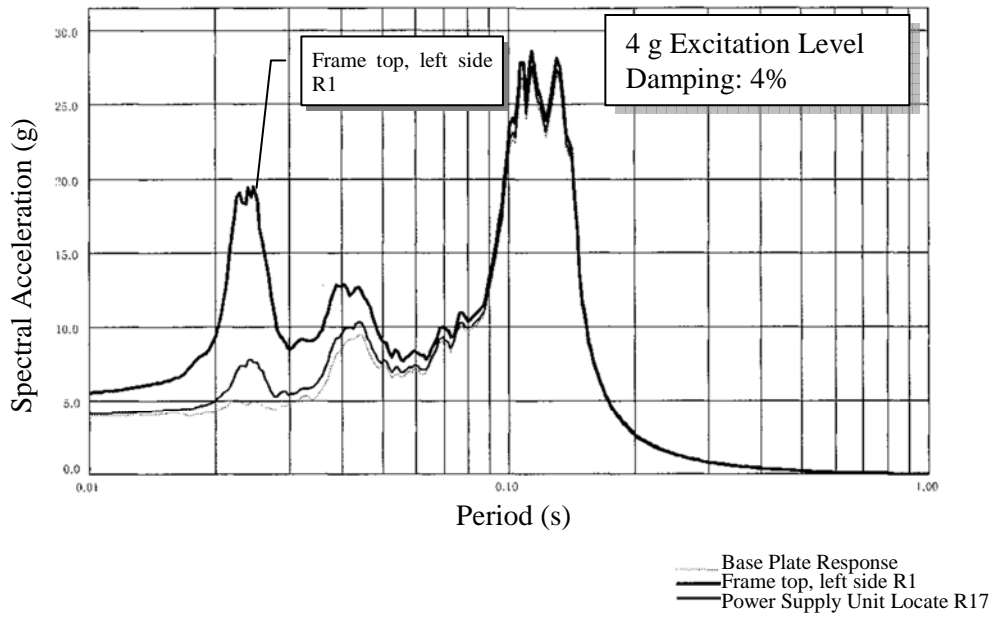


Figure B-47 Protection Instrument Rack – Rack RS – 4 g (Back and Forth)

The AC controller card installed in the Protection Instrument Rack malfunctioned at a 4 g input excitation in the side to side direction, which resulted in a 7.62 g at the installation point of the AC controller card. The component tests reported in September 2003 utilized analytical responses. The AC controller card was re-tested using the recorded response of the full scale Protection Instrument Rack. The following two RS's were for the investigation of the function limit capacity of the AC controller card.

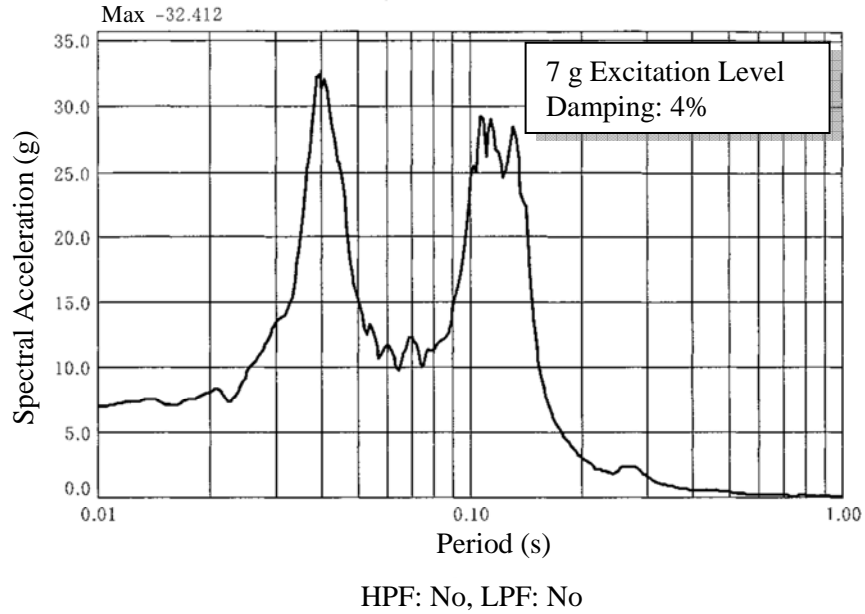


Figure B-48 AC Controller Card – 7 g Excitation (Non-malfunction)

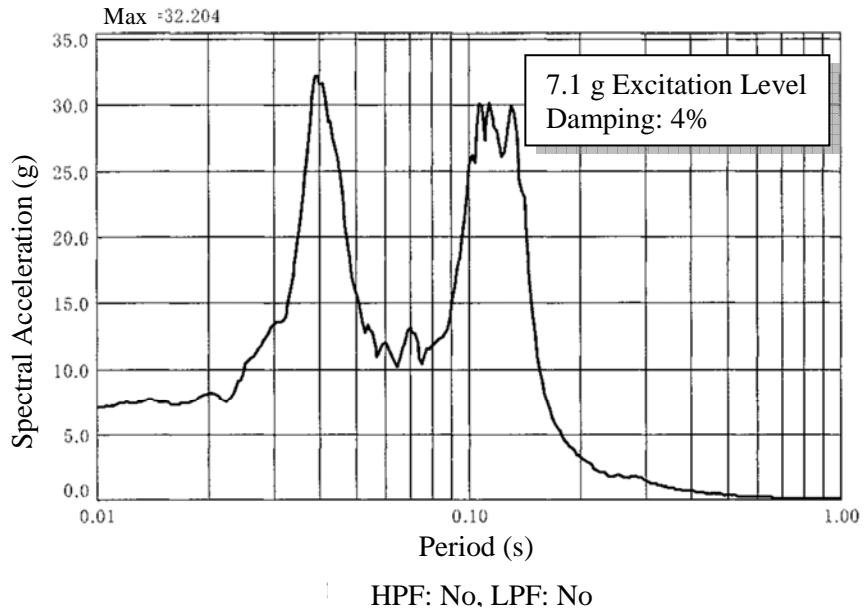
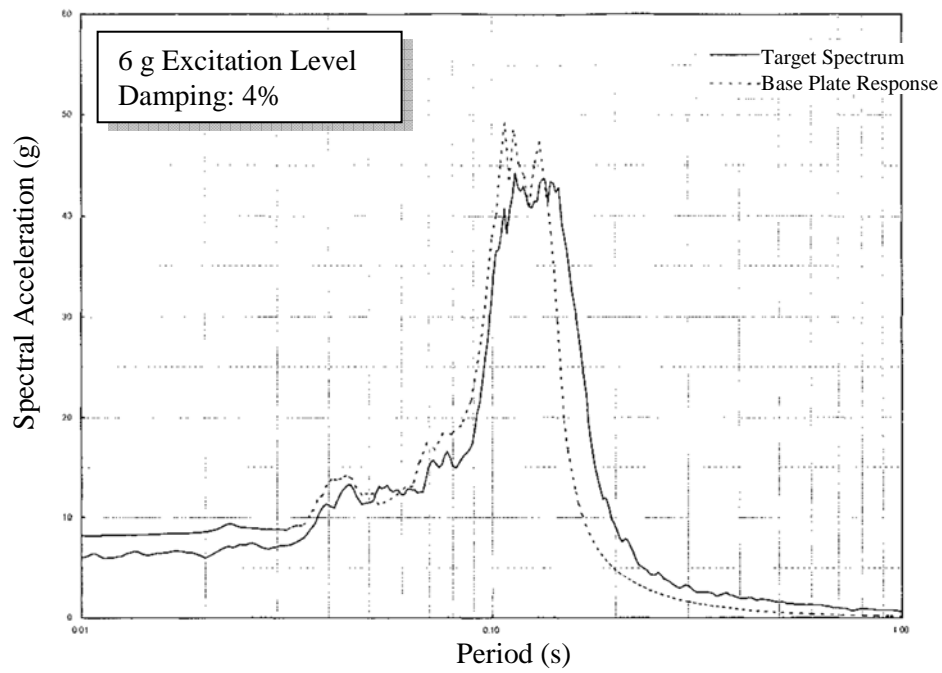
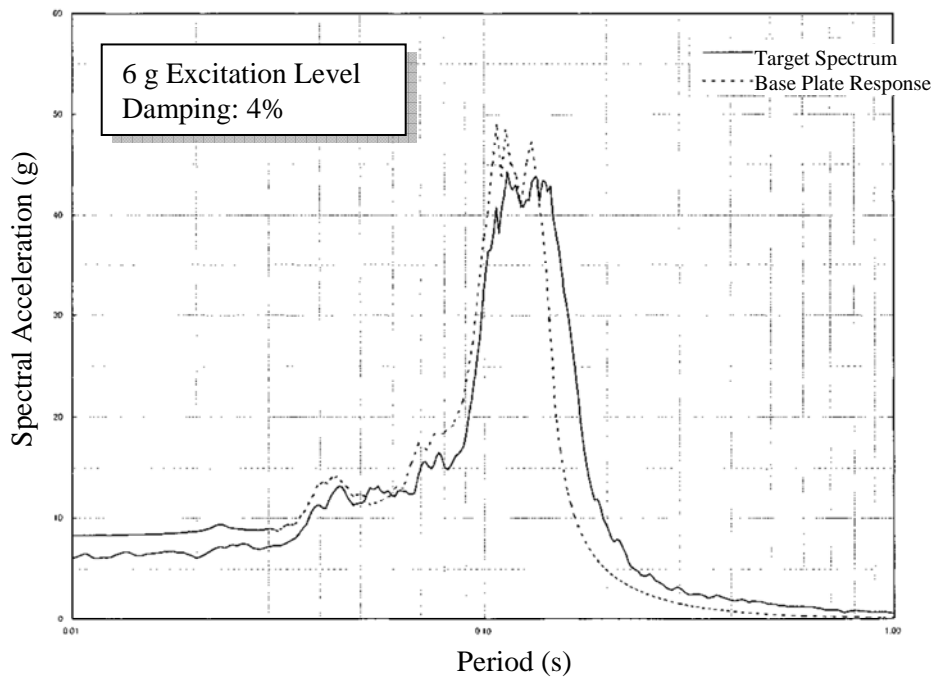


Figure B-49 AC Controller Card – 7.1 g Excitation (Malfunction)

B.2.4 Instrument Rack



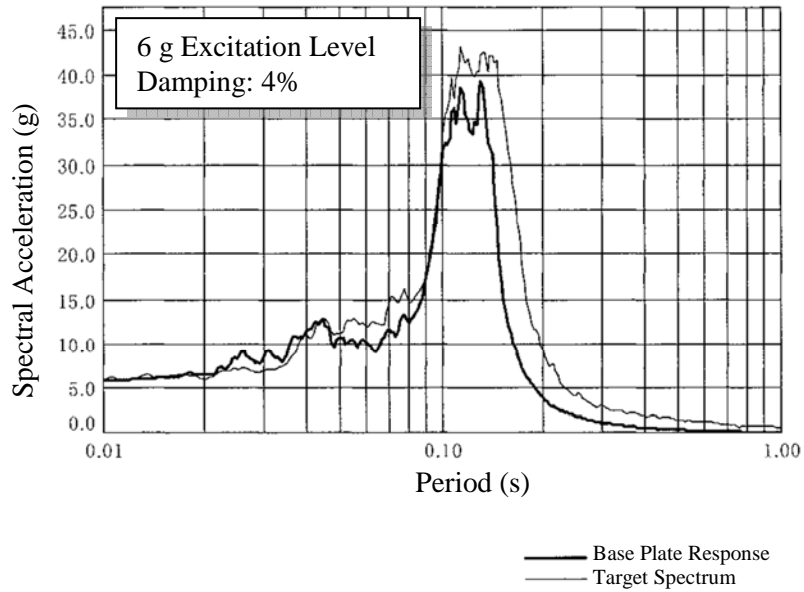
(A) Side to Side Direction



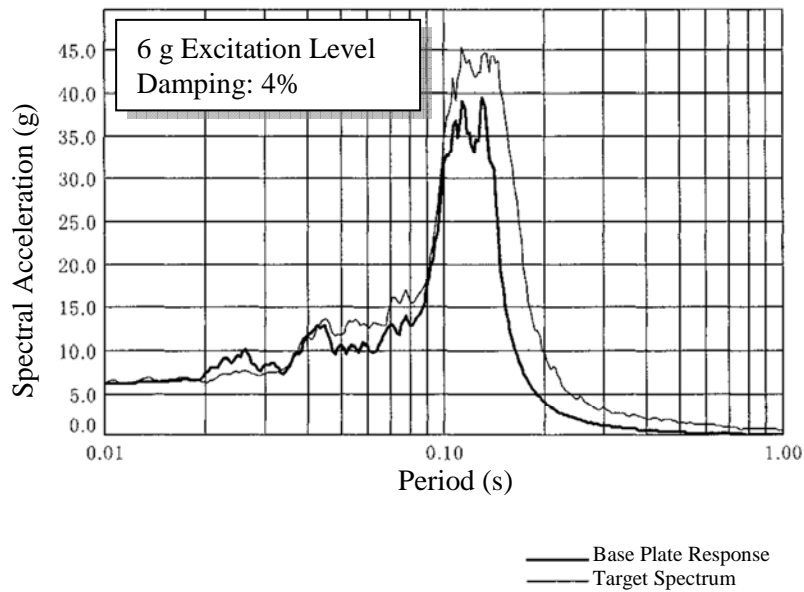
(B) Back and Forth Direction

Figure B-50 Instrument Rack – Base Plate RS – 6 g

B.2.5 Reactor Control Center



(A) Side to Side Direction



(B) Back and Forth Direction

Figure B-51 Reactor Control Center – Base Plate RS – 6 g

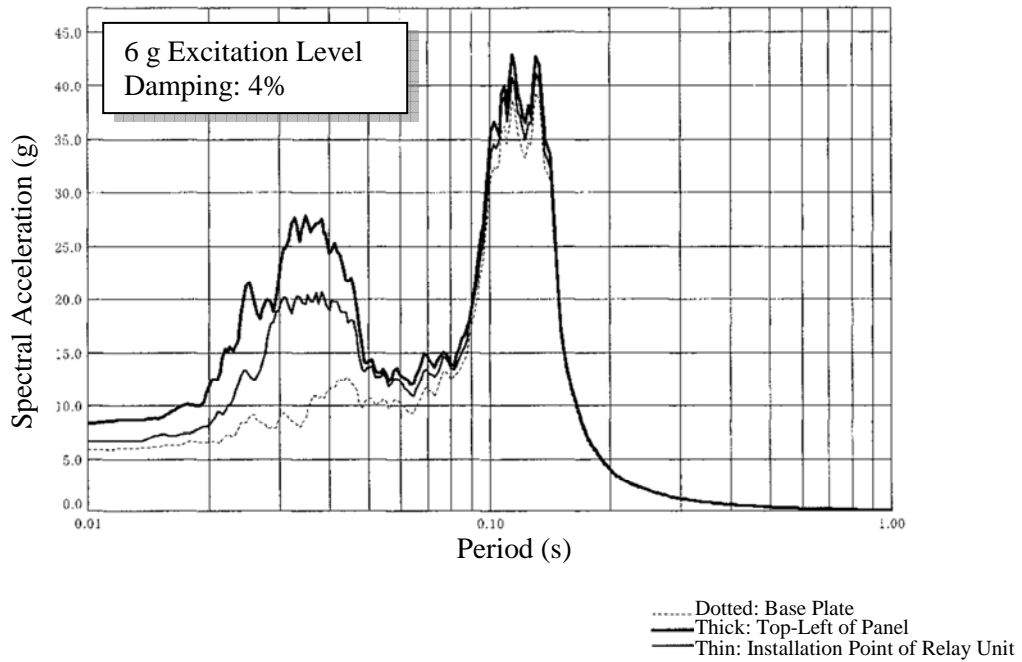


Figure B-52 Reactor Control Center – Panel RS – 6 g (Side to Side)

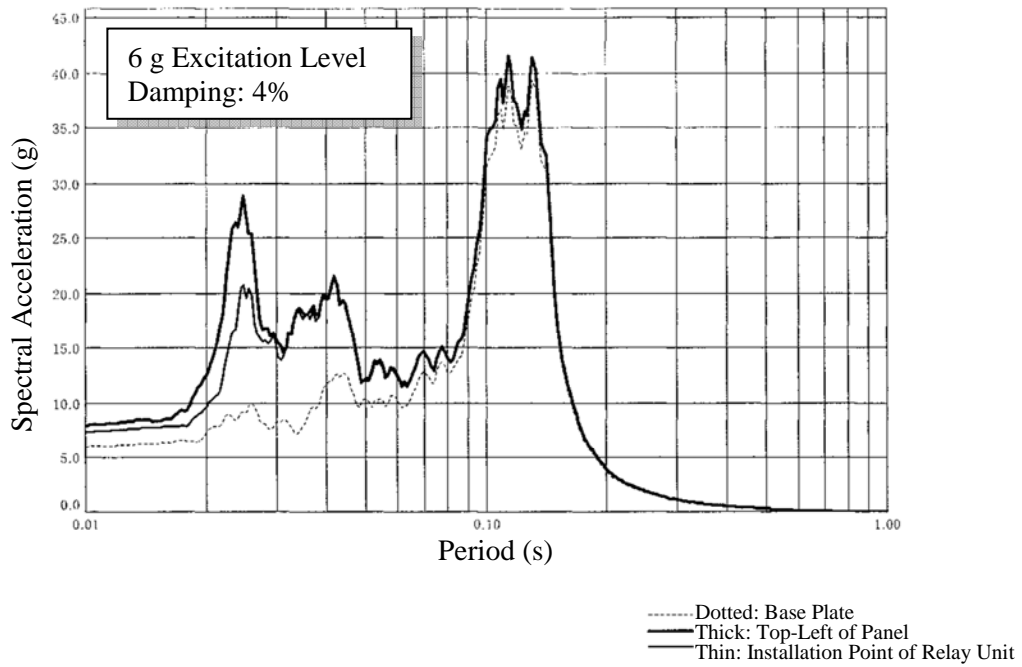
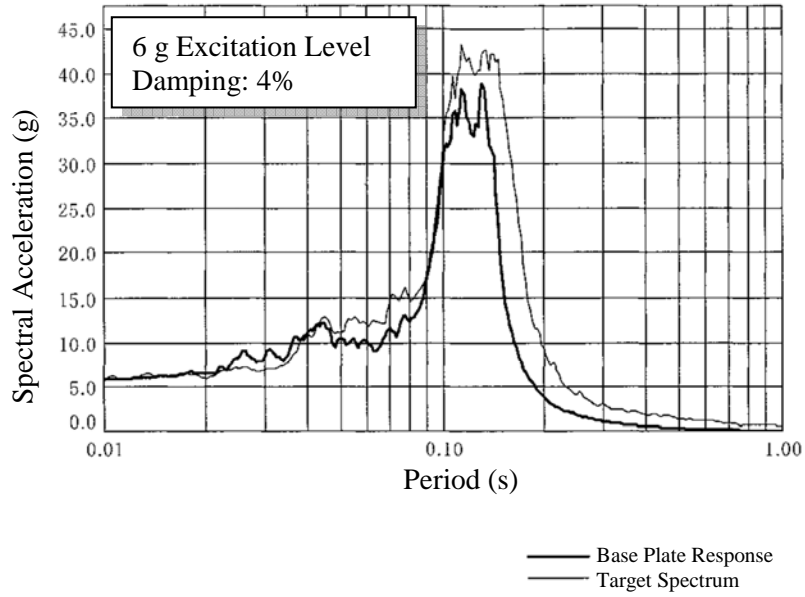


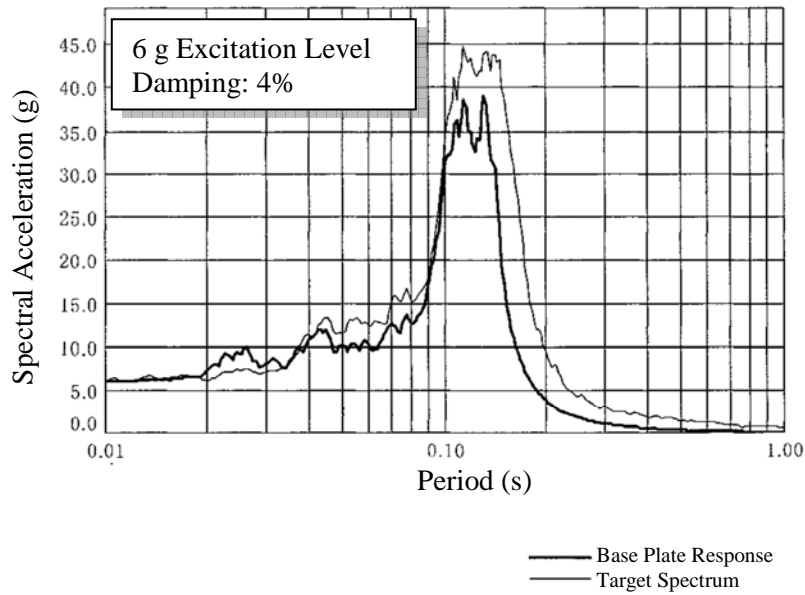
Figure B-53 Reactor Control Center – Panel RS – 6 g (Back and Forth)

B.2.6 Power Center

Several devices in the Power Center malfunctioned in the 6 g excitation test.



(A) Side to Side Direction



(B) Back and Forth Direction

Figure B-54 Power Center – Base Plate RS – 6 g

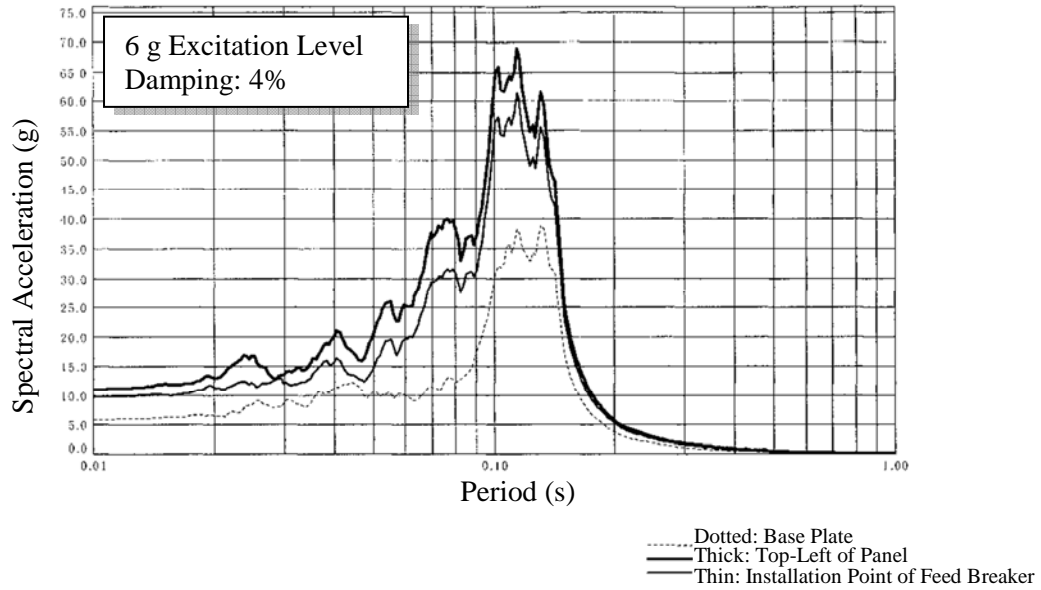


Figure B-55 Power Center – Panel RS – 6 g (Side to Side)

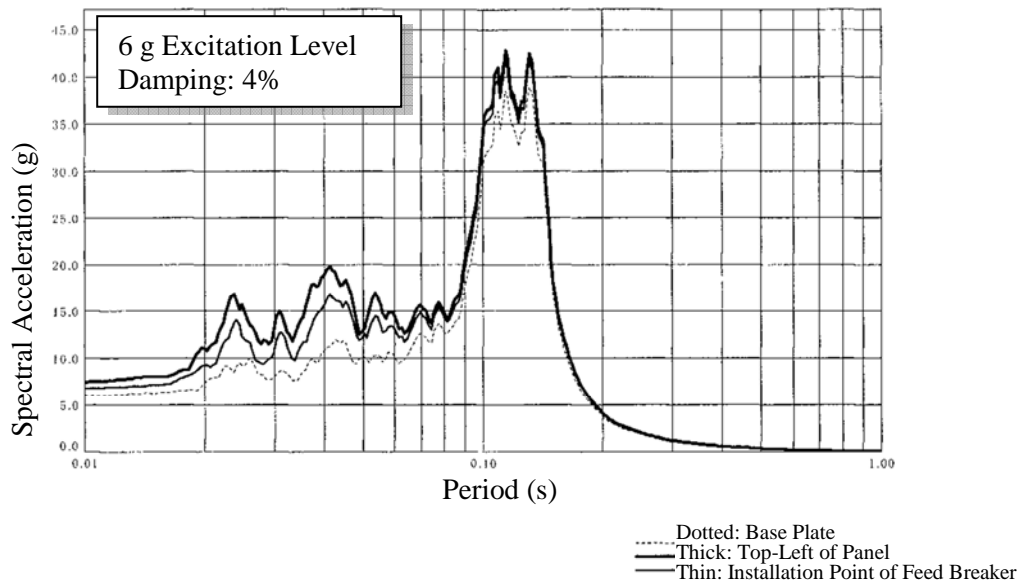


Figure B-56 Power Center – Panel RS – 6 g (Back and Forth)

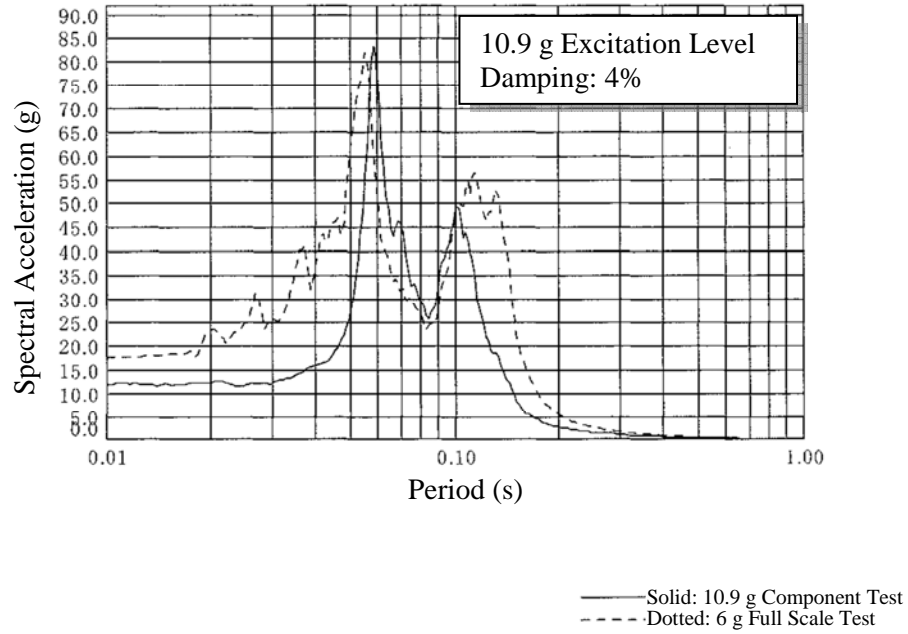
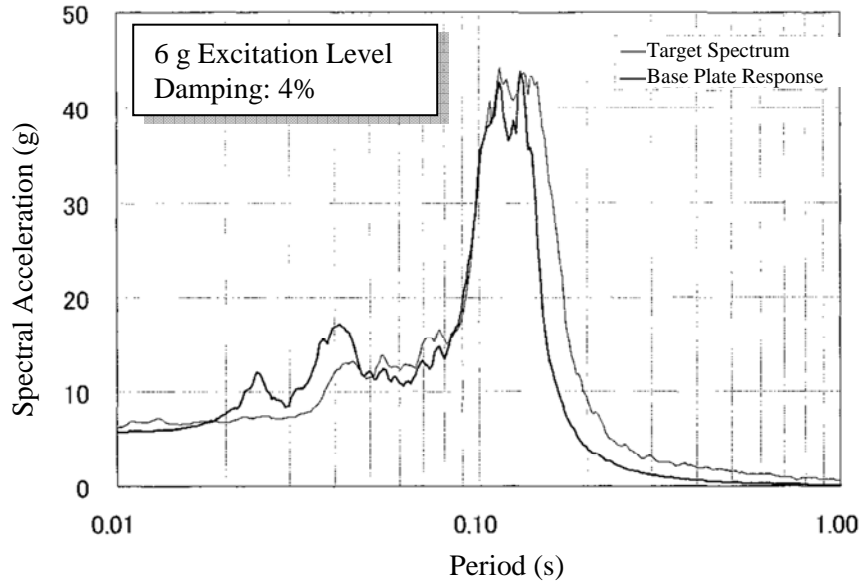


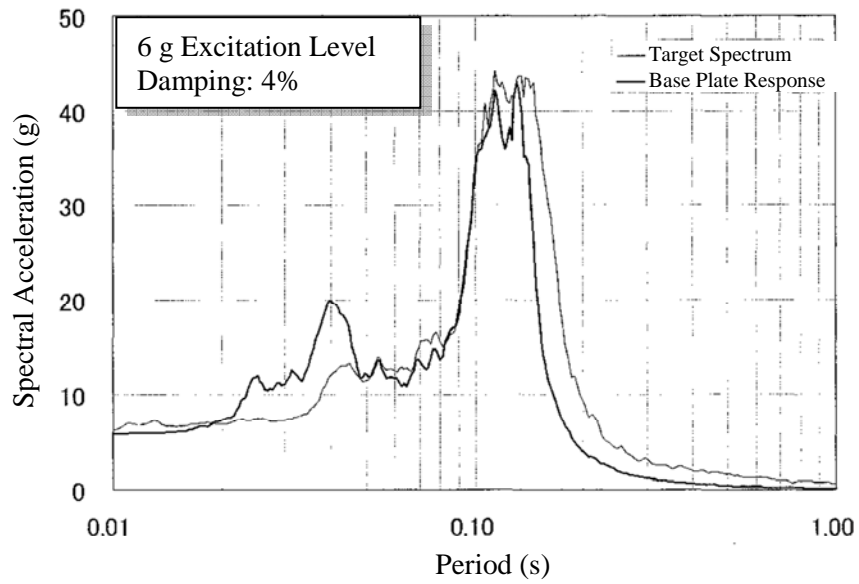
Figure B-57 RS of Ratio Differential Relay (TUB-2-D), Malfunctioned in 6 g Full Scale Power Center Test (Back and Forth, 10.9 g)

B.2.7 Metalclad Switchgear

Several devices installed in the Metalclad Switchgear malfunctioned in the 6 g full scale panel test.



(A) Back and Forth Direction



(B) Side to Side Direction

Figure B-58 Metalclad Switchgear – Base Plate RS – 6 g

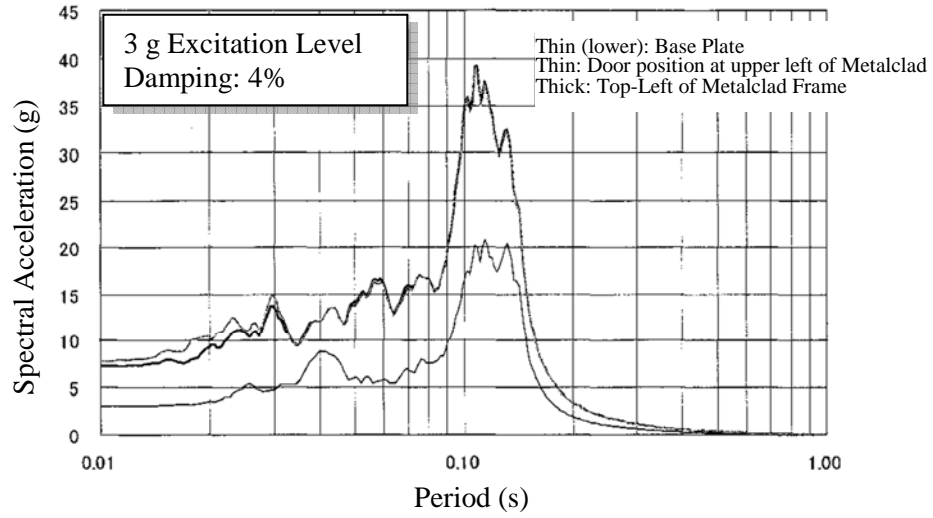


Figure B-59 Metalclad Switchgear – Panel RS – 3 g (Side to Side)

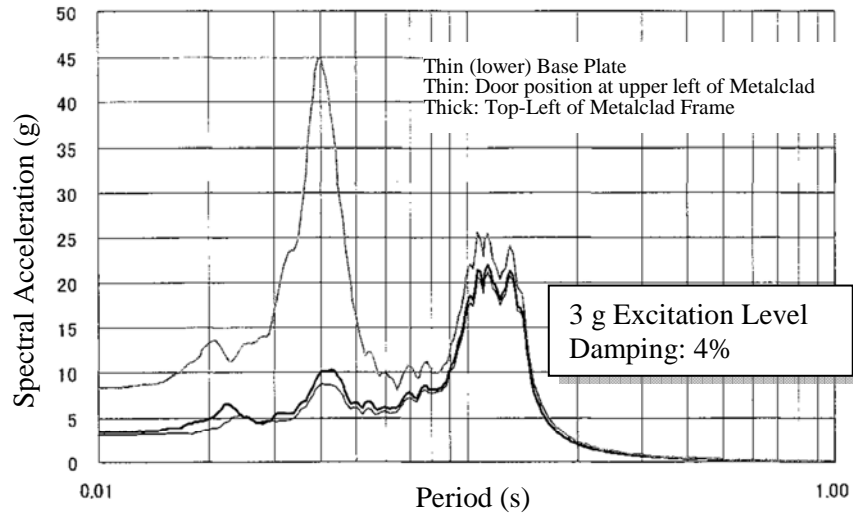
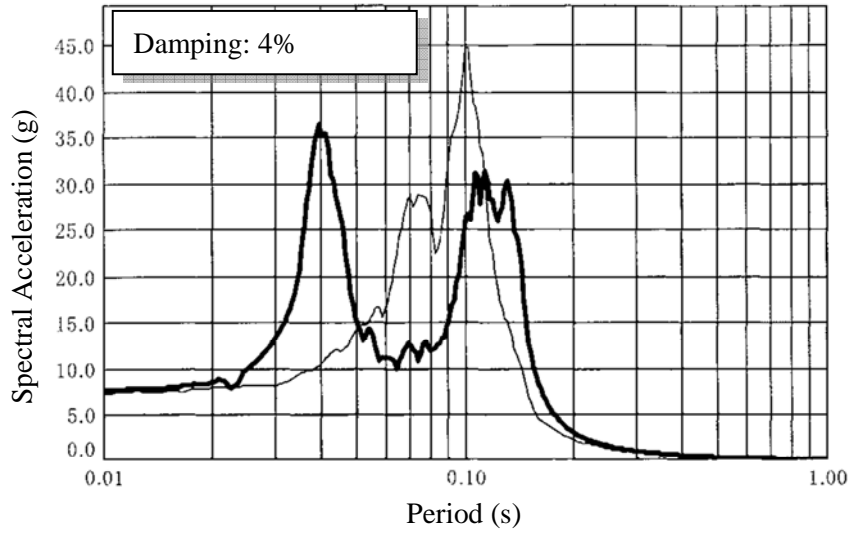


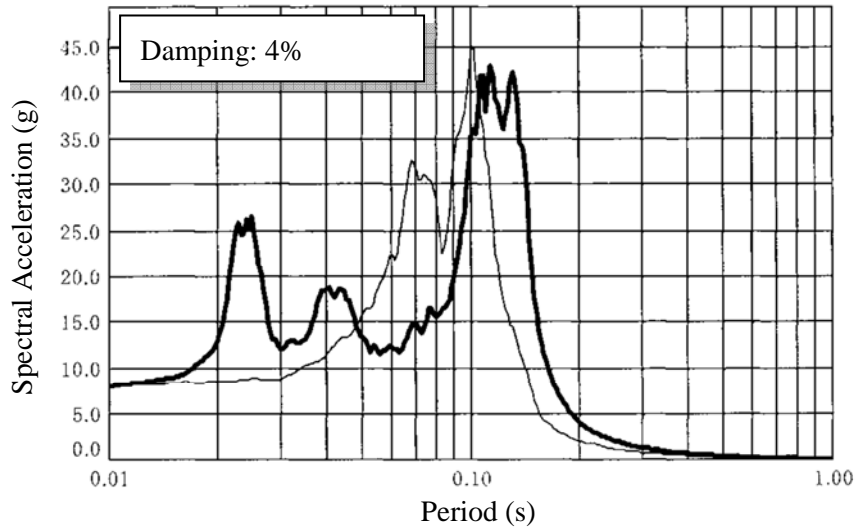
Figure B-60 Metalclad Switchgear – Panel RS – 3 g (Back and Forth)

B.2.8 Device Tests



(A) Side to Side Direction

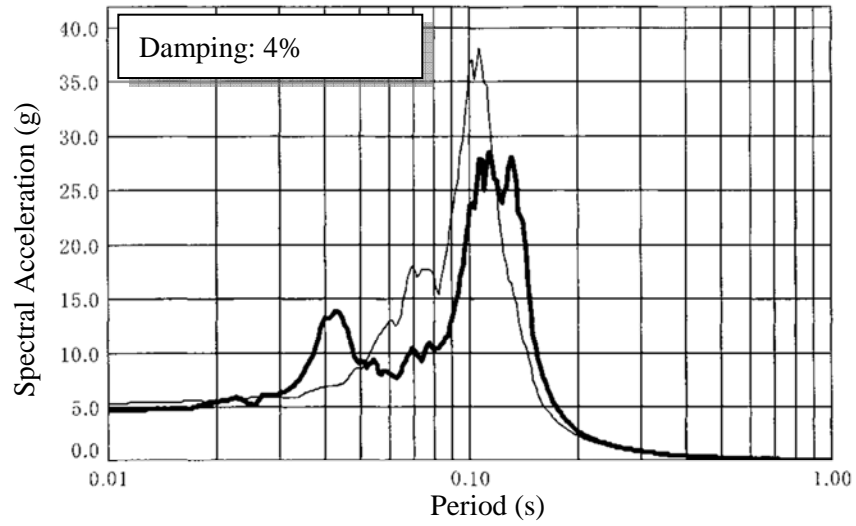
— Thin: Analysis
— Thick: Full scale test



(B) Back and Forth Direction

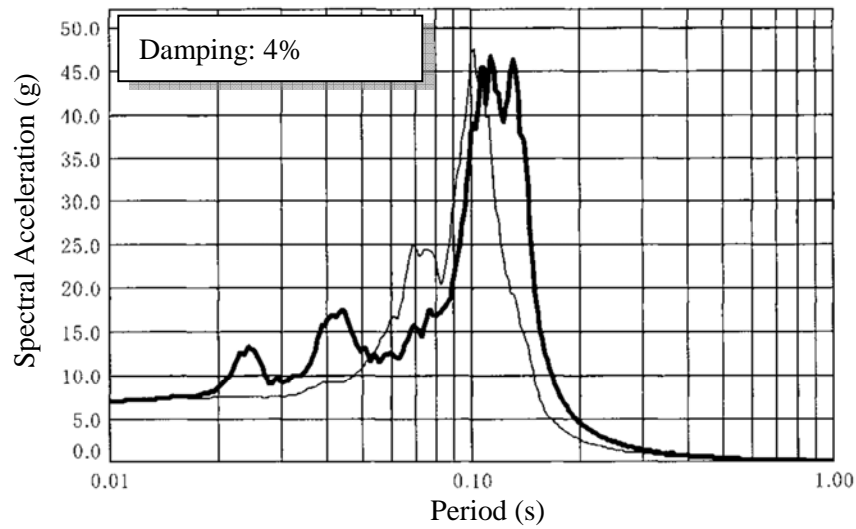
— Thin: Analysis
— Thick: Full scale test

Figure B-61 RS at Installation Points for Test Module (MHI S9166AW), Power Supply Module (MHI S9016AW), and Monitor Module (MHI S9146AW)



(A) Side to Side Direction

— Thin: Analysis
 — Thick: Full scale test



(B) Back and Forth Direction

— Thin: Analysis
 — Thick: Full scale test

Figure B-62 RS at Installation Points for Power Supply Equipment (MHI S9980UD) and Diode Unit (S9154UT)

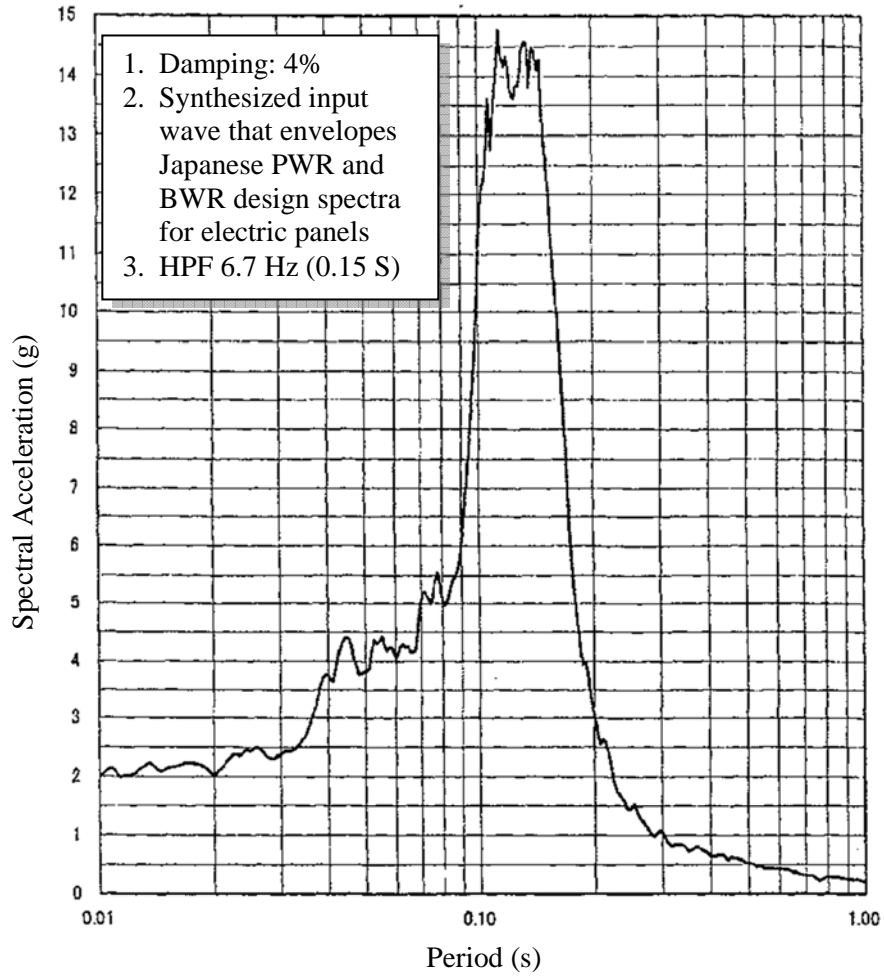


Figure B-63 RS for Differential Pressure Transmitter (MHI UNE13)

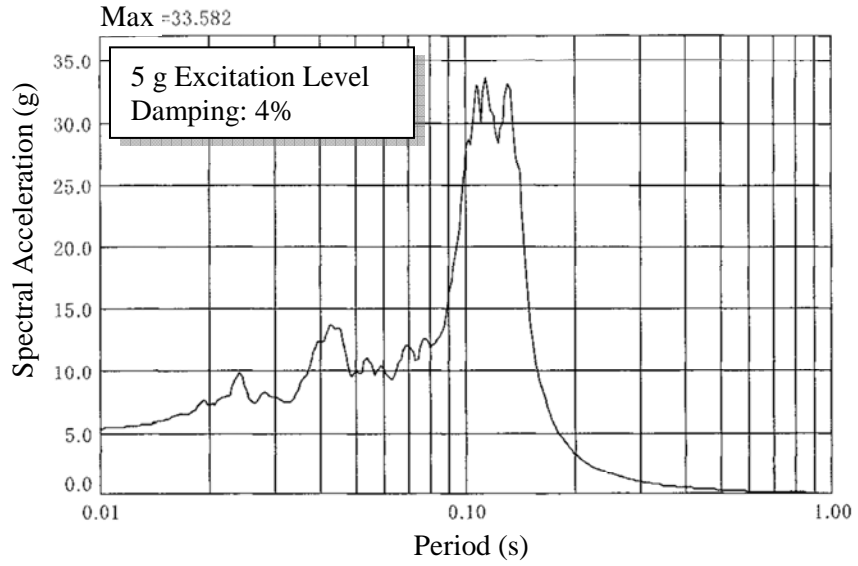


Figure B-64 RS of Recorded Time History for Feed Breaker (DS-416) in Power Center – 5 g

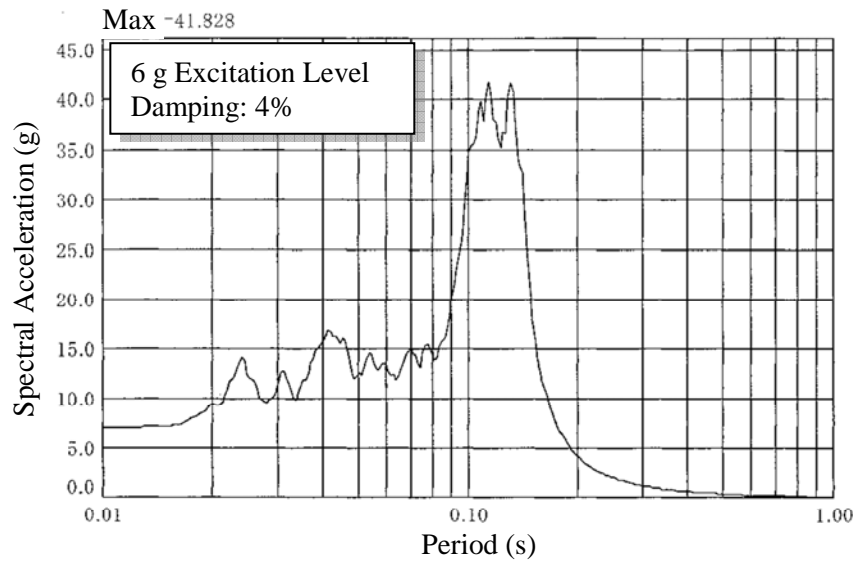


Figure B-65 RS of Recorded Time History for Feed Breaker (DS-416) in Power Center – 6 g

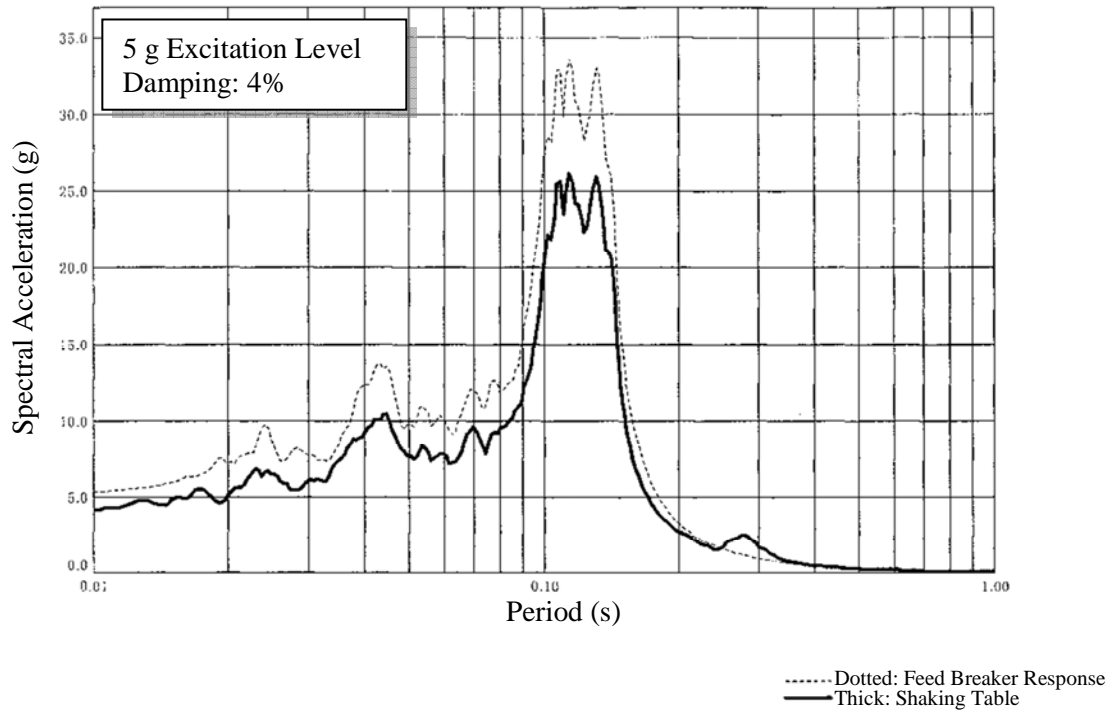


Figure B-66 RS for Feed Breaker (DS-416) in Power Center – Malfunction

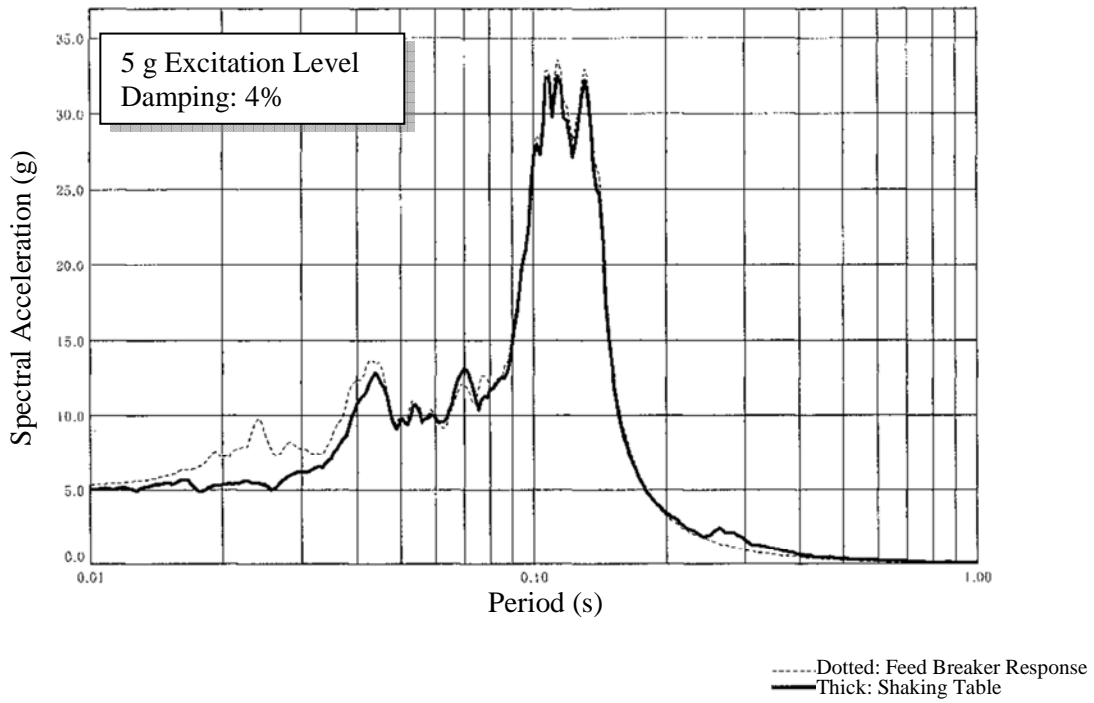


Figure B-67 RS for Feed Breaker (DS-416) in Power Center – Normal Function

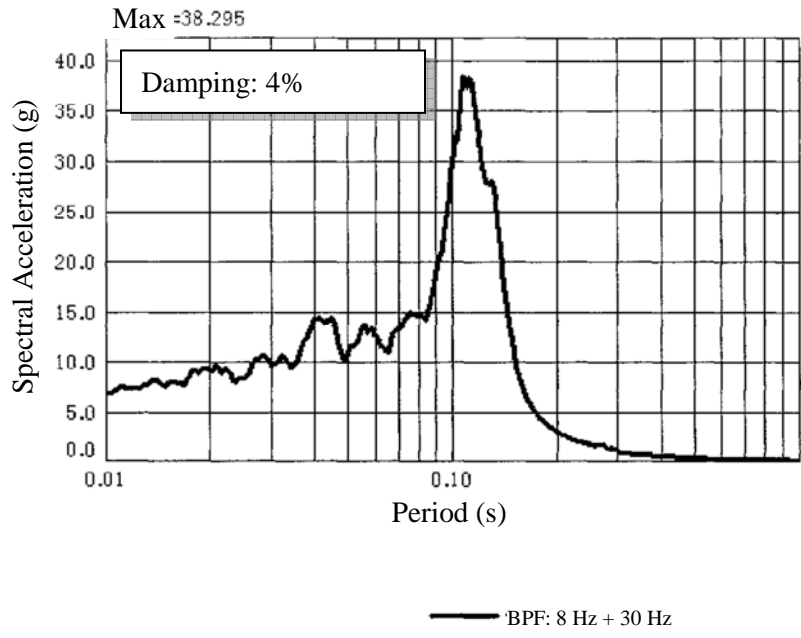


Figure B-68 RS for Feed Breaker (DS-416) in Power Center

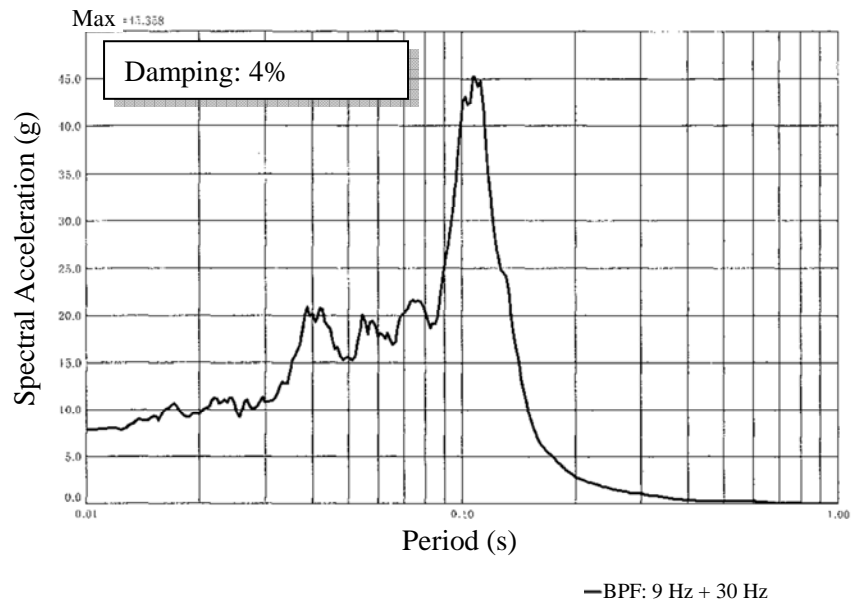


Figure B-69 RS for Feed Breaker (DS-416) in Power Center

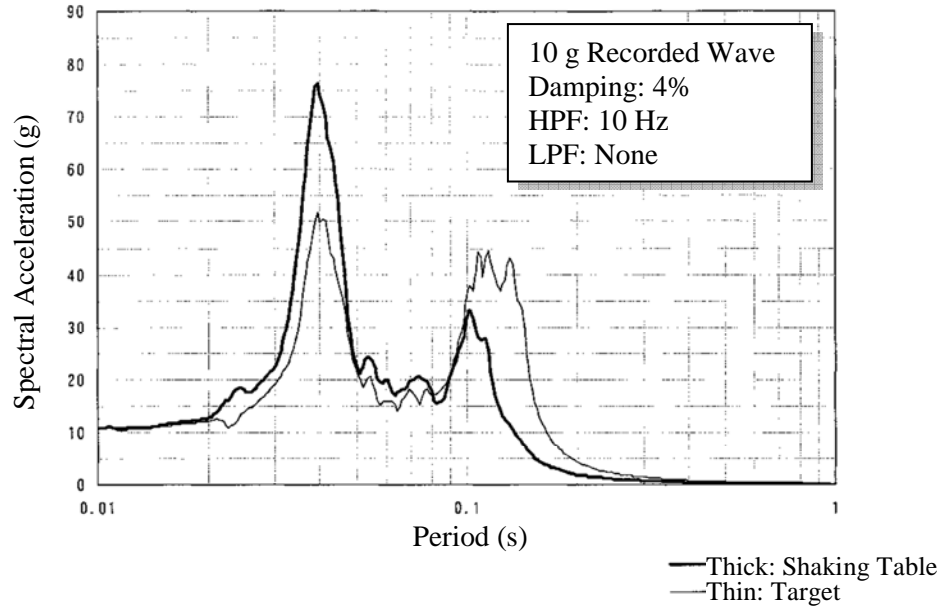


Figure B-70 Test Module (MHI S9166AW), Power Supply Module (MHI S9016AW), and Monitor Module (MHI S9146AW) – Recorded Wave 10 g (Side to Side)

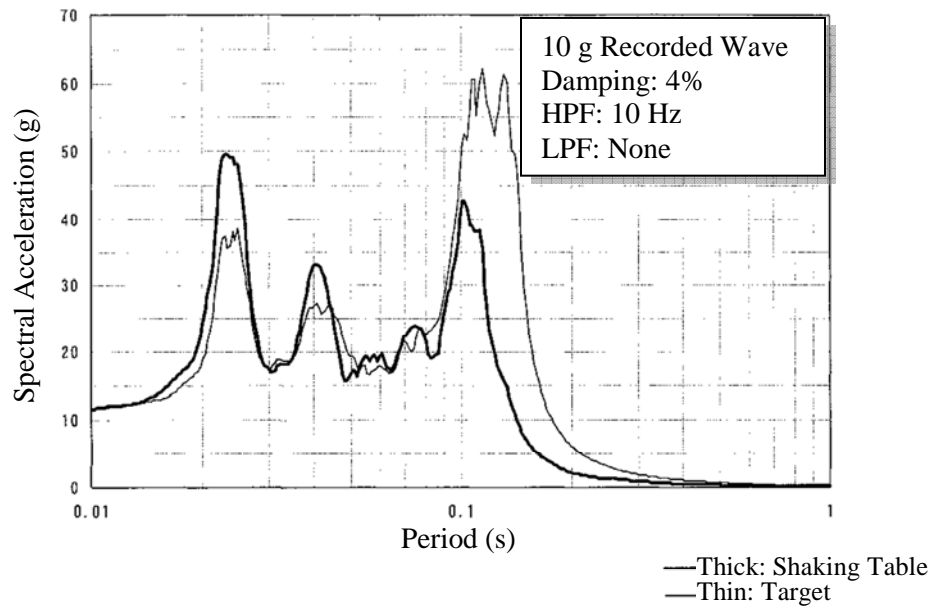


Figure B-71 Test Module (MHI S9166AW), Power Supply Module (MHI S9016AW), and Monitor Module (MHI S9146AW) – Recorded Wave 10 g (Back and Forth)

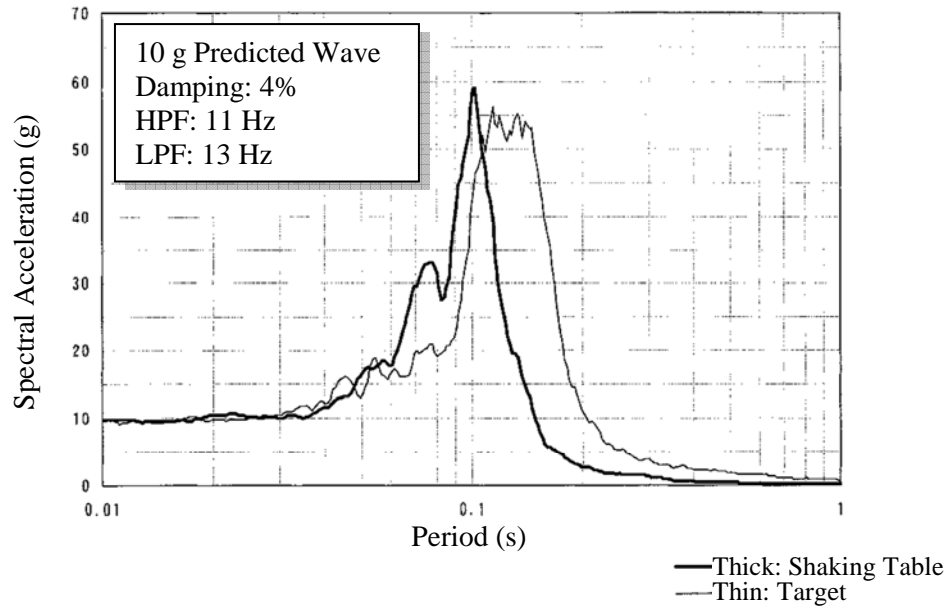


Figure B-72 Test Module (MHI S9166AW), Power Supply Module (MHI S9016AW), and Monitor Module (MHI S9146AW) – Predicted Wave 10 g (Side to Side)

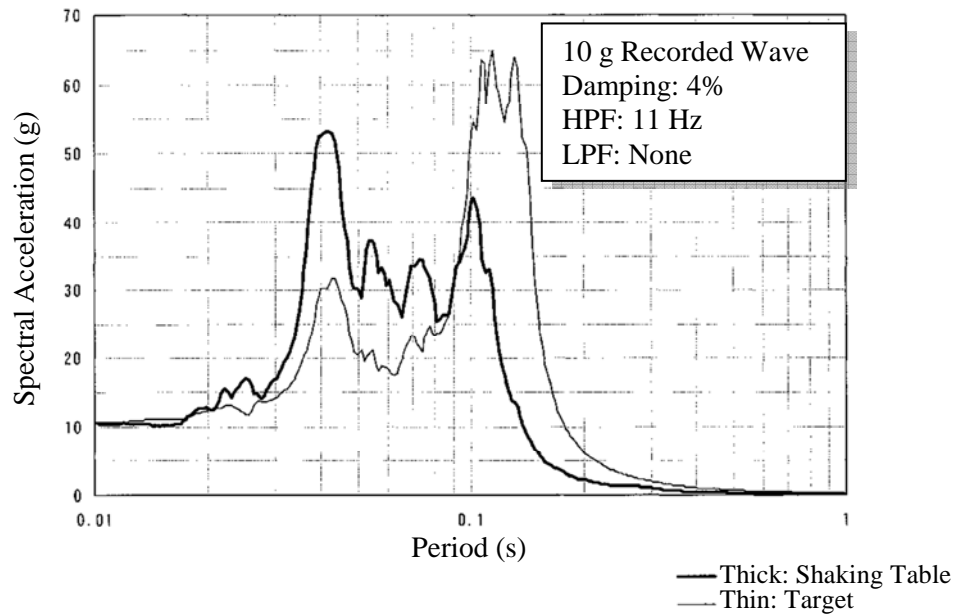


Figure B-73 Power Supply Equipment (MHI S9980UD) and Diode Unit (MHI S9154UT) – Recorded Wave 10 g (Side to Side)

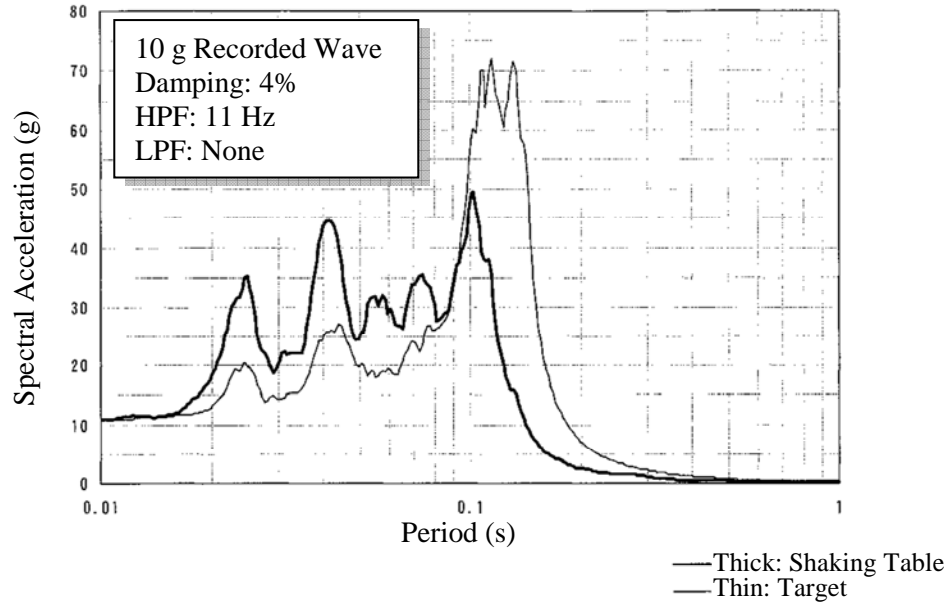


Figure B-74 Power Supply Equipment (MHI S9980UD) and Diode Unit (MHI S9154UT) – Recorded Wave 10 g (Back and Forth)

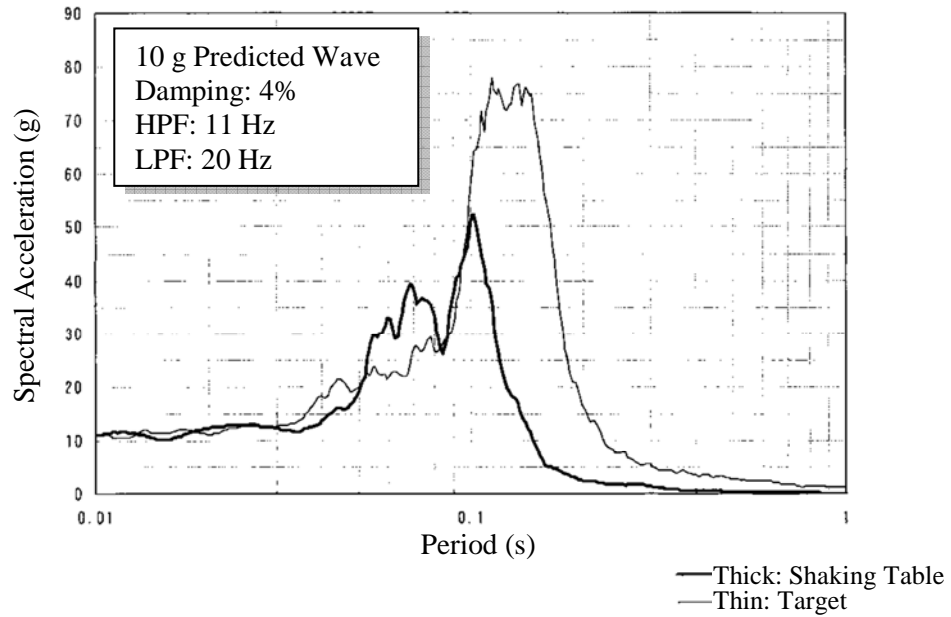


Figure B-75 Power Supply Equipment (MHI S9980UD) and Diode Unit (MHI S9154UT) – Predicted Wave 10 g (Side to Side)

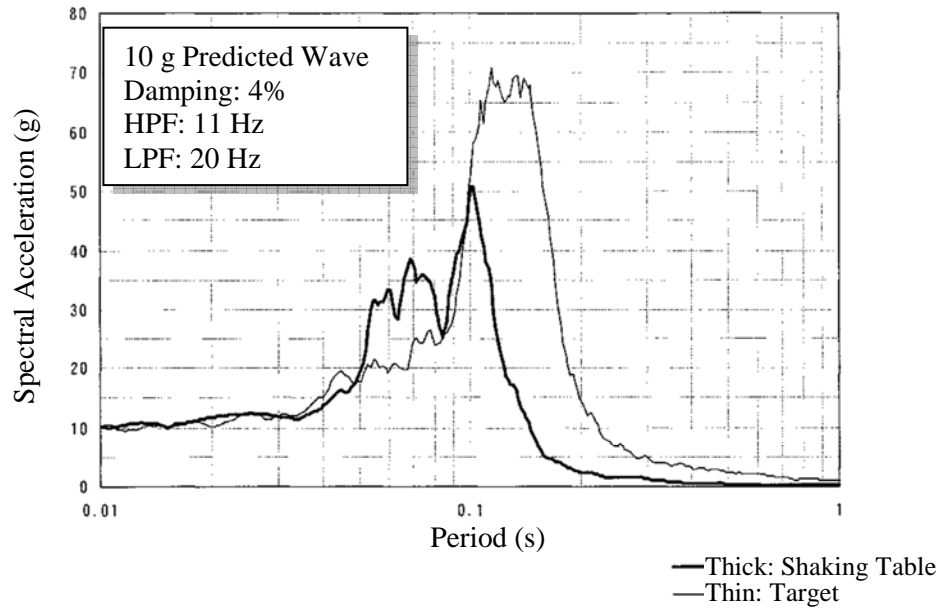


Figure B-76 Power Supply Equipment (MHI S9980UD) and Diode Unit (MHI S9154UT) – Predicted Wave 10 g (Back and Forth)

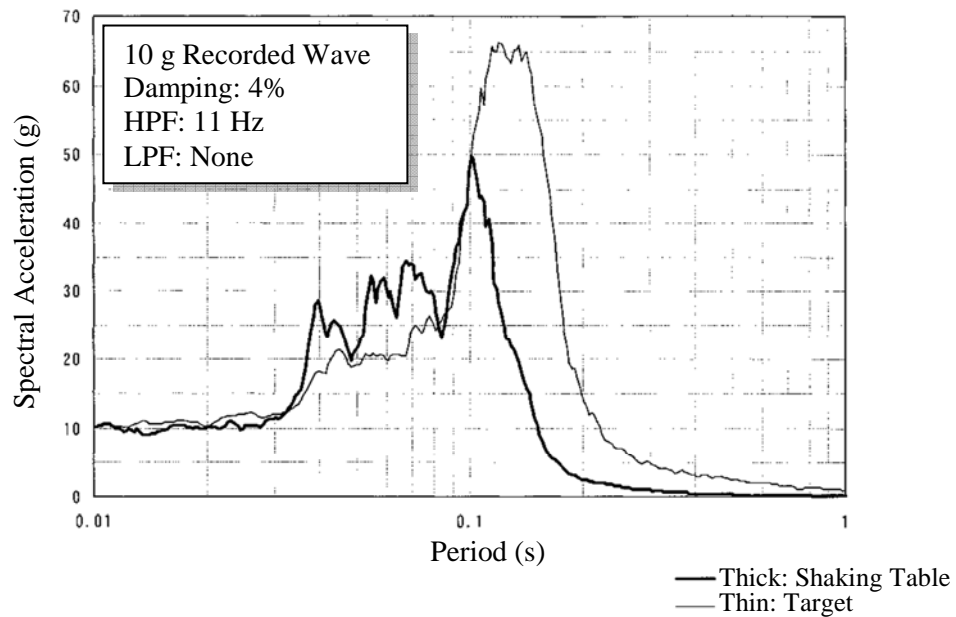


Figure B-77 Differential Pressure Transmitter (MHI UNE13) – Recorded Wave 10 g (Side to Side)

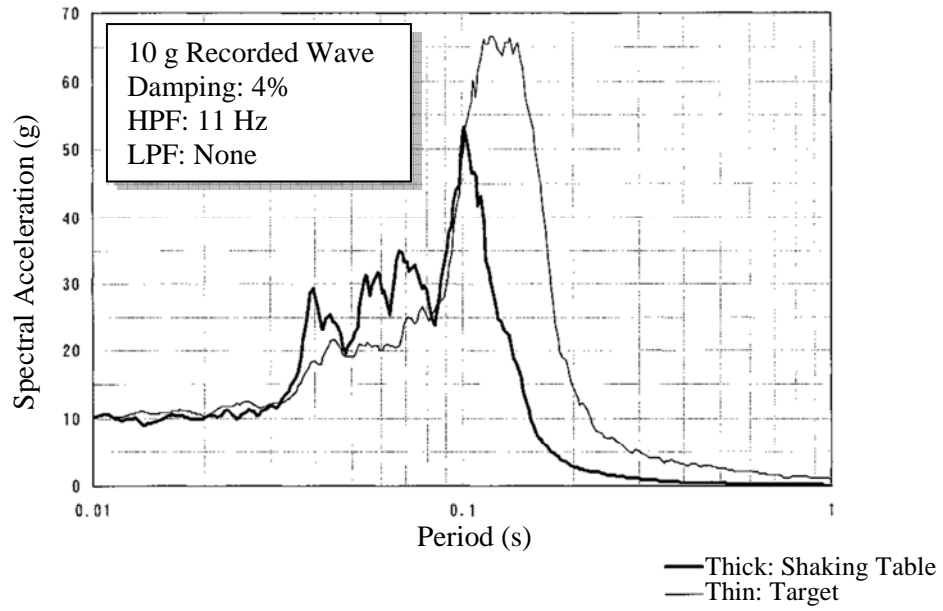


Figure B-78 Differential Pressure Transmitter (MHI UNE13) – Recorded Wave 10 g (Back and Forth)

NRC FORM 335 (9-2004) NRCMD 3.7 <p style="text-align: center;">BIBLIOGRAPHIC DATA SHEET <i>(See instructions on the reverse)</i></p>	<p style="text-align: center;">U.S. NUCLEAR REGULATORY COMMISSION</p> 1. REPORT NUMBER <i>(Assigned by NRC, Add Vol., Supp., Rev., and Addendum Numbers, if any.)</i> <p style="text-align: center;">NUREG/CR-7040 BNL-NUREG-94629-2011</p>				
2. TITLE AND SUBTITLE Evaluation of JNES Equipment Fragility Tests for Use in Seismic Probabilistic Risk Assessments for U.S. Nuclear Power Plants	3. DATE REPORT PUBLISHED <table border="1" style="width: 100%;"> <tr> <td style="width: 50%;">MONTH</td> <td style="width: 50%;">YEAR</td> </tr> <tr> <td style="text-align: center;">April</td> <td style="text-align: center;">2011</td> </tr> </table> 4. FIN OR GRANT NUMBER <p style="text-align: center;">JCN: N-6076/N-6998</p>	MONTH	YEAR	April	2011
MONTH	YEAR				
April	2011				
5. AUTHOR(S) R. Kennedy (RPK Structural Mechanics Consulting) J. Nie and C. Hofmayer (Brookhaven National Laboratory)	6. TYPE OF REPORT <p style="text-align: center;">Technical</p> 7. PERIOD COVERED <i>(Inclusive Dates)</i>				
8. PERFORMING ORGANIZATION - NAME AND ADDRESS <i>(If NRC, provide Division, Office or Region, U.S. Nuclear Regulatory Commission, and mailing address; if contractor, provide name and mailing address.)</i> <table style="width: 100%;"> <tr> <td style="width: 50%;"> RPK Structural Mechanics Consulting 28625 Mountain Meadow Road Escondido, CA 92026 </td> <td style="width: 50%;"> Nuclear Science and Technology Department Brookhaven National Laboratory P.O. Box 5000 Upton, NY 11973-5000 </td> </tr> </table>		RPK Structural Mechanics Consulting 28625 Mountain Meadow Road Escondido, CA 92026	Nuclear Science and Technology Department Brookhaven National Laboratory P.O. Box 5000 Upton, NY 11973-5000		
RPK Structural Mechanics Consulting 28625 Mountain Meadow Road Escondido, CA 92026	Nuclear Science and Technology Department Brookhaven National Laboratory P.O. Box 5000 Upton, NY 11973-5000				
9. SPONSORING ORGANIZATION - NAME AND ADDRESS <i>(If NRC, type "Same as above"; if contractor, provide NRC Division, Office or Region, U.S. Nuclear Regulatory Commission, and mailing address.)</i> Division of Engineering Office of Nuclear Regulatory Research U.S. Nuclear Regulatory Research Washington, DC 20555-0001					
10. SUPPLEMENTARY NOTES Syed Ali, NRC Project Manager					
11. ABSTRACT <i>(200 words or less)</i> <p>The Japan Nuclear Energy Safety Organization (JNES) is conducting a multi-year equipment fragility test program to obtain realistic equipment fragility capacities for use in the seismic probabilistic risk assessments (SPRAs) of nuclear power plants (NPPs) in Japan. This test program started in 2002 and is planned to continue until 2012. This program consists of the test of a series of safety significant equipment, which are scheduled in two phases. Phase I includes large horizontal shaft pumps, large vertical shaft pumps, electrical panels, and control rod insertion capability and Phase II includes fans, valves, tanks, support structures, and overhead cranes. As part of collaborative efforts between the United States and Japan on seismic issues, the U.S. Nuclear Regulatory Commission (NRC) and Brookhaven National Laboratory (BNL) participated in this program by evaluating the results of the JNES equipment fragility tests. The goal of this research effort was to compare the JNES fragility results with the fragility data typically used in current U.S. SPRAs and assess the impact that the new test results may have on current SPRAs and how this data can be utilized for future SPRAs. This report summarizes the BNL evaluation of the JNES equipment fragility test data and provides insights on the applicability and application of this data in U.S. SPRA practices.</p>					
12. KEY WORDS/DESCRIPTORS <i>(List words or phrases that will assist researchers in locating the report.)</i> Seismic equipment fragility, full-scale shaking table testing, seismic margin, seismic probabilistic risk assessment, design certification (DC) application, combined license (COL) application, high confidence low probability of failure (HCLPF) capacity, large horizontal shaft pump, large vertical shaft pump, electrical panel, control rod insertion, fans, valves, tanks, support structures, and overhead cranes	13. AVAILABILITY STATEMENT <p style="text-align: center;">unlimited</p> 14. SECURITY CLASSIFICATION <i>(This Page)</i> <p style="text-align: center;">unclassified</p> <i>(This Report)</i> <p style="text-align: center;">unclassified</p> 15. NUMBER OF PAGES 16. PRICE				